SPECIAL VOLUME

The Journal of Indian Geophysical Union

ISSN number 0971 - 9709

JIGU-IAGA Special Volume-2/2016

Geomagnetic Measurements, Observatories And Applications

based on

XVIth IAGA Workshop, 2014

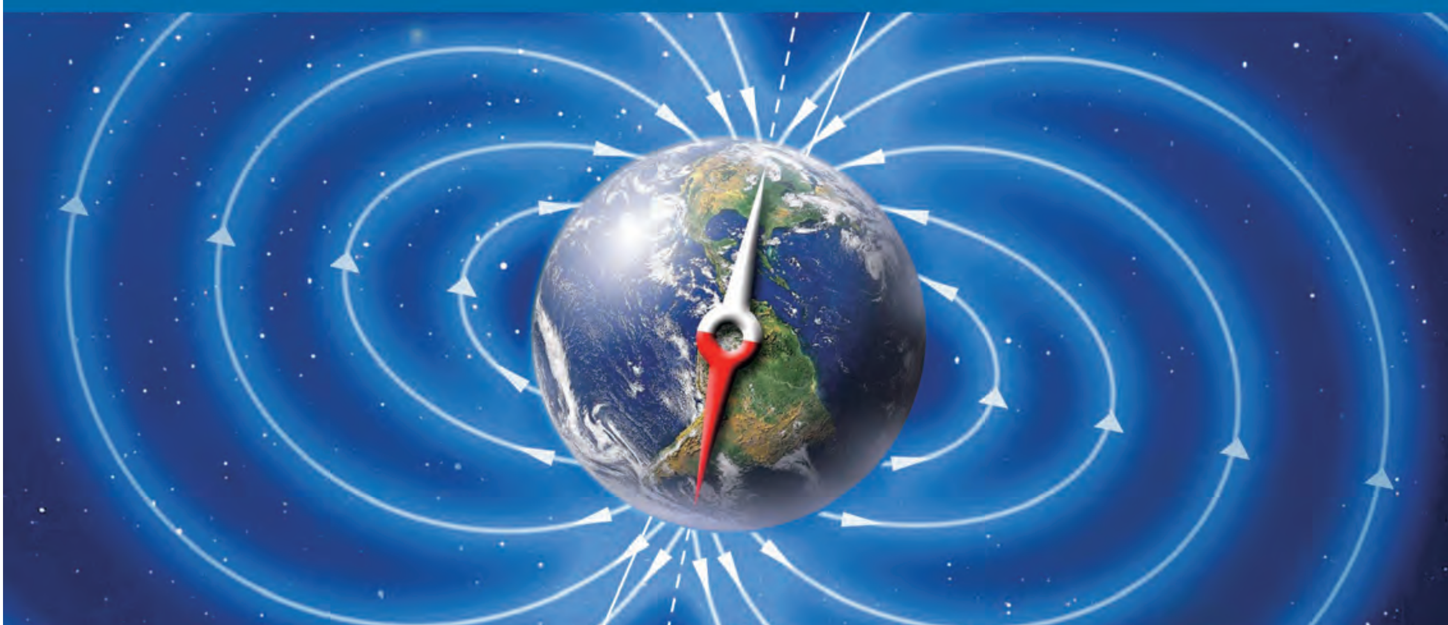

Guest Editors:
Nandini Nagarajan
Sergey Khomutov
Kusumita Arora

INDIAN GEOPHYSICAL UNION

The Open Access Journal with four issues in a year publishes articles covering
Solid Earth Geosciences; Marine Geosciences; and Atmospheric, Space and Planetary Sciences.

Annual Subscription
Individual Rs. 750/- and Institutional Rs. 2000/-
Payments should be sent by DD drawn in favour of "The Treasurer, Indian Geophysical Union", payable at Hyderabad.
For correspondence, please contact, Hon. Secretary, Indian Geophysical Union, NGRI Campus, Uppal Road,
Hyderabad - 500 007, India; Email: igu123@gmail.com; Ph: 040 27012799

CONTENTS

Preface

In 1986 the first IAGA Observatory Workshop was held in Ottawa; since then the biennial Workshops have guided and witnessed the progress in quality of data aquisition through improvements in instrumentation as well as observation and analyses practices by bringing together on a regular basis observers, researchers, and developers on the same platform for meaningful exchange of information and ideas. During 7-17 October 2014, the sixteenth International Association of Geomagnetism and Aeronomy (IAGA) Workshop on Geomagnetic Observatory Instruments, Data Acquisition and Processing was held in India for the first time jointly organized by the National Geophysical Research Institute (CSIR-NGRI), Hyderabad and the Indian Institute of Geomagnetism (IIG), Mumbai. It was of special importance to the organisers as the Golden Jubilee (1964-2014) of the Hyderabad Magnetic Observatory (HYB) was commemorated during this Workshop. With continuous recording and reporting of reliable and quality data over the last fifty years, HYB has emerged as an ideal, inland, low-latitude, international Key Magnetic Observatory, acknowledged by the International Association of Geomagnetism and Aeronomy (IAGA). The long data series has been used as input to main field model computations along with data from observatories all over the world. Significant contributions to studies of low-latitude geomagnetic phenomena have been made from these datasets, as well as magnetic pulsations and earth current measurements.

About sixty observers from thirty one countries participated in the measurement sessions, of which ten were trainee/novice observers. Thirty instruments were brought in for inter-comparison from respective observatories. Thirty more scientists arrived for the scientific sessions in the latter half of the Workshop. Germany, USA, Belgium, UK, S Korea, Hungary, Japan, Russia, Kazakhstan, Sri Lanka, Austria, Australia, Czech Republic,and South Africa were represented significantly. There were delegates from Ireland, Canada, Denmark, Israel, France, Spain, Ukraine, W Samoa, Maldives,Syria, Romania, Slovenia,Poland and Ukraine. There were thirty delegates from India: 10 from the IIG, 9 from NGRI, 3 from Survey of India (SOI) and 5 from different universities.

Participants create the flavour of a Workshop. The close knit geomagnetic observatory community is well known for its interactive and cooperative nature, which made this Workshop vibrant and fruitful. The organisers are grateful to all those who came to Hyderabad for this event and actively participated in all aspects.

After registration and ice-breaker on Monday, 6th October at CSIR-NGRI, the measurement sessions started on 7th October in the newly setup observatory of Choutuppal (CPL). There were a total of 9 pillars at CPL of which 6 were kept vacant for absolute measurements by participants. One pillar was used to install Autodiff or continuous comparison on all 5 days of the measurement sessions. The azimuths of these pillars had been pre-determined by teams from SOI and IIG. Calibration of PPM-s was also carried out during the session in a dedicated room in the Main Building. As a first, the measurement sessions included six lectures on basics of magnetic observatory practice and data processing. Three afternoon sessions of practical training and demonstrations were also held. For regular absolute observations and new experiments, observers occupied sixty slots of 90 minutes each. A special session on low-latitude azimuth observations was conducted with demonstration by expert team from the Survey of India, followed by animated discussions. The scientific efforts by the large international community were covered in detail by the local media.

Prof. Harsh Gupta, President IUGG and Chief Guest, inaugurated the scientific session of the Workshop on 13th October 2014. Acting Director CSIR-NGRI, Dr. Y.J. Bhaskar Rao, Director's nominee from IIG, Dr. S. Gurubaran, IAGA council member Dr. Archana Bhattacharyya, IAGA Div V co-Chair, Dr. Pavel Hejda, Chief Scientist from the MoES, Dr. B.K. Bansal, Head of Observatories, GFZ, Dr. Juergen Matzka spoke on the occasion. The past and present staff of the HYB Magnetic Observatory received commendations on their efforts to preserve high standards of data quality from Prof. Harsh Gupta to mark the golden jubilee of

HYB Observatory during the Inaugural session. Some of the Golden Jubilee invitees shared their memories of the early days at the observatory.

Six scientific sessions were held during three days with 45 oral and 35 poster presentations. The major topics covered were: the Golden Jubilee of HYB & Long data series, Observatory Instruments and Techniques, Observatory Data Acquisition and Processing, Scientific Applications of Observatory data and Repeat Stations, Results of Measurement sessions. A special session was held on the ongoing ICSU-sponsored initiative for new efforts for regional cooperation among data observers and users in the northern Indian Ocean region, 'Uniting and Networking the magnetic community in the northern Indian Ocean region (MAGNIO)'. The seventh and concluding session on the last day was organised as a panel discussion on 'Magnetic observatories of the future and Observatory networks and IAGA's supporting role'. Details of the different aspects of Workshop activities have been published in the Report 2014 by the organisers.

The success of this Workshop is due to the support given by IUGG, IAGA and ICSU. Agencies of the Government of India: MoES, DST, CSIR, INCOIS, and INSA, have provided critical financial support to the Workshop, which enabled its success, in particular, the Measurement Sessions which required specialized infrastructure. The organisers are indebted to these agencies and to the Directors and management of the host institutes, whose support made it possible to successfully host this prestigious event. For this Workshop the new CPL Observatory was established in record time! Gratitude is due to the many volunteers and support teams as well as colleagues from HYB, who have put in months of efforts before the Workshop and full days without sleep during the event.

This special volume of the Journal of the Indian Geophysical Union entitled 'Geomagnetic measurements, Observatories and applications of data from IAGA Workshop, 2014' consists of eighteen scientific articles contributed by participants, on three distinct thrust areas of geomagnetic observatory research, which formed the main themes of the Workshop. The articles are categorised into three sub-disciplines: Magnetometers and Measurements, Observatory Data and Practice and Applications.

In the first section on Magnetometers and Measurements, contributions are about design and improvements in performance with improved accuracy and stability of measurements. Details of a new theodolite WiDIF for repeat surveys, mechanical stability of suspended dIdD sensor, hardware developments to monitor characteristics of fluxgate for stable 1 sec values, determination of variometer alignment, temperature stability of LEMI-025 are presented.

The second section concentrates on Observatory Data and Practice, i.e. methods of processing and analyses of data at different observatories to monitor data quality and extract the maximum information. Contributions include articles on historical archives and their importance, experiments to determine performance of classical magnetometers, new software of enhanced data processing tools implemented at different observatories with complete visualisation, real time transmission, remote controlled trouble shooting, data quality of new observatory, assessment of temperature effects.

The last section on Applications has a very large scope. Contributions include articles on atmospheric tides and electrojet, dynamic aspects of solar flare effects, long term external field contributions in repeat station data, repeat surveys in India, secular variations in Indian region, ionospheric behaviour during seismic event.

The editors of this special volume thank all the authors, and reviewers for their prompt response and painstaking efforts and patience over the past year that have made this volume possible. We thank the editorial board of JIGU for agreeing to publish this special volume and specially, Dr P.R. Reddy, Chief Editor, JIGU, for his guidance and encouragement throughout this process.

Nandini Nagarajan
Sergey Khomutov
Kusumita Arora

Editorial

I deem it a privilege to write an editorial for the special volume of the Journal of Indian Geophysical Union (JIGU), guest-edited by three internationally reputed scientists. This publication assumes importance as it has clearly projected the relevance of establishing, maintaining and utilising magnetic observatories in generating quality data that has helped (and continues to help) in solving various problems of interest to specialists researching on magnetic storms, sunspot activity, solar flares, earthquake precursors and many other related problems.

I am happy to notice the significant camaraderie between technical experts, instrument developers and production specialists and scientists with theoretical and application oriented basic science background during the IAGA conference at CSIR-NGRI and post conference structuring of this special volume. They, as a single well knit community, have put at rest the ill-conceived opinion expressed by some sceptics that maintenance of observatories, data generation using routine procedures and analysis of the generated data using established processing algorithms cannot be categorised as part of established scientific research and those associated with these operations can at best be called as technical experts. A peep into the 18 well-articulated and structured manuscripts clearly show the significance of these data generation operations that require focused attention, constantly evolving innovative procedures, bundles of patience and perseverance and capacity to segregate noise from signal to better understand various natural phenomena that have direct impact on our very existence amidst chaotic unknown phenomena involving both the nature and the Man.

We would never have known about the 11 year sunspot maximum and minimum cycles, Plasma bubble and fox clouds, TEC signals prior to a high magnitude earthquakes, dynamics of Aurora lights, magnetic storms impact on communication networks and navigational electronics, Maunder minimum, impact of sunspot activity/ solar flares on climate change but for the impressive volume and length of data generated by committed technical experts cum scientists spanning over centuries.

It is indeed remarkable that contributors have meticulously referred the sequential development of instruments and techniques in the last hundred years and more in building their articles, as they strongly believe that the present day knowledge has evolved from past experiences, successes and failures. The historical development of analogue era and transition to digital era tells us the rich heritage associated with the modernisation of magnetic observatories.

I congratulate the three guest editors and contributors of 18 manuscripts for bringing out a significantly important publication. I thank the editorial team of this special volume, on behalf of JIGU editorial team, for selecting JIGU for publication of this volume.

P.R.Reddy
Chief Editor, JIGU

GEOLOGICAL SOCIETY OF INDIA

Prof. Harsh K. Gupta
President

Foreword - I

Geomagnetic observatories, which are the repositories of long time series of geomagnetic variation data, play a crucial role in global field modeling, space weather studies, studies of secular variations as well as records of local characteristics of the field behaviour. IAGA Observatory workshops, which focus on Geomagnetic Observatory Instruments, Data Acquisition and Processing are held once in two years at different Magnetic Observatories of the world, where Absolute and Variation instruments are compared and scientific applications of the resultant data are presented and discussed. These Workshops present an opportunity for instrument developers, observers and data users to come together to implement best practices for highly accurate absolute measurements and calibration and comparison of instruments and plan future directions of improvements in all related aspects. The Workshops are indeed a unique concept where one- half the duration is dedicated to hands-on measurement and calibration sessions, while another half is devoted to scientific deliberations regarding improvements in observations and their applications.

The XVI IAGA Workshop, 2014 was jointly organized by the National Geophysical Research Institute (CSIR-NGRI), Hyderabad and the Indian Institute of Geomagnetism (IIG), Mumbai, in the premises of CSIR-NGRI and its Choutuppal campus where about 90 scientists from 31 different countries participated. Instruments from 30 observatories were brought for calibration and measurements. This was the first time such a workshop was held in India. The Golden Jubilee (1964-2014) of the Hyderabad Magnetic Observatory (CSIR-NGRI) was commemorated by this workshop.

Six scientific sessions were held during three days with 45 oral and 35 poster presentations. The major topics covered Golden Jubilee of HYB & Long data series, MAGNIO, Observatory Instruments and Techniques, Observatory Data Acquisition and Processing, Scientific Applications of Observatory data and Repeat Stations, Results of Measurement sessions. The seventh and concluding session on the last day was organised as a panel discussion on 'Magnetic observatories of the future and Observatory networks and IAGA's supporting role'.

This special volume of the Journal of the Indian Geophysical Union presents 18 articles categorised into three major disciplines,which had been cores areas of deliberation during the IAGA Workshop: Magnetometers and Measurements, Observatory Data and Practices, Applications.

My appreciation goes to the scientists and officers who were responsible for the establishment and continuance of the Hyderabad Magnetic Observatory and conducted research on its high quality data. I compliment the IAGA scientists and researchers and commend the organising team led by Dr. Kusumita Arora for a very successful Workshop and a well planned special volume.

Harsh K. Gupta

Address for Correspondence: Koteswaram Professor, CSIR - National Geophysical Research Institute, Hyderabad-500 007,INDIA.
Tele/Fax: 040-27012866,Tel: 040-27155971(R) Email: harshg123@gmail.com

President, Geological Society of India
Immediate Past President, International Union of Geodesy and Geophysics
Member, Atomic Energy Regulatory Board
Formerly: Member, National Disaster Management Authority
Secretary to Govt. of India, Department of Ocean Development
Vice-Chancellor, Cochin University of Science & Technology
Director, National Geophysical Research Institute
Professor, University of Texas at Dallas, USA

Foreword - II

Geomagnetic observatories, which are the repositories of long time series of geomagnetic variation data, play a crucial role in global field modeling, space weather, secular variations as well as records of local characteristics of the field behaviour. IAGA Observatory workshops, which focus on Geomagnetic Observatory Instruments, Data Acquisition and Processing are held once in two years at different Magnetic Observatories of the world, where Absolute and Variation instruments are compared and scientific applications of the resultant data are presented and discussed. These Workshops present an opportunity for instrument developers, observers and data users to come together to implement best practices for highly accurate absolute measurements and calibration and comparison of instruments and plan future directions of improvements in all related aspects. The Workshops are indeed a unique concept where one- half the duration is dedicated to hands-on measurement and calibration sessions, while another half is devoted to scientific deliberations regarding improvements in observations and their applications.

This volume records the 16th in the series of IAGA Observatory Workshops, jointly organised by the National Geophysical Research Institute, Hyderabad and the Indian Institute of Geomagnetism, Mumbai, and held for the first time in India, at the Hyderabad Magnetic Observatory. This marked the occasion of its Golden Jubilee, and so the Workshop included a series of Special Sessions. It is wonderful to be able to recognise and celebrate the effort that goes into maintaining a high-quality, long-running geomagnetic observatory. Observatories, the data they record, and the careful calibration, processing and analysis that are performed on them are the 'backbone' of IAGA's science. Without them, we cannot produce our magnetic models such as the International Geomagnetic Reference Field, the indices that characterise the state and activity of the external magnetic field, the space weather forecasts and alerts that are becoming routinely issued by a number of agencies around the world, and we cannot undertake scientific research to understand and model the sources and generating mechanisms of the field, and the interaction between the various sources. In an increasingly technology-dependent world, where space weather has the potential to impact on societal well-being, the importance of our observatory network cannot be under-estimated. Those that run them are largely the 'unsung heroes' of our science, and with this Foreword, I would like to pay tribute to their commitment and dedication. Observatory Workshops are an opportunity for practitioners to come together, share best practice and new techniques, and spend some time in the company of others with the same professional interests. I know that the 16th Workshop was very successful and highly regarded by the participants, and I thank everyone involved in organising and running it.

Prof Kathy Whaler
Immediate past-President, IAGA

J. Ind. Geophys. Union (January 2016)
Special Volume-2/ 2016 pp: 9-18

WIDIF: A New DIFLUX Optimised for Field Use

J. Rasson, O. Hendrickx, J-L. Marin, F Humbled and Genzi Li[1]
Institut Royal Météorologique, Service Scientifique de l'IRM à Dourbes, B-5670 Viroinval, Belgium
jr@oma.be
[1]Beijing Aerospace Xinfeng Machinery Equipment Co., Ltd, No. 52 Yongding Road, Beijing, China

ABSTRACT
The project aims at solving the increasingly difficult problem of non-magnetic theodolite supply while at the same time providing the design a very compact DIflux electronics. Our design plans to integrate in one compact instrument the fluxgate sensor, electronics, a GPS receiver, clock, display and battery. Those elements should be made small enough to fit on the DIflux theodolite's telescope.

As all elements having a magnetic signature participate rigidly in transits with the telescope, their magnetic effects are compensated by the DIflux measurement protocol. In fact they are determined and eliminated as if they were part of the sensor magnetization.

The concept was tested on BOIF TDJ6E-NM nonmagnetic theodolites. It was tested in different magnetic observatories and repeat station conditions. Tests were carried out at different magnetic latitudes. They show a dependable behavior and the instrument is convenient in terms of use and transport.

The results of comparisons with classical DIfluxes are presented. The excellent absolute results demonstrate the validity of this new concept.

The TDJ6E-NM theodolite manufactured by the BOIF factory in Beijing, China in a nonmagnetic version was recently made available. We carried out extensive testing of metrological as well as magnetic properties on several units. The tests showed that the device is fully compatible with the requirements for a DIflux in an INTERMAGNET magnetic observatory.

Keywords: Geomagnetic measurement, Magnetic repeat station, Magnetic declination, Nonmagnetic, Diflux theodolite.

CONSIDERATIONS ABOUT THE DIFLUX

The DIflux is a relatively recent invention (*Tenani, 1941*). In the nineteen-seventies it has reached a level of maturity, thanks to the work of a number of colleagues (*Meyer and Voppel 1954, Serson and Hannaford 1956, Trigg 1970*). From 1971 Daniel Gilbert, Jacques Bitterly and Jean-Michel Cantin from IPG Paris continued the investigations and achieved a high level of precision so that it proved to be better in terms of accuracy, resolution and ease of use (*Bitterly et al. 1984*). Therefore the people in charge of making absolute geomagnetic measurements try to use it where ever possible and it is on its way to supplant other absolute geomagnetic measuring instruments, both in the observatory and in the field.

It is an instrument able to measure the value of the geomagnetic declination D and inclination I. The instrument consists of a non magnetic theodolite and a fluxgate sensor mounted on the telescope, so that optical and magnetic axes are parallel. The accuracy of a measurement with a DIflux depends on the accuracy of the theodolite and on its magnetic cleanliness. The accuracy of a theodolite can be measured by appropriate measurement techniques (*Deumlich 1980*) and the magnetic cleanliness can also be measured and improved so as to be below a given limit. Therefore we can put the DIflux in the class of the absolute instruments.

NON MAGNETIC THEODOLITE SUPPLY

We in the geomagnetic observatories are all concerned about the supply of nonmagnetic theodolites, an essential tool in our observation tasks. Concerns are of:

- Future availability,
- Rising costs,
- Decreasing quality.

Although we are producing the automatic Diflux AUTODIF, able to solve part of this supply problem, we realize that the manual DIflux will still be around for many years for reasons of cost, ease of use and portability. The present supply of nonmagnetic theodolites is based on discontinued units:

- ZEISS 010, 015 and 020
- Wild T16
- UOMZ 3T2KP.

These theodolites are mechanically demagnetized by exchanging the offending magnetic parts with nonmagnetic materials. Precision axles, screws, springs made of steel are replaced by aluminum, brass, and plastics.

NON MAGNETIC THEODOLITE QUALITY

Unfortunately, as our contacts with manufacturers and users of non-magnetic theodolites show, mechanical and

Figure 1. The TDJ6E from Beijing Optical Instrument Factory (BOIF). This instrument with a basic 6 arc seconds accuracy is available in a nonmagnetic version TDJ6E-NM

optical characteristics and specifications of the theodolites are degraded in the demagnetization process:

- Manufacturer 1 admits that their modified ZEISS are not as wear resistant as the original factory issue,
- Our use of Manufacturer 1 modified ZEISS has shown rather severe shortcomings: glass and metal parts loosen under vibration,
- Errors in eccentricity of graduated circles result in severe ambiguities for the reading of circles,
- A full calibration check of Manufacturer 1 modified ZEISS theodolites in a foreign optical workshop showed significantly degraded optical and accuracy specifications,
- In our experience, modified non-magnetic theodolites never come with detailed optical or metrological specifications.

We concluded: "There is a need for a quality, new-in-box, non-magnetic theodolite, available in quantity, obeying strict metrological, optical and non-magnetism specifications".

A COLLABORATION WITH BOIF

The Beijing Bofei Instrument Co., LTD (BOIF) in China is still able to produce the non-magnetic theodolites TDJ6E-NM (Figure 1). They were first demonstrated to us in the Kakioka IAGA workshop in 2004 by the staff of the Chinese Earthquake Administration (CEA). During the strict instrument testing sessions at this workshop, the TDJ6E-NM obtained good results in the DIflux intercomparison: systematic errors were below 3 arc seconds and the dispersion in the results were below 5 arc seconds in I and 6 arc seconds in D.

The decision was taken to approach BOIF to purchase a batch of their non-magnetic theodolites so that we could start the work on a new Diflux based on the BOIF instrument. During the next IAGA observatories workshop in Changchun, China in 2010 and with the help of the CEA, we met a BOIF engineer and had in depth discussions about their theodolites. As a result, the TDJ6E-nm model, 0.1 arc minute accuracy class device was selected for our project.

As can be seen in the specifications below, the TDJ6E is similar to the ZEISS-020, well known and used in the Observatory community.

DETAILED SPECIFICATIONS OF TDJ6E-NM

Setting the non-magnetism specifications

In our discussions with BOIF, we set the specifications for the overall non-magnetism of the theodolite. These are based but exceed the military specification STANAG 2897 (Ed. 3). This specification comprises two steps: idealization and magnetic signature testing. The specification calls for a magnetic signature after idealization below 1nT at a distance of 5 cm. The distance of 5cm is dictated by practical considerations so that the test can be carried out manually in front of a fluxgate sensor. Shorter distances would make the method too sensitive to distance errors and longer distances would be unrealistic compared to

Table 1. Results of the preproduction testing for non-magnetism.

	description	id1	id2	Magnetic Signature		
				as received	after idealization	
First_batch					@ 10mmm	@ 50 mm
a-1	telescope_tube	2A12	'2024	< 0.1 nT	< 0.1 nT	< 0.1 nT
a-2	mirror_support	2M2-M	ADC12	< 0.1 nT	0.4nT	< 0.1 nT
a-3	Brass_cup	CW4S2K	CuSM6	< 0.1 nT	0.3nT	< 0.1 nT
a-4	nut	NS105	Bzn15-20	< 0.1 nT	< 0.1 nT	< 0.1 nT
a-5	diagonal_eyepiece	2A12	-	< 0.1 nT	< 0.1 nT	< 0.1 nT
Second_batch						
b-1	bracket	nm-04-41		< 0.1 nT	< 0.1 nT	< 0.1 nT
b-2	cover_plate_left	nm-06-16A/B		< 0.1 nT	< 0.1 nT	< 0.1 nT
b-3	plummet_obj_mount	nm-08-01-		< 0.1 nT	0.6nT	0.1 nT
b-4	diopter_ring	nm-01-26		< 0.1 nT	< 0.1 nT	< 0.1 nT
b-5	levelling_knob	nm-02-6		< 0.1 nT	0.3nT	< 0.1 nT
b-6	horiz_axis	nm-04-33-0		< 0.1 nT	5nT	0.9nT

the distance between the Diflux fluxgate sensor and the theodolite 's alidade.

It is however difficult to relate the angular error on magnetic declination and inclination to the size of the magnetic signature because this depends on the magnetic latitude where the measurement is taken. The location of the magnetic pollution on the theodolite is also important to assess this relation: for instance a magnetic pollution located on the horizontal telescope axis is likely to be eliminated by the Diflux measurement protocol (*Gilbert & Rasson 1998*). On the other hand, magnetic pollution in the tribrach or in the lower part of the theodolite will for sure cause errors in the inclination.

For setting a specification for maximum magnetic signature we consider relationships linking the Diflux fluxgate measurements dD and dI in nanoTesla units with the angle readings δD and δI in degrees at mid-latitude, where H~20000nT and F ~50000nT:

$$\mathrm{atan}(dD/H) = \delta D \qquad \mathrm{atan}(dI/F) = \delta I \qquad (1)$$

The relations (1) give a value for dD=dI=1nT:

δD = 10 arc second,

δI = 4 arc second.

We believe this upper limit on the angular error level is adequate, given the angular accuracy specifications (see below). Moreover, these slight magnetic signature related effects bear mostly on δI (*Gilbert & Rasson 1998*).

TDJ6E-NM Theodolite specifications for non-magnetism

This specification is established as the result of a two steps approach: idealization procedure and magnetic signature measurement.

Idealization procedure

The idealization simulates the magnetic field environment to which the object under test will be subjected in its useful life. This environment is obviously both DC and AC fields. Therefore, the idealization magnetic field is the sum of:

- A DC field of 0.6 mT,
- An AC field (1Hz) starting at 6 mT decreasing to 0.2 mT, decrease occurring in steps not greater than 0.2 mT.

Magnetic signature measurement method

We use the Observatory DIflux in the Inclination measurement position in quiet field's conditions. We approach the object under test along the fluxgate axis until 5 cm from fluxgate. We then rotate randomly the object under test and record the max and min fluxgate readings. The magnetic signature M_s is defined as:

$$M_s = (\mathrm{max}-\mathrm{min})/2$$

Preproduction magnetic signature testing of theodolite parts

In order to strictly respect the non-magnetism specifications, BOIF sent us batches of theodolite parts for testing (Figure 2) of their non-magnetism.

We give in Table 1 the results of the magnetic signature testing both before and after idealization. It is noteworthy that the parts indeed get a detectable magnetic signature after the idealization procedure while they were all delivered with signature levels below 0.1nT. Item b-6 almost fails the test and was corrected by BOIF at production.

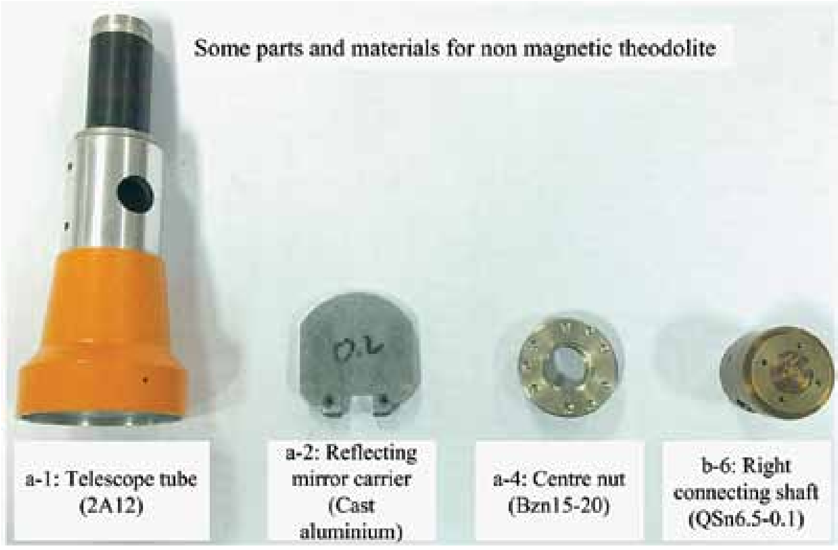

Figure 2. Theodolite parts from the TDJ6E-NM delivered for preproduction testing of the non-magnetism in Dourbes. See Table 1 for the results

TDJ6E-NM Theodolite specifications: operational, environmental, mechanical, metrological and optical

- Temperature operating range -20 to +50°C
- Ingress Protection rating: IP54
- Diameter of the horizontal circle: 94mm
- Diameter of the vertical circle: 76mm
- Circle graduation accuracy to ISO 17123-3 :±6 arc second or better for Vertical and Horizontal angular circles
- Reading microscope magnification Horizontal circle: 68x
- Reading microscope magnification Vertical circle: 65.4x
- Reading microscope image: erected, also with the diagonal eyepiece
- Color coded microscope reading field; simultaneous vertical and horizontal angle reading
- Telescope image: erected, also with the diagonal eyepiece
- Telescope magnification: 30x
- Optical plummet image (not erected) range of focusing: 0.5 - ∞ m
- Optical plummet magnification: 3x
- Optical plummet field of view: 5 degrees
- Tubular spirit level of the alidade tilt sensitivity: 30 arc seconds = 2mm
- Automatic vertical circle index accuracy: better than 1 arc second
- Automatic vertical circle index compensation working range: +/-2 arc minute
- Possibility to lock the automatic vertical circle index pendulum
- Height of horizontal axis: 207mm
- Dimensions: 286x163x130mm
- Weight: 4.3 kg

SPECIFICATION VERIFICATION IN DOURBES

As a sizeable batch of theodolites was purchased, it was decided to test the specifications of 8 randomly chosen units from the delivery. The tests concerned non-magnetism and angular accuracy specifications. The ISO 17123-3 standard was used for graduation accuracy test of the horizontal and vertical graduated circles.

Postproduction specifications testing: angular accuracy

A special pillar was set-up with 5 targets well distributed in azimuth for the horizontal circle test. Also the pillar was installed in front of a tall object (ionospheric sounder antenna) so that 4 targets covering 30° on the vertical circle were visible (Figure 3).

The results of this testing are given in Table 2. All theodolites passed the test since the results are within +/-6 arc seconds.

Postproduction specifications testing: magnetic signature after idealization

We used a large solenoid in order to apply the AC and DC magnetic fields required for the idealization (Figure 4). The observatory Diflux was used for the magnetic signature measurements.

We tested separately the theodolite, the tribrach and the two diagonal eyepieces (coudés). The results are presented in Table 3. All the theodolites under test passed.

Figure 3. Special set-up for testing the circle graduation accuracy according to the ISO 17123-3 standard

Figure 4. Our set-up for idealization. The reading on the teslameter is in Gauss.

Table 2. Final results of the 8 different TDJ6E-NM theodolites angular accuracy test.

Angular Accuracy ["] of Theodolites – summary of results

Theodolite reference #:	001	007	021	023	031	034	044	050
Horizontal Circle	4	4	4	4	6	4	6	5
Vertical Circle	2	4	4	2	3	4	1	2

Table 3. Magnetic signature of the theodolite elements in nT @ 5 cm. Coudé = Diagonal eyepiece.

Magnetic Signature [nT] after idealization – summary of results

Theodolite #:	001	007	021	023	031	034	044	050
Theo [A]	**0,2**	**0,4**	**0,0**	**0,3**	**0,2**	**0,4**	**0,1**	**0,2**
Tribrach [B]	**0,4**	**0,3**	**0,1**	**0,2**	**0,2**	**0,3**	**0,2**	**0,2**
Coudé ocular [C]	**0,0**	**0,0**	**0,0**	**0,0**	**0,0**	**0,0**	**0,0**	**0,0**
Coudé µscope [D]	**0,0**	**0,0**	**0,0**	**0,0**	**0,0**	**0,0**	**0,0**	**0,0**

Figure 5. The WIDIF Diflux as a combination of the TDJ6E-NM and the blue magnetometer console, mounted on the telescope. The console also comprises a GPS receiver, a clock, a battery and three LCD displays, one of them being visible here. Note also the second under plate, allowing using pillars fitted with 120° v-grooves.

THE WIRELESS DIFLUX (WIDIF) AND FLM4/A

The Wireless DIflux WIDIF is based on the TDJ6E-NM theodolite. The projected new Diflux is designed so as to mount the fluxgate sensor and the complete electronic console on the telescope (Figure 5). WIDIF is a compact DIflux magnetometer: the fluxgate sensor, fluxgate electronics, a GPS receiver, clock, several displays and a battery are kept small enough to fit onto the telescope. In that way we do not need a wired connection between the theodolite bearing the fluxgate sensor and the electronics console. We indeed do away with the cable joining the theodolite and the console.

How is it possible to get good measurements with the electronic console (which has a non-zero magnetic signature) so close to the fluxgate sensor? Elements with magnetic signature participate rigidly in all transits with the telescope: they are determined and eliminated as if they were part of the sensor magnetization error. So their magnetic effects are compensated by the DIflux measurement protocol just as the sensor magnetization error (*Gilbert and Rasson 1998*).

Widif electronics for a BOIF TDJ6E-nm theodolite is mainly intended for repeat station work. More conservatively, the FLM4/A electronics console connected by a wire to the theodolite is also available, mainly for Observatory work or when a backlit display is necessary (measurements at night), see Figure 10. Whatever the console execution, the theodolite electronics console consists of:

- 0.1 nT resolution fluxgate magnetometer with a LDC-20A Pandect fluxgate sensor
- GPS receiver disciplining a clock and able to indicate the Latitude and Longitude
- Circuitry to electronically trim of the sensor magnetization error
- A lithium polymer battery for powering the console during up to 6 h.

Outstanding features of the electronic console

The electronics package has been kept small so that it can fit in the tight space available on the telescope of the theodolite. It is necessary to leave all the telescope (focus and ocular) and theodolite controls readily accessible while maintaining the possibility to allow 360° transits and rotations of the telescope. It is also desirable to keep the centre of gravity of the telescope assembly on the horizontal and vertical rotation axes, so that the telescope keeps its position when released. As the instrument is to be deployed for fieldwork mainly, a quasi waterproof and mechanical protection is provided to the console.

Another key operational property resides in the fact that it must keep a constant magnetic signature over the course of a full DIflux measurement protocol of the declination and inclination. Besides it must provide access and view to the measured values whatever the position of the telescope is. Practically this means that 3 different

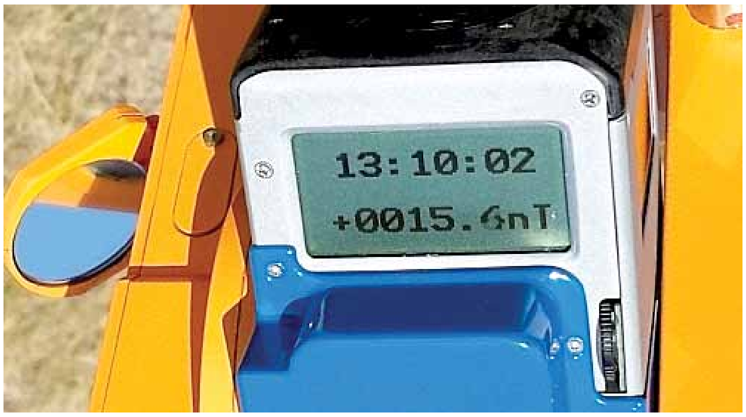

Figure 6. The WIDIF display during a measurement session. The display will change its orientation to fit the telescope position.

Figure 7. Measurement menu of the WIDIF at switch-on. Note the rocker switch (upper right) allowing to navigate the menu. It is extremely soft to activate and when idle, remains in the same position so as to keep the magnetic signature unchanged.

digital LCD displays are set-up around the telescope. Moreover the writing on the displays must always appear left-to-right and head up, so an automatic orientation of the displays must take place, controlled by a gravity sensing device on the telescope.

As several measurement menus are programmed in the console, a switch is provided for the operator to select between the different functions. Activating this switch should not disturb the measurement in any way, so it must be very soft to activate and not modify the magnetic signature. Finally, since the battery size is limited due to available space, the electronics design should ensure very low-power operation and save any microwatt where possible.

TESTING

Tests carried out in Dourbes

In order to test the finished WIDIF, intercomparison tests were carried out in our Dourbes magnetic observatory. We used the standard procedure of measuring the baseline of a variometer on the same pillar using

- The reference observatory Diflux,
- The WIDIF under test.

The tests in Dourbes involved a ZEISS010 with DImag88 electronics from EOPG, France. The WIDIF and ZEISS intercomparison was performed for a period of 90 days in the year 2014. The variometer is a LAMA fluxgate triaxial device installed in DFI orientation. Therefore D and I baselines can be computed without involving any other instrument.

Concerning the Declination D baselines, the agreement between the two is within 0.001° as shown by the black (WIDIF) and orange (ZEISS) fitted baselines. This level of agreement is quite satisfactory, as the angle reading resolution of the WIDIF is 0.0016° (0.1 arc minute), see Figure 8.

Concerning the Inclination I baselines, the agreement between the two is initially within 0.002° and tapering off to 0.001° and less at the end of the comparison session. This level of agreement is also quite satisfactory, as the vertical angle reading resolution of the WIDIF is 0.0016° (0.1 arc minute) albeit with less magnification as for the horizontal circle, see Figure 9.

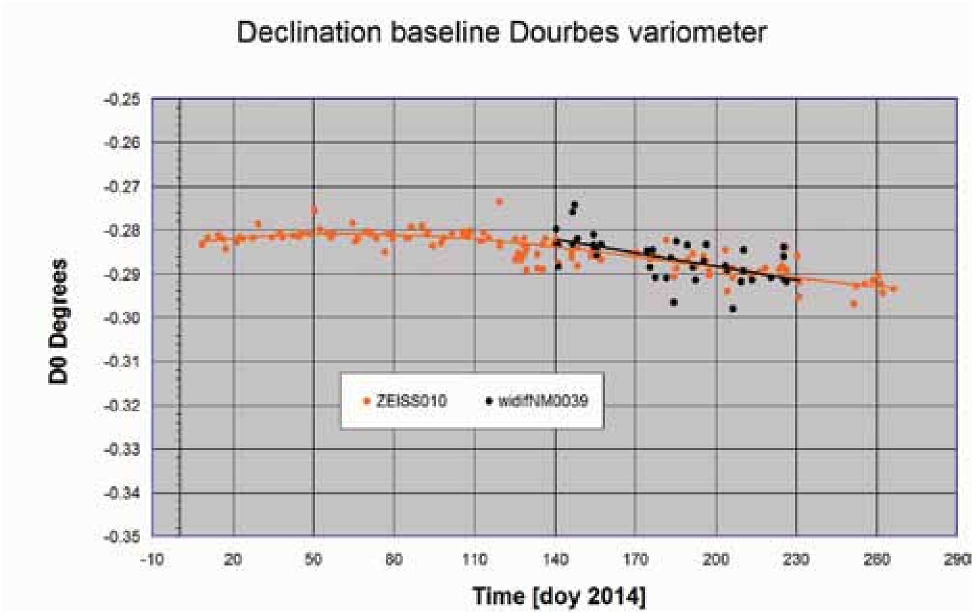

Figure 8. Declination baseline of the LAMA DFI variometer as measured by the ZEIS010 and WIDIF DIfluxes.

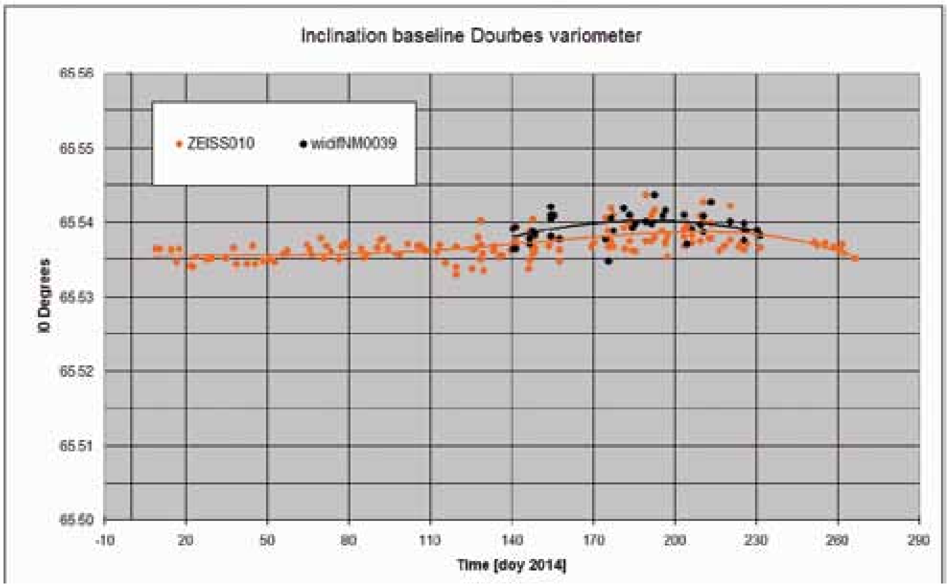

Figure 9. Inclination baseline of the LAMA DFI variometer as measured by the ZEIS010 and WIDIF DIfluxes.

Testing under different magnetic and illumination conditions

We gathered extensive experience of using the WIDIF for fieldwork and in the process, tried to improve the device. For instance, several modifications in the display interface were introduced as a result of the feedback from the field operators.

In general, the WIDIF proved to be very handy in the field. The GPS receiver providing accurate timing and geographical coordinates on the spot is very useful in repeat station work and when an astronomical geographic North determination has to be made (e.g. sun shot). We also had the opportunity to use the WIDIF for airport compass rose certification (Brussels airport) and for runway azimuth determination (Liège Airport) and appreciated its compact and lightweight construction. For compass rose work, about 20% less time was necessary to complete the job. One has to get used to the pendulum clamp however, which is activated for transport of the instrument. One should not forget to unclamp the pendulum before making readings on the vertical circle, as otherwise the automatic vertical circle index will be giving erroneous readings.

Figure 10. The FLM4/A DIflux electronics. This has the same functionalities as the WIDIF.

Table 4. The different observatories where the WIDIF was test

Observatory	Geomagnetic Inclination
Sodankyla, Finland	77°
Chambon-la-Forêt, France	64°
Sonmiani, Pakistan	38°
Chouttupal, India	24°
Trelew, Argentina	-43°

The reading of the WIDIF displays is easy and at all time convenient. Enough light must be available however, as the displays are reflective. For low light levels we recommend using the FLM4/A, which has a backlit display. In order to make sure the WIDIF Diflux is operational on the whole Earth, we carried out measurements in a variety of magnetic observatories, looking to get a high span of geomagnetic inclinations in the process. These observatories with their inclination values are listed in Table 4.

The WIDIF proved to be fully functional at those places. One of the 3 LCD displays would always be visible for zeroing the fluxgate output during the Diflux measurement protocol. The diagonal eyepiece was necessary to read the microscope in Chouttupal and Sonmiani, because the telescope is then in too steep a position to look directly in its ocular.

DETAILED SPECIFICATIONS OF WIDIF AND FLM4/A MAGNETOMETER CONSOLES

WIDIF fluxgate sensor & electronics specifications

Analog filtering of fluxgate output: Second order low-pass filter with 3 dB cut-off at 10Hz
Sampling frequency of the fluxgate signal: 30 Hz
Digital filtering of fluxgate signal: Box-car average over 900 ms
Displaying rate of fluxgate output: 5 Hz
Scale value accuracy: 1%
Range: +/-600nT
Automatic fluxgate sensor magnetization suppression with manual fine tuning.
Fluxgate sensor magnetization suppression range: +/-600nT

Battery life: 6 h including 1 GPS fix
Battery charging time: 2 h
LCD display technology: reflective

Version with wire FLM4/A:

This magnetometer console may also be used on the ZEISS 020/015/010 series of theodolites. It has the same functionalities as for WIDIF but plus:

- Larger battery
- Back-lit display
- Hi-reliability LEMO connector

The electronics console fits in the standard ZEISS theodolite boxes.

Ancillary devices

Lithium polymer battery charger
90° eye-pieces for microscope and ocular(non-magnetic, erect view)
Non-magnetic tools
120° V-groove under plate
Non-magnetic tripod
Sun shot filter
Operation manual

ACKNOWLEDGEMENTS

We thank the many colleagues who helped in the design and testing of the WIDIF: Pascal Jamme, Sebastian Pelliciuoli, Tero Raita, Benoît Heumez, Kader Telali, Kusumita Arora, Madeeha Ashfaque and Ayyaz Ameen. Dongmei Yang kindly connected us with BOIF.

REFERENCES

Bitterly, J., Cantin, J.M., Schlich, R., Folques, J. et Gilbert, D. 1984. Portable magnetometer theodolite with fluxgate sensor for earth's magnetic field component measurements, Geophysical Surveys v.6 p233-239.

Deumlich, F. 1980. Instrumentenkunde der Vermessungstechnik, VEB Verlag für Bauwesen, Berlin 1980.

Gilbert, D. and Rasson J.L., 1998. Effect on DIflux Measuring Accuracy due to a Magnet located on it, Proceedings of the VIIth Workshop on Geomagnetic Observatory Instruments, Data Acquisition and Processing, Scientific Technical Report STR98/21, pp168-171, Geo Forschungs Zentrum Potsdam.

Meyer, O. and Voppel, D. 1954. Ein Theodolit zur Messung des Erdmagnetischen Feldes mit der Förstersonde als Nullindicator, Deutsche Hydrographische Zeitschrift, v.12 p73-77.

Serson, P.H. and Hannaford, W.L.W., 1956. A portable electrical magnetometer, Canadian Journal of Technology, v.34 p232-243.

Tenani, M., 1941. Nuovo Metodo di misura della declinazione e della inclinazione magnetica, La ricerca scientifica, v. 20, p1135-1140.

Trigg, D.F. 1970. A portable D and I magnetometer, Geomagnetic Laboratory Report n°70-3, Direction de la Physique du Globe, Energie, Mines et Ressources, Ottawa, Canada.

J. Ind. Geophys. Union (January 2016)
Special Volume-2/ 2016 pp: 19-23

Monitoring of Long Term Mechanical Stability of a Suspended dIdD Sensor applying Optical Observation

László Hegymegi[1] , András Csontos[2], László Merényi[3]
[1] Mingeo Ltd., H-1142 Budapest, Ráskai Lea u. 20, Hungary,
hegymegi@mingeo.com
[2] Geological and Geophysical Institute of Hungary, Tihany Geophysical Observatory, H-8237 Tihany, Kossuth utca 91,
csontos.andras@mfgi.hu
[3] Geological and Geophysical Institute of Hungary, H-1143 Budapest, Stefánia utca 14,
merenyi.laszlo@mfgi.hu

ABSTRACT

Automatic geomagnetic measuring systems need additional solutions to monitor the variation of the reference frame of the sensor. Reference frame of a vector magnetometer is defined physically by the true direction of sensor's axes. Several methods have already been developed for establishing the correct adjustment of the sensor. Published methods were suitable to align the sensor but continuous monitoring of the reference frame was not ensured especially for declination measurement without an independent reference magnetometer. Introduction of the so called MGEN device to measure optical angle variation between the suspended dIdD sensor and an independent telescope is a new promising improvement. MGEN device was originally designed for astronomical monitoring purposes, but with some modifications it can be used to monitor small movements and rotation of nearby objects like magnetometer sensors. Our paper presents the device and the first long term results of the measurements.

Keywords: Reference frame, Optical monitoring, DIdD, Baseline.

INTRODUCTION

Several methods were developed to help the installation of magnetometers (necessary to add couple of references). Different types of magnetometers need different procedures to find the perfect orientation of the sensor. The user manuals give usually good instructions for the observers how to perform the installation. The manufacturers of magnetometers often provide certificate of the calibration too. However, after setting up the device the tilt of the pillar or variation of the temperature can modify the originally developed reference frame of the sensor. Suspension of the sensor can eliminate the tilt of the device but torsion of the system still can happen despite of the applied suspension. Unfortunately, different sources of errors (i.e. mechanical instabilities, temperature effect on the device, voltage dependence of electronics etc.) appear simultaneously. There are no general solutions to separate these errors and to correct the dataset afterwards. Usually, the observers summarise these errors as the variation of the baseline.

If we could independently monitor the mechanical variation of a sensor then we would have a better chance to identify the main reason of a baseline drift. This idea is more realistic if our device is essentially free from a few possible calibration errors.

From this point of view the advances of dIdD instrument become even more important:

Since the dIdD system is based on a nuclear magnetometer, this instrument can be qualified based on parameters of the nuclear magnetometers, i.e. accuracy, sampling interval etc. It also follows, that the scale factor and the offset do not need to be calibrated.

Only the following four values have to be calibrated for the determination of the reference frame of the device:

i.) I_0 value (I baseline),
ii.) D_0 value (D baseline),
iii.) orthogonality error of magnetic axes,
iiii.) the levelling error of the D coil axis.

By summarising above points, one can conclude that the dIdD reference frame is defined physically by the D coil and I coil axes. They should be orthogonal and the D coil should be horizontal, in the case of perfect alignment of the sensor.

The dIdD instrument provides good baseline stability. If we assume that the magnetic axes of the sensor is determined only by the mechanical position of the coil system then we should only monitor the coil's direction in the geographic reference frame and the orthogonality of the coil system.

The direct measurement of the orthogonality is resolved by current switching between the coils (*Heilig 2012*). Similar solution can be used for I baseline and for levelling of the D coil axes by applying suspended turning coil (*Hegymegi 2012*).

In order to have good information about the variation of declination baseline, the Lacerta MGEN autoguider optical device was incorporated into the system, to monitor the position of the sensor in horizontal plane. For this

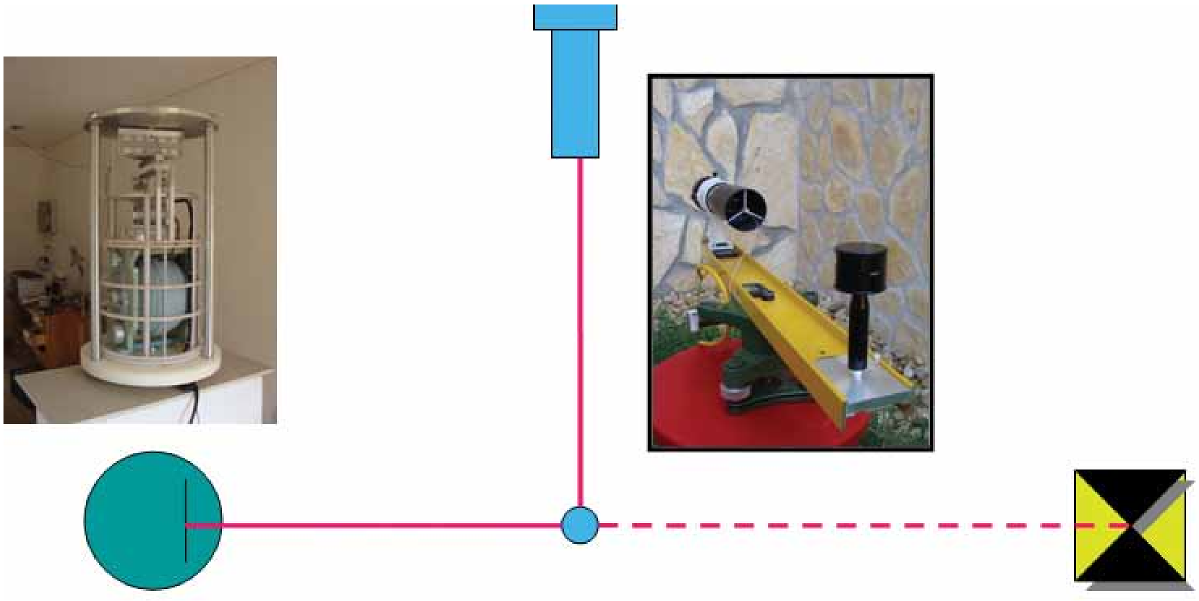

Figure 1. The configuration of the optical monitoring system

monitoring a reference point is required at a certain distance from the sensor. When we designed this system, our main goal was that the measurement resolution should be high enough if using in-the-room reference, or external reference (for example a point equipped with a GPS) at a bigger distance.

THE OPTICAL UNIT AND THE MEASURING SYSTEM CONFIGURATION

The Lacerta MGEN device was originally designed for astronomical applications. In order to use it for our tasks we needed to modify the unit.

Theoretically the D baseline of the dIdD is equal to the angle, which is measured between the true North and the plane perpendicular to D coil axes. In the observatory practice we need to measure only the variation of this direction if we have a chance to calibrate this value from time to time. If we attach a mirror on the suspended part of the dIdD sensor we can measure this variation directly. In this case it is enough to monitor the position of the light, which is reflected by the mirror.

In our test configuration the light is emitted by a small LED from the centre of the telescope. A prism turns the direction of the light at right angle to the mirror of dIdD sensor. The way of the light is practically the same back to the telescope (Figure 1.).

The MGEN device continuously calculates the centre of the light beam in the camera as X/Y sub-pixel values, and sends these horizontal and vertical coordinates to the data logger in 0.001 pixel-point resolution. This set-up is able to monitor the mutual positions of the camera and the mirror with very high resolution.

Technical specification of the camera:

CCD size	752x582 pixel
	2.7x3.65 mm
Depth	8 bit
Reading velocity	2 Mpixel/sec
Power consumption	
w. electronics	12 V DC
	max 200 mA
Operating temp.	-10 to +60 °C

A double prism system applied, where one prism directs the light to the mirror of the instrument and the other to the remote mirror. By screening one or the other the camera can measure the two angles.

In Tihany Observatory the calibration of the MGEN output is possible with absolute measurements on the absolute pier of the observatory. Therefore external reference mark was not used.

CALIBRATION OF MGEN DEVICE

Other question is the scale factor and the linearity of the MGEN device. In order to determine these parameters a calibration procedure was performed in Tihany Observatory (THY). The suspended sensor of dIdD was rotated along its vertical axis with several minutes of arc. After measuring for five minutes in the new position, rotation was performed again, and this cycle was repeated several times. The MGEN device recorded the actual values of rotation during the test. The true angle of rotation was calculated as a difference between the standard observatory declination data and the actual declination record of dIdD. The result of comparison of the two independent measurements shows that the linearity of MGEN device is good in the whole

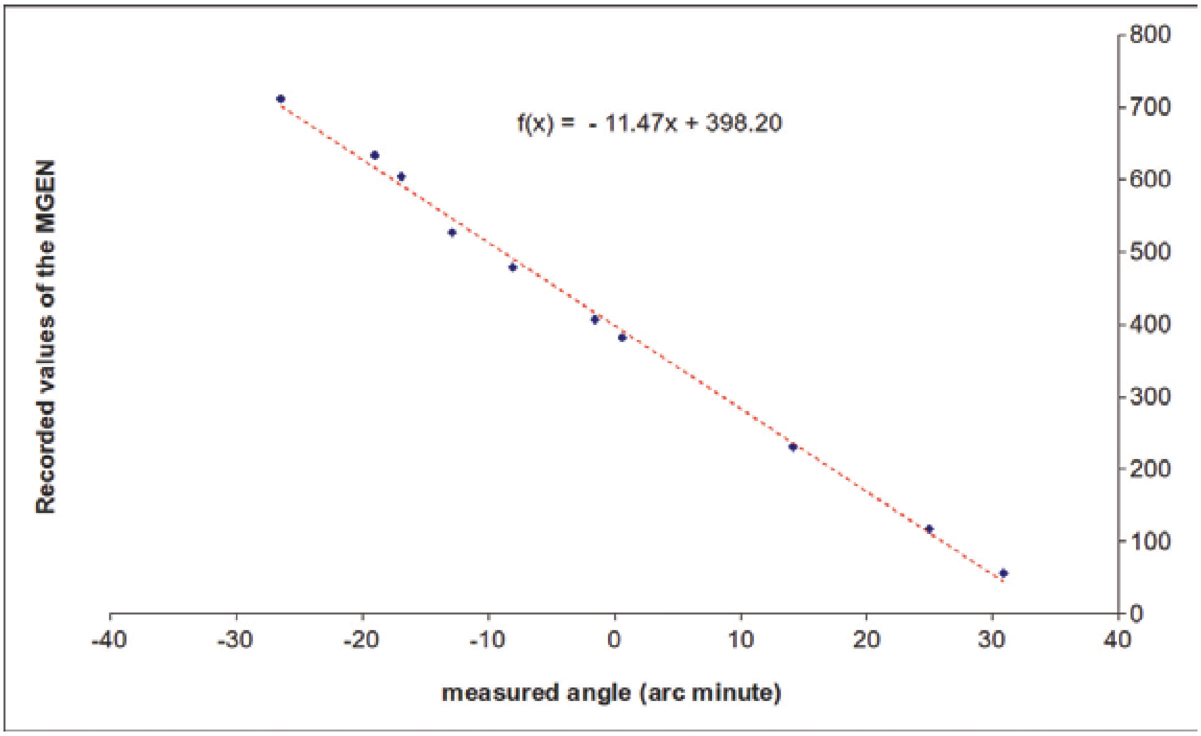

Figure 2. The result of the calibration of the MGEN scale factor

range i.e. 0-800 pixels (Figure 2.). The distance between the camera and the dIdD sensor was about 2.5 meters. The result of this measurement shows also that one pixel variation in MGEN corresponds to 5.23 arc second rotation of the dIdD sensor. The noise level of the system 0.03 pixels peak to peak gives about 0.16 arc second resolution.

The residuals of the procedure were processed too. The maximal values of the residuals did not exceed the range of 13 pixels. The residuals may come from the optical error of the telescope or the mirror.

LONG TERM dIdD BASELINE STUDY WITH MGEN

In order to test the utility of D baseline monitoring, we performed a long term measurement in THY from, during 16.08.2013 to 28.11.2013. The dIdD device was installed in the old variation house of the observatory. The declination baseline of the dIdD was monitored in two independent ways. We compared the output of the dIdD with the definite data of THY and with the MGEN record too. The temperature of the room was also recorded at two points with 0.001 °C resolution.

The variations of D baseline are presented with the temperature and the MGEN record (Figure 3). We used minute mean values for this study.

In this paper we analyse only the declination measurements of the instruments. Earlier studies (*Csontos 2012*) presented that the declination output of dIdD mainly depends on the direction of D axis (D_0 value). We found that the inclination base of the device was stable within 10 arc seconds during the study. The attenuated variation of the inclination base brings out rate of stability. We have noticed that the orthogonality of the coils, the horizontality of the D axis and especially the I_0 value were very stable during our test. As a consequence we can be sure that the variation of the declination base essentially indicates the variation of the D_0 value.

The declination baseline of dIdD device varied more than 40 arc seconds in the studied period. The MGEN record in horizontal plane shows about 25 arc seconds variation. The variation of the temperature does not show strong correlation with declination baseline. The MGEN record of horizontal rotation is more or less similar to temperature variation. This indicates a temperature effect on the mutual position of the devices or on the MGEN measuring system only.

A close observation of varied activity during entire test period helps in better evaluation of correlation between the dIdD baseline and the measured temperature. The close observation revealed that mechanical variations seem to be low. However, if we observe the curves from about day

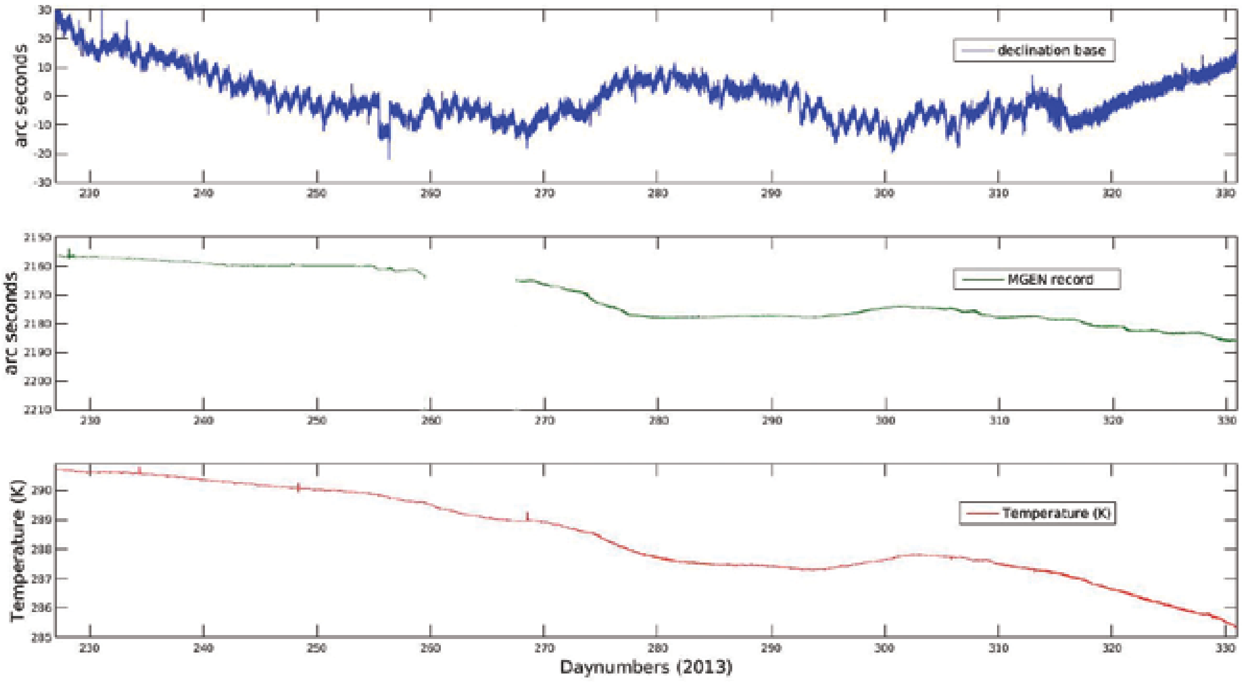

Figure 3. Difference values between the definite THY declination variation and the corresponding dIdD output, MGEN record of horizontal rotation and the temperature record

number of 270, then a better correlation (but with negative sign) can be realized.

Further tests are required to find out the reason of this experience.

FURTHER MECHANICAL EFFECTS IN THE DATASET

The appearance of "beginning drift"

After the installation of a magnetometer one usually notices appearance of a baseline drift. This drift is usually significant and its characteristic is exponential. During several tests we found similar effect in the MGEN record too. The device presented two minutes drift during two weeks, even though temperature was stable during this test. This experience shows that mechanical reasons of the "beginning drift" can be significant.

Earthquakes in the record

Several earthquakes (5 and 3 ML were the typical magnitude) occurred in Hungary in the period of the long term test. The centre of the earthquakes were about 200 km away from THY. The seismograms from a nearby Tihany seismograph station were available. The MGEN records during period of earthquakes were always disturbed. The amplitude of the MGEN "noise" always related to the seismograms from Tihany station.

CONCLUSIONS

We developed and tested a new optical device (MGEN) for geomagnetic monitoring purposes. The instrument measures the mutual direction of the camera and the target device. We found that the MGEN provides perfect stability for observatory tasks. The linearity and the resolution of the instrument are also good. The long term test shows that this monitoring system is also sensitive to the temperature variations.

In our first long term test we found that the expected correlation between the dIdD declination baseline and the measured temperature and mechanical variations is not always obvious. Probably the variation of the D_0 value is caused by different reasons not only the mechanical instability.

However, the observed mechanical effects i.e. "beginning drift" and the disturbances in the MGEN record during the time of the earthquakes show that the device is really efficient for the tasks.

This instrument can be a candidate solution of automatic observatories for monitoring the mechanical stability of the sensors.

REFERENCES:

Csontos A., D. Sugar, M. Brkić, P. Kovács, L. Hegymegi, 2012. How to control a temporary DIDD based observatory in the field? Special issue of "Annals of Geophysics" on 5th MagNetE Worksphop on European Geomagnetic Station Survey, Rome, Italy pp. 1085.-1094.

Hegymegi L., A. Csontos, B. Heilig, 2012. Results of the development of automatic baseline controlling DIDD (ABCD) magnetometer. XVth IAGA Workshop on Geomagnetic Observatory Instruments, Data Acquisition and Processing, June 4. – 14, Royal Institute and Observatory of the Spanish Navy San Fernando, Cádiz, Spain. (oral presentation)

Heilig B., 2012. Determining the orthogonality error of coil systems by means of a scalar magnetometer: application to delta inclination-delta declination (dIdD) magnetometers, Measurement Science and Technology. 23, 37001, doi: 10.1088/0957-0233/23/3/037001 (IF: 1.494 (2011), IC: 0, C: 0).

J. Ind. Geophys. Union (January 2016)
Special Volume-2/ 2016 pp: 24-29

Hardware Developments to Determine the Transfer Function of a 1-Second Fluxgate Magnetometer

A. Swan [(1)], T. Shanahan[(1)], C. Turbitt [(1)], J. Rasson[(2)]

[(1)] British Geological Survey, United Kingdom,
apsw@bgs.ac.uk
[(2)] Institut Royal Météorologique, Belgium,
jr@oma.be

ABSTRACT

With the introduction of the INTERMAGNET standard for 1-second magnetic data and the development of new fluxgate magnetometers to meet this standard, it has become increasingly necessary to ascertain the transfer function of magnetometer systems.

Here we describe a black box test device developed by the British Geological Survey (BGS), which is based on a principle devised by the Institut Royal Météorologique (IRM), used to determine the timing accuracy, amplitude and phase response of a fluxgate magnetometer. This device was used to evaluate two commonly used systems deployed within INTERMAGNET observatories; the DTU FGE for 1-minute data and the 1-second standard Lemi-025. Here we also describe tests carried out to determine the noise characteristics of these magnetometers.

The test methodologies and results are presented, alongside previously presented timing measurements for comparison and validation of the test device.

Keywords: Magnetometer, Transfer-function, Timing, 1s- standard.

INTRODUCTION

Now that the specifications for INTERMAGNET 1-second data have been defined and manufacturers are releasing products that claim to meet this standard, it has become increasingly important for INTERMAGNET Observatories (IMOs) to independently ascertain the transfer function of their instrumentation and to not solely rely on the manufacturer's claims.

To aid IMOs in this, BGS has designed and constructed a simple to use calibration device that can be used by non-technical staff and without the need for any specialist external equipment. The device is designed to be used in conjunction with a Helmholtz coil and to make use of the linear least squares parameter estimation method developed by IRM (*Rasson, 2008, 2009*) by outputting an accurately time-stamped periodic signal, or by outputting a time-stamped step signal, a Fast Fourier Transform (FFT) tool can be used to analyse the impulse response of the system.

DEVICE SPECIFICATIONS

To accurately test the timing characteristics of a 1-second standard fluxgate magnetometer the absolute time accuracy relative to UTC of any used calibration device must be of an order of magnitude above the 10ms time-stamp accuracy laid down by the INTERMAGNET 1-second standard. To achieve such accuracy the device designed by BGS utilises the 1 Pulse-Per-Second (1PPS) TTL output from a Garmin 18LVC GPS receiver in conjunction with a PIC18F45K20 8-bit embedded microcontroller to give a measured timing-accuracy of less than 1μs for any output signal.

The external Helmholtz coil with inductance (~2 mH) and resistance (~74 ohms) is designed to easily fit over any fluxgate magnetometer sensor without perturbing the setup and has a measured time-constant of less than 30μs with a -3dB point of 5.9kHz with a scale value of 448nT/mA. The combined time-delay and time-constant of the calibration device and Helmholtz coil is easily an order of magnitude above the 1ms requirement of a 1-second magnetometer calibration test system.

The embedded microcontroller controls all functions of the calibration device: it reads in and stores the NMEA string from the GPS in a temporary buffer; it constantly monitors for the 1PPS and derives its timing accuracy from this; it controls a 20x4 Hitachi LCD to display time/date and user input information; it drives the output signal to the coil with an adjustable amplitude between 15mV & 500mV, corresponding to an applied field of between 90nT & 3000nT; it inputs user parameters by means of push-button switches.

The device has an internal 12V battery, whose voltage is displayed on the LCD and can also be run from a 12Vdc external power supply. A green LED indicates the presence of the 1PPS and flashes every second when the GPS is acquired. A blue LED indicates the on/off state of the output voltage.

The calibration device can be used to either output a periodic square wave with period, amplitude, start date/time and number of cycles selected by the user, or can be

Figure 1. Calibration Device

used in step-function mode, where the user can select the amplitude and start & finish date/time.

Whilst in output mode, the device will constantly check for the presence of the 1PPs and, if lost will terminate the test run, displaying an error message with the number of test cycles completed (in periodic mode), or the finish time in step mode.

The time, date and acquisition status of the GPS are constantly displayed on the LCD and an error message is displayed if the GPS is disconnected or if no valid GPS signal has been acquired.

TIMING TESTS

To validate correct operation of the device, tests were carried out on two commonly used fluxgate magnetometers in IMOs (the DTU FGE-K and the Lemi-025), using two differing techniques; FFT analysis of the system impulse (*Shanahan, 2009*) and least squares parameter estimation of a periodic signal (*Rasson, 2008, 2009*).

A 24-bit Earthdata PS6-24 seismic digitiser, sampling at 200Hz was used in conjunction with the calibration device in step response mode with an applied step size of 100nT to determine the phase and amplitude response of the FGE-K fluxgate magnetometer by using the impulse response method. The FGE-K was tested with and without the RC low pass filter (LPF) on the output stage.
Figures 2 & 3 show the phase and amplitude response, which compare favourably with the results carried out by Shanahan using a FGE-J fluxgate electronics and Guralp DM24 digitiser, again showing that with the removal of the RC filter the group-delay remains constant and linear within the pass band range.

Note the presence of 50Hz mains signal in the response, highlighting the need for adequate anti-aliasing filtering to ensure that this signal is not folded back into the pass band range.

The impulse method was not used to analyse the Lemi-025 as the magnetometer acquisition system digitises the signal and outputs at too low a sample rate (10Hz & 1Hz).

In total four time series tests were carried out on the DTU FGE-K and Lemi-025 magnetometers as per the Rasson method at periods of 4, 8, 16 & 32 seconds to determine the timing and amplitude responses, with the results presented in Figures 4 & 5 and Table 1.

Results for the FGE-K fluxgate correlated with those of the impulse test shown in Figures 2 & 3. The Lemi-025 tests indicate that the group-delay and amplitude response for all tested time periods meets the INTERMAGNET 1-second standard (10ms and -3dB).

NOISE TESTS

To quantify the instrument noise of the two fluxgate magnetometers, each type was tested in turn in a near zero magnetic field for four hours within a custom built mu-metal shield with a specified external signal attenuation of 114dB, shown in Figure 6.

Each magnetometer was configured to output at 1 sample per second. The Lemi-025 was tested as the complete delivered unit, with its own custom built 24-bit digitiser. The ADC used for testing the FGE-K fluxgate noise was an Earthdata 24-bit digitiser designed for seismic applications. The ADC is a delta-sigma modulator with a dynamic range of over 150dB, primary sample rate of 192 kHz and consists of a Finite Impulse Response (FIR) digital filter with an out-of-band attenuation of 120dB.

The Noise Power Spectral Density (NPSD) is calculated using the Welch-Periodogram method used by Shanahan (2009). A total of 14, 2048 point sections were averaged with Bartlett windowing applied. The Discrete Fourier Transform (DFT) was then produced using the FFT algorithm with the negative frequencies folded into the spectrum to obtain the total noise power.

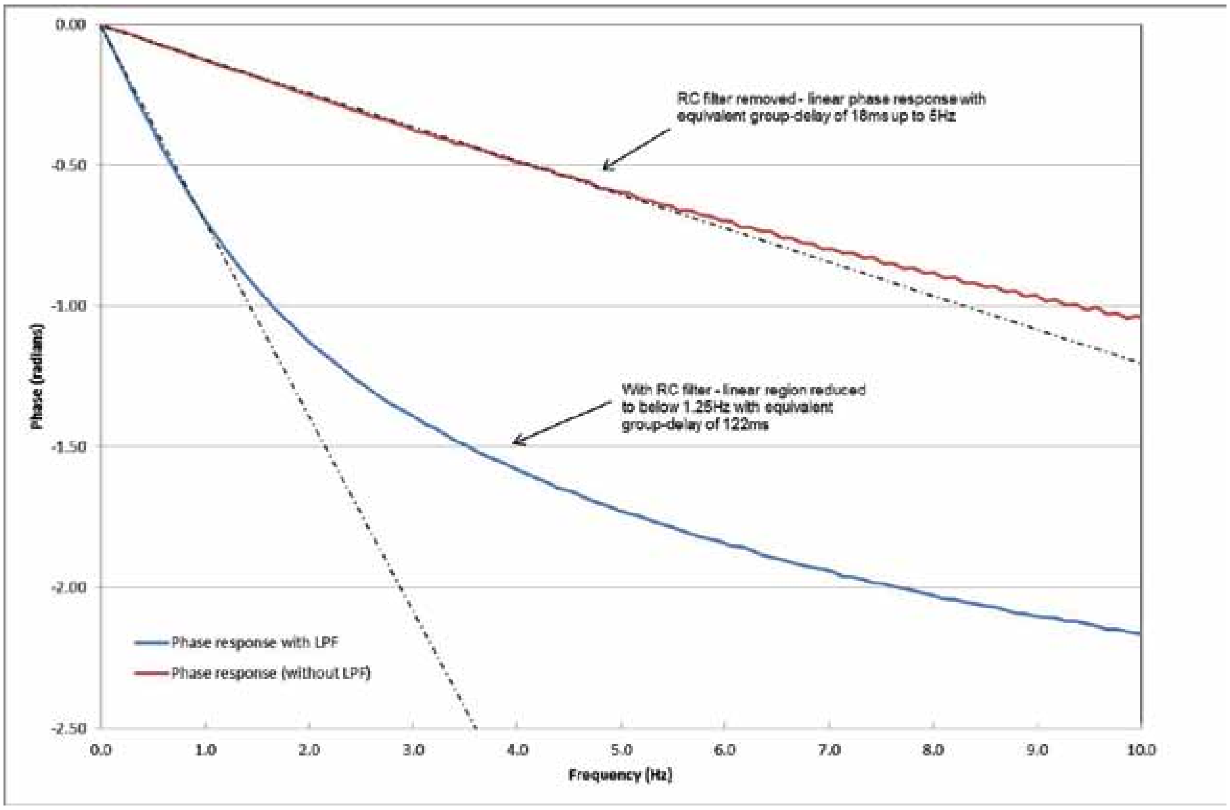

Figure 2. Phase Response of DTU Fluxgate With and Without Output Filter

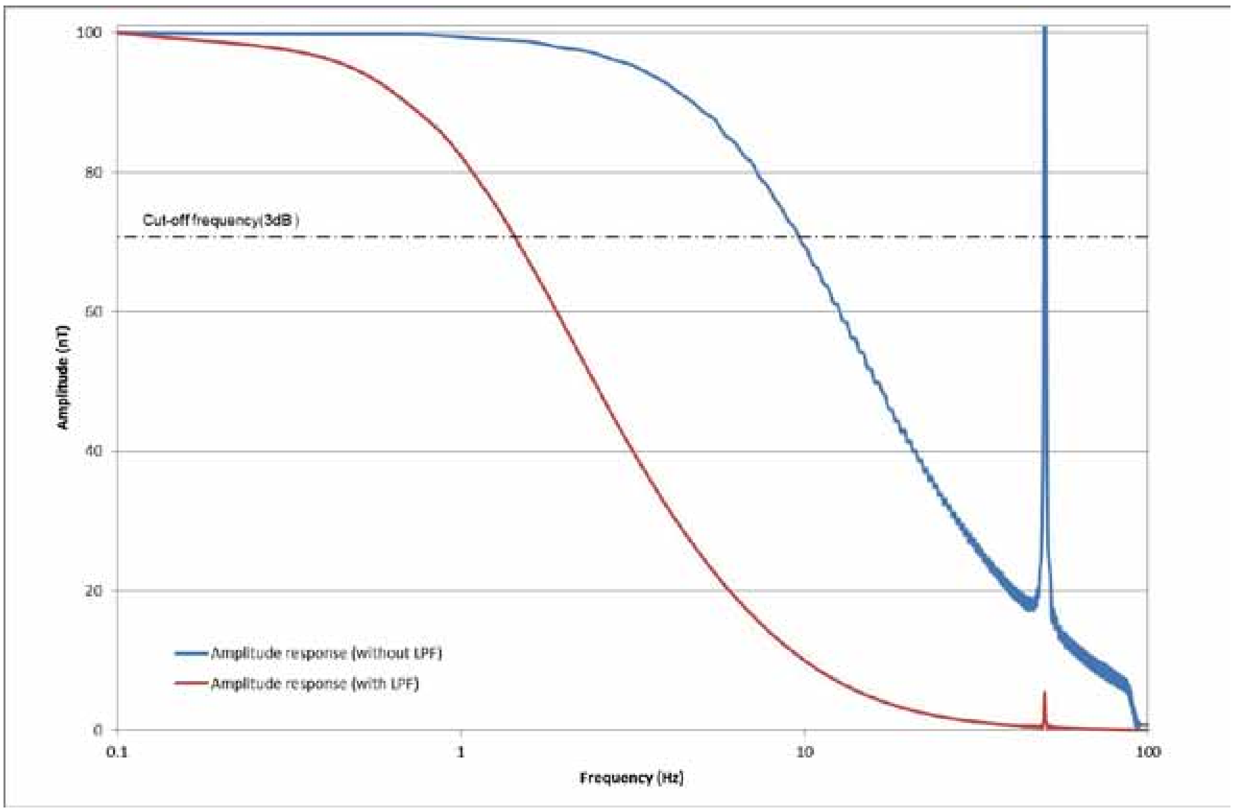

Figure 3. Amplitude Response of DTU Fluxgate With and Without Output Filter

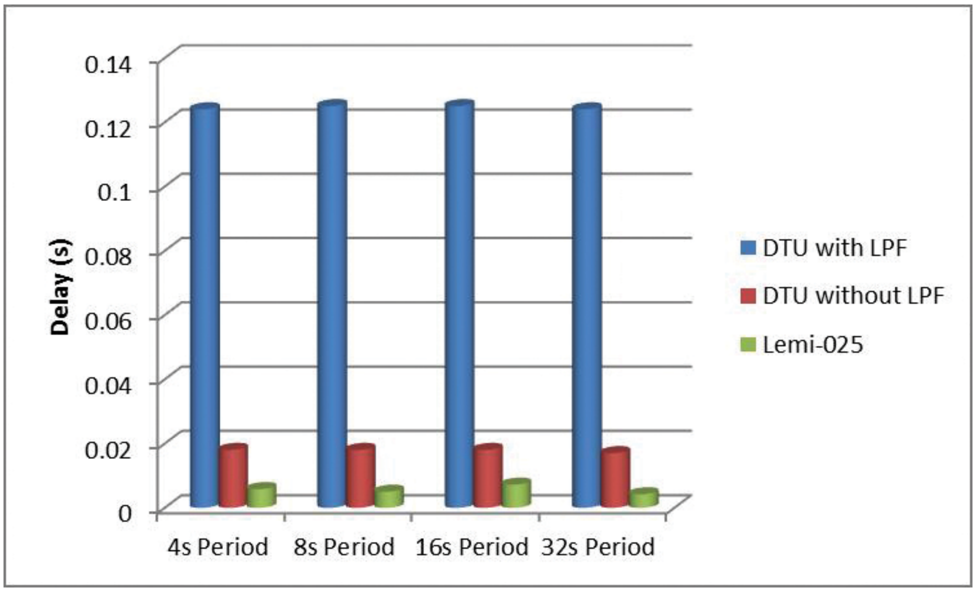

Figure 4. Timing delay of series tests

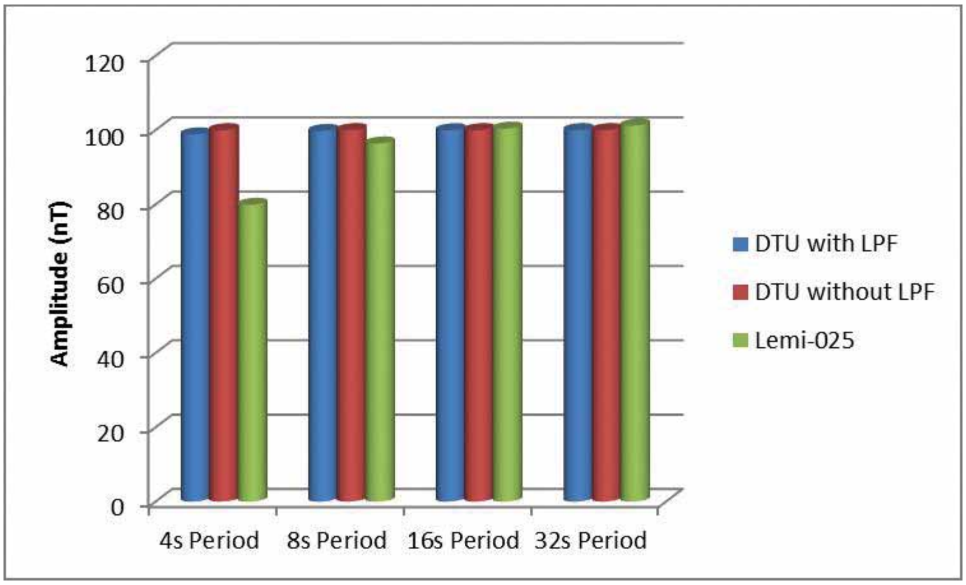

Figure 5. Amplitude Response of series tests

Period (s)	Lemi-025		DTU (with RC filter)		DTU (without RC filter)	
	Delay (s)	Amp. (%)	Delay (s)	Amp. (%)	Delay (s)	Amp. (%)
4	0.006	79.86	0.124	98.81	0.018	99.95
8	0.005	96.35	0.125	99.74	0.018	99.97
16	0.007	100.36	0.125	99.94	0.018	99.96
32	0.004	101.19	0.124	99.96	0.017	99.98

Table 1. Time series test results

Figure 6. Interior view of mu-metal shield pictured without lid

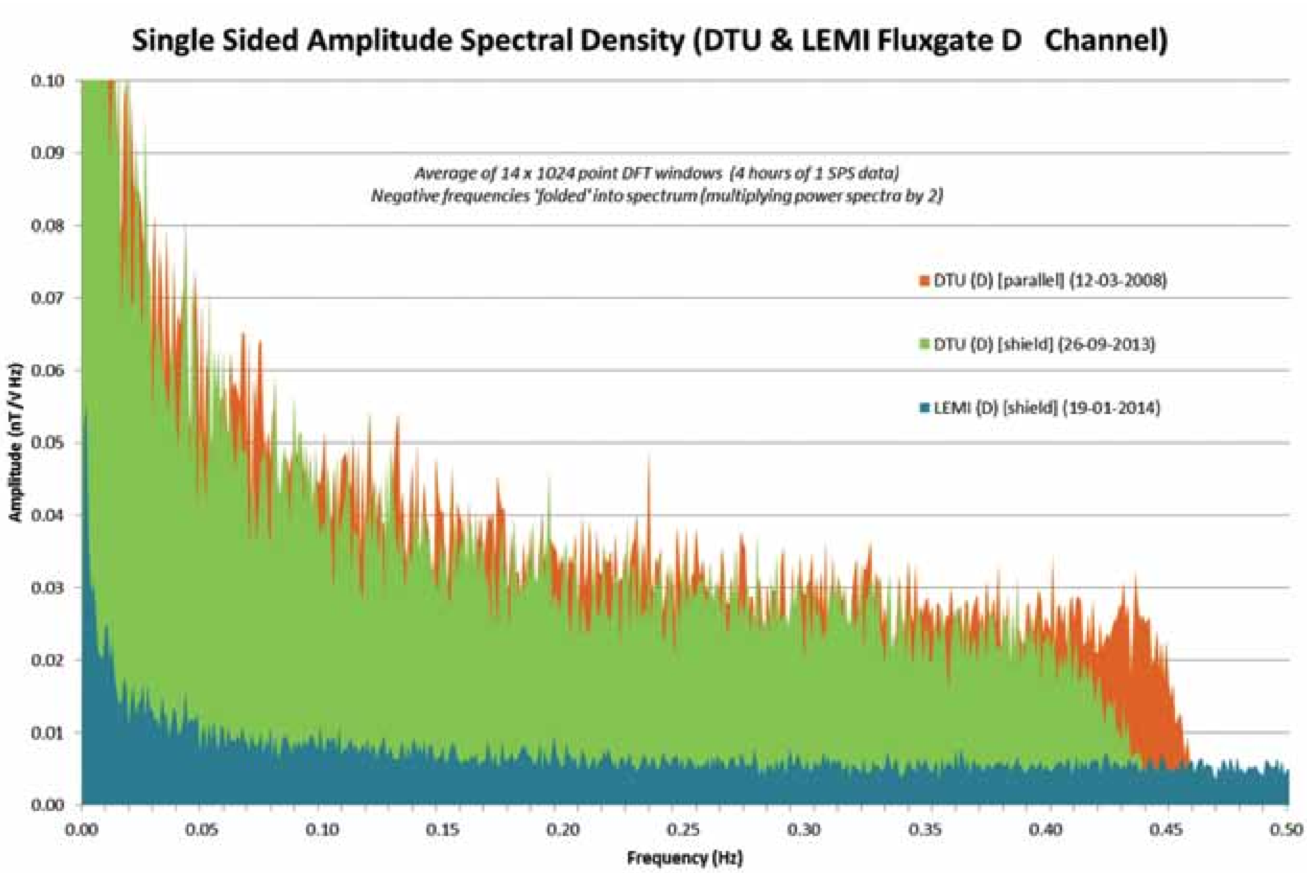

Figure 7. Noise Power Spectral Density

The NPSD results for the FGE-K fluxgate compare favourably with the parallel method tests on a FGE-J conducted by Shanahan (*2008*), showing a total RMS noise (up to the Nyquist rate of 0.5Hz) of 0.04nT. The difference in roll-off rates up to the Nyquist shows the differing filter responses of the Guralp and Earthdata digitisers.

The results indicate that the Lemi-025 meets the noise requirements of the 1-second standard with a noise level of 9pT/√Hz at 0.1Hz.

CONCLUSIONS

The hardware we have developed has proved to be an effective testing device to determine the timing characteristics of any fluxgate magnetometer. The device has demonstrated to be easy to use and has delivered comparable and reliable results using two differing testing methods.

The results confirm that with the removal of the RC low-pass filter the DTU FGE-K's group-delay remains constant and linear at a value of 18ms throughout the 1-second standard pass band. With a high enough sample rate on the recording digitiser this group-delay value can be easily time-shifted to meet the - INTERMAGNET time-stamp accuracy standard for one-second data.

The DTU FGE-K meets the 1-second standard amplitude requirements in the pass-band and with additional filtering can be made to satisfy the amplitude requirements of the stop-band. However, as previously determined by Shanahan (*2009*) the DTU FGE, with a noise level of 40pT/√Hz at 0.1Hz does not meet the noise requirements of the INTERMAGNET standard for one-second data.

The Lemi-025 tests show that the unit meets the timing requirements laid down in the INTERMAGNET time-stamp accuracy standard for one-second data, with a group delay for all test periods well below that of the stipulated 10ms. The amplitude results indicate that the Lemi performs well within the pass-band range. However, more tests need to be carried out to fully quantify the unit's performance within the stop-band.

The noise test of the Lemi-025 are promising and indicate that the Lemi meets the INTERMAGNET 1-second noise standard. However, these tests do not measure the long-term stability of the magnetometer and further tests need to be carried out to quantify the long-term characteristics of the Lemi-025.

REFERENCES

Rasson, J., 2008. Testing the Timing accuracy of 1s INTERMAGNET Variometer, INTERMAGNET Technical Note, TN0004 V0.1

Rasson, J.L., 2009. Testing the Time-Stamp Accuracy of a Digital Variometer and its Data Logger, Proceedings of the XIIIth IAGA Workshop on geomagnetic observatory instruments, data acquisition, and processing: U.S. Geological Survey Open-File Report 2009–1226, 225-232

Shanahan, T.J.G., Turbitt, C., 2009. Evaluating the Noise for a Commonly Used Fluxgate Magnetometer – for 1-second Data, Proceedings of the XIIIth IAGA Workshop on geomagnetic observatory instruments, data acquisition, and processing: U.S. Geological Survey Open-File Report 2009–1226, 271 p.

Turbitt, C.; Matzka, J.; Rasson, J.; St-Louis, B.; Stewart, D., 2013. An instrument performance and data quality standard for INTERMAGNET one-second data exchange, 186-188 Proceedings of the XVth IAGA Workshop on Geomagnetic Observatory Instruments and Data Processing, Boletín ROA No.03/13, Royal Institute and Observatory of the Spanish Navy, Cadiz, Spain.

J. Ind. Geophys. Union (January 2016)
Special Volume-2/ 2016 pp: 30-36

The FGE Magnetometer and the INTERMAGNET 1 Second Standard

Lars William Pedersen,[1] and Laszlo Merenyi [2]

[1] DTU Space, Denmark,
lawp@space.dtu.dk
[2] Geological and Geophysical Institute of Hungary, H-1143 Budapest, Stefánia utca 14,
merenyi.laszlo@mfgi.hu

Based on presentation from the XVI IAGA workshop, Hyderabad, INDIA, October 7—16, 2014.

ABSTRACT

During the years 2012-2014, the Danish Space Center, DTU Space, has developed, tested, and implemented new features of the well known 3-axis FGE Fluxgate Magnetometer. Measurements show that the FGE is suitable for the new INTERMAGNET one second standard thanks to its good linearity and stability, even though the noise in the high frequency band is too large. With a good data acquisition system, such as the Magrec-4B/ObsDaq from Mingeo, it is possible by filtering correctly to keep the time stamp below the 10 ms limit.

Key words: FGE magnetometer, Fluxgate sensors, INTERMAGNET, Linearity, Group delay.

INTRODUCTION

The new INTERMAGNET standard for 1 second data (*Turbitt, 2013*) demands magnetometers with good linearity, high stability and low noise, and fast dataloggers with accurate timing and sharp filtering.

The FGE magnetometer has proven over the last decades to have very good stability and new lab tests show a very good linear frequency response up to 20 Hz.

We have used the Hungarian Magrec-4B datalogger system with ObsDaq v.5.5 A/D converter (ADC) from Mingeo for the tests, since this system can correct delays separately on each channel and can apply the digital filter developed within the PLASMON project. This filter fulfills the new demands for the frequency response: the filter is linear from DC to 0.2 Hz and has more than 60 dB attentuation at 0.5 Hz and above. With the Magrec-4B and ObsDaq ADC, operating at 128 Hz sampling rate and using GPS time synchronization together with proper delay correction for a magnetometer channels, the time stamp accuracy relative to UTC is better than 10 ms.

A new feature for the FGE is the development of an electronic board for differential output of the three components X, Y and Z, which makes it possible to upgrade older FGE systems to use fast seismic dataloggers or similar instruments (like Magrec-4B/ObsDaq datalogger system) in parallel with the old datalogger systems. This gives better noise characteristics, frequency response and timing accuracy.

THE NEW INTERMAGNET ONE SECOND STANDARD

INTERMAGNET has made a new standard for 1 second data describing the demands for magnetometers, data acquisition system, calibrations and observatory practice. These specifications need to be fulfilled to accept data as 1 second data.

These demands can be divided in different groups:

- Linearity: The magnetometer shall be linear in the pass band DC to 0.2 Hz with maximum gain/attenuation of 3 dB and constant phase response less than +/- 10 ms.
- Stability: The demands for stability is the same as the old standard for 1 minute data: Maximum component scaling and linearity error: 0.25 % and maximum component orthogonality error: 2 mrad
- Timing: Data logger system shall have time stamp accuracy better than 10 ms (with GPS time for example) and the data resolution shall be 1 pT which demands a high resolution (24 bit) AD converter.
- Filter: The low pass filter shall be very sharp (starting at 0.2 Hz) and attenuate with minimum 50 dB at 0.5 Hz, which demands a very good digital filter.
- Noise: The pass band noise level for DC – 8 mHz is the same as for 1 minute data: <100 pT RMS. But since the power in the signal for higher frequencies up to 0.2 Hz is very small, the noise level in the band of 8 mHz - 0.2 Hz shall be smaller: ≤10 pT/√Hz at 0.1 Hz.
- Also the maximum offset error between absolute observations should be less than +/- 2.5 nT.

FREQUENCY TESTS OF THE FGE

The transfer function of the magnetometer (both sensor and electronics) can be measured in several different ways. Three parameters are interesting due to the INTERMAGNET demands: linearity, delay and phase. We have chosen two different tests to measure these parameters: a multiple frequency test (MFT) where each frequency is analyzed, and a square wave test with Fourier analysis.

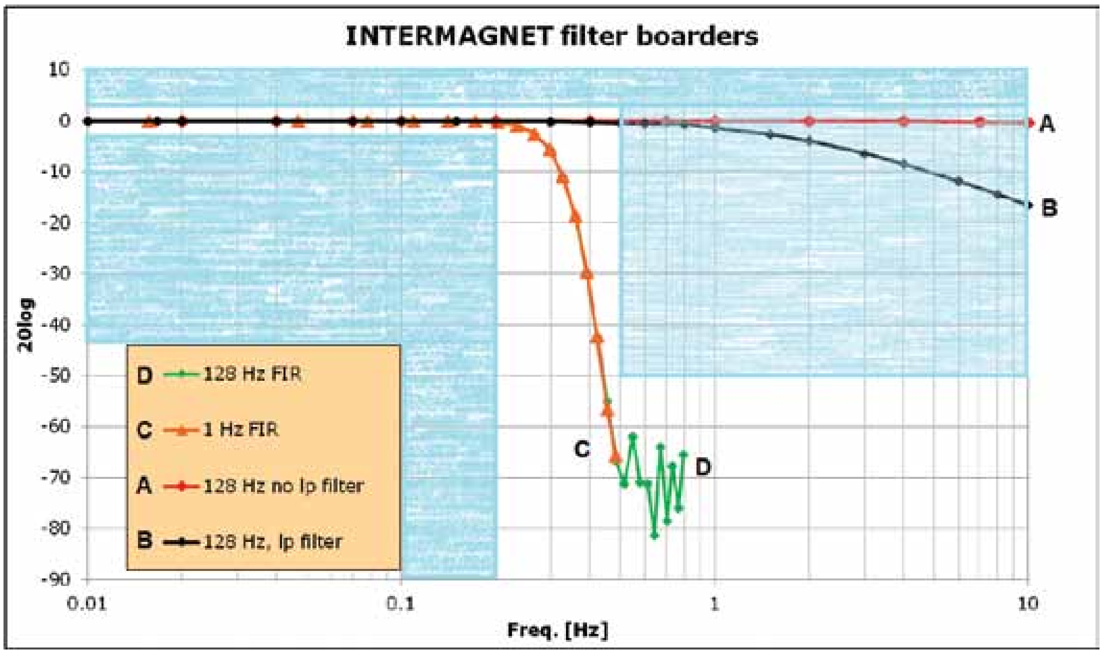

Figure 1. Magnitude plot of INTERMAGNET filter demands. Blue shaded borders mark out the very narrow band between 0.2Hz and 0.5Hz where the INTERMAGNET filter has to attenuate with 50 dB. The four curves show the FGE response with different filtering: A: FGE analog output without any filter, B: FGE analog output with normal 1 Hz lowpass filter, C: FGE analog output with PLASMON FIR filter (1 Hz data filtered from 128 Hz data), D: FGE analog output with PLASMON FIR filter (128 Hz data)

MULTIPLE FREQUENCY TEST (MFT)

In the MFT setup we have placed 3 normal fluxgate sensors in a zero field cylinder with 7 layers of u-metal to cancel out the natural geomagnetic field and noise, such as 50 Hz. In the cylinder the sensors are placed in a coil so we can add different magnetic signals to the sensors from a waveform generator. This generator is controlled by a computer that also collects the data.

A FGE magnetometer electronics measures the signal from two (X and Y) of the three fluxgate sensors, while the third channel (Z) is used for measuring the reference signal from the waveform generator. All three signals are acquired through a newly developed differential output board (DiffOut) and a 24 bit ObsDaq ADC with 128 samples/s rate, and data are stored in the computer. Since the third channel is used as reference there is no need for any synchronization between waveform generator, ADC and computer. The ADC and computer were previously tested with same signal on all 3 channels to verify that all 3 channels are sampled simultaneously. (The ADC used for the tests works without an input multiplexer, as it has three independent analog inputs sampling in parallel).

In each test a number of cosine frequencies between 8.3 mHz (120 s) and 60 Hz with various amplitude and cycles are programmed and executed. For each frequency, the recorded signals are analyzed using a Levenberg-Marquardt-leveling algorithm, the amplitude of the sinusoidal signals are measured for all 3 channels, and the delays between the two sensor channels and the reference channel are measured. From the delays, the phases between X, Y and reference Z are calculated.

Unlike the square wave test mentioned later, this test focuses on certain frequency bands, such as 0.1 Hz – 1 Hz, and analyze it in detail using a large number of frequencies.

Square wave test

The other test used to quantify the magnetometer transfer function is a square wave test.

A square wave signal with the base frequency f_{sq} can be described as a serial of sinusoidal waves with odd harmonic frequencies (1, 3, 5, ..) based on f_{sq}:

$$x_{sq}(t) = \frac{4}{\pi}\left(\frac{1}{1}\sin(2\pi f_{sq}t) + \frac{1}{3}\sin(6\pi f_{sq}t) + \frac{1}{5}\sin(10\pi f_{sq}t) + \ldots\right)$$

This means that if a square wave signal goes through a 'black box', it is possible to find the transfer function of this black box by analyzing the output signal via the FFT. Both gain and phase can be calculated for each frequency, but sample timing has to be very precise to get the right phase. If the amplitudes of the harmonic frequencies are normalized by multiplying with $2k$-1 (1, 3, 5,.) then the gain transfer function of the magnetometer can be found.

Geological Survey of Canada has made a test system for magnetometers called 'GPS Interface Mark 7, variable pulse generator' (*Olfert, 2013*).

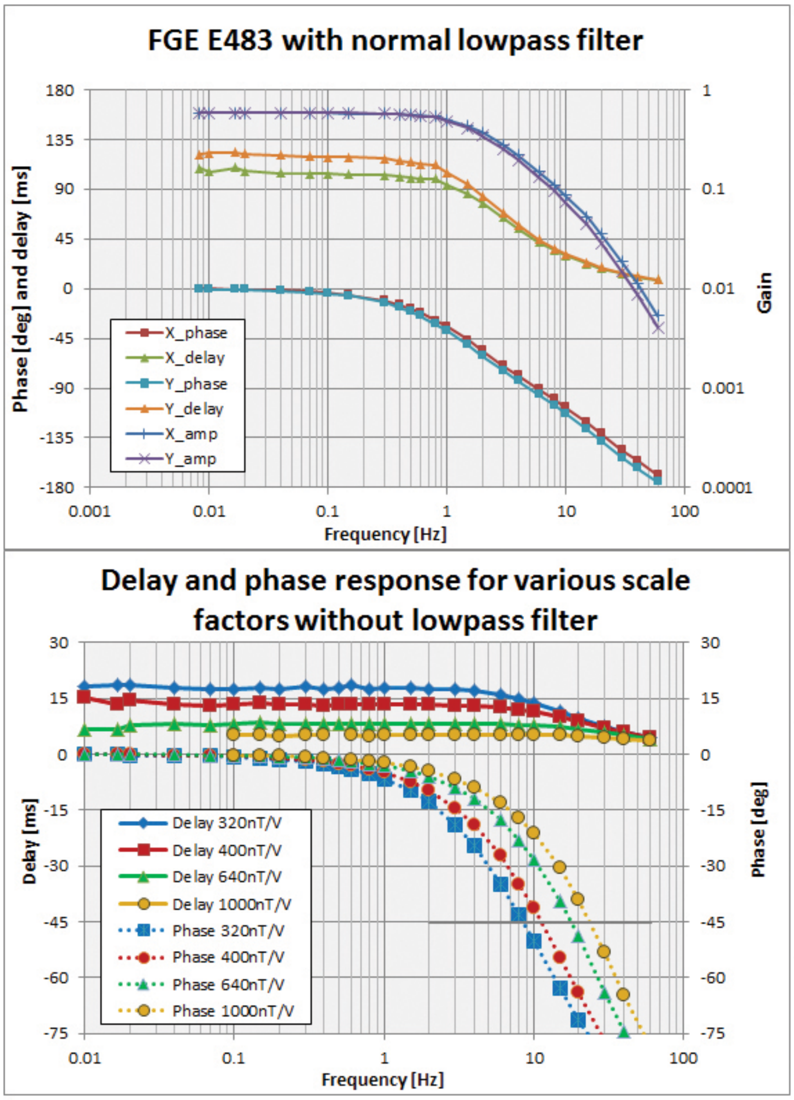

Figure 2. Transfer function of a normal FGE with lowpass filter (upper plot), and delay and phase for various scale factors without lowpass filter (lower plot), all measured with MFT-test.

This system gives a square wave magnetic signal through a coil to a magnetometer at a small distance. It can be used at geomagnetic observatories to test magnetometers without disturbing the magnetometer setup, since the coil is placed close to the sensor without touching it. If the coil is placed in the right angle (45 degrees) close to a 3 axis magnetometer, it is possible to obtain a similar response for all 3 axes at the same time.

The data acquired will be a 'square wave like' signal without the highest frequencies depending on the magnetometers transfer function.

It is possible to analyze data in the frequency domain up to half the sample frequency, so with a normal sample rate of 1 Hz, data can be analyzed up to 0.5 Hz.

It is normally necessary to sample at least 512 seconds of data to obtain a robust result. This is shown in Figure 1 where curve C is data sampled with 1 Hz and the signal is a 64 second long square wave. Curve D is the same square wave signal sampled at 128 Hz, but the data analyzed is the FIR filtered 128 Hz data.

MEASUREMENTS ON THE FGE MAGNETOMETER

Several sets of fluxgate sensors and FGE electronics with different scale factors and filters have been tested in the laboratory at DTU Space using the two test methods.

Most FGE magnetometer electronics produced over the last 20 years have a first order lowpass filter with a cutoff frequency $f0$ = 1.6 Hz (*Pedersen, 2013*), so this has been tested carefully on several different old and new FGE electronics. Since the actual cutoff frequency is determined by the lowpass filter capacitor whose tolerance is 20, $f0$ can change ±20% from its nominal value. A normal test of 2

Table 1. Group delay and cutoff frequencies versus Scale factor

Scale Factor [nT/V]	Delay [ms]	f0 [Hz]
320	18	8
400	14	11
640	9	17
1000	5	25

Table 2. Change in sensor constants over years

	Years between calibrations	Sensor constants changes between calibrations		
FGE no		X o/oo	Y o/oo	Z o/oo
S0100	19	-0.4	0.2	0.1
S0101	20	2.0	-1.8	2.3
S0110	19	0.1	0.0	6.3
S0130	17	-0.2	0.6	-0.1
S0176	14	9.2	-0.1	1.3
S0228	8	0.5	0.3	0.4
S0260	9	4.0	3.6	0.0
S0288	3	0.1	0.0	0.0
S0291	6	-0.6	0.3	-0.9
S0291	1	0.3	0.4	0.0
S0335	3	-0.2	-0.1	0.0
S0336	6	-1.1	-1.1	-0.1
S0373	3	-0.2	-0.2	0.0

Table 3. Change in orthogonality between calibrations

	Years between calibrations	Orthogonality changes between calibrations		
FGE no		X-Y mrad	Z-X mrad	Z-Y mrad
S0100	19	0.1	-2.4	1.9
S0101	20	-0.3	0.1	-3.2
S0110	19	-0.1	3.5	4.9
S0130	17	-0.5	-0.1	0.9
S0176	14	-0.6	-0.2	-0.4
S0228	8	0.4	-0.1	-2.2
S0260	9	0.3	0.3	-0.1
S0288	3	-0.4	0.2	-0.7
S0291	6	0.6	-0.4	0.2
S0291	1	0.1	0.0	0.1
S0335	3	0.2	1.3	0.9
S0336	6	0.5	-0.5	-0.3
S0373	3	0.0	0.0	0.0

or 3 channels in a FGE with lowpass filters mounted can therefore give results with a large spread of delays.

The upper plot of Figure 2 shows the results for 2 channels of the 3 measured parameters in the MFT-test: the amplitude (gain), the phase and the delay. The green and orange curves show that the group delay of X and Y are constant at around 100 ms and 115 ms up to 1 Hz. The cutoff frequency of the lowpass filter is found to be around 1.5 Hz (where the phase is -45 degrees).

Since the group delay can vary 20-30 ms between the 3 channels with lowpass filters, it will be necessary to measure the delay in each channel in each FGE electronic.

The measured delay should be taken into account when producing 1 second data conforming the INTERMAGNET standard.

If the lowpass filter is removed from the electronics, then the delay is mainly controlled by the magnetometers gain in the feedback loop. This is actually the scale factor of the magnetometer which normally is set to a value between 320 nT/V and 1000 nT/V. A high scale factor results in a higher cutoff frequency and smaller delay.

The lower plot in Figure 2 shows the result of MFT tests of 4 FGE's with different scale factors all without lowpass filters. The -45 deg points of phase response curves indicate *f0* cutoff frequencies between 8 Hz and 25 Hz, while the delay plots shows group delays between 18 ms and 5 ms. These results are summarized in Table 1.

PERFORMANCE OF THE FGE MAGNETOMETER

The FGE magnetometer has shown its stability over many years use. More than 300 instruments have been setup round the world during the last 30 years, and only 13 of them have needed to be repaired and recalibrated in the last 10 years. The data from these recalibrations shown in Table 2 reveals that the sensor sensitivity changes only a few thousandths between calibrations even after 10 years. Also the orthogonality between the 3 sensors in the marble cube (Table 3) is very stable and the measured changes are only parts of a mrad.

Noise level of the FGE was measured with sensors inside a zero field cylinder. The measured one second data exhibited around 35 pT_{RMS} noise on average. In the 8 mHz - 0.2 Hz band this means about 80 pT/√Hz average noise level density that exceeds the INTERMAGNET specified noise limit at 0.1 Hz. The noise spectrum is not totally homogenous within this range, the amplitude slightly decreases as frequency increases, especially from DC 0.008 Hz to 0.1 Hz, so at 0.1 Hz the noise density can be slightly lower than the average density, but still above the limit.

Despite of the higher noise it is however still possible to deliver 1 second data to INTERMAGNET, since noise is often not the critical issue and it can easily be seen in data.

DATA ACQUISITION SYSTEMS

For INTERMAGNET minute data the sample timing and resolution is not as important as for INTERMAGNET 1 second data. To produce minute data, it is typical to use a slow 16-bit ADC such as the ADAM-4017.

In the new 1 second standard the timing, the resolution and the filtering have become a big issue, and therefore we have tested and used a newer datalogger system from Mingeo in Hungary: Magrec-4B (*Merenyi, 2014*) with a 24-bit ADC called ObsDaq v.5.5 (*Merenyi, 2013*). This is a fast datalogger system supporting a sample rate of 128 Hz or more, so there is no problem with aliasing from 50/60 Hz signals. The datalogger can apply different filtering, including a 2 step FIR filter originally developed for the PLASMON project (*Heilig, 2012*). This filter fulfills the demands from INTERMAGNET, so it was used in most of our tests. In Figure 1 it can be seen how this FIR filter cuts off between 0.2 Hz and 0.5 Hz.

The ObsDaq ADC supports two sampling modes: free-run mode and triggered mode. In triggered mode the sampling is kept synchronized to an external timing signal, for example to a GPS-PPS signal, resulting in very high time stamping accuracy (better than 0.1ms). However, in all of our tests, we used the free-run mode. In this mode the A/D sampling is not synchronized to any external clock and there is some time sliding due to errors of ObsDaq internal clock. At 128 Hz sampling rate, the times of free-run mode samples are slowly fluctuating relative to UTC seconds with up to ± 3.9 ms. Magrec-4B can determine UTC time labels with ±1 ms accuracy for these samples, using its GPS. Depending on the filter calculation method, this ± 3.9 ms fluctuation will result in ± 3.9 ms timing errors in1 Hz data, or it can be corrected by the filter. Even in the first case, the total time stamping error stays below ±5 ms.

With the Maglin software for the Magrec datalogger it is possible to test the delay of each channel, using a GPS controlled square wave signal, like the Canadian system. It is possible to measure delay within ± 2 ms, and these delay values can be stored and used in the datalogger correcting for the delay.

THE NEW DIFFERENTIAL OUTPUT BOARD DIFFOUT

The FGE magnetometers were originally designed with single ended analogue output for the 3 magnetic channels and for the two temperature sensors. This configuration has been adequate until now, but new fast and precise data loggers like seismic acquisition systems often need differential signals.

DTU Space therefore has developed a small electronic board (*Pedersen, 2014*) that can be built into the FGE box and provides differential output of X, Y and Z. Each channel uses high quality amplifiers and arrays of matched resistors to get very good performance:

- Low temperature coefficients below 0.01 nT/Kelvin.
- Linear to much higher than 1 kHz.
- User selected high accuracy gain of 1, ½ or ¼. (Attenuation factor of 1, 2 or 4)
- 2 user selectable options for filtering: 1st order lowpass filter or no filter.
- It can run in parallel with the original single ended output.

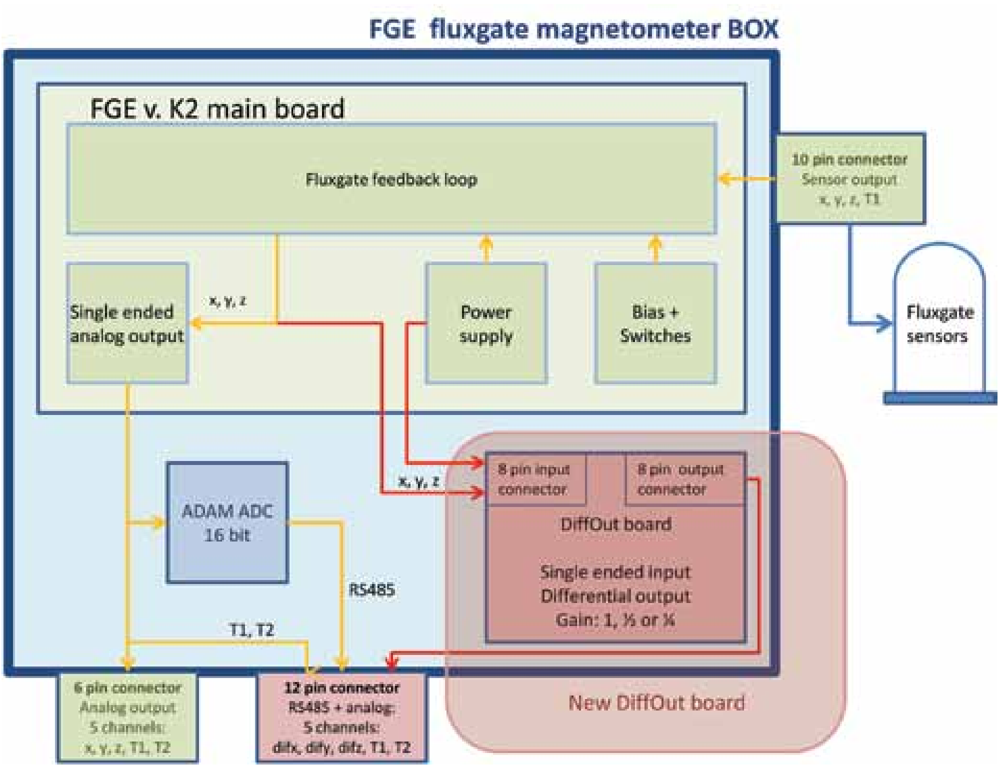

Figure 3. DiffOut board in the FGE box.

The DiffOut board is mechanically mounted in the FGE box and connected to power (+/- 15 V) and to ground on the FGE board. The input of X, Y and Z are connected on the FGE board just before the single ended output amplifier, so the signals are the same but without the lowpass filter. The 3 differential outputs and the ground can be connected to a 12 pin connector on the box, as seen in Figure 3.

In this way the 3 magnetic channels can be measured in two independent ways without affecting each other.

CONCLUSIONS

Except for the noise at 0.1 Hz, the FGE magnetometer can fulfill all the instrument demands of the new INTERMAGNET standard for 1 second data:

- Linear from 8 mHz to 1.5 Hz with the original lowpass filter.
- Linear up to 8-25 Hz without filter depending on scale factor.
- Orthogonality between sensors are better than 2 mrad and can be less than 1 mrad.
- Scaling and linearity are better than 0.25%.
- Group delay is stable up to 1 Hz or more.
- Long term stability is very good.

Since the FGE magnetometer is the main instrument in many geomagnetic observatories round the world, and it is not typical or popular to make any changes in a long time running proven system, an important question arises: how the original FGE can be upgraded for the new INTERMAGNET one second standard? Our answers are the following:

- Use better data acquisition systems with faster and higher resolution AD converters, GPS timing control and digital filtering.
- Use parallel acquisition with old and new dataloggers to compare data for a period.
- Determine the group delay of the magnetometer and use this information to correct the timing of the one second data.

The FGE electronics has been sold mostly in two versions: without digital output (only single ended analog output) or with digital output, where a 16 bit ADC is build into the box. Almost all FGE's have the 1st order lowpass filter included.

If parallel acquisition is desired, it is recommended to install the DiffOut board to obtain the 3 channels out in parallel without interfering between the original and new datalogger. With the DiffOut board bypassing the lowpass filter, the delay is low and well known.

If the original output with lowpass filter is used, beware of the big group delay. This should either be measured and taken into account for each channel in the software or should be eliminated by removing the filter capacitors on the FGE main electronic board. Then the group delay can be found in table 1, and it will only vary a few ms.

ACKNOWLEDGEMENTS

A special thanks to Jan Raagaard Pedersen from DTU Space for his help, good ideas and knowledge during the testing process.

Thanks to Geological Survey of Canada for letting us test and use the square wave system.

Thanks to Mingeo for their corporation with the ObsDaq ADC, when we needed to change software.

REFERENCES

Heilig, B., Vellante, M., Reda, J., Raita, T., Sutcliffe, P., Merényi, L., Csontos, A., Kovács, P., 2012. PLASMON EMMA for Near Real Time Monitoring of the Plasmasphere, XVth IAGA Workshop On Geomagnetic Observatory Instruments, Data Acquisition and Processing, San Fernando, Spain, 4-14 June

Merenyi, L., 2014. Magrec-4B, Magnetic data collection platform. Mingeo Ltd, manual, http://www.mingeo.com/prod-magrec4b.html

Merenyi, L., 2013. ObsDaq, 24 bit ADC. Mingeo Ltd, manual, http://www.mingeo.com/prod-obsdaq.html

Olfert, N., 2013. GPS Synchronised Magnetic Pulse Generator System. NRCAN Short manual

Pedersen, L. W. 2013. FGE Fluxgate Magnetometer ver. K2. DTU Space manual, http://www.space.dtu.dk/english/research/instruments_systems_methods/3-axis_fluxgate_magnetometer_model_fgm-fge.aspx

Pedersen, L.W. 2014. Differential output amplifier for the FGE magnetometer. DTU Space manual http://www.space.dtu.dk/english/research/instruments_systems_methods/3-axis_fluxgate_magnetometer_model_fgm-fge.aspx

Turbitt, C., Matzka, J., Rasson, J., St-Louis, B., Stewart, D., 2013. An instrument performance and data quality standard for INTERMAGNET one-second data exchange, http://nora.nerc.ac.uk/507228/1/Turbitt_etal_IAGAworkshop_OneSecondDataExchange_2013.pdf

J. Ind. Geophys. Union (January 2016)
Special Volume-2/ 2016 pp: 37-41

Determination of Variometer Alignment by using Variation Comparison with DI3-Flux

Philip Heinisch[1], Hans-Ulrich Auster[1]

[1]Institut für Geophysik und extraterrestrische Physik, Technische Universität Braunschweig, Mendelssohnstrasse 3, D-38106 Braunschweig, Germany, p.heinisch@tu-braunschweig.de

ABSTRACT

By comparing magnetic field variations measured by two separate magnetometers the alignment of the individual axis of one of these magnetometers can be determined relative to the other one. The motivation for this analysis was to determine the attitude of the magnetometer equipped lander "PHILAE" on the surface of Comet 67P/Churyumov-Gerasimenko with respect to the mother spacecraft, the ESA satellite ROSETTA. The algorithm has been tested in the geomagnetic observatory at Niemegk. The DI3-Flux method for absolute measurement was used in this case, to predetermine the orientation of a three component reference magnetometer within the geographic reference system with an accuracy much better than 1arcmin. After performing the absolute measurement the three component reference fluxgate magnetometer can be operated as variometer and compared to the variations measured by the observatory variometer(s). A correlation analysis then allows the determination of all six angles of misalignment (non-orthogonality and orientation) of the observatory variometer with respect to the DI3 system by comparing both measurements. We discuss the algorithm and limitation of this method. We show that all variometer alignment errors can be determined with an accuracy of better than 0.1°.

Keywords: Variometer, Magnetometer, Alignment, Variation, Comparison.

INTRODUCTION

The initial motivation for the development of a method to determine the orientation of a three axis magnetometer relative to a reference magnetometer came from the ESA ROSETTA mission (*Glassmeier et al., 2007a*). As part of this mission the lander PHILAE was released to comet 67P/Churyumov-Gerasimenko. This lander as well as the orbiter is equipped with fluxgate magnetometers to measure the ambient magnetic field and for investigating the plasma environment and magnetization of the comet and its tail.

Because PHILAE is not equipped with dedicated navigation instruments, the position and attitude during the Descent and Landing Phase (SDL) and after touchdown must be reconstructed using results from scientific instruments. The tri-axial fluxgate magnetometer of the Rosetta Lander Magnetometer and Plasma Monitor package (ROMAP) (*Auster et al., 2007*) as well as the two tri-axial fluxgate magnetometers from the Rosetta Plasma Consortium (RPC-MAG) (*Glassmeier et al., 2007b*), were all switched on during these phases, which gave the unique ability to use the combined results from both experiments to reconstruct the attitude by magnetic field measurements.

Therefore an algorithm for determining these mission critical parameters from the magnetic field measurements was to be developed and initial ground tests should provide the necessary expertise for applying a similar method under the harsh conditions of the ROSETTA mission.

Additionally the determination of observatory variometer alignment errors, even if not specified explicitly in the observatory standards (*Jankowski and Sucksdorff, 1996*), might be of interest, especially for instruments, which cannot be recalibrated in external calibration facilities, because they are impossible to replace once installed, without interrupting the observatory baseline.

ALIGNMENT DETERMINATION PROCESS

The alignment of the variometer axis is determined by comparing the three dimensional spatial orientation of low frequency variations in the earth's magnetic field with observations of a reference variometer with known axis alignment. Using low frequency variations instead of a DC signal has the advantage that measurement errors caused by offsets can be neglected. Scale factor and non-orthogonality errors are below 10^{-4} and therefore considerably lower than the ratio between signal (about 10 nT) and resolution (10 pT).

To ensure the process is not influenced by sensor temperature dependence or sensor noise, very low frequencies in the range of the daily magnetic field changes had to be excluded. Higher frequencies were also not usable, because the signal periods are too short and therefore, depending on the sampling rate, not enough data points are available for accurate comparison.

The alignment reconstruction process for the variometer x-axis is illustrated as an example in Figure

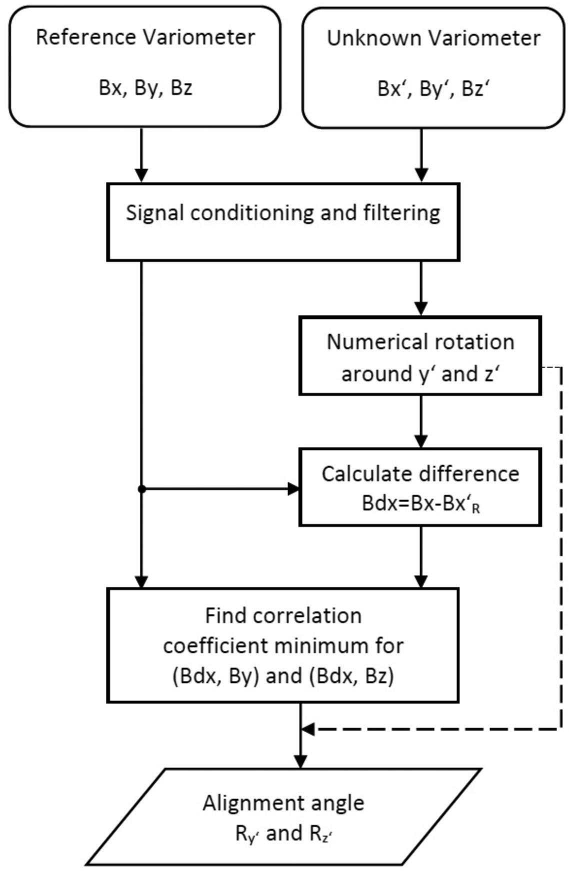

Figure 1. Illustration of the alignment reconstruction process exemplarily shown for the x-axis.

1. To determine the axis alignment the signal from each component is numerically rotated around the two other perpendicular components. Afterwards the signal from the axis that is used as reference is subtracted from the unknown axis' signal. The correlation coefficients between this difference signal and the remaining two perpendicular reference components are then minimized by continuously rotating to reconstruct the alignment. This way all six angles describing the orientation and orthogonality error of the unknown variometer can be determined.

Depending on the magnetic background conditions and the field activity, the length of the input signal necessary for this method, ranges from about 30 minutes to 14 hours. Using even longer intervals has no further advantages, as temperature effects limit the accuracy and the additional data leads to no significant increase in statistical significance.

As the algorithm depends on comparing low frequency variations, the accuracy of the results depend mostly on the level of variance in the magnetic field, which can be quantified by the standard deviation of the signal. Since signal variance alone is not a sufficient criterion for accurate alignment reconstruction, because the fluctuations could be caused by local interference, the correlation coefficients between the absolute values of both input signals were considered, too. To get a quality parameter, the mean standard deviations for the components are weighted with the correlation coefficient between the absolute values.

To further check the results, the alignment results can be used to rotate the data from the variometer with unknown alignment into the coordinate system of the reference variometer. The correlation coefficients between the individual components before and after rotation can then be compared to get an estimate of the quality of the results.

MEASUREMENTS PERFORMED AT NIEMEGK OBSERVATORY

The process described above was applied to the two Niemegk observatory variometers "Ng0" and "Ms0" relative to a reference variometer using the DI3-Flux setup [Hemshorn et al., 2009]. As only the main observatory variometer Ng0 is in a climate controlled environment, the Ms0 and reference variometer are subject to daily temperature variations which had to be taken into account by filtering ultra-low frequency variations from the signals, as discussed above.

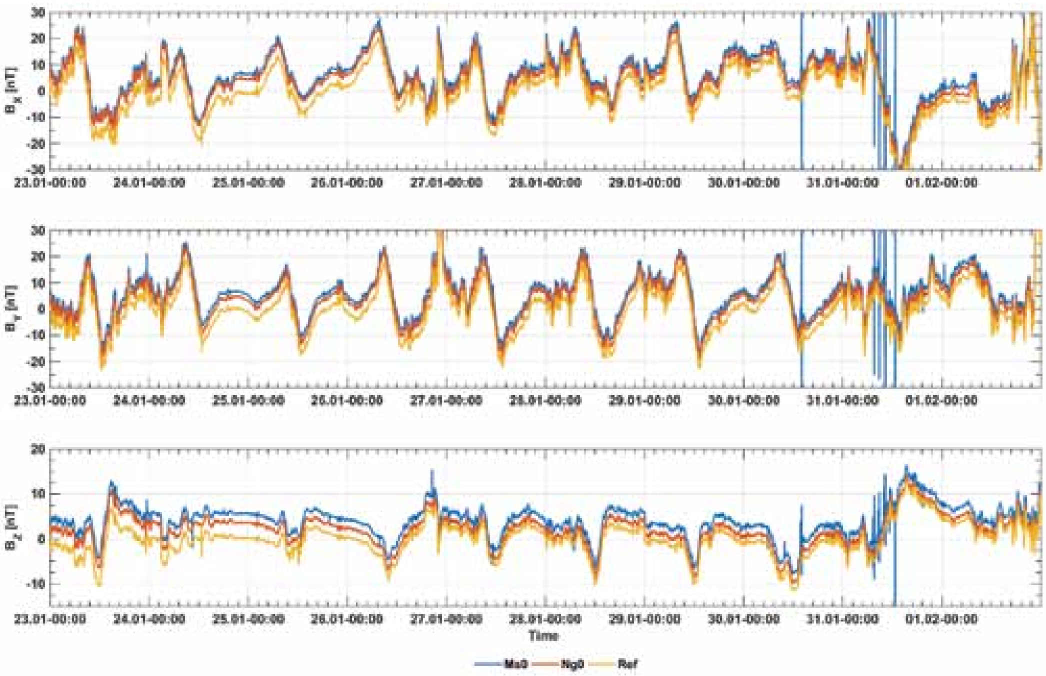

Figure 2. 10-day raw input dataset for the two Niemegk variometers "Ms0" and "Ng0" and the reference variometer "Ref". Ms0 and Ng0 were shifted by 6nT and 4nT respectively for better visibility.

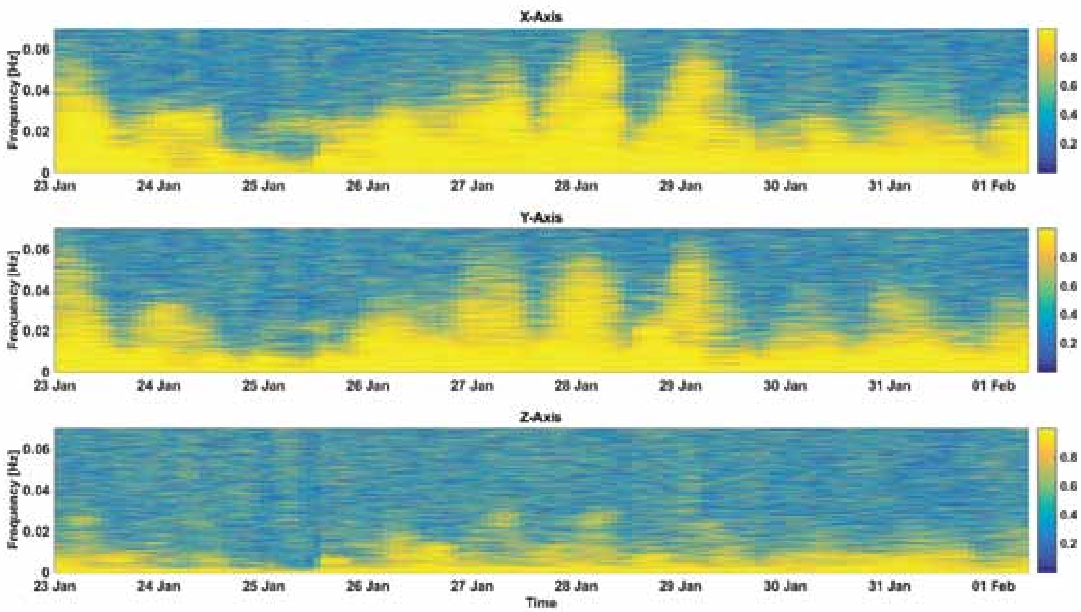

Figure 3. Dynamic coherence spectra between the reference variometer and Ng0 signal. Each interval has a length of 14h with an overlap of 7h.

In total 10 days of data observed from 23.01.2014 until 01.02.2014 were used, as shown in Figure 2, even though much less would have been sufficient. This way it was possible to separate the entire dataset into smaller intervals of about 14h, which were then individually processed. This way it was possible to exclude intervals with strong external interference and use a statistical approach for error determination.

In the next step, a band-pass filter was used to remove frequency components not suitable for alignment reconstruction, as described above.

The dynamic coherence spectra for the three components of the Ng0 and reference variometer shown in Figure 3 shows clear differences in the presentations of coherent wave activity. Especially around the 24th and the 28th of January strong coherent waves with a maximum frequency

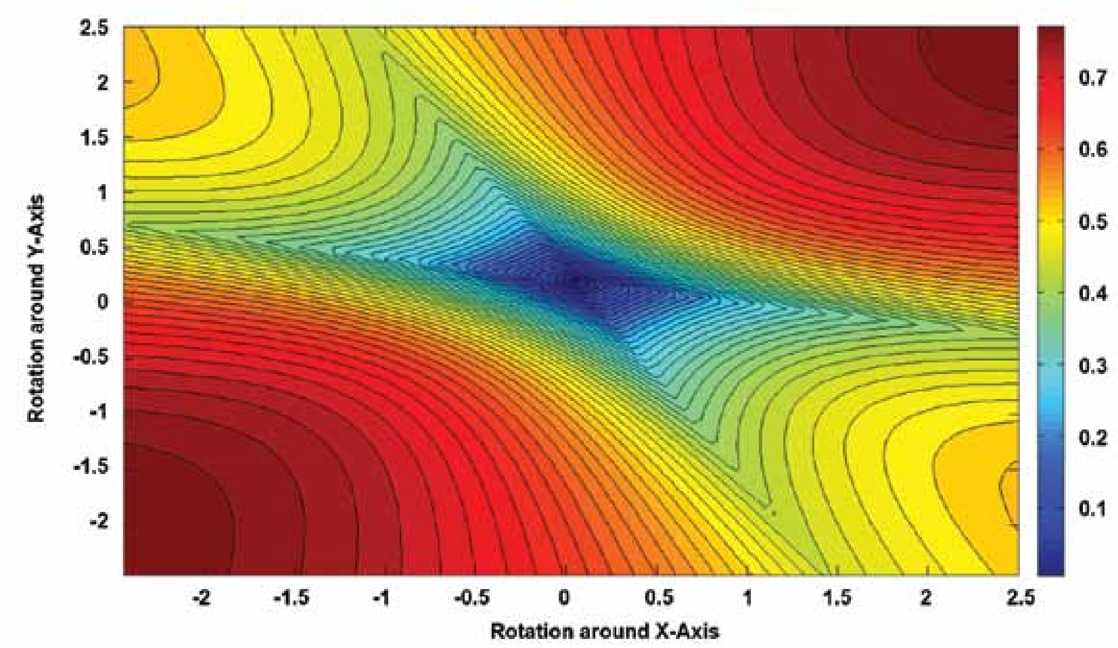

Figure 4. Mean correlation coefficient between the Ng0 z-axis differences and the x- and y-components depending on the corresponding rotation angles. The alignment result is given by the minimum in the middle.

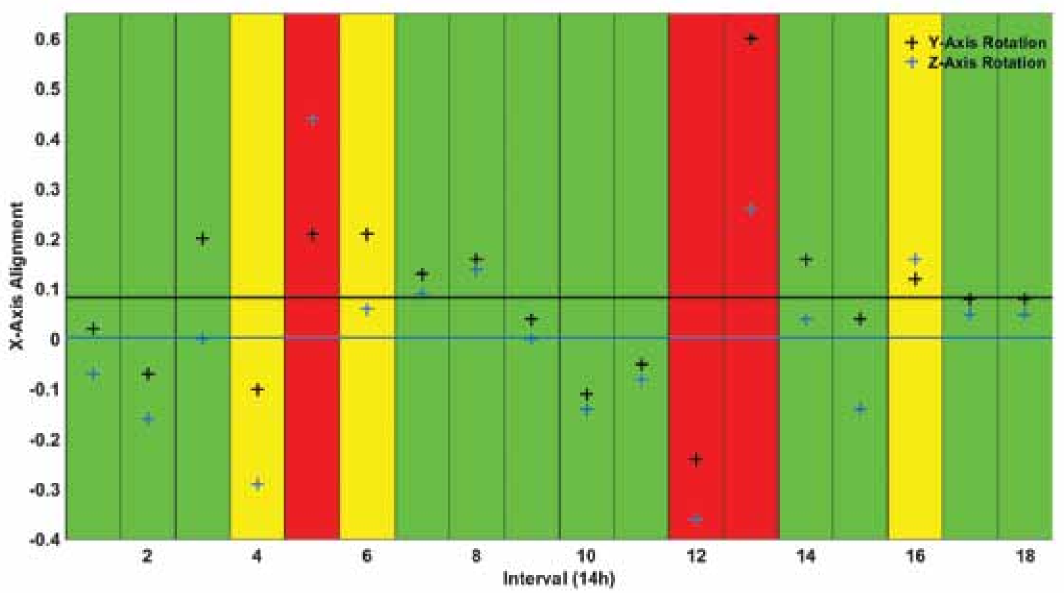

Figure 5. X-Axis alignment results for the Ng0 variometer, the blue lines denotes the y-axis rotation and black the z-axis rotation. The corresponding mean values are indicated by the two lines. The color coded background illustrates the data quality.

of 0.06Hz were detected, which is in the range of Pc3 and Pc4 pulsations. To reduce the impact of local interferences and noise, frequencies above this threshold were removed by filtering the signals. Because coherent structures in the z-component are as expected not as frequent as in the other two components, the error of this method for the z-axis alignment is bigger than for the x- and y-components.

The intermediate results are shown for one of the intervals of the Ng0 z-axis in Figure 4. As shown in Figure 1 the algorithm determines the minimum of the mean correlation coefficient between, in this case the Ng0 z-axis differences and the reference variometer x- and y-components, depending on the corresponding rotation angles to reconstruct the alignment. This sharp minimum is clearly visible in Figure 3 as the mean correlation decreases to zero in the middle of the figure. The process is done for all three axes to determine all six alignment angles and then repeated for all of the individual intervals.

Table 1: Mean alignment results for Ng0 and Ms0 using individual 14h intervals.

	Ng0	Ms0
Ortogonality X/Y	0.00°	0.00°
Ortogonality X/Z	0.02°	0.00°
Ortogonality Y/Z	0.03°	0.02°
Orientation X vs. vertical axis	0.02°	-0.06°
Orientation Y vs. vertical axis	0.01°	0.04°
Orientation Z vs. geogr. north	-0,18° (w)	2,72° (e)

The final Ng0 alignment results for the individual intervals are shown for the x-axis as an example in Figure 5. The color coded background indicates the data quality, as discussed above.

The mean alignment results for all intervals and both variometers are shown in table 1. Orthogonality errors of the observatory variometers as well as errors in the alignment versus horizontal plane are very small. The orientation within the horizontal plane depends on the time of variometer installation. Thus the results are in the expected range and validate that the proposed method is applicable for the determination of the axis orientation.

CONCLUSION

Using the presented method, it was possible to verify variometer orientation with accuracies better than 0.1° using the DI3-Flux setup. Applied to both Niemegk observatory variometers the orthogonality and vertical alignment errors were determined to be below 0.1°. The alignment in the horizontal plane is 0.18° (w) for NG0 and 2.72 (e) for MS0. Thus by using the DI3-flux absolute measurement this method can be offered for orientation verification for observatory variometers without interrupting the continuous data acquisition process.

As intended, an algorithm derived from this method was used very successfully to reconstruct the attitude of the ROSETTA PHILAE lander on the surface of comet 67P/Churyumov-Gerasimenko, using concurrent magnetic field observations by the orbiter magnetometer RPC-MAG and the lander magnetometer ROMAP with an accuracy better than 15° (*Heinisch et al., 2015*). The results were not only used for scientific analyses (*Auster et al., 2015*), but also to narrow down the possible landing sites and as input for the prediction of the possible communication slots, which were used to reestablish contact with PHILAE in June 2015.

ACKNOWLEDGEMENT

We thank the Niemegk Observatory team for supporting and conducting the comparison of DI3-Flux measurements with the variometer data.

REFERENCES

Auster, H. U., et al., 2007. 'ROMAP: ROSETTA Magnetometer and Plasma Monitor', *Space Sci. Rev.*, 128, 221-240.

Auster, H. U., et al., 2015. 'The nonmagnetic nucleus of comet 67P/Churyumov-Gerasimenko', *Science*, DOI: 10.1126/science.aaa5102

Glassmeier, K. H., et al., 2007. 'RPC-MAG: The Fluxgate Magnetometer in the ROSETTA Plasma Consortium', *Space Sci. Rev.*, 128, 649-670.

Glassmeier, K. H., et al. , 2007. 'The ROSETTA Mission: Flying towards the Origin of the Solar System', *Space Sci. Rev.*, 128, 1-21.

Heinisch P., et al., 2015. 'Attitude-Reconstruction of ROSETTA's lander PHILAE using two-point observations by ROMAP and RPC-MAG', *Acta Astronautica*, in press.

Hemshorn, A., et al. 2009. 'DI-flux measurement of the geomagnetic field using a three-axial fluxgate sensor', *Measurement Science and Technology*, 20, doi:10.1088/0957-0233/20/2/027004

Jankowski, J. & C. Sucksdorff 1996. 'IAGA Guide for magnetic measurements and Observatory Practice'. *Warsaw: International Association of Geomagnetism and Aeronomy*. p. 51. ISBN 0-9650686-2-5.

J. Ind. Geophys. Union (January 2016)
Special Volume-2/ 2016 pp: 42-46

The Temperature Stability of LEMI-025 1-Second Variometer: Case Study in the Icheon Observatory

Sooncheol Hong [1], Jung-Hoon Kim [1], Andriy Marusenkov [2], László Hegymegi [3], András Csontos [4]

[1] SETsystem, Inc., 16-3 Gangnamdaero 8, Seocho, Seoul, Korea,
kim@setsystem.co.kr

[2] Lviv Centre of Institute for Space Research of NANU and SSAU, 5A Naukova St., 79040, Lviv, Ukraine,
marand@isr.lviv.ua

[3] Mingeo Ltd., H-1142 Budapest, Ráskai Lea u. 20, Hungary,
hegymegi@mingeo.com

[4] Geological and Geophysical Institute of Hungary, Tihany Geophysical Observatory, H-8237
Tihany, Kossuth utca 91,
csontos.andras@mfgi.hu

ABSTRACT

The temperature characteristics of the 1-second variometer were studied in the real operation environment. For estimations of the instrument thermal drift the two approaches based on the total field difference and base values analysis were used. The total temperature drift was decomposed to the console and the sensor ones using considerable differences in the temperature variations of these units. The significant non-linearity of the temperature dependencies of the variometer electronic unit was revealed. The temperature corrected total field difference did not exceed ± 0.5 nT during about one year.

Keywords: Variometer, Sensor, Temperature drift.

INTRODUCTION

The South Korea Icheon geomagnetic observatory, which belongs to Korean Space Weather Center (KSWC) of Radio Research Agency (RRA), was upgraded in May-June, 2013. The new places both for the recording instruments as well as for the absolute measurements were built. The new set of the recording instruments includes the Overhauser magnetometer GSM-19, the fluxgate magnetometer LEMI-025 with the gimbals suspended sensor, the data acquisition system MAGREC and DI-flux meter for performing absolute measurements. As a result of the proper installation the devices were free from possible instrumental errors i.e. inaccurate scale factors, orientation errors etc. Due to the underground installation at the depth approximately 3 meters, the Overhauser and fluxgate sensors' temperature daily variations are quite small (0.1 – 0.3 Celsius degree). In contrast, the consoles' diurnal temperatures vary considerably (up to 10 Celsius degrees). The sensor and console temperatures have also significant seasonal variations (Figure 1, curves Ts and Te respectively). The aim of the present study is to estimate the temperature drift of the LEMI-025 magnetometer in the real operation conditions. Two approaches for estimation thermal drift were used: a) the comparison of the total field time series computed using the variometer records with the scalar magnetometer data; b) analysing the variometer base values obtained as a result of the absolute measurements.

DATA PROCESSING – THE TOTAL FIELD DIFFERENCE ANALYSIS

In accordance with the first approach, the total field values computed using bias fields and the variometer 1-minute data were compared with the Overhauser magnetometer records – so called delta-F test – the common INTERMAGNET observatories practice for data quality control *(INTERMAGNET TECHNICAL REFERENCE MANUAL, 2012)*. This method was usable only to test the H and Z components. (The contribution of D component to the calculated total field value is practically zero.)

The data were analyzed separately at the two intervals: a) from September, 11^{th}, 2013 till March, 14^{th}, 2014; b) from March, 28^{th} till August, 26^{th} 2014. The variometer bias fields applied at each interval were slightly different; as a result some shift between dF values at each interval exists (Figure 1, curve "dF").

Taking into account different behaviours of the electronic unit (Te) and sensor (Ts) temperatures the attempt to separate the contributions of the temperature drifts of the console and the sensors was made.

In order to separate effects of the sensor and console temperatures on dF we select the subintervals with approximately stable sensor temperature T_s (with maximal deviations <1.6 °C) and built the plots dF vs. the console temperature T_e. In this plot dF – Te points from each interval are concentrated near some average line. However,

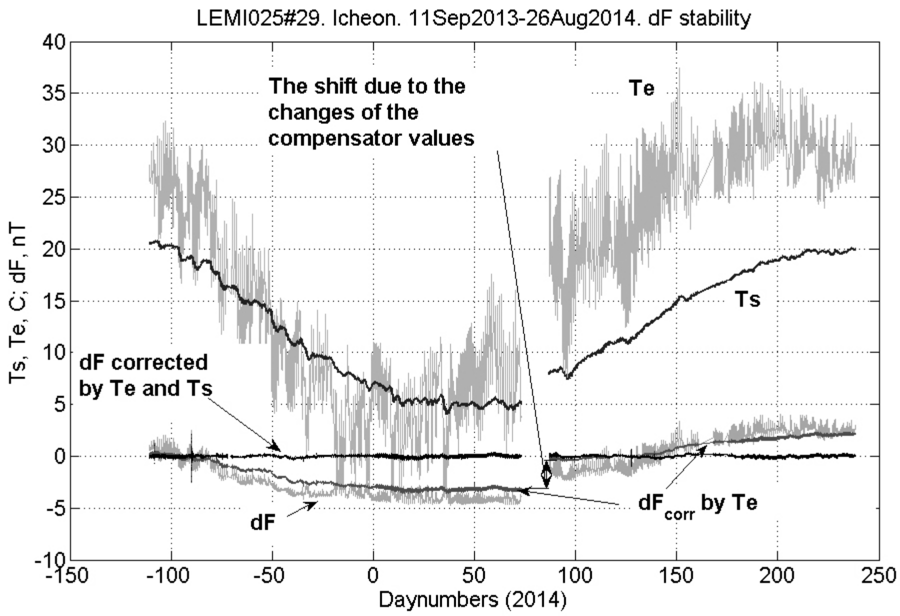

Figure 1. The total field difference (dF) and the magnetometer temperatures.

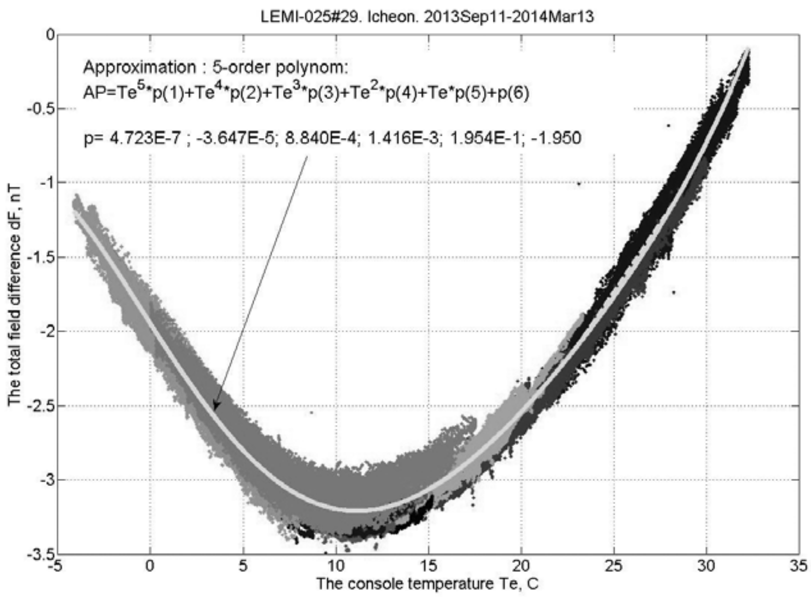

Figure 2. The total field difference (dF) dependence on the console temperature. The data subsets with the nearly constant temperature of the sensor are marked by the same grey colour hue.

the dF values taken at the same Te, but from the different subintervals, are shifted, as we assumed, due to the influence of the sensor temperature Ts. Correcting these shifts between subintervals the common set of the pair dF-Te was combined and, then, approximated by the 5-order polynomial fits (Figure 2). It has to be noted that the dependency dF on the console temperature Te is strongly non-linear and even changes its sign at the proximity of Te≈10.5°C. The non-linear dependencies at the both intervals are consistent and satisfactory correlate with thermal drift specifications of the voltage reference LTC1027, used in the variometer, and with the results of laboratory tests of the compensator current thermal stability, which creates the bias fields. So, we assume that drifts along H and Z components are caused by the common source – the voltage reference. Therefore, these drifts are proportional to the bias values along these components and could be corrected using thermo-drift estimations based on the dF analysis.

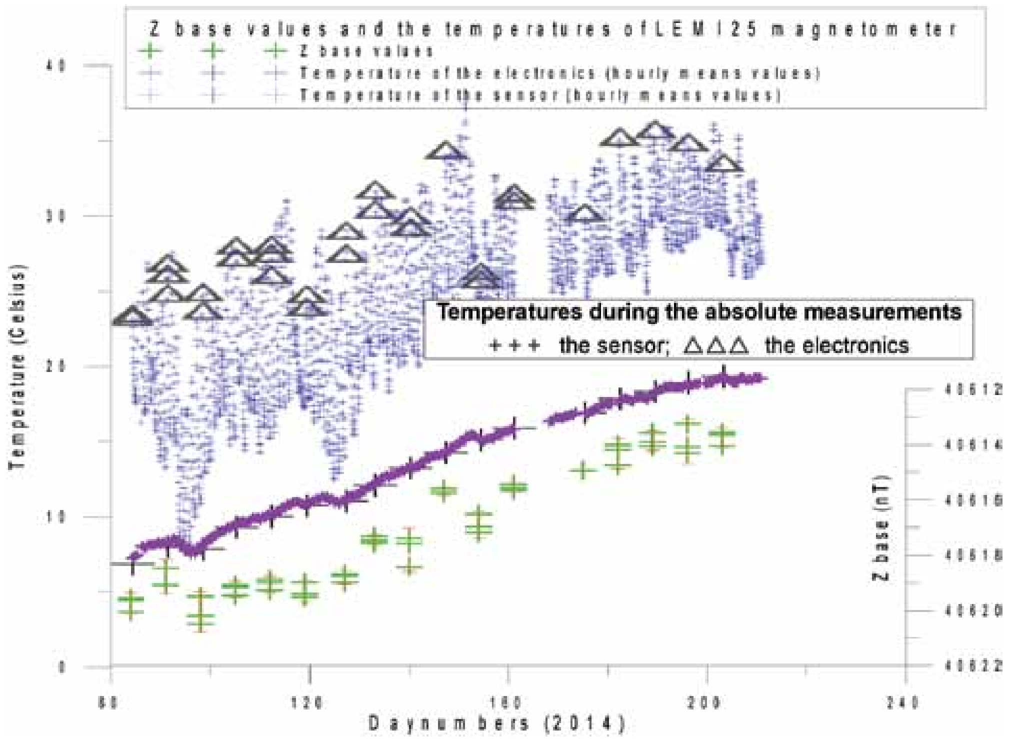

Figure 3. Variation of the temperature and the Z base values of LEMI-25 device

After correcting the console temperature dependence by polynomial approximation (curve "dF_{corr} by Te" in Figure 1) we estimated the sensor temperature influence basing on its seasonal variations. The dF values also show non-linear dependence on the sensor temperature – the 3-order polynomial approximation was used to correct this dependence. The dF values after correcting temperature drifts and the shift due to the bias values change are given in Figure 1 (curve "dF corrected by Te and Ts") – there is no observable long-term drift and all corrected values do not exceed ± 0.5 nT during one year.

DATA PROCESSING – ANALYSIS OF BASE VALUES

We selected a period of the data set which was mostly free from instrumental problems. We used the 1st, 2nd and 3rd complete set of daily absolute measurements for our work. We discarded the absolute values, if we found extreme outputs of the diagnostic parameters I.e. the misalignments and the offset of the sensor.

Figure 3. shows the variation of the temperature and the Z baseline during 130 days. We can see the different characteristics of the two temperature variations. We can also notice a significant temperature effect on the Z component. In Figure 3. it is clearly seen that the fluctuations of the measured temperatures (sensor and electronics) at the time of absolute measurements has a different behavior. This different fluctuation of two temperature variations give us the chance to separate temperature effects on the sensor and the on the electronics.

The next step was the computation of temperature coefficients. We used numerical optimization. We calculated the temperature corrected base values(Z_{BC}): $Z_{BC}=Z_b+(T_s-10)*Z_{CS}+(T_e-20)*Z_{CE}$, where Z_b is calculated Z base, T_s is the temperature of the sensor, Z_{CS} is temperature coefficient of Z sensor, T_e is the temperature of the electronics, and Z_{CE} is temperature coefficient of electronics. Let us note, that the drift of base values always has the opposite sign in respect to the magnetometer drift, because the sum of the base values and the variations yields the real value of the measured component almost free from the instrumental errors. We selected the sign of the coefficients Z_{CS}, Z_{CE} in such a way, that it represents the polarity of the temperature drift of the magnetometer data.

We used hourly means of Z sensor and electronics' temperature values corresponding to each absolute set of measurements. We assume that only the temperature dependence has caused the drift in baseline values . In such a case temperature corrected base values should be free from any drift and any scatter too. We also supposed that the temperature dependence is a linear function of temperature and it does not vary in the time. Of course, our assumption about linearity of the temperature dependence is not completely correct, especially for the electronics drift, as it was revealed by the delta-F analysis. However, during the absolute measurements the electronics

Table 1. Console temperature coefficients (Te=15 – 35 °C)

	dF estimations	Base values' estimations
B_H=30160 nT	0.12 nT/ °C [1]	(0.04 … 0.05) nT/ °C
B_Z=40620 nT	0.16 nT/ °C [1]	(0.14 … 0.16) nT/ °C
F=50593 nT	0.2 nT/ °C	0.16 nT/ °C [2]

[1] calculated in assumption of the common source of the thermal drift — the voltage reference thermal dependence
[2] the value calculated from the components' temperature coefficients

Table 2. Sensor temperature coefficients (Ts=15 – 22 °C)

	dF estimations	Base values' estimations	Difference
B_H=30160 nT	0.15 nT/°C [1]	-(0.2 … 0.23) nT/°C	-(0.35 … 0.38) nT/°C
B_Z=40620 nT	0.2 nT/°C [1]	0.46 … 0.47 nT/°C	0.26 … 0.27 nT/°C
F=50593 nT	0.25 nT/°C	0.24 … 0.25 nT/°C [2]	**≈0.0 nT/°C** [2]

[1] calculated in assumption of the common source of the thermal drift — linear thermal expansion of the compensation windings
[2] the value calculated from the components' temperature coefficients

temperature mostly fluctuates between 15-35 °C and in this range the magnetometer temperature dependence could be satisfactory approximated by the linear function (see Figure 2). Previous studies show that the most of the fluxgate magnetometers have large temperature coefficients and their behaviour depends significantly on the amplitude of the temperature change. Thus, the determination of a general temperature coefficient, as a correction factor is very limited *(Csontos, 2007)*. Anyway, the instrumentation of a common INTERMAGNET observatory let us to use only the presented methods for base value correction especially in the case of D component.

In our case 42 complete sets of absolute measurements were corrected for temperature. We selected the maximum of corrected values [MAX(Z_{BC})] and the minimum of the same values [MIN(Z_{BC})] after every numerical iteration. Our task was to find the minimum of MAX(Z_{BC})-MIN(Z_{BC}) expression by applying different coefficient values. The corresponding temperature coefficients are Z_{CS} = 0.46 nT/C° and Z_{CE} = 0.14 nT/C°. Using similar method we determined the temperature coefficients of the two other sensors. In the case of H sensor we found: H_{CS} = -0.20 nT/C° and H_{CE} = 0.04 nT/C°. For the D sensor D_{CS} = 0.07'/C° and D_{CE} = -0.03'/C°, where H_{CS} is a temperature coefficient of H sensor, D_{CS} is a temperature coefficient of D sensor, D_{CE}, H_{CE} is temperature coefficients of the electronics. We find that in the case of D component that the residuals are significant. The original drift of D component did not show any similarity with the temperature variation.

Alternatively the RMS value of the 42 temperature corrected absolutes set was processed too. Numerical iterations were performed to determine the temperature coefficients. The predefined expectation was that the RMS of temperature corrected absolute measurements should be minimal.

In the second case the corresponding temperature coefficients are Z_{CS} = 0.47 nT/C° and Z_{CE} = 0.16 nT/C° and H_{CS} = -0.23 nT/C° and H_{CE} = 0.05 nT/C°. Our conclusion was that the result does not depend significantly on the method used to obtain coefficients.

RESULTS AND DISCUSSION

We compare the estimations of the LEMI-025 temperature drift coefficients based on the total field difference and the base values methods. The base values estimations were conducted only at the limited time interval from March, 28 till August, 26th 2014, when the sensor temperatures mostly varied in the range 15-22 °C and the console temperatures – in the range 15 – 35 °C. In these temperature ranges the non-linearity of the thermal characteristics is not very strong, so we compare the temperature coefficients of the linear approximations of the temperature drifts (Table 1 and Table 2). The delta-F estimations of the components' temperature coefficients H_{dFs}, H_{dFe}, Z_{dFs}, Z_{dFe} were calculated using following expressions:

$$H_{dFs} = F_{dFs} \cdot B_H / F \ , \ H_{dFe} = F_{dFe} \cdot B_H / F \ ,$$
$$Z_{dFs} = F_{dFs} \cdot B_Z / F \ , \ Z_{dFe} = F_{dFe} \cdot B_Z / F \ ,$$

where F_{dFs}, F_{dFe} – the total field difference sensor and electronics temperature coefficients;
B_H, B_Z – horizontal and vertical components of the magnetic field;
F – the total field intensity.

The base values' estimations of the total field difference temperature coefficients F_{CS}, F_{CE} were calculated as follows:

$F_{CS} = (H_{CS} \cdot H_{CS} + Z_{CS} \cdot Z_{CS})^{½}$, $F_{CE} = (H_{CE} \cdot H_{CE} + Z_{CE} \cdot Z_{CE})^{½}$.

Both approaches give the mutually consistent estimations of the console temperature drift (Table 1). The small difference in the H component drift estimations could be explained by the deviation of the drift from the linear dependence.

The H and Z sensors' temperature drift estimations based on the delta-F and base values analysis look completely different, whereas the temperature coefficients of the total field difference almost coincide (Table 2). Correcting base values' estimations of H and Z components drifts by those obtained from the dF estimations, we found that the residual drifts (Column "Difference" in Table 2) could be very well explained by the sensor tilt. The possible sensor tilt is in contradiction with our expectation that the suspended sensor has to have very good vertical orientation and compensate pillar tilts. The further study is necessary to carry out for clarifying this behaviour.

CONCLUSIONS

The analysis of the temperature characteristics of the 1-second variometer LEMI-025, deployed in the upgraded observatory Icheon, South Korea, was carried out. The two complementary approaches – delta-F and base values analysis – were used. The latter allows us to determine the components' temperature coefficients, whereas the first of them effectively detects contributions to total field difference during the time intervals of absolute measurements. The considerable different effects of the sensor and electronics temperature variations was used to separate the temperature coefficients of the sensor head and the console. The significant non-linearity of the temperature dependencies, especially for the console, was revealed. The dF values after correcting temperature drifts do not exceed ± 0.5 nT during about one year.

The observed peculiarities of the console temperature characteristic is in good agreement with the laboratory tests of the temperature behaviour of the voltage reference used to form the bias fields along H and Z components. This fact gives us background to consider the voltage reference instability as a common source of the H and Z components' drifts due to the electronics temperature variations. We also supposed, that the sensor compensation windings, creating the bias fields, have equal temperature coefficients. Taking into account these assumptions, the temperature coefficients for total field difference, estimated by the delta-F method, were decomposed to estimate the coefficients of each sensor in proportion to the intensity of H and Z components. The comparison of delta-F and base value estimation reveal good agreement for the electronics temperature coefficients. The sensor temperature coefficients for components H and Z, estimated by the both methods, are significantly different. However, this difference could be explained by the sensor tilt. The reasons of the possible tilt of the suspended sensor need to be carefully studied in future. Obtained estimations of the temperature characteristics could be used for the correcting variometer data, but, due to the limited capabilities of such correction, it is recommended to consider possibility to stabilize the temperature of the instrument, especially its electronic unit. Using a temperature stabilized environment is the best way to reach very accurate measurements.

REFERENCES

Csontos A., L. Hegymegi, B. Heilig, 2007. 'Temperature Tests on Modern Magnetometers', Publs. Inst. Geophys. Pol.. Acad. Sc. C-99 (398) 171-177.

Intermagnet Technical Reference Manual, Version 4.6 2012. Edited by: Benoît St-Louis, 2012 http://www.intermagnet.org/publications/intermag_4-6.pdf.

J. Ind. Geophys. Union (January 2016)
Special Volume-2/ 2016 pp: 47-53

Observatory Data as a Proxy of Space Weather Parameters: The Importance of Historical Archives

P. Hejda
Institute of Geophysics of the CAS, Bocni II, 14131 Prague, Czech Republic,
ph@ig.cas.cz

ABSTRACT
Old geomagnetic observations are traditionally understood to be an important source of information about the structure and temporal behaviour (secular variation) of the internal geomagnetic field. A compilation of geomagnetic data from various parts of the world, recorded over several years allowed Gauss (*1839*) to separate the magnetic field into its parts of internal and external origin, and to prove that most of the geomagnetic field was of internal origin.

Each day satellites produce a huge amount of data on processes on the Sun, in the solar wind and in the Earth's environment, however, their span of operation is too short to allow for understanding of these processes and changes therein in the long term. On the other hand, geomagnetic observatories have been in operation for about 180 years; back ward reconstruction of solar processes may be possible based on the time series of various indices derived from observatory data that reflect responses to different combinations of solar wind parameters. Thus, digitization of these analogue observatory records and their printed records has become nowadays an exigent task. This paper contains a historical review of magnetic studies and measurements since the 16th century, followed by a case study in digitizing old magnetograms from the Prague-Clementinum Observatory. The problems connected with digitization, scaling and further processing of the data are discussed and preliminary results presented.

Key words: Geomagnetic observatory, Geomagnetic indices, Sunspot numbers, Space weather.

INTRODUCTION: REVIEW OF MAGNETIC OBSERVATIONS

Jonkers et al. (*2003*) collected over 150,000 declination measurements and nearly 20000 inclination measurements made between 1510 and 1930. The first sustained series of measurements at a single site in Greenwich showed that the geomagnetic field was subject to time-dependent change. Regular measurements of declination were started in Greenwich in 1816 to assist in the calibration of ships' compasses. The first measurements of declination in Paris were performed in 1541, and the Royal Astronomical Observatory was founded in Paris in 1667. Also regular measurements of inclination were carried out since 1671. A method for absolute measurements of magnetic intensity was proposed by Gauss (*1833*). The method combines vibration and deflection experiments in order to separate the intensity of the magnetic field and magnetic moment of the magnet used in the experiment. The method has now been re-interpreted by Van Baak (*2013*). In 1833, Gauss and Weber finished the construction of the magnetic observatory in Göttingen and developed or improved instruments to measure the magnetic field, such as the unifilar and bifilar magnetometer. The Göttingen Observatory became the prototype for many other observatories worldwide. The method of absolute determination of magnetic intensity made it possible to calibrate instruments locally.

Construction of instruments and improvements in observatory practice was not the purpose of Gauss' work, but just a tool for understanding of the nature and basic properties of the Earth's magnetic field. Gauss and Weber, therefore, joined the activity of Alexander von Humboldt in establishing a worldwide chain of observatories, known as the Göttingen Magnetic Union, which made simultaneous measurements at specific intervals (term days). The results were published in six volumes of the Results of Observations of the Magnetic Union (*Gauss and Weber, 1837-1843*). The simultaneous measurements started with 9 European observatories (6 of them in Germany) in 1836 and the number increased to 31 observatories in 1841: 18 in Europe (Berlin, Breda, Breslau (Wroclaw), Brussels, Christiania (Oslo), Copenhagen, Cracow, Geneva, Göttingen, Heidelberg, Kremsmünster, Leipzig, Makerstoun, Marburg, Milano, Prague, Stockholm, Uppsala), 4 in Russia (St. Petersburg, Ekaterinburg (Sverdlovsk), Nertschinsk, Barnaul), 3 in India (Shimla, Madras, Trivandrum), Auckland Island, Cambridge (US), Cape of Good Hope, St. Helena, Toronto, Van Diemens-Land (Tasmania). Most of them measured declination and horizontal intensity, others only declination. Publication of the Results ceased in1843. Prague Observatory discontinued these measurements in 1849.

Gauss and his collaborators believed that it would take just a few years of worldwide common observation of geomagnetic phenomena to unravel the mysteries of geomagnetism. It turned out that this view was

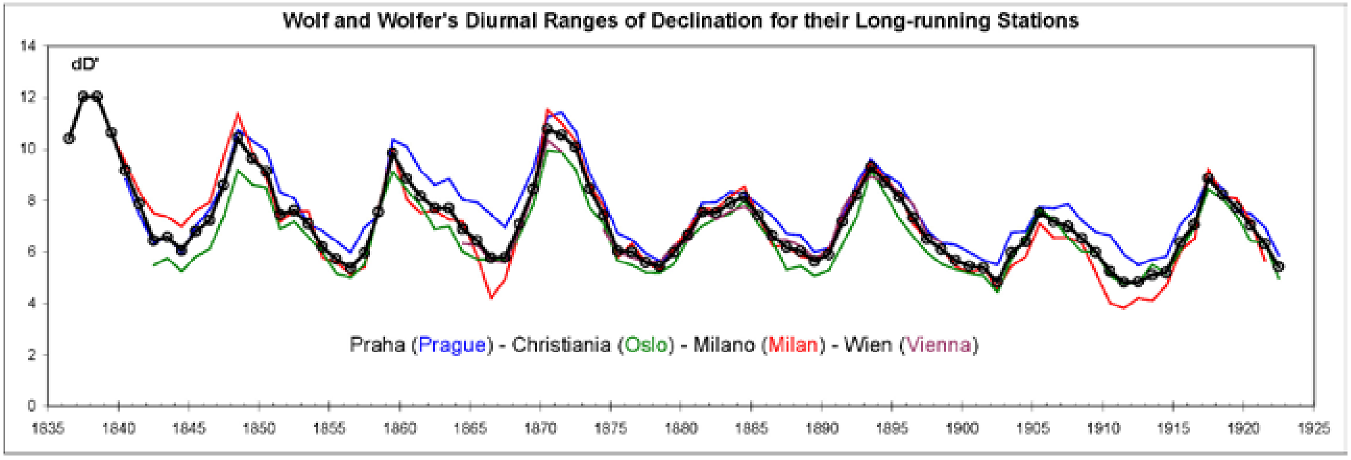

Figure 1. Diurnal ranges of declination obtained by Wolf and Wolfer from observatories in Prague, Oslo, Milano and Vienna and sunspot numbers (black curve), (Svalgaard, 2012)

too optimistic. However, considerable progress in the understanding of geomagnetism was achieved. Already in the third volume of Results, Gauss (*1839*) published the general theory of geomagnetism where he introduced the concept of spherical harmonic analysis and applied it to magnetic field measurements.

Most observatories operating within the Göttingen Magnetic Union were closed already in the 1840's or 1850's. Just a few observatories established before 1850 were in operation up to the year 1900 or later. According to the information about observatories from the regional reports in (*Gubbins and Herrero-Bervera, 2007*) and from the list of observatory yearly means in the WDCs, these were Clausthal, Colaba, Greenwich, Göttingen, Helsinki, Kew (London), Milano, Munich, Oslo (Christiania), Prague, Ekaterinburg (Sverdlovsk), Toronto and Wien.

OBSERVATORY DATA AS A PROXY OF SPACE WEATHER PARAMETERS

In 1806, Alexander von Humboldt organized regular night observations of magnetic declination. On December 21, he observed strong magnetic deflections and noticed the presence of northern lights overhead. Von Humboldt concluded that the magnetic disturbances on the ground and the auroras in the polar sky were two manifestations of the same phenomenon. He called this phenomenon magnetic storm.

The next step from atmosphere – solid Earth relations to true solar – terrestrial relations was taken by Edward Sabine (*1852*) and Rudolf Wolf (*1852*), who found an association between the sunspot cycle and geomagnetic activity. The impact of solar activity on the geomagnetic field was incontrovertibly proven seven years later. In September 1859, Richard Carrington saw by chance a bright outburst of light in a group of large sunspots, which was 17 hours later followed by an extremely strong magnetic storm. Its strength was recently estimated at Dst ~ 1600nT (*Tsurutani et al., 2003*). This event attracted public attention not only due to the extreme northern lights, but also due to the disruption of telegraph transmissions (*Boteler, 2006*).

Sunspot number is the oldest observed space weather (SW) parameter. These observations date back to the 17th century. As the time series of sunspot numbers were rather heterogeneous due to non-uniform methodology used in deriving them, Rudolf Wolf started a thorough revision around 1850 and defined a standard procedure for their derivation. In 1852, he discovered a connection between sunspots and the diurnal variation of the geomagnetic field and subsequently used the diurnal variation of declination to re-calibrate the sunspot numbers. Telescopic observations of sunspots were made by several observers as early as 1609 (*Stern, 2002*). The rapid increase in the number of observations and their quality was interrupted by the long period between 1645 and 1715 (the Maunder Minimum) when sunspots nearly disappeared. After sunspots became frequent again, they were not investigated systematically. Around 1850 Wolf began a search of historical sunspot observations, and during the next 40 years he produced a record of the sunspot number from 1700 onwards. His index is known as the Wolf Sunspot Number. It is defined as ten times the number of sunspot groups plus the number of individual sunspots, all multiplied by a correction factor for each observer. As the sunspots were observed by hundreds of observers, the homogeneity of the time series is the main concern.

Wolf realized that the connection between sunspots and diurnal variation of the geomagnetic field could be used as an independent check of the calibration of sunspot numbers. As the diurnal variation displays a strong seasonal dependency, the comparison was done on the basis of annual means. Wolf and his successor Wolfer carried out this comparison continuously using declination data from the observatories of Oslo, Prague, Milano and Wien (Vienna) (Figure 1). The results, published annually under the title Astronomische Mitteilungen, represent the first systematic study of the approximation of terrestrial phenomena with extraterrestrial, and vice versa. It was recently shown (see e.g. *Mursula et al, 2009*) that because the relation between the daily declination range and sunspots varies with season, the relation between the corresponding yearly averages is rather arbitrary and unreliable. It, however, does not detract from the importance of the Wolf's pioneering work.

In spite of Wolf's discovery, the mechanisms by which processes on the Sun can influence the Earth's environment remained unclear until the satellite observations in the 1960's. Since then, substantial progress has been achieved in our knowledge of Space Weather including the ability of short-term predictions. The complexity of geomagnetic variations has been characterized by various indices of geomagnetic activity. Their comparison with satellite observations revealed that some of them are closely related to solar wind parameters.

Julius Bartels defined the u-measure as the monthly or yearly mean of the unsigned differences between the mean values of the H-component on two successive days (expressed in units of 10nT). Svalgaard and Cliver (*2005*) found that essentially the same results are obtained using the mean over the whole day, over a few hours or only one hour. In the extreme, the same result is obtained even from a single night value. They also changed the scaling to units of 1 nT and called the index IDV (InterDiurnal Variability). The advantage of the IDV-index consists in the ability to compute a homogeneous series also for observatories with just a few recorded observations per day. However, such an advantage can be realised only when there exists at least one point value within a fixed night time. Comparison with satellite data has shown that on a timescale of a year the IDV-index is correlated with the Interplanetary Magnetic Field magnitude B, and, on the other hand, is insensitive to solar wind speed, V. It thus provides basic information about the yearly average of IMF 100 years before the satellite era (*Svalgaard and Cliver, 2005*, Figure 6).

Svalgaard and Cliver *(2007*) also introduced the IHV-index (InterHourly Variability) defined as the sum of the absolute values of the six differences between hourly values of any of the geomagnetic components for the seven hours spanning local midnight. The IHV-index averaged over Bartels rotation is a good proxy of BV^2. The index can be modified to hourly means instead of hourly point values. However, attention must be paid to proper recalibration (*Mursula and Martini, 2006*). As most observatories published printed yearbooks with hourly means derived from photo registration in the "pre-digital" era, there exists a vast quantity of valuable data that can be used for computation of improved quality of the IHV-index.. However, the oldest observatories in the 19th century (including Prague) often carried out manual measurements with just a few point values per day; the IHV-index thus cannot be calculated.

More detailed information about the utilization of geomagnetic observatory data for space weather studies has been detailed by Svalgaard (*2009*), He wrote: "As geomagnetic variations have been monitored for ~170 years with [for this purpose] constant calibration, we have a data set of immense value for understanding long-term changes in the Sun. We argue that all efforts must be expended to preserve and digitize these national and scientific treasure troves."

GEOMAGNETIC MEASUREMENTS AT PRAGUE OBSERVATORY

The observatory had its seat in the Clementinum College situated in the Old Town, close to the Charles Bridge. At the beginning of 18th century, an astronomical tower was built there, and in 1752 the Astronomical Observatory was established. An uninterrupted series of high quality temperature measurements dates back to January 1, 1775 and is well known to climatologists all over the world (*Sima, 2001*).

Kreil commenced work at the observatory of the Vienna University and in 1831 became assistant at the observatory de La Breda of Milano. He introduced magnetic observations there and participated from the very beginning in simultaneous measurements within the Göttingen Magnetic Union. In 1838 he was transferred to the Prague Observatory, of which he became Director in 1845. His main interest was in magnetic observations. He installed similar magnetic instruments at Prague, as he had used in Milano in order to continue his research. In view of the interest in science, reigning in Prague, he found willing collaborators there, and commenced regular hourly observations. Regular magnetic observations were started in July 1839 (*Kreil, 1842*). The equipment of the observatory were similar to the prototypes used in Göttingen. Simultaneous measurements at specific intervals (term days) within the Göttingen Magnetic Union were performed until 1849. In the first decade, measurements with a frequency of 2 minutes were also carried out during periods of magnetic storms. Due to increasing urban noise from the beginning of the 20th century, the observations were limited to the declination only, and the observatory was closed in 1926.

From the very beginning all measurements were published in the yearbooks called Magnetische und Meteorologische Beobachtungen zu Prag. The yearbooks contain tables of variation observations (magnetic and meteorological), reports on absolute magnetic measurements and discussions concerning their conversion to physical units. Variation observations were published

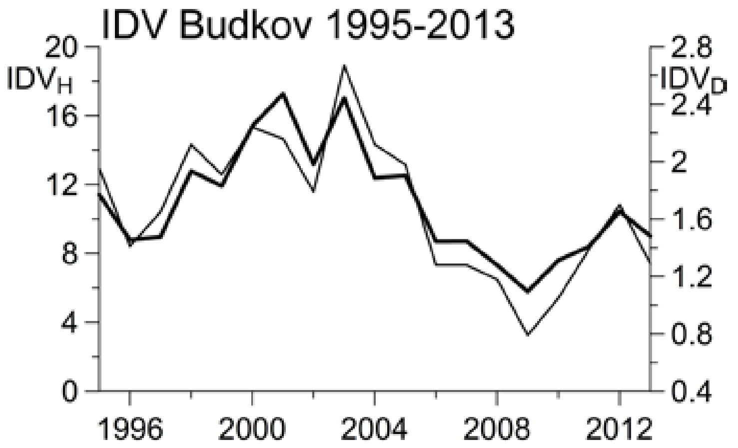

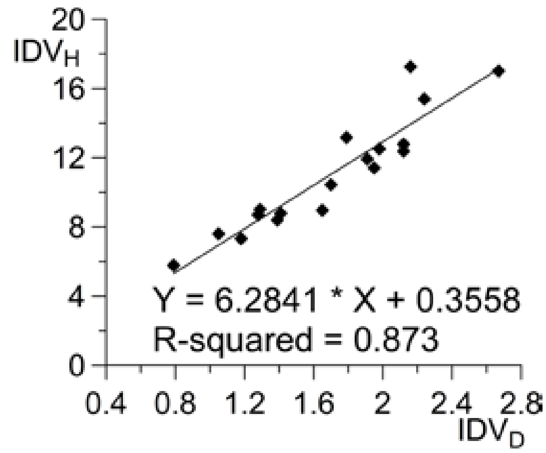

Figure 2. Left: Yearly means of the IDV-index computed from the horizontal intensity (IDVH thick line) and declination (IDVD – thin line) of Budkov Observatory. Right: IDVH vs. IDVD and the linear fit by rms. The index was calculated from momentary values at 21:20 UT, which corresponds to the calculation of IDV from Prague Observatory data in the period 1855-1904.

Table 1. Summary of daily measurements published in the yearbooks Magnetische und meteorologische Beobachtungen zu Prag.

Vol.	Years	Components	Time of measurements	Comments
1	1839 Jul - Dec	D, H, I	5, 6, 7, 8, 9, 10, 11, 10:30, 11:30, 12:30, 13, 13:30, 14:30, 15:30, 16:30, 18, 19, 20, 21, 22	scale units
1	1840 Jan – Jul	D, H, I	0, 2, 6, 7, 8, 9, 10, 11, 12, 13, 14, 15, 16, 17, 18, 19, 20, 21, 22, 23	scale units
2	1840 Aug – Dec	D, H, I	0, 2 or 4, 6, 8, 10, 12, 13, 14, 16, 18, 20, 22	scale units
2	1841 Jan – Jul	D, H, I	0, 4, 6, 8, 10, 12, 13, 14, 16, 18, 20, 22	scale units
3-4	1841 Aug 1843 Dec	D, ΔD, H, ΔH, I	6, 8, 10, 12, 13, 14, 16, 18, 20, 22	scale units ΔD = difference D(t) –D(t-5min), and similarly for ΔH
5-6	1844-45	D, ΔD, H, ΔH, I	6, 8, 10, 12, 13, 14, 16, 18, 20, 22	scale units not I at 22 h
7-11	1846 – 1850 Apr	D, ΔD, H, ΔH	6, 8, 10, 12, 13, 14, 16, 18, 20, 22	scale units
11-13	1850 May – 1852 Dec	D, H, ΔH, I	6, 8, 10, 12, 13, 14, 16, 18, 20, 22	scale units
14	1853	D, H, I	6, 14, 22	scale units
15-30	1854-69	D, H, I	6, 8, 10, 14, 22	scale units
31-32	1870-71	D, H, I	6, 10, 14, 18, 22	scale units
33-44	1872-83	D, H, I	6, 10, 14, 18, 22	scale units, D and H also in physical units
45-50	1884-89	D, H	6, 10, 14, 18, 22	physical units
51-53	1890-92	D, H	6, 10, 14, 22	physical units
54	1893	D, H	6, 7, 14, 21	physical units
55 - 65	1894-1904	D, H	7, 14, 21	physical units
66 - 78	1905-1917	D	7, 14,21	physical units; increasing urban noise

in scale units (scale-divisions) until 1871. In the period from 1872 to 1883 data in scale and physical units were published and from 1884 only data in physical units. Time stamps in the yearbooks show Göttingen astronomical time. Compared with Prague astronomical time the difference is 18 minutes. According to astronomical convention, 0 h is midnight and 12 h noon. The summary of magnetic variations is given in Table 1. The time of measurements in the Table corresponds to the Göttingen "civic time", i.e. 12:00 corresponds roughly to 11:20 UT.

DIGITISATION OF YEARBOOKS

Although some summary data were used already by Wolf and his successor Wolfer for calibration of sunspot numbers, the data as a whole stayed available only in the printed form of yearbooks. The recent interest in historical data, documented among others also by the project "Long-term reconstruction of Solar and Solar Wind Parameters" supported by the ISSI grant for 2012-2014, led us to the decision to digitize the data. In the first stage, all volumes of the yearbooks were scanned and transferred into pdf files. They are available via the author's web page *http://ig.cas.cz/en/geomagnetika/hejda*. Although the OCR was part of the scanning process, the adjacent text files contained too many errors to be useable for data digitization. The manual digitization was carried out by means of spreadsheets with pre-programmed templates that allow also for preliminary data check and repair of rough errors: computed monthly means were compared with monthly means published in the yearbooks. All declination and horizontal intensity data of regular observations have already been digitized. The digitization of the data from the disturbed periods will follow.

CONVERSION FROM SCALE UNITS TO PHYSICAL VALUES

The observations were published in scale units until 1871. While considered a drawback at first glance, this in fact had several advantages. The observatory staff understood that data users would have to convert the data to physical units and, therefore, provided not only variometer observations, but also all data obtained during absolute measurements. They are not limited by the parameters for conversion from scale to physical units that were set by editors of the yearbooks. Presently, everything is available for checking the calculations and correcting their errors, if needed. The usual formula for conversion from scale units to physical values is

physical_value = base_value + scaling_factor · (scale_units + instrument_corrections).

The scaling factor for declination or inclination is a geometrical problem of conversion from divisions on the scale to the angle (in degrees and arc minutes). Instrument corrections are not used. The base value must be obtained by comparison with absolute measurements, as the data are transferred (reduced) to the site of the absolute measurements.

The physical unit of horizontal intensity was Gauss emu ($=10^4$ nT). We converted it to nT in our outputs. As the magnetization of the needle depends to the temperature, the instrument corrections are far from being negligible if the temperature is not kept constant. On the time scale of years one must also account for the aging of the magnets. The calculation of parameters thus requires comparison of series of absolute measurements with variation observations. All declination data from 1840 to 1871 were converted to physical units. The scaling of the horizontal intensity requires a more detailed study of the comments presented in the yearbooks, because there were several interruptions and discontinuities caused, e.g., by fibre rupture and other accidents. Only the period from 1855 to 1871 has been processed so far.

The base value and instrument corrections are not important for space weather applications based on short-term variations (daily or interdiurnal), provided the daily variation of temperature is neglected. As the variation instruments were installed in a building with thick walls, this condition was satisfied. The daily variation was usually a few tenths of degree Reaumur (1°Re=1.25°C). Although the IDV index as per definition is calculated from the unsigned difference between the horizontal intensity at consecutive local midnights, the index can also be computed for any hour and for any magnetic element without losing the "IDV signature" (*Svalgaard and Cliver, 2010; Svalgaard, 2014*). This finding is of great importance, because the observations in the early 19th century are noisier than later observations, and the computation of the average of more data series, or their comparison, can improve the quality of the results. We have tested the substitutability of data on the yearly means of the IDV computed from the horizontal intensity, IDV_H, and from the declination, IDV_D, of the Budkov Observatory data for the period 1995-2013, and the results are satisfactory, see Figure 2. This fact can be used not only for improving the performance of the IDV index, but also as a test of the mutual consistency of the scaling factors of the horizontal intensity and declination. As the scaling of the declination is just a matter of geometrical arrangement, the scaling factor is stable. The value of 1 division on the scale changed from 27.226″ in 1839 to 29.064″ in 1872. The comparison of IDV_D with IDV_H can thus be interpreted as a test of the scaling factor of the horizontal intensity. A similar approach has already been applied by Svalgaard (*2014*) in identifying

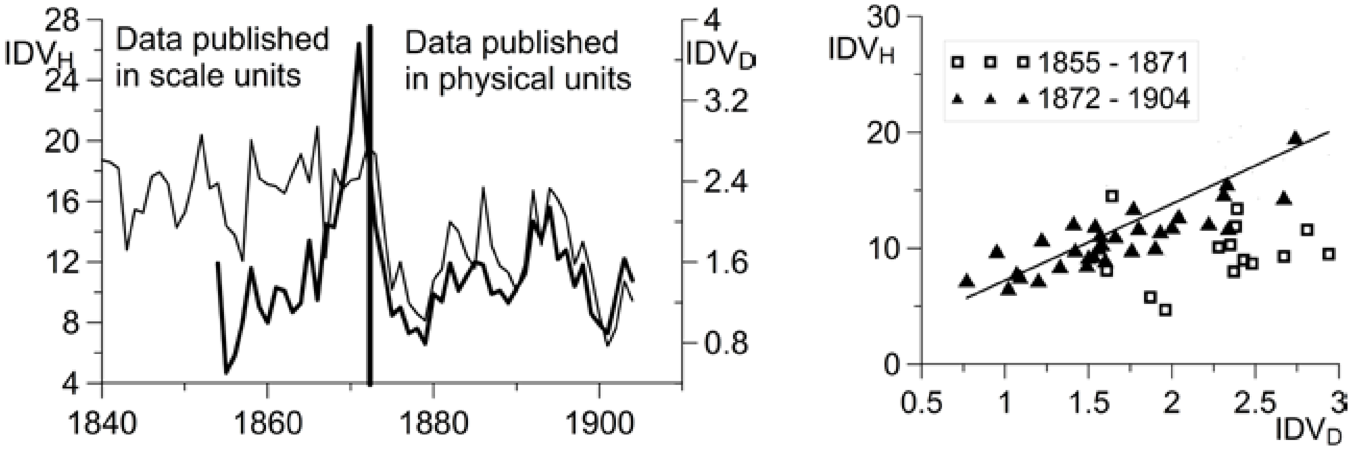

Figure 3. Left: Yearly means of the IDV-index computed from the horizontal intensity (IDVH thick line)and declination (IDVD – thin line) of Prague Observatory in the period 1855-1904. Right: IDVH vs. IDVD and the linear fit by rms. The index was calculated from momentary values at 22:00 Göttingen civic time (about 21:20 UT). Low values of IDVH before 1866 indicate a problem in scaling factors.

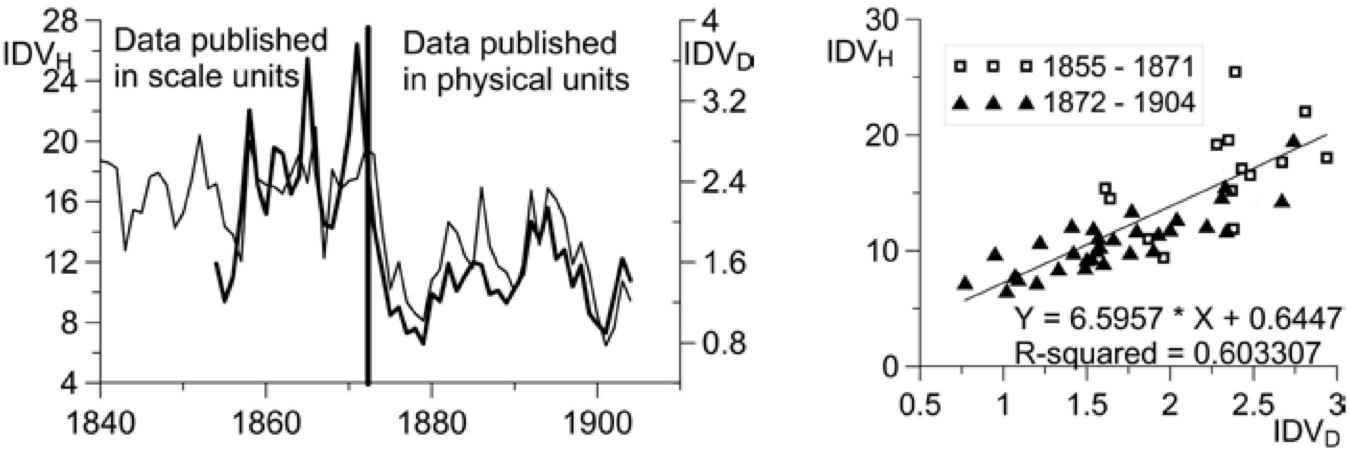

Figure 4. Left: Yearly means of the IDV-index computed from the horizontal intensity (IDVH thick line) and declination (IDVD – thin line) of Prague Observatory in the period 1855-1904. Right: IDVH vs. IDVD and the linear fit by rms. Improved correlation after the error was fixed and the scaling factor corrected.

errors in the scale values for the magnetic elements of the Helsinki Observatory.

Figure 3 shows the results of the test of IDV_H and IDV_D in the period from 1855 to 1904. We can see that the relation between IDV_H and IDV_D in the period 1855-1866 is much lower than after 1866. A check of volumes XVII (1856) to XXVII (1866) provided no explanation. However, we found the following footnote in volume XXVIII (1867): "by mistake, the scaling factors presented in Volumes XVII (1856) to XXVII (1866) were not related to physical units (Gauss) but to the horizontal intensity (about 1.9 Gauss)". This means that the scaling factor in this period should be multiplied by 1.9. After this correction, both the IDV_D and IDV_H look much more consistent (see Figure 4). However, these results must still be considered as preliminary and further analyses are required.

CONCLUSIONS

Modern science is based on experimental data and measurements. The data are mostly acquired in laboratories by pre-planned and carefully prepared experiments. By contrast, the laboratory of geophysical research is the entire planet Earth and the experiments are prepared by Mother Nature herself. Geophysical research depends on long-term continuous observations spread all over the globe. These precious data should be fully exploited.

The importance of historical data for space weather studies is manifold. On the one hand, historical data allows backward extension of data series of geomagnetic indices, which bear important information about physical properties of the solar wind in the past. On the other hand, newly derived geomagnetic indices and their alternates represent a suitable tool for detecting and correcting errors in the scaling factors of old magnetic data.

The stable operation and accuracy of absolute measurements at Prague Observatory for over 60 years in the period 1849-1926, provides a valuable resource to extend the series of geomagnetic indices backward in time. This would also be compared with the few long data series available (Greenwich-Kew, Helsinki). The digitization and processing of this data is in progress and first results are presented here.

ACKNOWLEDGEMENTS

The research was supported by the Grant LM2010008 of the Ministry of Education, Youth and Sport of the Czech Republic. Helpful comments of the reviewers is acknowledged

REFERENCES

Boteler, D.H., 2006. The super storms of August/September 1859 and their effects on the telegraph system. Adv. Space Res., v.38, pp.159-172.

Gauss, C.F., 1833. Intensitas vis magneticae terrestris ad mensuram absolutam revocata, Göttingen Geselschaft der Wissenschaften, Germany (English translation displayed at http://www.21stcenturysciencetech.com/translation.html).

Gauss, C.F. and W. Weber, 1837-1843. Resultate aus den Beobachtungen des magnetischen Vereins im Jahre 1836-1841 (6 volumes), Verlag der Dieterchschen Buchhandlung, Göttingen.

Gubbins, D. and E. Herrero-Bervera, 2007. Encyclopedia of Geomagnetism and Paleomagnetism. Springer, ISBN/13 : 978-1-4020-3992-8.

Jonkers, A. R. T., A. Jackson, and A. Murray, 2003. Four centuries of geomagnetic data from historical records, Rev. Geophys., v.41, no:2, doi:10.1029/2002RG000115.

Kreil, K., 1842. Magnetische und meteorologische Beobachtungen zu Prag, Wiener Zeitschrift für Physik, Chemie und Mineralogie, v.1, pp:18-37.

Mursula, K., and D. Martini, 2006. Centennial increase in geomagnetic activity: Latitudinal differences and global estimates. J. Geophys. Res., v.111, A08209, doi:10.1029/2005JA011549.

Mursula, K., I. Usoskin, and O. Yakovchouk, 2009. Does sunspot number calibration by the "magnetic needle" make sense? J. Atmos. Solar-Ter. Phys., v.71, no.17-18, pp:1717-1726.

Sabine, E., 1852. On periodical laws discoverable in the mean effects of the larger magnetic disturbances. R. Soc. Lond. Philos. Trans., pp:103–124.

Sima Z., 2001. Astronomy and Clementinum. National Library of the Czech republic, ISBN 80-7050-484-6

Stern, D., 2002. A millennium of geomagnetism, Rev. Geophys.,v.40, no.3, pp:1007-1035, doi:10.1029/2000RG000097, 2002.

Svalgaard, L., 2009. Observatory Data: a 170-year Sun-Earth Connection. In: Love, J.J., ed., Proceedings of the XIIIth IAGA Workshop on geomagnetic observatory instruments, data acquisition, and processing: U.S. Geological Survey Open-File Report 2009–1226, pp:246-257.

Svalgaard, L., 2012. How well do we know the sunspot number. Presentation at Colloquium at HAO, Boulder.

Svalgaard L, 2013. Solar activity – past, present, future. J. Space Weather Space Clim., v.3, no.A24.

Svalgaard, L., 2014. Correction of errors in scale values for magnetic elements for Helsinki. Ann. Geophys., v.32, pp:633–641, doi:10.5194/angeo-32-633-2014.

Svalgaard, L., and E. W. Cliver, 2005. The IDV index: Its derivation and use in inferring long-term variations of the interplanetary magnetic field strength, J. Geophys. Res., v.110 , A12103, doi:10.1029/2005JA011203

Svalgaard, L., and E. W. Cliver 2007. Interhourly variability index of geomagnetic activity and its use in deriving the long-term variation of solar wind speed, J. Geophys. Res., 112, A10111, doi:10.1029/2007JA012437.

Svalgaard, L., and E. W. Cliver, 2010. Heliospheric magnetic field. J. Geophys. Res., v.115, no.A09111, doi:10.1029/2009JA015069.

Tsurutani, B. T., W. D. Gonzalez, G. S. Lakhina, and S. Alex, 2003. The extreme magnetic storm of 1–2 September 1859,J. Geophys. Res., v.108, no.A, pp:1268-1275, doi:10.1029/2002JA009504, 2003.

Van Baak, D.A., 2013. Re-creating Gauss's method for non-electrical absolute measurements of magnetic fields and moments. Am. J. Phys. v.81, no:10, pp:738-744, http://dx.doi.org/10.1119/1.4816806

Wolf, J.R., 1852. Neue Untersuchungen über die Periode der Sonnenflecken und ihre Bedeutung. Mittheil. der Naturforsch. Geselschaft in Bern, v.245, pp:249-270.

J. Ind. Geophys. Union (January 2016)
Special Volume-2/ 2016 pp: 54-61

Methodological and Software Approaches to Processing of Magnetic Measurements at Observatories of IKIR FEB RAS, Russia

Sergey Y. Khomutov
IKIR FEB RAS, Paratunka, Kamchatka, Russia
Mirnaya str., 7, Paratunka, Elizovskiy district, Kamchatka region, 684034 Russia
khomutov@ikir.ru and hom@ngs.ru

ABSTRACT
Main methodological principles of the softwares used for processing the data of magnetic observatories of IKIR FEB RAS, Far East, Russia are presented, which are prepared using mathematical package MATLAB and Octave as set of scripts and functions with open code. The ultimate goal of the processing steps is to achieve the full vector of the magnetic field at every minute, including reported and adjusted data calculation. The softwares are designed so that: (a) visualization of data during all steps of processing is available; (b) intermediate files of partially processed data are not produced, only primary data are used during any step of processing, the additional procedures, such as noise removing, temperature correction accounting and so on, are used as separate modulus and files. The processing steps have been applied to data of different magnetometers to establish robustness of the method. The block diagrams of magnetic data processing and the examples of service files and screenshots are presented.

Keywords: Magnetic Observatory, Software, Magnetic data processing.

INTRODUCTION

The magnetic data obtained at magnetic observatories (MOs) are very important for fundamental and applied sciences. MOs are connected to world observational networks with specified standards of high quality data. At present, the INTERMAGNET is the most significant network of MOs (see *INTERMAGNET Technical reference manual, 2012*). The high standards of the specifications of the magnetometers, the method of the measurements and formats of the resulting data are defined for INTERMAGNET observatories (IMOs). But methods, algorithms and software of the data processing adopted at each IMO are defined by individual observatories; there are no set standards for these procedures.

Recent publications, including the presentations at IAGA 2014 Workshop in Hyderabad (XVI IAGA Workshop, 2014), have shown that the prospects of having system of completely automated measurements at IMOs seem unlikely in near future. Therefore the current system of magnetic observations in accordance with INTERMAGNET standards is continued. In absence of unified and standardized method for processing and analysis of the data obtained by IMOs, it is difficult to ensure delivery of uniform quality of quasi-definitive and definitive data for all IMOs, especially for organizations that have several IMOs and for IMOs in remote locations without a full team of observatory scientists. Transmission of data in near real time is a priority of INTERMAGNET, which is easily achievable with today's technology of telecommunication. But the gaps in the "IMO – GIN" link are clearly visible due to lack of effective and user-friendly software, which may be used directly at IMOs.

The Institute of Cosmophysical Research and Radio Wave Propagation of the Far Eastern Branch of Russian Academy of Science (IKIR FEB RAS) have four magnetic observatories located at the Far East in wide range of the latitude (see Table 1). Three of these MO are observatories of the INTERMAGNET. MOs are equipped by modern vector and scalar (FGE DTU, GSM-90, GEM dIdD, POS-4) and absolute (DIflux LEMI-203, MAG-01H, POS-1, GSM-19W) magnetometers and systems for current and definitive processing of the data.

ALGORITHMIC AND SOFTWARE REALIZATION

MATLAB (and similar free package Octave) is used as the platform for the data processing software presented here. The software packages provide a scripting environment; the advantage of text format scripts being that they can be easily modified for the unique configuration of each observatory. MATLAB have expanded possibilities of the graphics that is very important for the visualization of data. Some standard tools, which allow read/write of wide variety of data formats and sufficient memory for large datasets are additional advantages of these platforms. In software of IKIR MOs we used only command window mode, without any visual-like applications.

Because all four observatories are divisions of the single institute, there is no problem with unification of the software - almost all of the modules, scripts and files have the same structure. Differences arise mainly because of differences in hardware used: each type of magnetometer generate unique types of raw data files. For example there are significant differences for the HDZ-variometer (eg, FGE-DTU) and FDI-

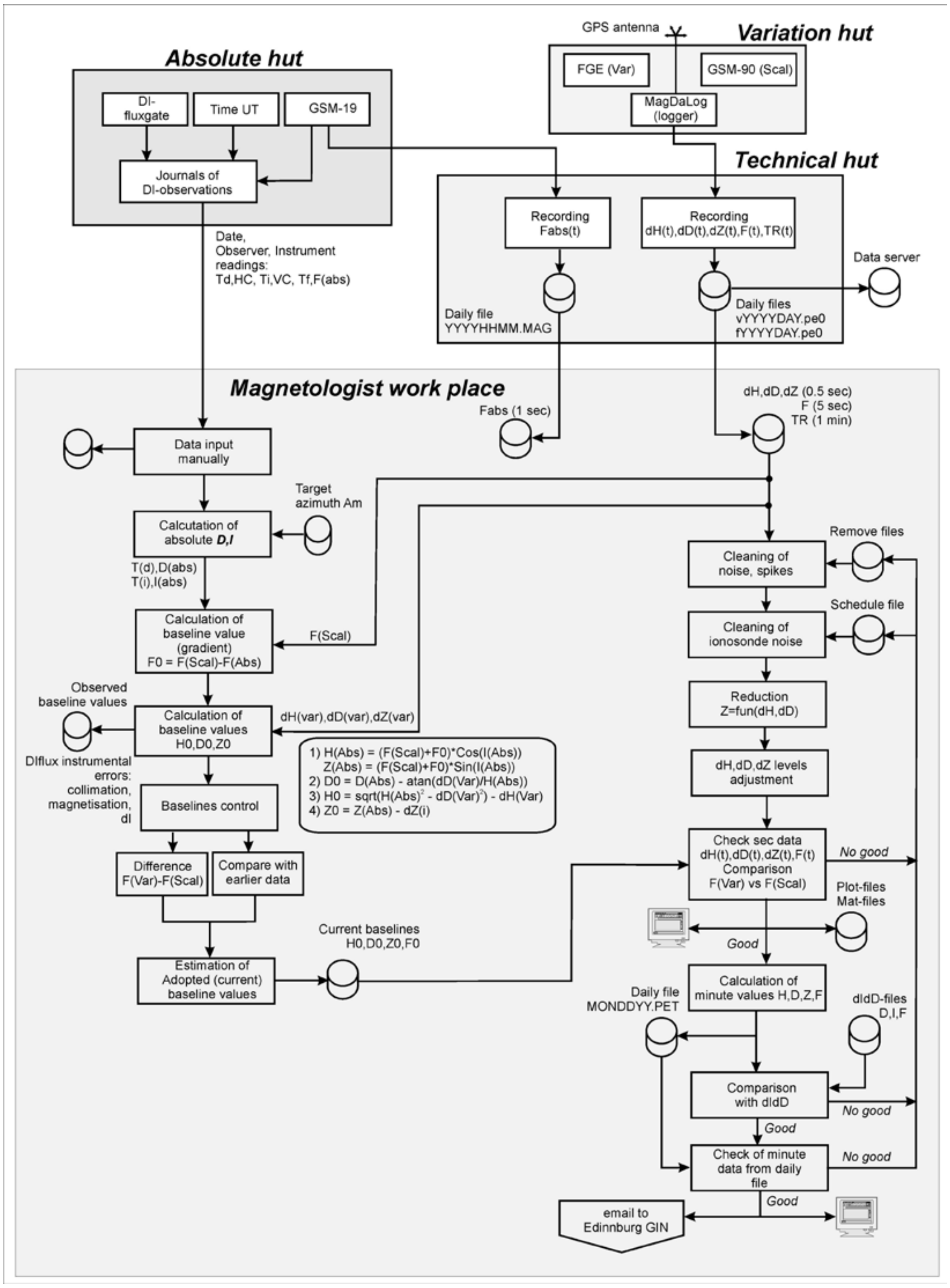

Figure 1. Diagram of the processing of the magnetic data of the main vector magnetometer FGE at observatory "Paratunka"

Table 1. The observatories of IKIR FEB RAS, the Far East, Russia

Observatory	Year	IAGA	IMO	Geograph		Geomag	
Cape Schmidt (Chukotka)	1967	CPS	No	68.9	180.6	64.0	231.5
Magadan (Stekolniy)	1965	MGD	2009	60.1	150.7	52.0	213.1
Paratunka (Kamchatka)	1968	PET	2013	53.0	158.3	45.8	221.5
Khabarovsk (Zabaykalskoe)	1968	KHB	2013	47.7	134.7	38.4	202.5

variometer (dIdD GSM-19FD). However, for the same type of devices the software is almost identical, for example, for the fluxgate FGE and MAGDAS. There are also differences in processing the results of the absolute observations, depending on the used magnetometers and techniques.

The general scheme for processing of magnetic measurements (by FGE only, as example) is presented at Figure 1. Most of the steps are routine in observatory practice. A few additional blocks will be explained in the main section of the article. The block "Reduction of Z=fun(dH,dD)" is used to remove the dependence of component Z from variations of horizontal components dH (about 1.3%) and dD (about 0.1%); the possible reason of this dependence is non-orthogonality of sensor Z to horizontal plane. The block ""Journals of DI-observations" means hand-filled form of observations, with readings of vertical (HC) and horizontal (VC) circles of a theodolite and values of total field F.

THE MAIN PRINCIPLES

Long experience of practical work at MOs, the standards and manual of INTERMAGNET and interaction with colleagues have allowed us to identify some principles, which can be used for methodical structuring of software (s/w) to be used at IMOs.

(1) Processing of the results of the measurements must be performed directly at the observatory, directly after the measurements, and by the staff of the observatory (magnetologists)

This approach enforces quick detection of problems with the magnetic measurements and quick estimation of the situation at the observatory in order to plan and take appropriate and effective solutions. The most common problem that arises is the lack of qualified personnel. However, if the observatory meets INTERMAGNET standards, i.e. there is good control of the basic operating environment of the variometer, then the work requirements on staff is minimised and staff with the necessary skills are more likely to be available.

(2) Input file for any stage of processing should be the primary data; creation and use of files of intermediate data should be kept to a minimum

The ordinary practice during the processing of magnetic data (for example, the calculation of the minute values of different status) generates a large number of intermediate files after execution of each step often simply due to changes of format, which are not explicitly tagged as output. For example, the application of the temperature corrections to the raw data file FILE0 leads to the creation of FILE1, next removing of noise - to FILE2, the adoption of the baseline values - to FILE3, etc. An alternative would be to use the transparent processing, where each procedure (temperature correction, obtaining of total field components, etc.) is one of consecutive and mandatory phases of the script. Thus intermediate files generated, will reside only in the computer's memory and output files contain only final results. In our s/w the script reads the original data at each stage of processing; the information to initialise each step is stored in the script itself.

The efficacy of this approach can be illustrated by the processing of the measurements of the main fluxgate vector magnetometer FGE to remove large amplitude noise recorded during occurrence of strong earthquakes (see module "Cleaning of noise, spikes" at Figure 1). Because the FGE sensors are suspended by a gimbaled joint, seismic movement of the pillar swings the sensors, introducing artificial signal to the magnetic data. Figure 2 show a part of record of D component during 19 May, 2013, which shows the effects of an earthquake of magnitude 6.5 at distance of 340 km from IMO PET (Paratunka), Kamchatka. The effects of the aftershocks are also visible in the magnetic data. It is clear that these oscillations with amplitude up to 100 nT must be removed. The magnetologist visually estimate the time interval of the earthquake effect from the plots and note to special text file the record similar "2013 05 19 18.6948 18.8508 111", where it is pointed the date, started and finish times of the interval and flags of applicability to the H,D,Z components. After restarting, the script reads this record and flags the data (in memory) with the symbol NaN (Not-a-Number) to indicate that these data aren't to be used during the next steps of processing. The effects are visible as a gap in the plot of Figure 2. For the next earthquake the new line "2013 05 19 19.3648 19.4154 111" are added to the file and so on.

This technique can be applied for removal of regularly recurring noise. For example, during the vertical sounding of the ionosphere by the ionosonde placed at the distance about 300 meters from magnetometers, there may be the pulses up to 1-2 nT in FGE data. The repetition of the sounding is 15 minutes. Figure 3 show the differences F(var)-F(scal) with clearly visible spikes. The procedure of the removing of this noise (see module "Cleaning of ionosonde noise" at Figure 1) use the information from special file with records similar to "2013 05 18 00 00 00 2013 05 20 23 59 59 15 +042 +049", where date and time of the beginning and ending of the sounding, interval between sessions (in minutes) and beginning and ending of the noise interval (in seconds) relatively to sounding session start time are presented; for example, the magnetic data during 14:45:42-14:45:49, 19 May, 2013 will be replaced by NaNs. The results are presented at Figure 3 (middle and lower panels).

Another example of this approach can be the correction of jumps in records (see module "dH,dD,dD levels adjustment" at Figure 1). The shifting of the data by the appropriate constant value allows to fix the problem.

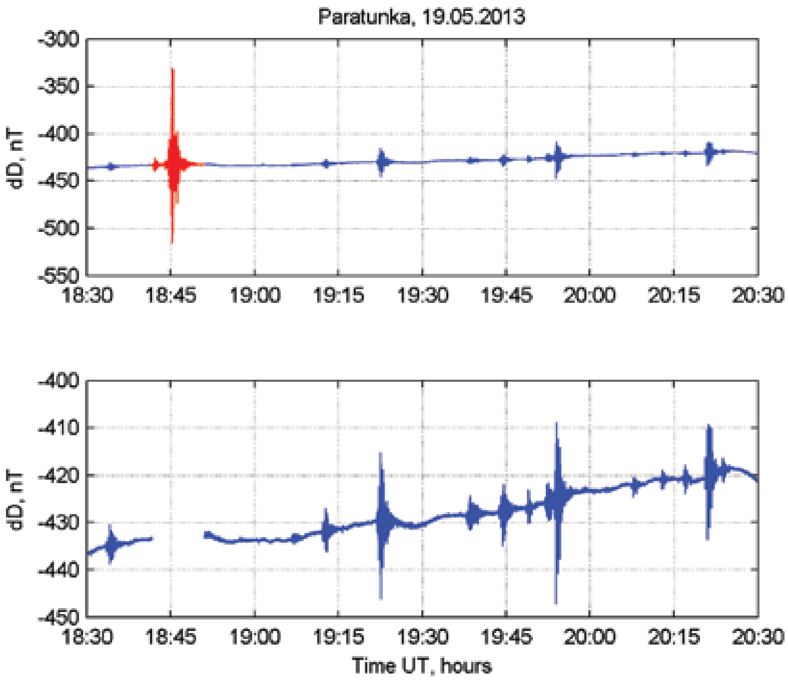

Figure 2. The example of the removing of the earthquake effect on the suspended fluxgate sensors during earthquakes. Upper panel: initial record; lower panel – record with the removed main shock effect.

Figure 4 shows the part of the records of D components of the fluxgate FGE, when after the earthquake of February 19, 2015 levels of all components were changed. The information in special file with lines similar "2015 02 19 16 33 20 2015 02 19 23 59 59 -02.32 +01.470 +01.00 +00.00", where the start and finish of the corrected interval and values of shifting are presented, is used by script. The initial and resulting plots are shown at Figure 4.

(3) Routine processing, nominally everyday, must generate data with the status close to quasi-definitive, i.e. taking into account the real baselines and after removing of the noise

Efforts made to achieve high quality, near quasi-definitive data at the end of each day will necessarily have several benefits including generation of good quality quasi-definitive and definitive data very quickly

- the estimation of the current (adopted) baseline values would be performed almost immediately after the absolute observations to provide "real-time" control of the quality of the absolute observations and quality of the baselines
- generation of total field vector time series for different magnetometers for effective comparison between heterogeneous data that can be used to quickly identify potential problems
- filling of gaps with data from backup device(s) in case of data gaps in main vector magnetometer, by simple substitution of "9s" in files in IMF or IAGA2002 formats by good values

Figure 5 show an example of data plots and difference plots of everyday processing, where the comparison of the horizontal component H of the main vector magnetometer FGE with data of the backup magnetometer GEM dIdD and Japanese fluxgate device FRG-601 is presented. This comparison is simple to achieve since the adopted baselines of all magnetometers were obtained on daily basis as close to "quasi-definitive" mode, without any delay. Similar plots are made for other components and for other devices. These differences allow detection of noise up to 0.1 nT against the background variations with range up to tens of nT. The magnetometers installed in different pavilions or at different pillars in the same pavilion function as gradiometers with the base ranging from meters to tens of meters.

(4) the maximal visualization of data should be provided at every step of the processing

The visual presentation of the results of the measurements and processing are powerful tools for the analysis of the large amount of data. By default, packages MATLAB and Octave offer graphical functions that provide for scaling, annotating, marking, returning coordinates, etc. and these are used in the developed software. The goals of graphical possibilities of the software are:

- the simplification of the perception of complex graphs (e.g., several curves in one panel)
- the indication (by color markers) of the poor data or deleted data
- re-scaling graphs to zoom in on details, which allows information to be interpreted directly from the curves

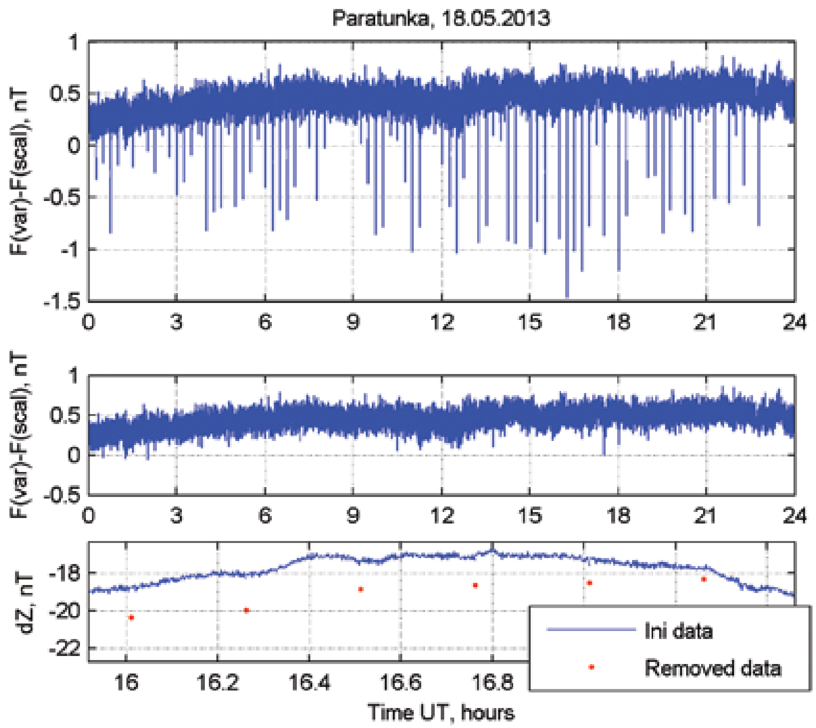

Figure 3. The example of the clearing of the noise in the magnetic data from the vertical sounding.

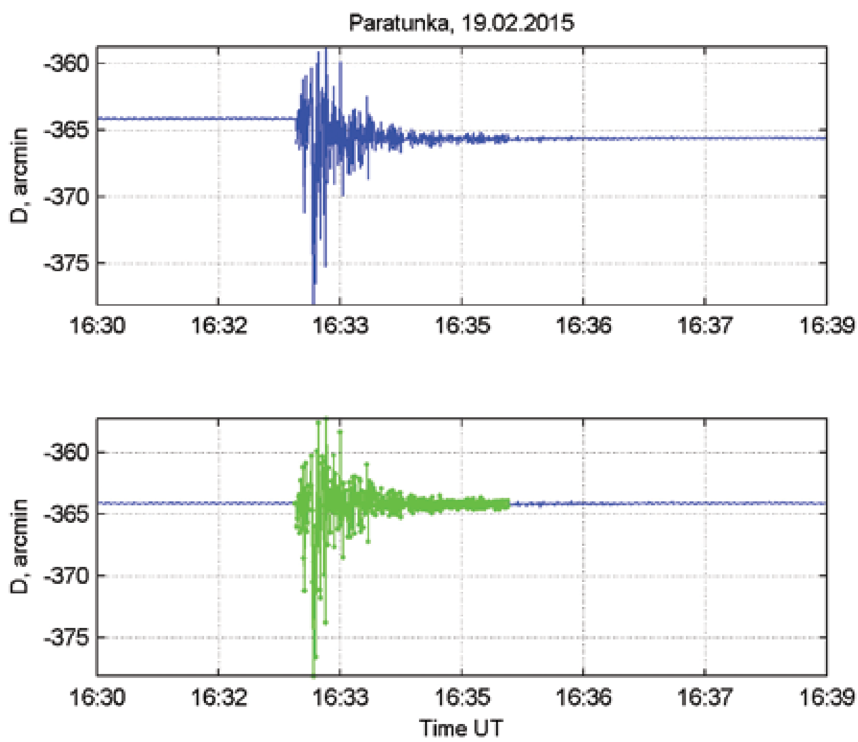

Figure 4. The example of the correction of the jump in the record level after strong earthquake. Upper panel – initial data with jump of -1.5' in D component, lower panel – after correction of jump and removing of earthquake effect (marked by dot).

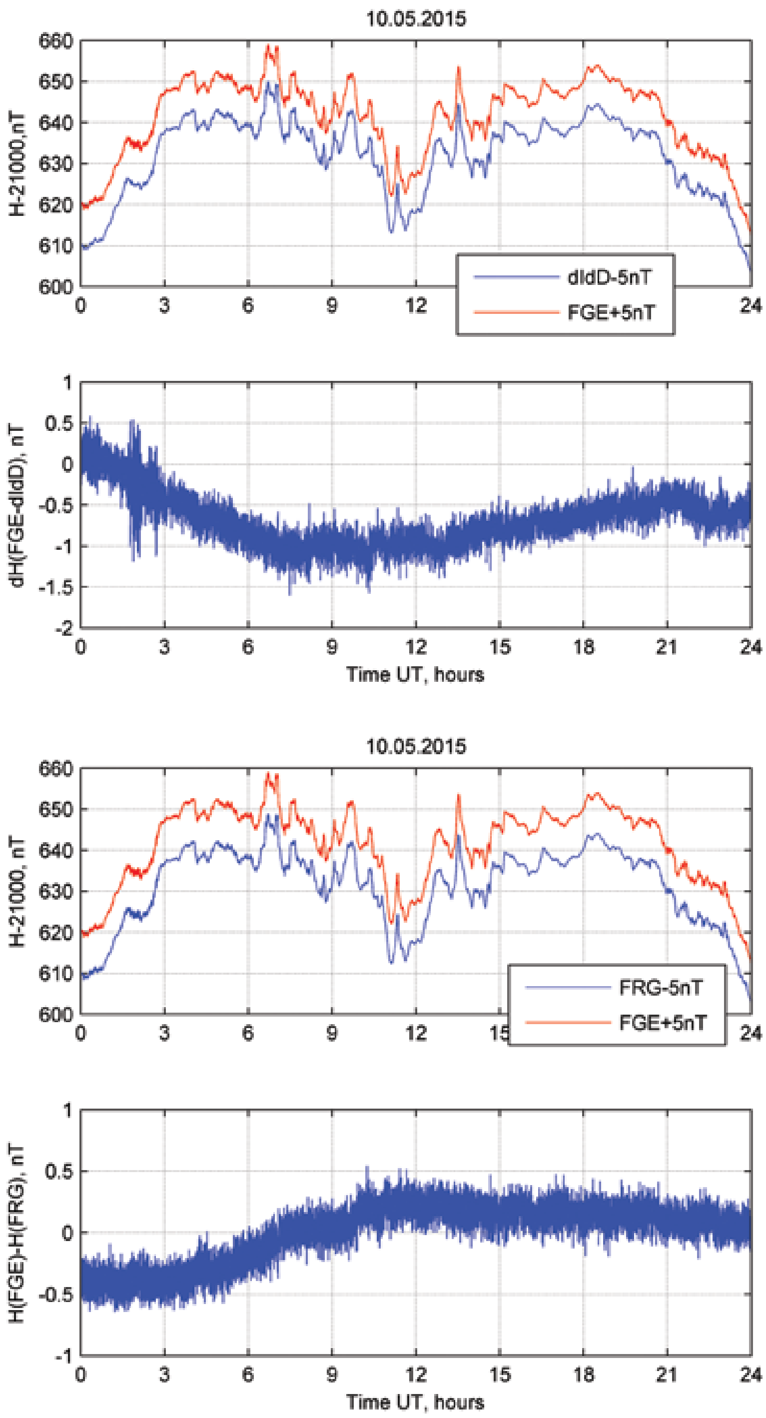

Figure 5. Comparison of the second values of the horizontal component H of the main vector magnetometer FGE (IMO PET) with data of GEM dIdD (two upper panels) and Japanese fluxgate variometer FRG-601 (two lower panels). Total values of H were calculated with "quasi-real" baselines.

Figure 6 presents the graphs, which are plotted during the processing of the absolute observations. These plots make it simple for the magnetologist to compare observations with recorded field values, allowing them to evaluate the accuracy of the absolute observation form, typing data to file and to determine the behaviour of the field at these points of time (disturbances, noise etc.).

Figure 7 presents the results of the absolute observations after processing of baselines as obtained from two DIflux (LEMI-203 and Mag-01H) by five observers, marked in

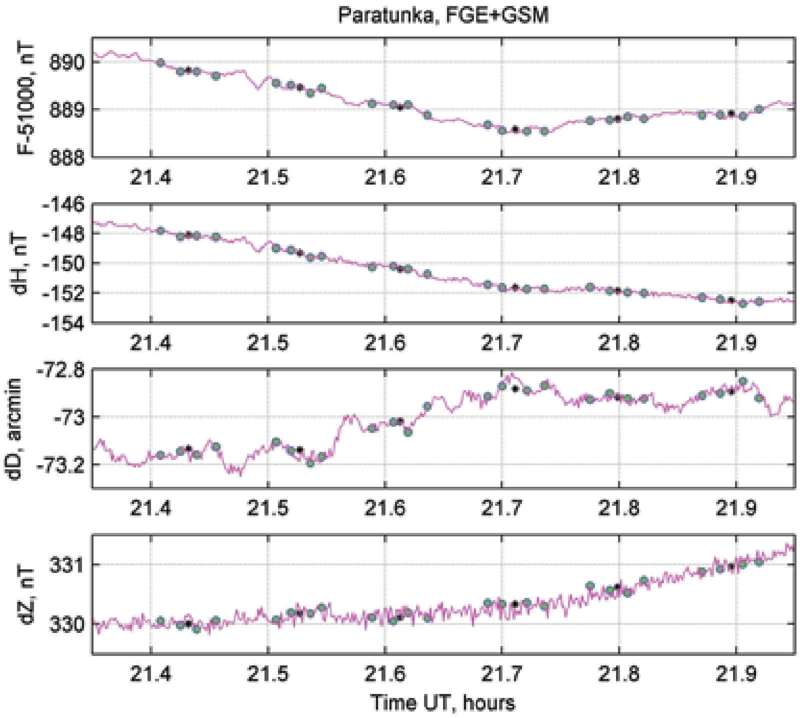

Figure 6. The plot of the data of the vector (dH, dD, dZ) and scalar (F) magnetometers during the processing of the results of the absolute observations. Solid curves are initial (second) data, circle markers indicate the values at time of "zero-position" of the DIflux during absolute observations and asterisk are the averages of the field values and time data.

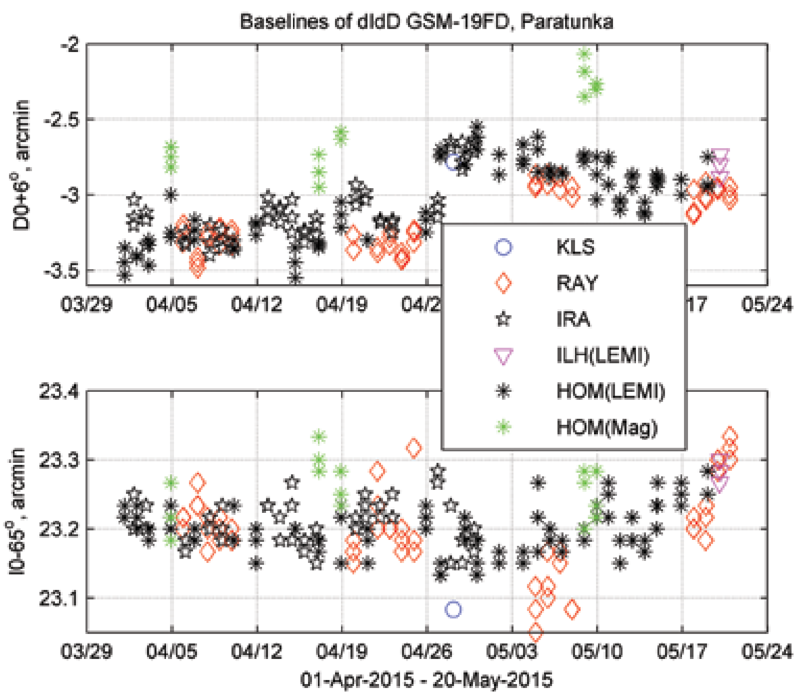

Figure 7. The example of the graphs of the baseline values for dIdD (IMO PET), which the observer can see after the processing of absolute observations.

different colors and symbols. Similar plots are generated directly after processing each absolute observation, such that the observer can estimate the quality of results and correct data or reject resulting baseline values.

Similar plots to those shown in Figures 2-5 are displayed at every step of processing, aimed at highlighting similarities and differences. For example, the showing of the variations dH,dD,dZ at separate panels allow easy scaling of every curve by amplitude. Presentation of three curves in single plot make it easy to select data fragments of interest by time. It is also important to note that all the principles presented above which are realized at magnetic observatories of IKIR FEB RAS primarily focused on the processing of the worst-case situations: crashes and hardware failure, noise, mistakes of magnetologist during manual work and so on. It is clear that under ordinary conditions all procedures can reliably operate in automatic mode.

CONCLUSIONS

Over the recent decades a lot of progress has been made in the standardisation of equipment and services for acquisition and publication of data in magnetic observatories around the world. However, there are problems with processing and the primary data analysis, the methods of which have been developed by observatories in their own traditions and do not conform to a uniform framework of Standard Operating Procedures (SOP). Availability of an efficient, comfortable and user oriented software for such processing for all the steps of data generation would make a huge difference to reporting of quality data to the global network.

The observatory of IKIR FEB RAS uses a new program to process magnetic data both for everyday reporting and for the preparation of quasi-definitive and definitive data. Software was developed under MATLAB and OCTAVE packages, have open source code and can be expanded and modified to specific instruments and possibilities of every observatories. The basis of the software incorporated several methodological principles generally oriented to work with the data by magnetologist directly at observatory, including under abnormal situations. Some part of software is also used at other INTERMAGNET observatories (Novosibirsk, Yakutsk, Alma-Ata).

ACKNOWLEDGEMENTS

The author thanks the colleagues from magnetic observatories "Klyuchi" (Novosibirsk) and "Khabarovsk", especially Olga Fedotova and Zinaida Dumbrava, for useful discussions during practical application of developed software. I wish to thank Stanislav Nechaev and Hans-Joachim Linthe for the good ideas and important advices. The work is supported by Russian Scientific Foundation, grant #14-11-00194. The author is very grateful to the referees and the Editorial Advisor for comments and corrections made in the manuscript. They greatly improved the method and quality of presentation.

REFERENCES

INTERMAGNET TECHNICAL REFERENCE MANUAL. Version 4.6. Edited by: Benoît St-Louis, 2012. 92 p.

XVI IAGA Workshop on Geomagnetic Observatory, Instruments, Data Acquisition and Processing, Oct. 7-16, 2014, Hyderabad, India. Abstract Volume. 2014. 55 p.

J. Ind. Geophys. Union (January 2016)
Special Volume-2/ 2016 pp: 62-66

The One Second data collection system in Polish geomagnetic observatories

Jan Reda, Mariusz Neska

Institute of Geophysics Polish Academy of Sciences,
ul.Ksiecia Janusza 64, 01-452 Warsaw, Poland
jreda@igf.edu.pl, nemar@igf.edu.pl

ABSTRACT

Over the last half decade, recording of Earth's magnetic field with a sampling rate of 1 second is becoming a new standard in geomagnetic observatories, especially in case of observatories belonging to INTERMAGNET (International Real-time Magnetic Observatory Network). Observatories belonging to our institute, which is responsible for all Polish geomagnetic observatories, have successfully introduced such a 1-sec data collection system. This system consists of a magnetometer, a special digital recorder, and appropriate hardware for processing and sending the data to the data collection centres. We use different types of magnetometers, both the most popular ones equipped with flux-gate sensors and the older ones equipped with Bobrov-type quartz variometers. Both types of magnetometers are characterized by low noise and good long-term stability. One-second data are not only stored on hard disks but also sent to INTERMAGNET GIN (Geomagnetic Information Node) in Edinburgh in real time. The typical real-time delay when providing data to GIN is less than 5 minutes. Therefore such data can be used in real-time applications, e.g. space weather forecasts.

Keywords: Geomagnetic observatory, INTERMAGNET, Real time data, Magnetometer.

INTRODUCTION

There is growing demand for 1 second magnetic variation data. Another important issue is to provide data in near real-time, i.e. with the minimum possible delay. The 1 second data are needed by space physicists studying rapid variations of external origin, such as ULF waves and sudden impulses (*Chulliat et al., 2009*). Near real time data becomes particularly crucial for issues related to space weather forecasting. 1 second data recording in geomagnetic observatories has also become very important because of SWARM and CHAMP satellite missions,to minimize spatiotemporal aliasing, in collating the data with these low-Earth-orbiting magnetic field satellites. Detailed ground-space analyses require 1-second observatory data (*Love and Finn, 2011*).

The only institution in Poland performing standard stationary observations of the geomagnetic field is the Institute of Geophysics, Polish Academy of Sciences (IGF PAS). Such observations consist of a continuous one-second recording of changes of three orthogonal components of the geomagnetic field, and of absolute measurements of the elements of the total geomagnetic field that are carried out regularly.

Currently such observations are conducted in all three observatories of our institute, i.e.:

- The Central Geophysical Observatory at Belsk (BEL, Central Poland),
- The Geophysical Observatory at Hel (HLP, north of Poland),
- The Polish Polar Station at Hornsund (HRN, Spitsbergen)

Routine digital geomagnetic field recordings were initiated in Polish observatories in the first half of the 1980s. Since 1984 Belsk Observatory has begun recording with a digital recorder using tape cassettes developed in our institute. Undoubtedly, this was a turning point compared to analog recording on photographic paper used before. The introduction of digital technology in observatories increased the comfort of observation, reduced the likelihood of human mistakes, and at the same time gave the opportunity of faster sharing of observation data.

A few years after implementation of digital recording techniques, BEL observatory joined the INTERMAGNET in 1992 (*Love and Chulliat, 2013*). HLP and HRN Observatories became members of INTERMAGNET in 1999 and 2002, respectively.

Initially, the sampling period was only 30 seconds with an A/D resolution of 12 bits, and dynamic range ±500 nT. In the following years the digital recording system was modernized. Both resolution of A/D conversion and sampling frequency were increased. A continuous recording with a sampling period of one second began in Belsk observatory in 2002.

INTERMAGNET enjoys a high prestige due to the fact (among others) that it brings together modern observatories providing high-quality data. Joining INTERMAGNET has brought not only prestige to our magnetic observatories, but also has had a positive impact on their development. The best evidence for this is the inclusion of our observatories in the Quasi-Definitive program and the delivery of real-time one-second data to INTERMAGNET.

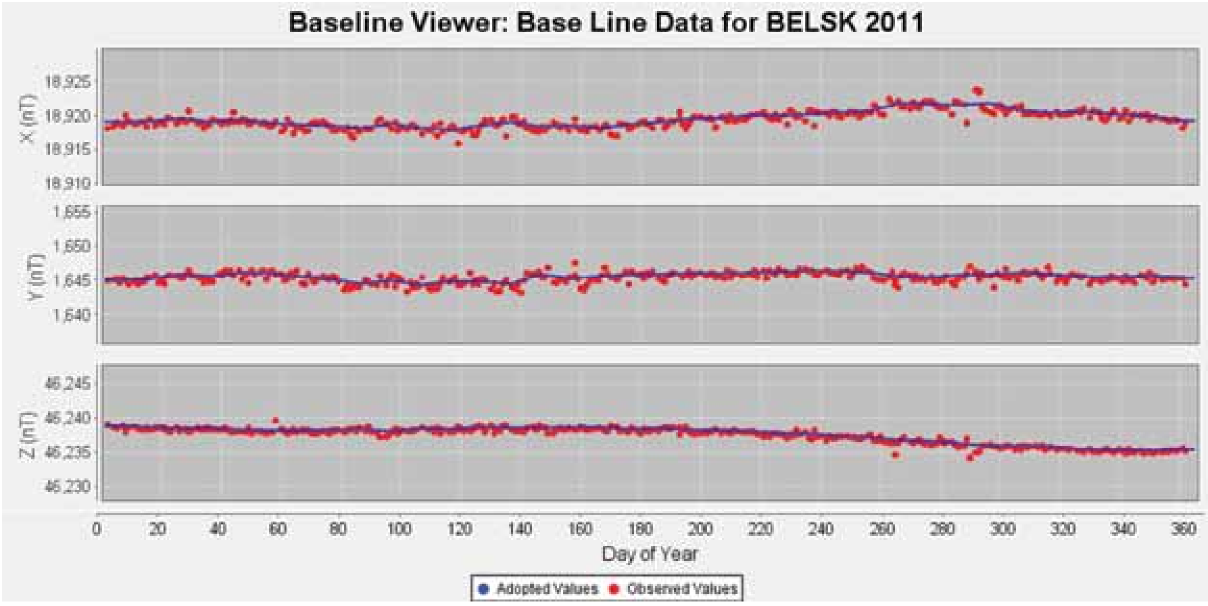

Figure 1. Baselines of PSM magnetometer from the Belsk Observatory.

MAGNETOMETERS

Observations of the Earth's magnetic field consist of absolute measurements and continuous recording of geomagnetic field changes.

Absolute measurements are conducted in the same way in most observatories of the world, i.e., by measuring both inclination (I) and declination (D) by means of a D/I-fluxgate magnetometer, and the total field (F) by a proton magnetometer.

We use the following D/I-fluxgate magnetometers:

- Belsk observatory: ELSEC-810 and GEOMAG-03 (manufacturer: GEOMAGNET).
- Hel and Hornsund observatory: FLUX-9408 (manufacturer: Institute of Geophysics PAS).

For total field measurements, we use PMP-8 and PMP-5 proton magnetometers that have been developed and produced in our institute.

The pool of variometers, i.e., the magnetometers used for recording geomagnetic field variations is more varied. In Belsk and Hel mainly PSM (Polish: Przenona Stacja Magnetyczna, English: portable magnetic station) magnetometers constructed in our Institute are used (*Jankowski et al. 1984*). These magnetometers were produced in small series from the late 1970s to the late 1990s. The basis of their construction is the Bobrov quartz variometer. Bobrov variometers consist of magnets and mirrors suspended on quartz fibres. Originally, such variometers were used for classical recording on photographic paper. In PSM magnetometers, photoelectric converters are added to the classical Bobrov variometers. Due to photoelectric converters and negative feedback, PSM magnetometers produce analog signals proportional to changes of the magnetic field. Even today the metrological parameters of PSM magnetometers are only minimally lower than those of the best flux-gate magnetometers. They have a good long-term stability and low noise. The disadvantages of PSMs are their complicated installation and service, large dimensions and weight, and considerable power consumption. Figure 1 illustrates the stability of a PSM magnetometer.

Standard PSM magnetometers have a 0.3 Hz analog low-pass filter, but in the exemplars used in our observatories the cut-off frequency has been increased up to 3 Hz. However, it should be noted that the sampling of analog signal is carried out with a frequency of 12,800 Hz.

Nowadays, we use fluxgate-type magnetometers in the Polish Polar Station Hornsund at Spitsbergen for the measurement of field changes. For the primary data set, a modern GEOMAG-02 magnetometer manufactured by the Ukrainian company GEOMAGNET is deployed. An older one (LEMI-03, also Ukrainian, made by Centre of the Institute of Space Research (*Korepanov et al., 1998*) is used as a backup magnetometer.

The most important reasons for the use of GEOMAG-02 magnetometer are the following:

- Low noise level and good stability,
- Cardan-suspended variometer sensor, which is very important in arctic conditions because of freezing / unfreezing ground during autumn and spring.
- Friendly use by the rotating shift personnel.
- The magnetometer is equipped with both analog output and flash memory-based digital data logger.

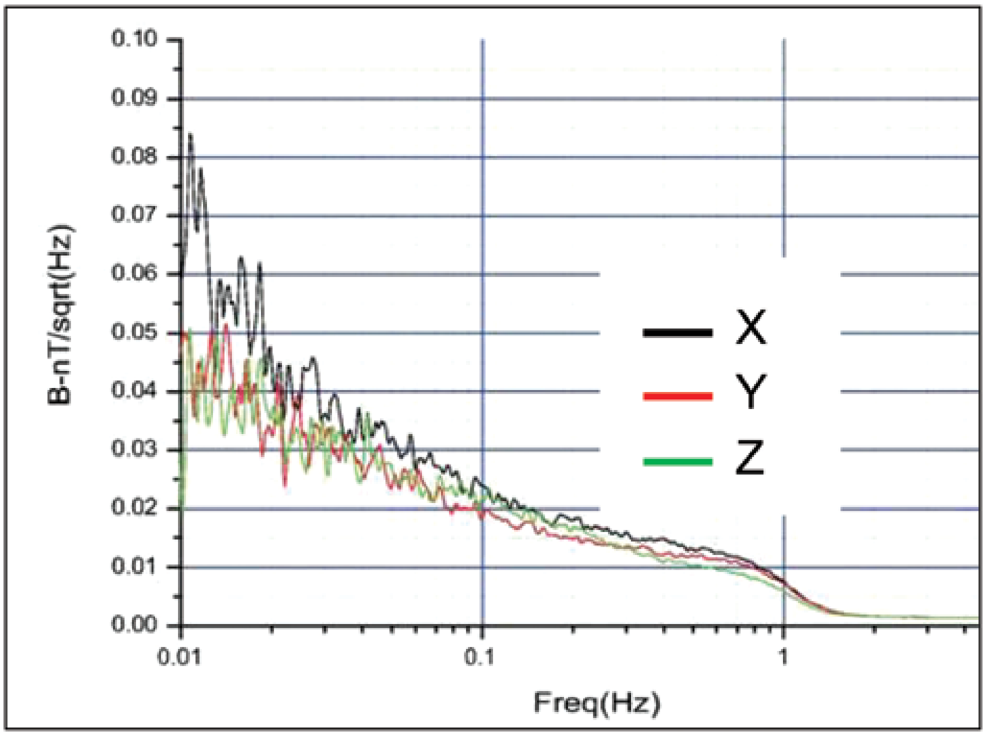

Figure 2. Noise characteristics of GEOMAG-02 magnetometer.

The noise characteristics of GEOMAG-02 magnetometer is shown in Figure 2.

DATA ACQUISITION SYSTEM

All geomagnetic observatories belonging to IGF PAS have very similar data acquisition systems with regard to:

- conversion of analog signals from magnetometers to digital format,
- data processing consists of generating and updating binary and metadata files,
- conversion of data to file formats required by INTERMAGNET or cooperating institutions,
- sending data to data centres,
- providing real-time data in graphical form on the Institute's webpage.

A block diagram of such a system is shown in Figure 3.

One of the basic parts of the data acquisition system is the Network Data Logger (NDL) for geomagnetic field changes recording. The basic parameters of this NDL logger are listed in Table. 1.

Both the setting of recording parameters and the data transfer from the NDL data logger are possible via ethernet interface. The recorded data is stored on a compact flash card and access to it is carried out via ftp protocol; it is typically defined as a cron job (scheduled every minute). Short raw NDL data files are processed and archived in binary format. Meta data information (scale values, base of registration, and many other parameters) for each observatory are stored in text files. Binary and metadata files are input to further processing. In the next steps the data is converted to many formats for different purposes. The most important of them are listed below:

- One-second IAGA2002 format (INTERMAGNET, Regional Warning Center - Space Research Centre, Polish Academy of Science, and as a reference for many field measurement campaigns by induction sounding methods, e.g., *Neska 2007*)
- One-minute IMFV1.23 format (INTERMAGNET, http://rtbel.igf.edu.pl)
- One-second IAGA format (IMAGE project, Hornsund only)
- One-second EMMA binary format (PLASMON project)

IAGA2002 files are sent to INTERMAGNET every minute whereas reported one-minute IMFV1.23 files are sent every 5 minutes. In case of one-second data it is very important to send data to international data centers with the shortest delay possible. An example statistics for the delay between sent data and real time is shown in Figure 4. One-second data is used, e.g., for space weather forecast. Quasi-definitive and definitive one-minute data are prepared manually (e.g., final bases are adopted and peaks are removed) and sent to INTERMAGNET after the

Table 1. Main parameters of NDL data loggers

AD conversion	sigma-delta 24 bits
Timing	GPS receiver
Analog inputs	6 channels, ±10V
Sampling periods	1.25ms, 2.5ms, 5ms , 10ms, 20ms, 50ms, 100ms, 200ms, 500ms, 1s, 2s, 5s, 10s, 20s, 30s, 60s
Internal sampling of analog signal	12,800 per second
Analog filtration	Anti-aliasing low-pass filter 200 Hz, 18 dB/oct
Digital filtration	FIR - low-pass filter, IIR - high-pass filter
Mass storage device	Compact Flash
Communication interface and protocols	Ethernet, TCP/IP, ftp
Power supply	12V DC / 300 mA

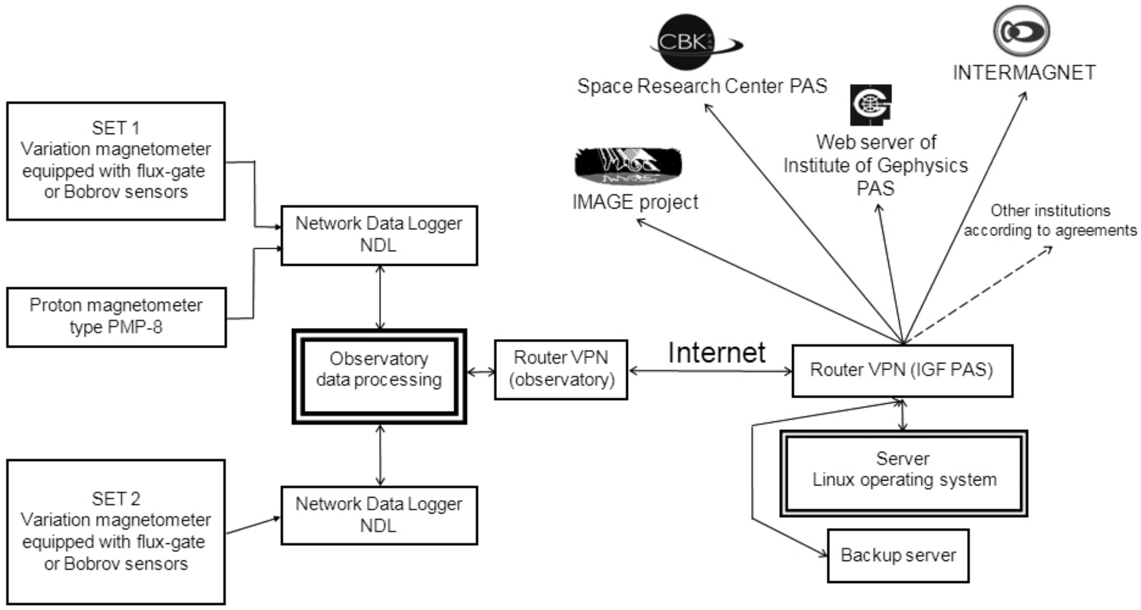

Figure 3. Block diagram of data acquisition system

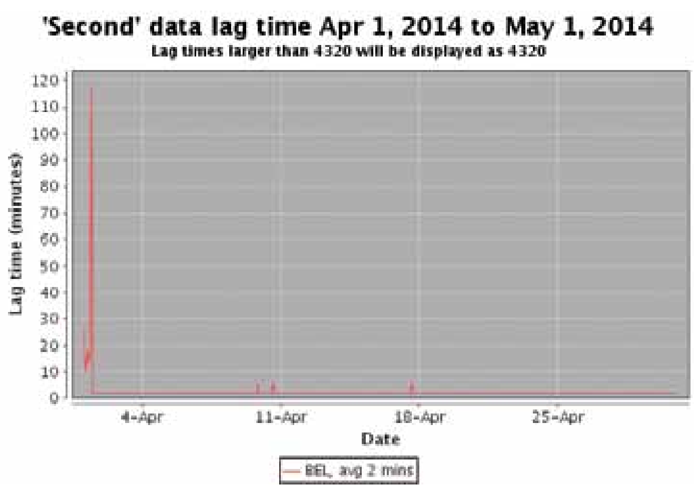

Figure 4. Lag time (Belsk/April 2014) defined as the amount of time between the current time and the time of the latest data sample received by the GIN. This plot has been automatically generated by web application working on Edinburgh INTERMAGNET Geomagnetic Information Node.

end of every month and year, respectively. These software utilities are compatible only with the in-house built NDL logger at present. The DDF format is also not a standard one. Therefore, the details of software do not have wider applicability. Adaptation of this software to run on other hardware platforms is yet to be developed.

SUMMARY

All three geomagnetic observatories of the Institute of Geophysics, Polish Academy of Sciences, participate in and contribute to the INTERMAGNET. They are not uniformly equipped with the same magnetometers. However, the metrological parameters of the magnetometers used by them are similar; they are characterized by low noise and good stability. All observatories deliver their one-second data in real time. The average lag time for sending one-second data to INTERMAGNET is two minutes provided that the internet works properly.

ACKNOWLEDGEMENT

This work was supported by the Ministry of Science and Higher Education of Poland, within statutory activity No 3841/E-41/S/2015.

REFERENCES

Chulliat A., Savary J., Telali K. and Lalanne X., 2009. Acquisition of 1-second data in IPGP magnetic observatories, Proceedings of the XIII[th] IAGA Workshop on Geomagnetic Observatory Instruments, Data Acquisition and Processing, June 9-18 2008, Golden, USA

Jankowski J., Marianiuk J., Ruta A., Sucksdorff C.and Kivinen M., 1984. Long-term stability of a torque balanced variometer with photoelectronic converter in observatory practice, Geophys. Surveys 6, 367-380.

Korepanov V., Best A., Bondaruk B., Linthe H. J., Marianiuk J., Pajunpaa K., ... & Reda J., 1998. Experience of observatory practice with LEMI-004 magnetometers. Rev. Geofis, 48, 31-40.

Love J. J. and Chulliat A., 2013. An International Network of Magnetic Observatories, Eos Trans. AGU, 94(42), 373.

Love J.J. and Finn C.A., 2011 The USGS Geomagnetism Program and Its Role in Space Weather Monitoring. Space Weather. 9 , S07001, doi: 10.1029/2011SW000684.

Neska A., 2007. On the use of fast registrations of observatories as a reference for magnetotelluric measurements, In: XII IAGA Workshop on Geomagnetic Observatory Instruments, Data Acquisition and Processing, Publs. Inst. Geophys. Pol. Acad. Sc., C-99 (398), 315-322.

J. Ind. Geophys. Union (January 2016)
Special Volume-2/ 2016 pp: 67-75

The new magnetic observatory at Choutuppal, Telangana, India

Kusumita Arora, K. Chandrashakhar Rao, L. Manjula, Suraj Kumar, Nandini Nagarajan
CSIR-National Geophysical Research Institute, Hyderabad, India
karora@ngri.res.in

ABSTRACT
Hyderabad Magnetic Observatory (HYB) of CSIR-NGRI, has 50 years of uninterrupted and stable recording of magnetic variations. These observations have contributed to global data, which is the basis of the main field model of the Earth's magnetic field, as well as several studies of low-latitude magnetic phenomena, and regional induction anomalies. With upgraded instruments, HYB became an INTERMAGNET observatory in 2009. With rapid urbanisation and introduction of Hyderabad Metro Rail project in the vicinity, it was imperative to establish an alternate observatory to continue the geomagnetic data series.

The campus of the former Choutuppal Geo-electric observatory provided a suitable location. Preliminary observations in 2012 and continuing observations thereafter, have led to provisional recognition of Choutuppal (CPL) as a magnetic observatory by International Association of Geomagnetism and Aeronomy (IAGA). Assessment of the quiet magnetic environment, minimising effects of temperature fluctuations in the construction of a primary variometer room, and stabilisation of power supply and internet connectivity have been achieved over the last three years.An evaluation of baselines, data quality and stability at CPL in comparison with HYB, is presented here.

Keywords: Magnetic observatory, Variation measurement, Absolute measurement, Baselines, Choutuppal, IAGA workshop 2014.

HISTORY OF MAGNETIC MEASUREMENTS AT HYB AND CPL

Hyderabad Magnetic Observatory, HYB (1964-present) and Choutuppal Geoelectric Observatory (CPL) (1967-1991) were set up in the center of the Indian peninsula and Ettaiyapuram Observatory (ETT) was set up at equatorial latitudes at the southern tip of the Indian peninsula (*Sanker Narayan, 1964; Sanker Narayan et al,1966, 1967; Sanker Narayan et al, 1978*) with the intention of studying concurrent low latitude magnetic phenomena at all frequency ranges. The geo-electric measurements at CPL were based on orthogonal 500m electric dipoles and magnetic pulsations were measured with solid core induction coils. Both quick run and ultra quick run photographic records were generated using highly sensitive galvanometers. Equatorial pulsation data and earth current measurements at CPL also contributed significantly to contemporary knowledge about the propagation and seasonal characteristics of magnetic pulsations (*Sarma et al, 1969; Sastry et al, 1982;*) and induction coil measurements of magnetic pulsations in 1969 (*Sarma et al, 1969; Sastry et al, 1990*).

HYB is situated just outside the influence of the quiet-day equatorial electrojet and is free from anomalous oceanic or geological induced effects and provides an ideal low-latitude location to monitor ionospheric and magnetospheric signals. With continuous recording and reporting of reliable and quality data over the last fifty years, HYB has emerged as an ideal, inland, low-latitude, international Key Magnetic Observatory, acknowledged by the International Association of Geomagnetism and Aeronomy (IAGA). The long data series has been used as input to main field model computations along with data from observations all over the world. Significant contributions to studies of low-latitude geomagnetic phenomena from daily magnetic variation, as well as magnetic pulsations and earth current measurements have been made from these datasets (*Srivastava, 1966; Srivastava and Abbas, 1977; Srivastava and Prasad, 1979; Srivastava et al, 1982; Sastry et al, 1982; Rao and Sarma, 2003; Rabiu et al, 2007, 2012; Rabiu & Nagarajan, 2007; Arora et al, 2014*).

Hourly values of magnetic variation as well as analyses of equatorial magnetic pulsations were reported from HYB and CPL (*CSIR-NGRI Report, 1972*).From 1972 hourly values are published in Indian magnetic data volumes and uploaded to WDC Kyoto (*Svendsen et al, 1990*).With digital instruments and technical support from Niemegk Observatory, GFZ, HYB produced 1-min data since 2008. The absolute measurements continued to be made using a DI fluxgate magnetometer and proton precession magnetometer. HYB became an INTERMAGNET observatory in 2009. Barely three years later, due to activities associated with Metro rail construction in the neighbourhood, within a distance of 500 m, deterioration of data quality at HYB was expected. An alternate magnetic observatory needed to be established, in order to continue the valuable 50-year data series, without interruption. To this end magnetic measurements commenced at Choutuppal in 2012. This paper is a commentary on the initiation and development of the new observatory and an evaluation of the new data series.

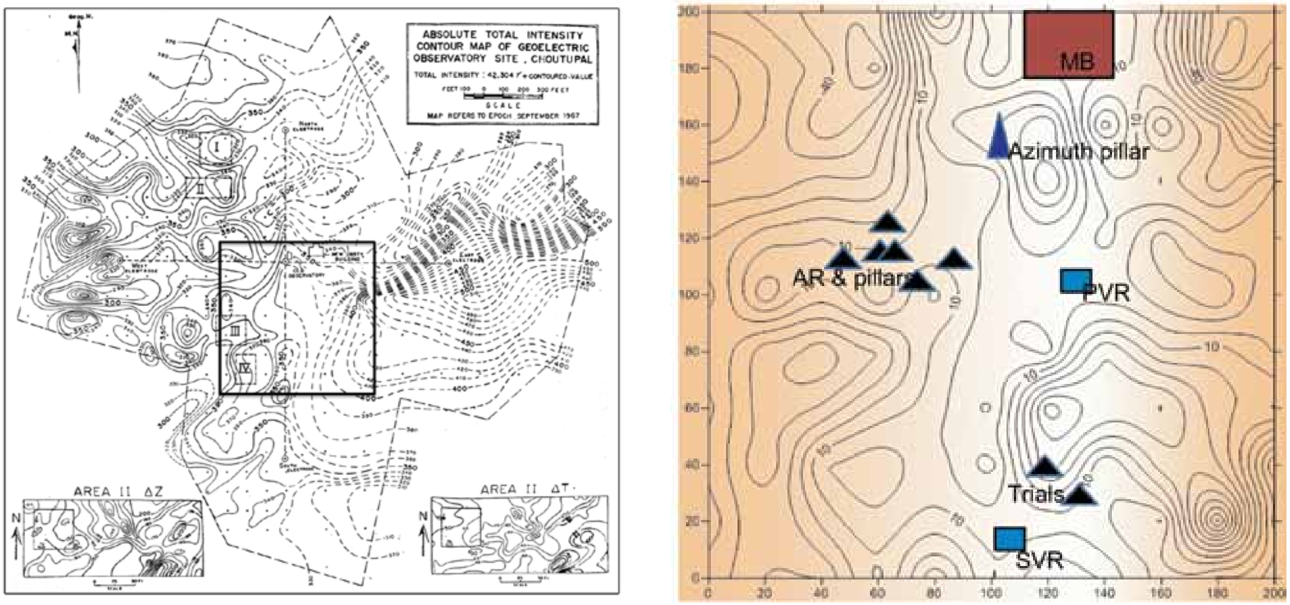

Figure 1. a) Contour map of the magnetic anomaly survey of the entire campus conducted in 1967; the black outlined square is the designated area for the new observatory. b) The area designated for the new magnetic observatory was re-surveyed in 2012 and locations of the different buildings and pillars are indicated within the 200mx200m area.

CHOUTUPPAL CAMPUS AS AN ALTERNATIVE LOCATION

The 0.4 sq km campus of the erstwhile geo-electric observatory in Choutuppal, situated 60 km due east of HYB, in geologically similar Archaean granite-gneiss terrain and semi-arid conditions, located more than 5 km away from any major road network, was a natural choice for setting up the new observatory. Preliminary measurements, as well as a magnetic survey were carried out to confirm the suitability of the new location for a medium term observatory. Within the approximately star shaped layout of the Choutuppal campus, the northern part is devoted to hydrogeological experiments; towards the south a geothermal observatory has been established. A 200 m x 200 m area in the central part was demarcated with the Main Building at its north-central periphery. The outline of the area is superimposed on the contour map of the magnetic anomaly survey of the entire campus, conducted in 1967 (Figure 1a; *Sanker Narayan et al, 1967*). Such an area is sufficiently far away from the boundary of the campus to ensure that local activities outside the campus may not have significant contribution to the measurements.

A detailed magnetic survey was made of the demarcated area in November 2012. Three areas were identified where the changes in magnetic field were within 12 nT; these were designated to be the sites of Primary Variometer Room (PVR), Secondary Variometer Room (SVR) and Absolute Room with the Absolute pillars, shown in Figure 1b. The ongoing trial measurements were located close to the site of the SVR to enable uninterrupted recording during the period of construction.

Trial measurements of magnetic variation data were started in early 2012, about 200 m south of the Main Building, away from internal roads and pathways, where two stable pillars were constructed for the DI measurements and the scalar magnetometer; the instruments were protected with wooden boxes. For the variometers, two pits were dug into the underground about 1m in depth and lined with marble and Styrofoam, in which the fluxgate sensor and data loggers were installed. The pillars and pits were covered with sheds of natural materials for protection against rain and direct sun. Solar panels were used to power the system. Absolute measurements were made about once in 15 days during the year, care being taken to make measurements early in the morning or late in the evening so that temperatures during measurements were mostly around 30°C.

STANDARDISATION OF MAGNETIC DATA SERIES FROM CHOUTUPPAL CAMPUS

Standardisation of the new data series and evaluation of its suitability to continue the data series of HYB has been accomplished between 2012 and 2015. Trial measurements started with recording of continuous three component variation data with GEOMAG02M fluxgate sensor and electronics and Overhauser PPM. The quality of data was good with high signal-to-noise ratio. The measurements were continued, establishing satisfactory baseline stability and comparisons with HYB. A set of sample data from one day in 2013 is shown in Figure 2.

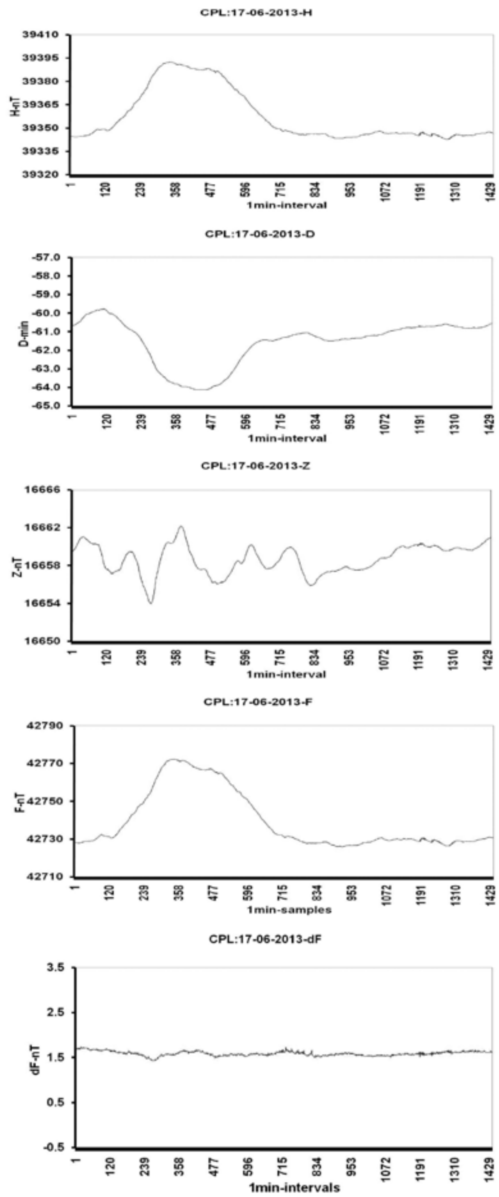

Figure 2. Sample data set showing the three component data, scalar data and ΔF, recorded in 2013.

Temperature variations were monitored closely to plan for sufficient thermal insulation to keep daily variations to within 1°C in the semi-arid weather conditions of Choutuppal. As expected, the most important challenge of the Choutuppal measurements lay in controlling the temperature and its variations in the vaults where the variometers placed. The mean annual temperature is high at 26.7°C , with monthly and daily ranges of around 11°C. Despite best efforts at insulating the instruments, the sensor and logger experienced significant temperature swings, varying between 1 to 1.5°C daily and as much as 4°C annually, which affected the quality of the trial data. Daily temperature changes at CPL are significant when compared with HYB variometer where temperature fluctuations are within 0.1°Cas shown in Figure 3, top panel. The effect of temperature on fluxgate measurements is observed as a sag in the red line of ΔF for CPL compared to the blue line of HYB, in Figure 3, bottom panel. Efforts were continued to minimize temperature effects over 2013 and diurnal temperature effects in Choutuppal reduced to 1 nT or better.

Frequency of absolute measurements was increased to achieve baseline stability within 1 nT. One min variation data during 2012-2013, had some interruptions and jumps during the planning phase due to changes of pillars and instruments. These would stabilise later during 2014-15. The H,D,Z baselines (2012-2014) are shown in Figure 4. The baseline plots had some scatter, attributable to short

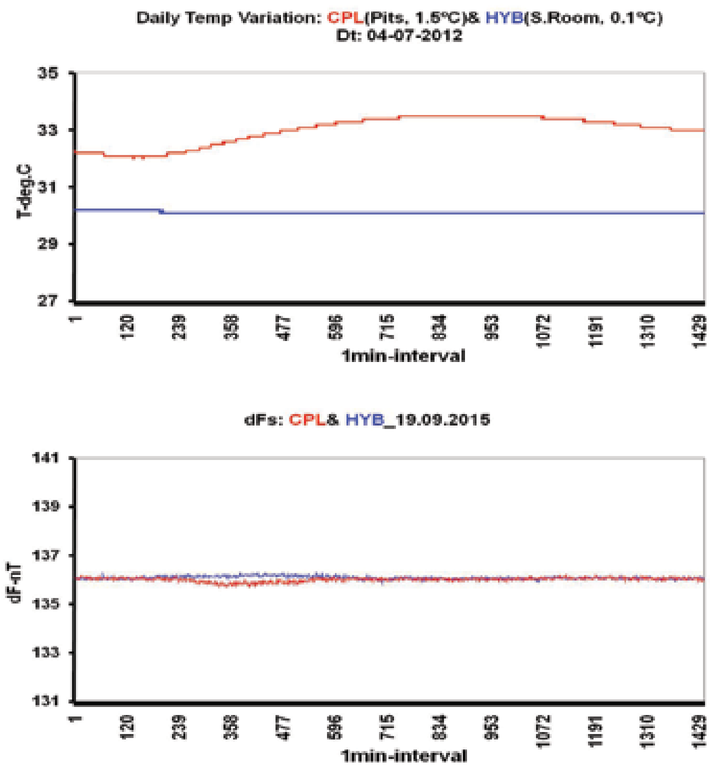

Figure 3a. Average daily temperature variation in HYB and CPL, b. Effect of temperature on ΔF –comparison between CPL and HYB.

and somewhat irregular record length. The jump in all the components at the beginning of 2014 is attributable to a change in instrument.

The total field scalar data, at 5s sampling of the HYB Overhauser was increasingly affected by noise generated by construction activities of the Metrorail, shown in Figure 5 bottom panel. The top panel of Figure 5 shows the superimposed curves of F(HYB) and F(CPL) at 5s sampling interval, on 31 May 2013. The noise in the HYB data is clearly seen. The difference curve in the bottom panel further highlights the noise of the HYB PPM data. Average daily variation in total field between the two locations is about 2nT.

The trends of variation data of HYB and CPL were compared by obtaining histograms of their first differences, as independent check of quality of data at each location. First differences are obtained by subtracting each minute value from the previous one; first differences of a representative month of data from the years 2012, 13, 15 for each component are shown in Figure 6.

Histograms of differences at HYB and CPL in red and blue respectively show elongated Gaussian distributions for the three cases for three components. From a statistical standpoint, daily variation in H, would comprise of small differences ~0.0 -0.1 nT during 6 hours of night time. Daily variations averaging 60 nT over 8 hours of daytime (0800-1600) would result in large number of differences in 0.1-0.2 nT range (60nT/8x60min=0.12). More rapid changes before and after the noon peak, and disturbances, would provide some of the larger differences. Variations in D and Z are half the amplitude and show correspondingly less smooth Gaussian distributions. Similar distributions have been obtained for both HYB and CPL, over several months, attesting to the stability and close similarity of variations at the two observatories.

CONSTRUCTION OF PRIMARY VARIOMETER ROOM AND ABSOLUTE PILLARS

The construction of Primary Variometer and Absolute Room was started in June, 2013. The dimensions of the former were 12ft by 16 ft and 12 ft in height. It is constructed in the form of a buried vault with just 2 ft above surface. The dimensions of the Absolute Room, built above ground are 16 ft by 8 ft and 11 ft in height; the pillars are 40 inch above ground with 7.5 ft below ground for long term stability. The construction material used was tested non-magnetic sandstone sourced from about 120 km away. Instead of regular bricks, stone constructions with ceilings reinforced by wooden planks were used. The PVR is double walled. The roof is fitted with thick layers of Styrofoam. The primary digital fluxgate magnetometer and recording unit were installed in

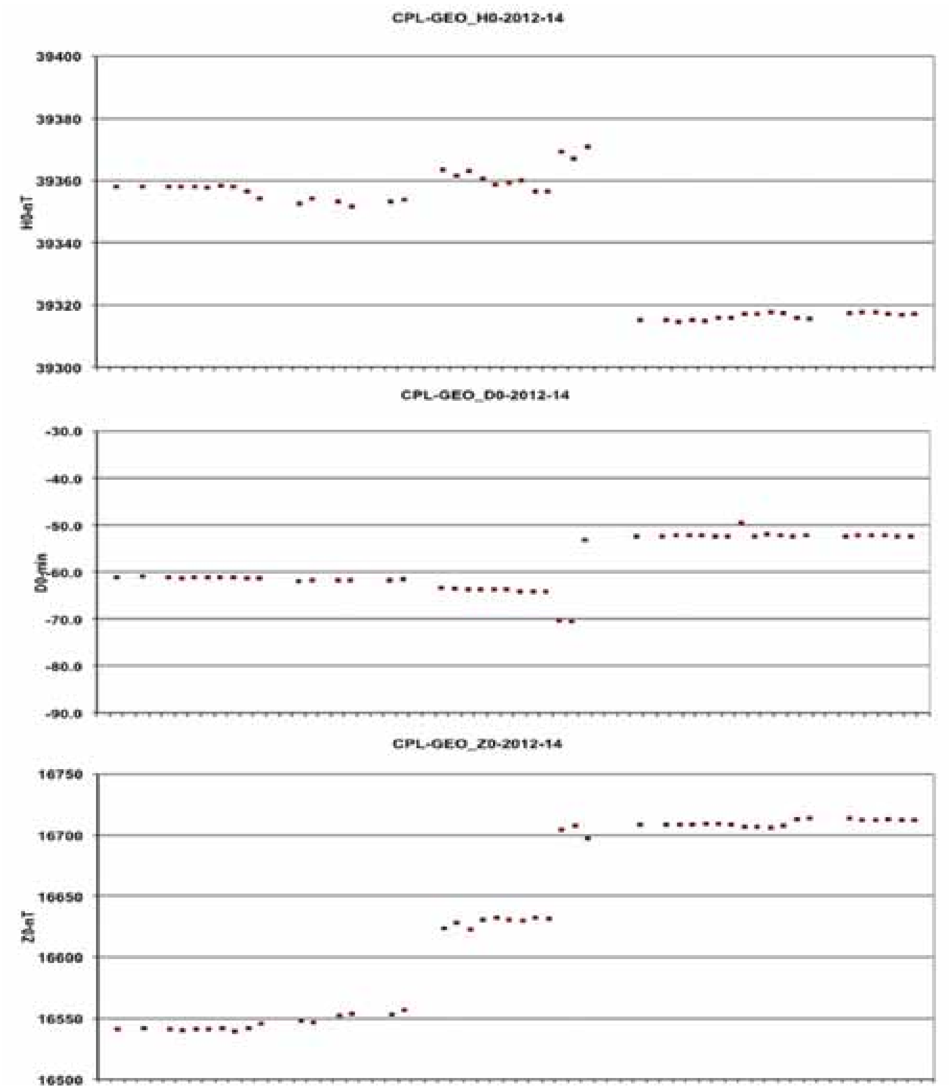

Figure 4. H,D,Z baselines, 2012-13

the primary variometer room in February 2014. However, issues of irregular power supply, fluctuations in solar powered backup and installation of dedicated internet connectivity had to be resolved. The primary variometer measurements have been uninterrupted since January 2015. The electronics and computers were housed in the control room of the main building. Solar panels of is it >3 kW capacity was installed to power the recording system independently; as Choutuppal experiences 90% sunny days, this is sufficient for uninterrupted clean power supply. Prior to supply of solar power, sharp voltage fluctuations and deviations from the standard 50 Hz supply played havoc with the electronics, which had to be rectified painstakingly. Dedicated internet lines were setup. In a remote area where both power supply and internet are very uncertain, completion of these activities took a lot of time and investment. Efforts to improve power supply and internet continued. In mid 2014, the new observatory at Choutuppal was provisionally assigned the IAGA code, CPL. The baselines and ΔF for the first half of 2015 show the significant improvements compared to 2012, as seen in Figure 7.

Seven absolute pillars were constructed, 2 positioned within the demarcated Absolute Room and five outside. An azimuth pillar was constructed south-west of the Main Building, about 300 m from the Absolute pillars. Azimuth was determined by geodetic (Stellar)and DGPS observations made by the Survey of India (SOI) and Indian Institute of Geomagnetism (IIG) as well as NGRI GPS team and relative positions of all 7 pillars were determined and the azimuth correction for each was assigned. From the coordinates the azimuths of baselines between the pillars and azimuth pillar were estimated. The measurements from the different methods agreed within 30 second of each other. D observations were carried out on each pillars to find out the pillar differences, which shows a range of 2.5 minutes. The results of the azimuth computation are given in Table 1.

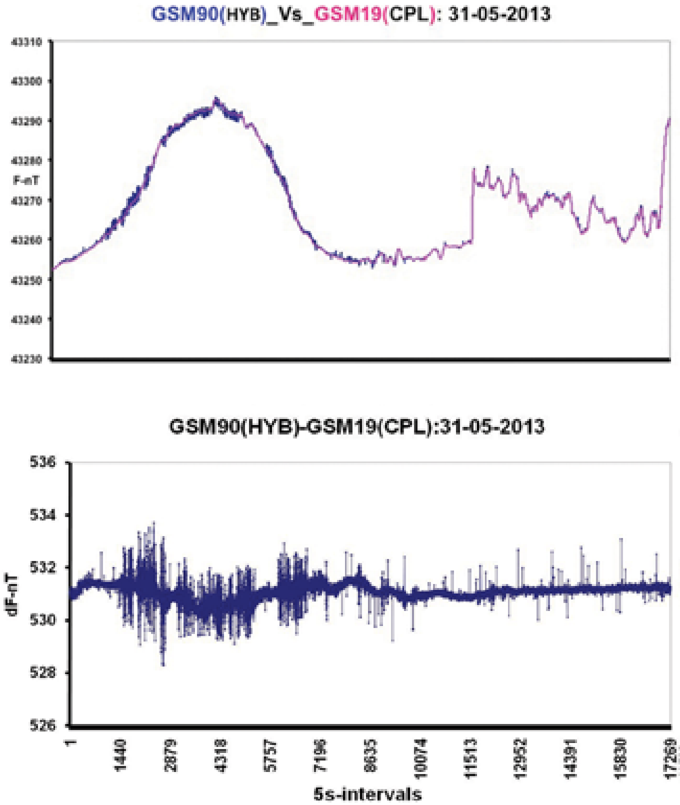

Figure 5. Noise in HYB Overhauser data

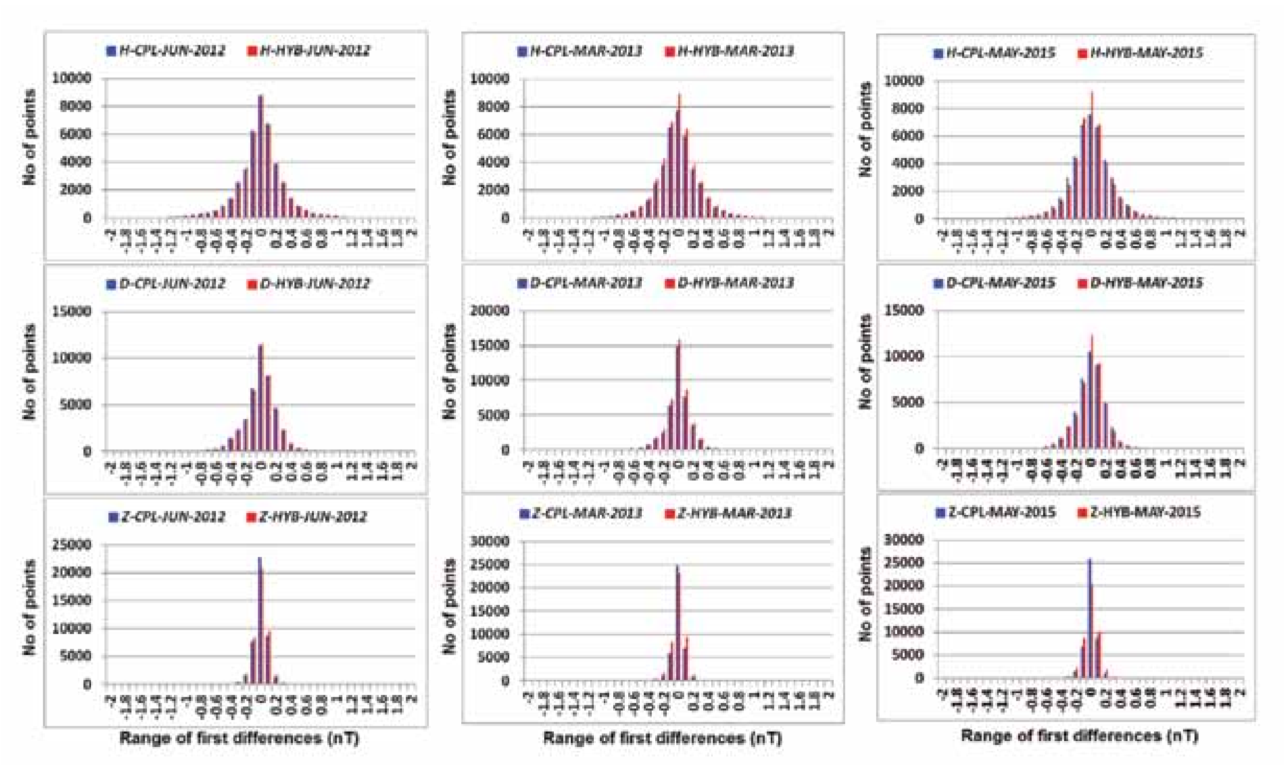

Figure 6. Comparison of first differences of three component data from HYB and CPL shows very similar nature of data distribution.

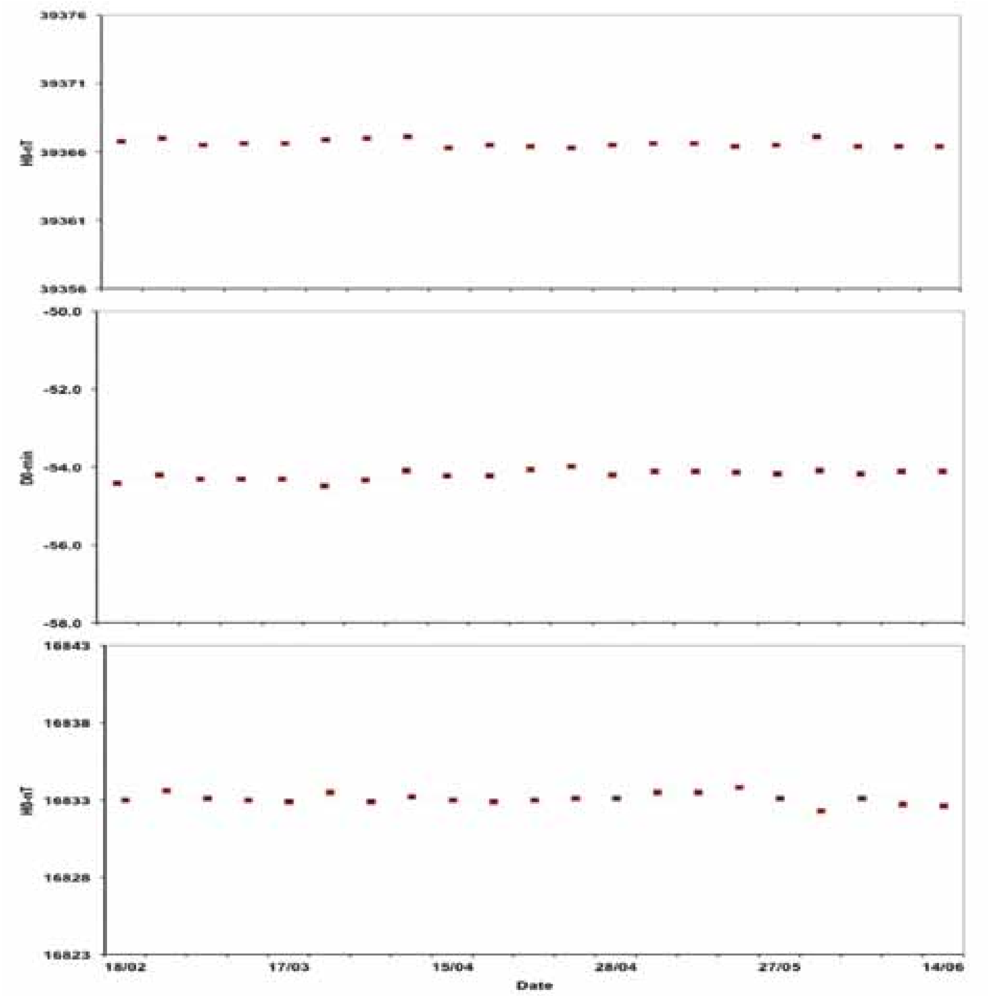

Figure 7. H,D,Z, Baselines of CPL, Feb to June, 2015

Table 1. Azimuth corrections for the absolute pillars

Pillar no	Azimuth Deg min sec	D corr (min)	dFcorr (nT)
1	42 22 31	0	0
2	41 07 19	-0.43	4.8
3	41 45 42	0.41	-2.4
4	38 15 35	0.55	18.6
5	39 35 58	-0.68	14.4
6	44 59 57	-1.78	-7.4
7	45 51 13	-1.28	-15.9

INTERCOMPARISON DURING XVI IAGA OBSERVATORY WORKSHOP, 2014

The XVI IAGA Observatory Workshop was held at CSIR-NGRI, Hyderabad, 7-16 October, 2014. About 60 observers attended the measurement sessions at CPL Observatory. Of these the measurements of the more experienced observers compare well with the baselines established for CPL. About 4 sets of declination-inclination observations were made by each observer, over 5 days. The observations were carried out on 7 absolute pillars. The appropriate declination correction was applied to each observation. A summary of the 3 best measurements of declination (D) and inclination (I) angles, of thirty four observers, are shown in the plots in Figure 8. It is seen that most measurements cluster about the mean between +/- 0.2 min for Dand +/- 0.3 min for

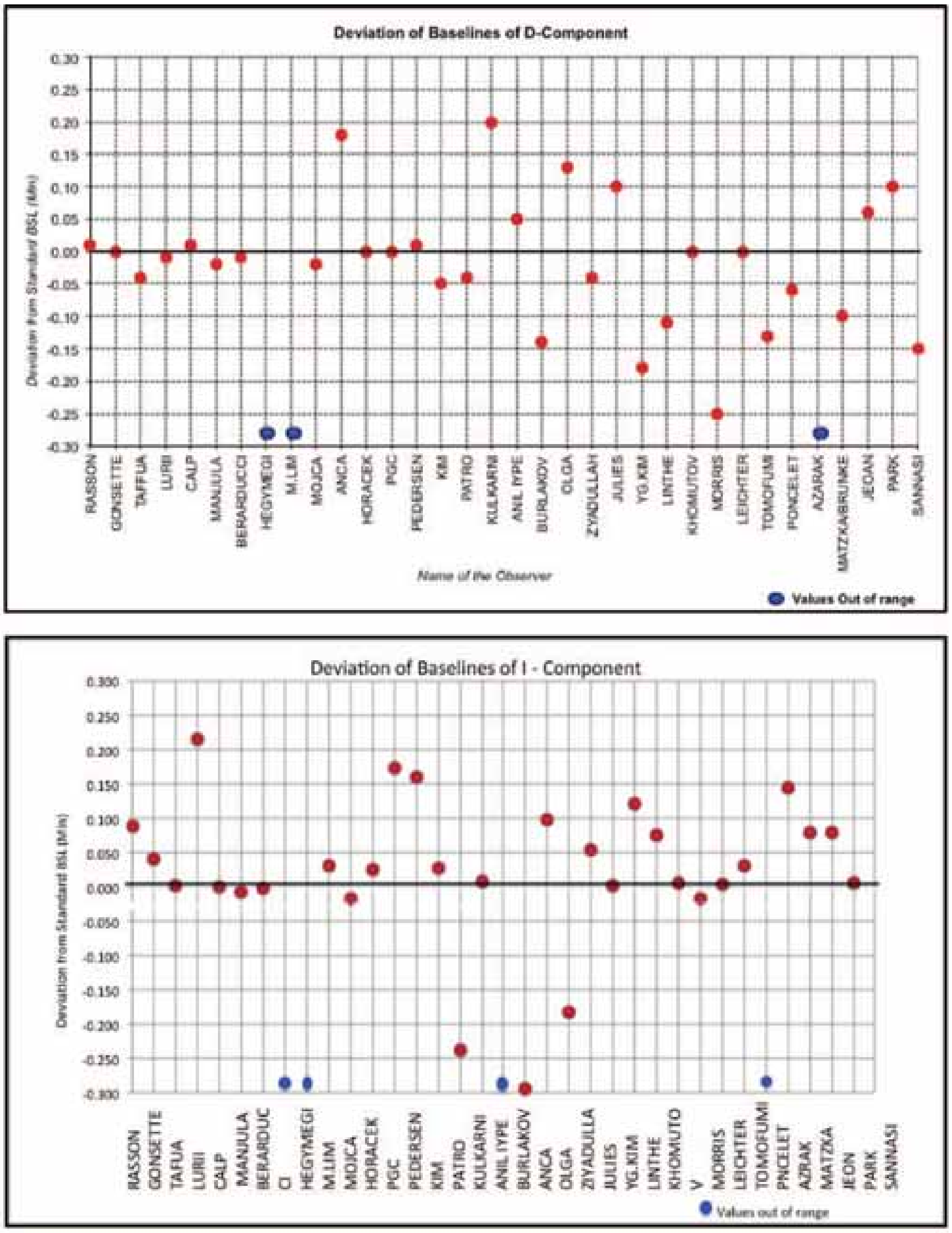

Figure 8. D and I observations during IAGA Workshop, October 2014.

I. Comparisons with measurements made by AUTODIF were also found to be satisfactory (*Arora and Veenadhari, 2014*). This was an additional affirmation of the stability of the environment, enabling accurate magnetic variation measurements at the recently established observatory CPL. Procedures for permanent assignment of the IAGA code are underway.

SUMMARY

HYB observatory has reported stable baselines and values of low-latitude variation, with suspended La Cour systems, as well as upgraded digital fluxgate magnetometers for 50 years. Due to external electromagnetic effects generated by the introduction of Metro rail about 500m from the observatory, it was decided to commence alternate recordings. A digital fluxgate magnetometer and Overhauser were installed for trial measurements at CPL, about 60 km from HYB, in 2012. The initial variations were compared and found satisfactory. Temperature fluctuations were further minimized to obtain long term stability of baselines at CPL. In 2014, the 3-axis Fluxgate Magnetometer Model FGE, assembled and calibrated by DTU, Space, Denmark with digital recording made by GFZ Potsdam was installed in the double walled, semi-underground primary variometer house at CPL. Both sets of data were reduced to obtain stable baselines in 2015.

Performance of the variometers was compared with observations at HYB over the period 2012-2015. Presentation of the on going data comparisons validates the establishment of this observatory. In future, this data will serve as an extension of the HYB data series.

ACKNOWLEDGEMENTS

Establishment of the new magnetic observatory at Choutuppal in record time has been possible due to the sustained support of Director, CSIR-NGRI and Project Director, HEART (PSC0203). Dr. H.J. Linthe of Adolf Schmidt Observatory Niemegk of GFZ, Potsdam, has played a key role in setting up the new primary variometer through an ongoing GFZ-NGRI collaboration.

REFERENCES

Arora, Kusumita, Phani Chandrasekhar N., Nandini Nagarajan, Ankit Singh, 2014. Correlations between sunspotnumbers, interplanetary parameters and geomagnetic trends over solar cycles21–23. Journal of Atmospheric and Solar-Terrestrial Physics114(2014)19–29.

Arora, Kusumita and Veenadhari B., 2014. XVI IAGA Workshop on Geomagnetic Observatory Instruments, Data Acquisition And Processing. Report submitted to IAGA, http://www.ngri.org.in/iaga2013_14/pdffiles/IAGA_2014_%20Report.pdf

CSIR-NGRI Report, 1972. Rapid Variations of the Earth's magnetic field. Geolectric Observatory, Choutuppal, Nalgonda.

Rabiu A. B., Onwumechili C.A., Nagarajan N., Yumoto K., 2012. Characteristics of equatorial electrojet over India determined from a thick current shell model Journal of Atmospheric and Solar-Terrestrial Physics, Volume 92, p. 105-115. 10.1016/j.jastp.2012.10.014

Rabiu A. B., Nagarajan N., 2007. Equatorial electrojet parameters in Indian sector Inter-relationships between the thickness, width and intensity of the equatorial electrojet in Indian sector. Bulletin of the Astronomical Society of India 35:645-654.

Rao Madhusudhan, Sarma, S.V.S., 2003. Solar cycle dependence of Pi2 pulsation activity in the equatorial region of India. Journal of Atmospheric and Solar-Terrestrial Physics, 65, 941 – 945.

Sanker Narayan, 1964 Establishment of a magnetic observatory at NGRI; Bull NGRI, 2, 115-122.

Sanker Narayan P.V., Srivastava, B.J., Y.S. Sarma, 1966. Modifications of the temperature compensation system of the La Cour variometers at the NGRI Magnetic Observatory, Hyderabad. J. Indian Geophysical Union, 3, 51-58.

Sanker Narayan P.V., Ramanujachary K.R., Sarma S.V.S., Zybin K.U., 1967. Establishment of a geolectric observatory by the NGRI, Hyderabad, at Choutuppal, Nalgonda; Bull NGRI, 5, 155.

Sanker Narayan P.V., Sastry T. S., KRR, SVSS Morgunov 1more, 1978. Equatorial Geomagnetic and Geoelectric Observatory of N.G.R.I at Ettaiyapuram (T.N.), India. Geophysical Research Bulletin Vol.16, No.4

Sarma Y. S., Sankernarayan P.V. , Ramanujachary K.R., Sarma S.V.S., K.YuZybin and Makaraov V.I., 1969. Three component induction magnetometer for recording geomagnetic micropulsations at the Geoelectric observatory at Choutuppal. Bull. NGRI7, pp. 51–65.

Sastry, T.S., Sarma, Y.S., Sarma, S.V.S and Sanker Narayan, P.V, 1982. Daytime Pi pulsations at equatorial latitudes. Geophysical Research Bulletin, 20(3), 91-108

Sastry, T. S., Prasad, S. N. , Srivastava, B. J. and M. Someswara Rao, 1990. Vertical electric profile at Choutuppal (Hyderabad) in peninsular India.Physics of The Earth and Planetary Interiors,Vol. 59, Issue 4, pp 229-232.

Srivastava, B.J. 1966. On the occurrence of large SSC amplitudes in the horizontal intensity of the geomagnetic field in middle latitudes around local mid night, J. Geomag. Geoelctr., 18, 437-442.

Srivastava, B.J and Abbas, H. 1976. Diurnal variation of geomagnetic SFE's and SSC's at Hyderabad, Indian. J.Radio space physics, 5, 307-310.

Srivastava, B.J and Abbas, H., 1977. Geomagnetic secular variation in India-Regional and local features, J.Geomag. Geoelectr. 29, 51-64.

Srivastava, B.J, and Prasad, S.N, 1979. The lunar and solar daily geomagnetic variations at Sabhawala and Hyderabad, Geophysical Journal of the Royal Astronomical Society, 57, pages 159–169.

Srivastava, B. J., Prasad, S.N., Singh,B.P., Arora, B.R., Thakur, N.K and Mahashabde, M.V, 1982. Induction anomalies in geomagnetic Sq in peninsular India, Geophys. Res. Lett., 9(10), 1135-113.

Svendsen, K.L., Davis, W.M., McLean, S.J., Meyers, H. 1990. A report on geomagnetic observatory operations. NOAA, NGDC, Boulder, Colorado, USA.

J. Ind. Geophys. Union (January 2016)
Special Volume-2/ 2016 pp: 76-79

System for Recording Variations of Earth's Magnetic Field at the "ALMA-ATA" Geomagnetic Observatory

O.I. Sokolova, A.A Andreev, G.V. Burlakov, O.L. Kachusova, O.N Kryakunova, Yu. N Levin, N.F. Nikolaevskiy

Institute of the Ionosphere, National Center for Space Research and Technology
Kamenskoe plato, Almaty, Republic of Kazakhstan
olgsokolova@yandex.ru

ABSTRACT

Modern equipment allows recording and monitoring of the geomagnetic field variations in INTERMAGNET Magnetic Observatories with high quality and resolution. However, many INTERMAGNET Magnetic Observatories have various problems of man-made origin that have negative effects on geomagnetic observation: noise in the recorded data or breaks in the record because of hardware or software failures, etc. We present a system, which enables remotely controlled re-start of the recording system after an interruption, applied to the measuring equipment and parameters of measurement of variations of Earth's magnetic field at the "Alma-Ata" geomagnetic observatory. This system makes it possible to improve the quality of our geomagnetic observations.

Key words: Geomagnetic field, Measurement, Recording, Monitoring.

INTRODUCTION

Kazakhstan's first geomagnetic observatory was put into operation in 1963, near Almaty city. From this time the "Alma-Ata" geomagnetic observatory (code IAGA – AAA; geographical coordinates: 43.25ºN, 76.95ºE; geomagnetic coordinates: 34.3ºN, 152.7ºE) began to measure the geomagnetic activity in the Republic of Kazakhstan. At present the observatory produces regular observations of the geomagnetic field in near real time. The observatory uses the following devices: two fluxgate magnetometers (LEMI-008 and LEMI-018) for continuous recording of variations of X, Y, Z components of the geomagnetic field; the DI-flux magnetometer LEMI-203 for absolute measurements of the magnetic declination D and magnetic inclination I; the scalar Overhauser proton magnetometer POS-1 for absolute measurements of total intensity F of the geomagnetic field. The observatory also calculates in real time the local K-index of geomagnetic activity for a quantified description of the disturbances of the geomagnetic field. At present the database of the "Alma-Ata" geomagnetic observatory include: hourly mean values of (H, D, Z) from 1963 to 2009; 1- second data files of (X, Y, Z, F) from November, 2003 up to the present; one-minute data files of (X, Y, Z, F) from November, 2003 up to the present; a local K-index of geomagnetic activity from 1996 up to the present. These data are submitted to the website (http://geomag.ionos.kz) of "Alma-Ata" geomagnetic observatory. In November, 2005 the observatory became a full member of the INTERMAGNET. The INTERMAGNET imposes the strict requirements of quality on each member INTERMAGNET Observatory (IMO) [*Nechaev, 2006, Benoît, 2011, Jankovski and Sucksdorff, 1996*]. Modern equipment allows recording and monitoring of the geomagnetic field variations in IMO with high quality and resolution. However, many IMO have various problems of man-made origin that have negative effects on geomagnetic observation [*Okawa et al, 2007*]. At present AAA commonly faces the problem of noise in the recorded data or breaks in record because of hardware or software failure. We present a newly devised system allowing remote start and control of the measuring equipment and parameters of measurement. We find that this system has improved quality of our geomagnetic observation and minimized data gaps.

REMOVAL OF NOISE IN TOTAL INTENSITY F MEASUREMENTS AT THE "ALMA-ATA" GEOMAGNETIC OBSERVATORY

For measurement and recording of total intensity F of geomagnetic field in the "Alma-Ata" geomagnetic observatory, we have used the POS-1 Overhauser magnetometer. It consists of a sensor and the electronic block, which is connected with the recording personal computer (PC) via the RS-232 interface (Figure 1). The computer is configured to continuously measure the total field intensity, F, at five second sampling rate in automatic mode. The obtained data are processed and transferred to the database for storage.

Longtime use of magnetometer POS-1 has shown that significant noise, commonly of man made origin are also recorded along with signal. The noise is produced from various sources of electromagnetic radiation surrounding the observatory, which interfere with the sensor and power-supply circuits. The main part of noise is due to defects in uninterrupted power supply and electric grounding of the

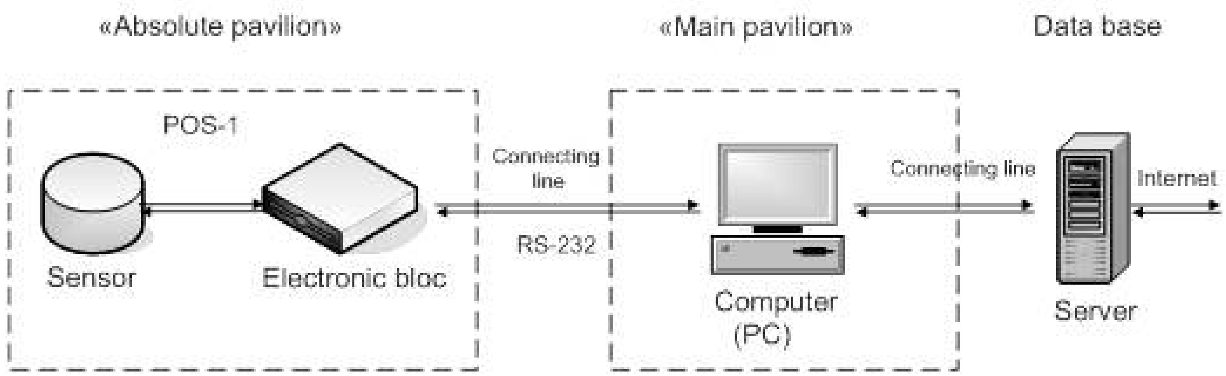

Figure 1. Scheme of equipment connection: distance about 10 m between "Absolute pavilion" and "Main pavilion"; distance about 100 m to Server with data base

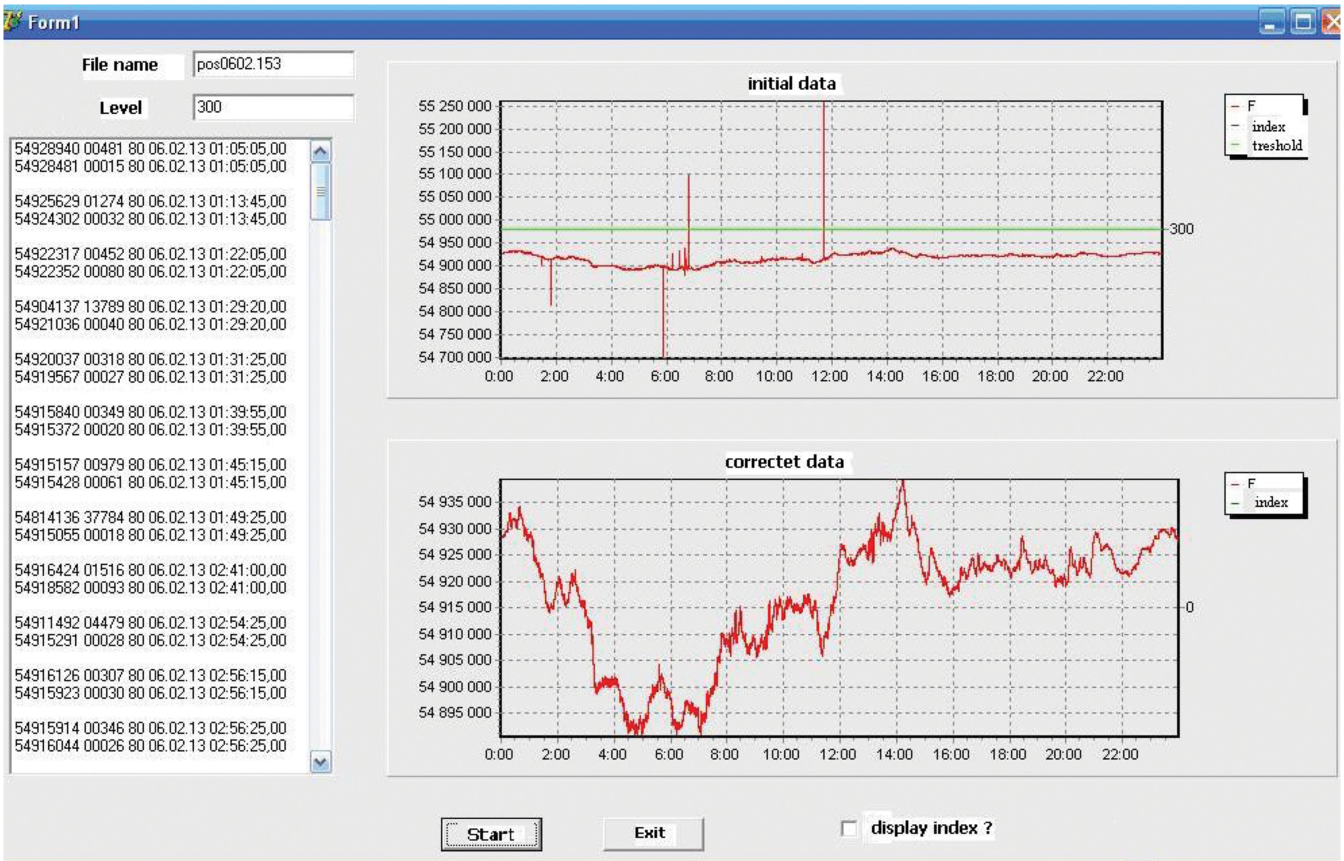

Figure 2. Graphic interface of the program of filtration of pulse noise

equipment, which affect the equipment and cause pollution of recorded data. A program to filter the data is used to remove spikes in the data set. Additionally, the POS-1 calculates the QMC as well. QMC (quality of measurement condition) is a root-mean-square error of determination of frequency of a signal precision, expressed in nT. The magnitude of QMC strongly depends on external noise during measurement. If QMC is a minimum and its value lies within 10-50 pT, noise is practically absent. If QMC is greater than 50 pT, the interferences are non-trivial. If this value is more, the interference is considerable. The filtering program uses QMC values for the analysis of spikes in geomagnetic data. If a spike is detected, the program eliminates it from a dataset and replaces it by the average value. The program works in the semi-automatic mode and is started manually after the process of recording of the daily data file is completed. Then the file with corrected values is saved automatically to the database of the observatory server. The graphic interface for program that filters the data is presented in Figure 2.

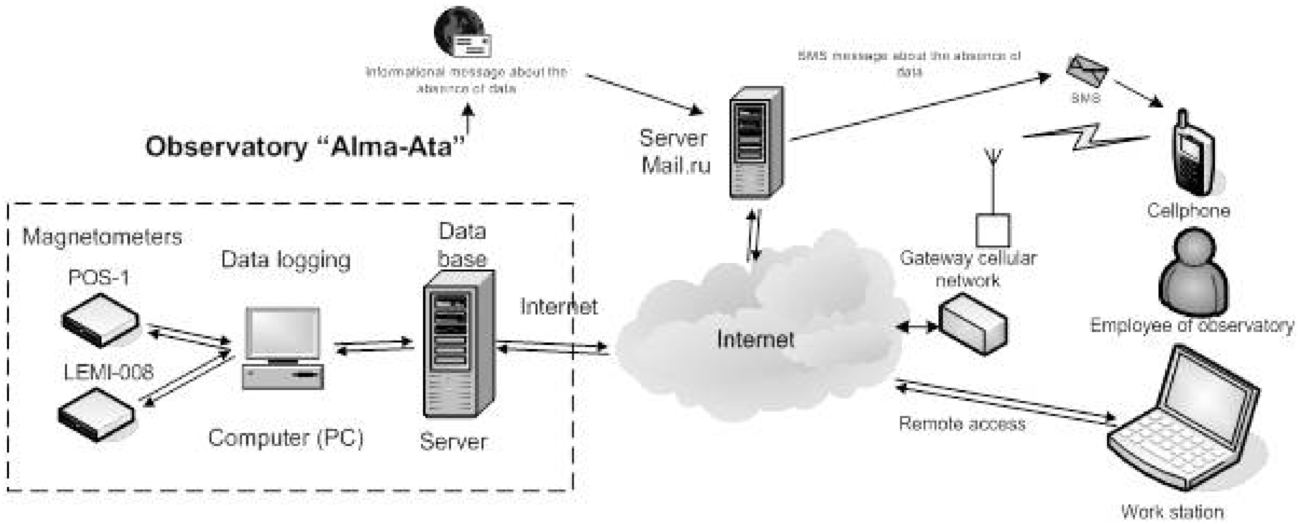

Figure 3. Remote control system

In the upper panel of Figure 2, a daily data array with noise is presented. The lower panel shows the view of the data array, after removal of the spikes. It is possible to filter and process data by starting the program directly on the recording personal computer. Additionally protected remote access to this computer from any other computer is ensured through Internet, which allows initiating the program of filtering remotely for a more efficient data recording process. In case of "hangup" of the software there is also an opportunity to reboot it remotely.

REMOTE STARTING OF DIGITAL MAGNETOVARIATION STATION OF THE "ALMA-ATA" GEOMAGNETIC OBSERVATORY

In the "Alma-Ata" geomagnetic observatory the digital three-component fluxgate magnetometer LEMI-008 is used to record the X, Y, and Z components of magnetic field variations. It consists of the fluxgate sensor and the electronic block, which provide transformation, processing and accumulation of information on variations of geomagnetic field, and, also transfers this information to the recording computer via the RS232 interface. The built-in GPS receiver corrects the time of internal clock. On the recording computer, one-second data of X, Y, Z components of measured geomagnetic field are acquired in the automatic and continuous mode. The obtained data are sent to the server for storage. During operation it became clear that periodically in recording data there are gaps because of hardware failure in the electronic block or owing to "hangup" of the recording software "Lemi Manager". It is possible to restore recording by restarting of the program or the electronic block. It was also noticed that the built-in GPS receiver sometimes loses connection with the satellite, which leads to loss of synchronization with UTC.

To restart the electronic block of LEMI-008, short-term shutdown of the supply voltage (12 volts) is reinstated by triggering a special program written on Delphi 7. The protection program prevents casual starting of reset process of electronic LEMI-008 block. For authorized starting of reset program, the corresponding code is entered in the window of the restarting program by pressing "START" button. This initiates the restarting process of LEMI-008 .

REMOTE CONTROL OF MAGNETOMETERS AND RECORDING SYSTEM AT THE "ALMA-ATA" GEOMAGNETIC OBSERVATORY

The proposed method of remote control of functioning of the equipment of the "Almaty" geomagnetic observatory is based on the information communicated to observatory staff about a break in the geomagnetic data record by means of SMS messages. If the data from the magnetometers POS-1 or LEMI-008 does not come to the database of observatory for more than 10 minutes, the server displays the corresponding information message. The special imagAllert.exe program (written on Delphi7) forms and sends this information message in the form of an e-mail to the special e-mail address on the Mail.ru e-mail server, as in Figure 3.

On the "mailbox" of this address, special settings are made, which allow the Mail.ru resource to form the SMS message about receipt of the e-mail to this address. SMS comes to the cell phone of the employee of the observatory, who after obtaining the notification about a problem with the data transmission, can remotely access the protected server, using the internet server or the recording personal computer. Further, the staff, in online mode, can find out the reason of the data transmission stop and, if necessary, restart the magnetometer or the software (POS_manager or LEMI_manager). Besides, the software "Remote access" enables restart of the recording computer.

CONCLUSION

The newly designed system allows not only deletion of noise, but also enables continuous recording of the geomagnetic data at the "Alma-Ata" observatory. This process was successfully applied several times during the past year at AAA. Remote restarting also allows operation without coming close to the sensor logger that reduces quantity of electromagnetic interferences and accelerates a restarting process. This ensures reduction of total number of days of lost data. The created system allows re-start and control of the measuring equipment and parameters of measurement of variations of Earth's magnetic field at the "Alma-Ata" geomagnetic observatory.

ACKNOWLEDGMENTS:

This work was performed under the Republican Budgetary Program 055 "Scientific and (or) scientific - technical activity", the subprogramme 101 "Grant financing of scientific researches" within the "Creation of Collecting System of Experimental Geophysical Data on the basis of Modern Information Technologies and Its Use in Research of the Near-the-Earth Space".

REFERENCES

Benoît St-L, 2011. INTERMAGNET Technical Reference Manual. Ver4.6. Edinburg. UK. 2011. pp. 23-26

Jankovski, J. and Sucksdorff, C., 1996. Guide for magnetic measurements and observatory practice// 1996, Warsaw, pp. 87-157.

Nechaev, S., 2006. Guide to stationary geomagnetic observations. Irkutsk: Publishing House of the Institute of Geography SB RAS, 2006, pp. 98-122

Okawa, T., Tokumoto, T., Nakajima, S., Owada, T., Toya T, Muromatsu, F., Kumasaka, N. and Koike, T., 2007. Development of artificial Geomagnetic disturbances monitoring system. Publ. Inst. Geophys. Pol. Acad. Sc., C-99 (398), Warsaw, 2007, pp. 183-188

J. Ind. Geophys. Union (January 2016)
Special Volume-2/ 2016 pp: 80-85

Calibration Experiments conducted at ETT observatory, 1980-2000

K. Saratchandra, N Rajendra Prasad, T.S. Sastry, Nandini Nagarajan
Hyderabad Magnetic Observatory, National Geophysical Research institute, Hyderabad 50007 INDIA
Email: nandini_ngri@yahoo.com

ABSTRACT
Data standards at Hyderabad (HYB) and Ettaiyapuram (ETT) magnetic observatories in the era of suspension variometers and secondary calibrated absolute magnetometers could be maintained only bycontinuous evaluation and self-consistent data reduction. Experiments were devised at these observatories using minimal equipment, without calibration facilities,to compare and calibrate absolute and variation magnetometers in situ. Of these experiments three are described here:

i) Determination of the thermal coefficients of the La Cour suspended magnets and assessment of the impact of diurnal temperature variation, within the wooden, thermally insulated variometer room at ETT.

ii) Evaluation of the effect of H-variation (diurnal range ~100nT) on the La Cour D-variometer at ETT, that was dynamically balanced in the'astable' position, with torque equal to the force exerted by ambient H-component. The H-field, around the D-variometer was increased in steps, using the Helmholtz coils of the assembly, to estimate the coefficient of change in D for every 10nT increase in H. This was used to re-calibrate declination values at ETT.

iii) Improved constant current source, bias coil assembly and in-house proton precession magnetometer(PPM) were deployed in the experiment. Baselines obtained from two different methods of vectorised measurement, Nelson's method and Serson's method, were compared for equatorial latitudes, against those obtained from DIFlux. Serson's method of vectorised measurements was found to be optimal for low values of vertical component.

Keywords: Calibration of observatory magnetometers, Equatorial vertical field measurements, Experiments on magnetometers.

INTRODUCTION

Hyderabad Magnetic Observatory (HYB, 17.4ºN,78.5ºE) and the Equatorial Observatory, Ettaiyapuram (ETT, 09.2ºN, 78.0ºE) were established in 1964 and 1978 respectively (*Sanker Narayan, 1964; Sanker Narayan et al, 1978*).The two observatories operated similar quartz suspension La Cour variometers and used calibrated secondary absolute standards, Quartz Horizontal Magnetometer (QHM) for H and D, and Zero Balance Magnetometer(BMZ) for Z, and yielded consistent continuous magnetic variation data. In the processing of data, checks were made to verify consistency and identify causes for baseline drift. One of the primary causes for drifting baselines and variation data was temperature change. The variometers at HYB were placed in a semi-underground double-walled vault with variation of temperature ~1° C. At ETT, where the variometers were installed above ground in a wooden insulated building, temperature variation was greater. This was a primary concern. Therefore thermal coefficients of the La Cour suspended magnetic were initially experimentally determined at HYB (*Sanker Narayan et al, 1966*) and later at ETT in 1980, and some results are presented below.
The D diurnal variations are of low amplitudes at low latitudes. It had been suggested that sensitivity of the La Cour D variometer improves considerably in the astable position i.e. the D Variometer magnet north pole pointing towards magnetic south, with sufficient torsion given to the suspending thick quartz fibre. In this orientation sensitivity is high due to magnetic repulsion and high torsion exerted by the thick suspension quartz fibre (*MacComb,1952*). This was the 'astatic' equilibrium position of the D variometer suspension installed at ETT. Later it was noticed that D-variation at ETT showed anomalous diurnal signature, the probable cause being the large diurnal range of H (~100nT) at an equatorial observatory. In order to investigate this and quantify the effect of H variation on D variation, an experiment to estimate the effects of calibrated increase of H-component, with simultaneous absolute measurements was performed. The ETT hourly variation data was revisited to correct this effect and an artifact of apparent EEJ effects in D-variation was eliminated (*Saratchandra et al, 2002*).

Careful checks of baselines also showed effects of ambient temperature and humidity on the secondary calibrated standards; QHM and BMZ. This had a seasonal effect on baseline determination. By means of careful measurement and recording of ambient conditions, these effects were minimized. It was recommended by the Danish Meteorological Institute (DMI), that absolute magnetometers be re-calibrated against a standard every 2 years. However it was not possible to complete these checks against external standards as regularly as advised. The inter-comparison of Balance Zero Magnetometers, posed a challenge. Usual practice was to compare these instruments against the baselines at Alibag Magnetic

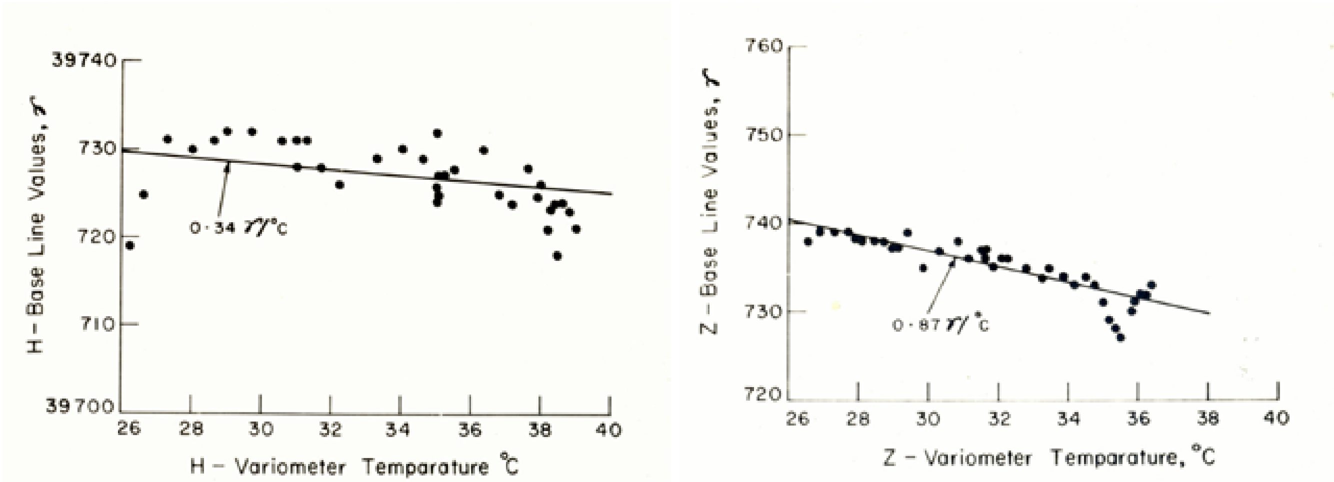

Figure 1a,b. Thermal coefficients of H and Z variometers (ETT) determined by heating and cooling of the variometer room, over a few hours, while continuously makingabsolute measurements at a nearby location.

Observatory (ABG). The settings of the collar magnet of the BMZ were different for HYB and ABG, giving an offset to values. Further, at ETT, near the equator, no collar magnet was used, therefore intercomparison at higher latitudes, was not feasible. Thus it was not possible to calibrate these instruments against ABG baselines. Efforts were made at NGRI to develop an absolute standard that could be used to monitor the QHM and BMZ. A proton precession magnetometer with a set of vectorising coils was developed (*Sarma et al, 1975*). After several improvements to the vectorising coil assembly and the constant current source, testing of the vector proton precession magnetometer (VPM) assembly and a novel method of vectorising at low latitudes were also carried out at ETT, comparing it with absolute measurements of the DI Flux magnetometer (*Saratchandra et al, 1999*). The efficacy of the method is reported below.

The three experiments are presented below along with their results.

DETERMINATION OF THERMAL COEFFICIENTS OF LA COUR VARIOMETERS

An experiment was conducted to obtain the thermal coefficients of La Cour variometers, at HYB (*Sanker Narayan et al, 1966*). Based on this, and an observed change of 1ºC/day in the double walled variometer vault, it was established that HYB variation data was free from thermal effects. A similar exercise was carried out at ETT in 1980 where the variometers were installed above ground, in a wooden walled housing. There was a concern that temperature effects might be large at ETT. In January 1980, the variometer room was heated from 25ºC to 40ºC, and cooled gradually and the temperature of the variometers was recorded every 5 min. At the same time, absolute experiments were carried out to determine baselines of H,D and Z, throughout the day. The absolute measurements were made using QHM and BMZ, and the values were reduced to a base temperature, from the values recorded. This satisfied the condition of stable absolute values. Plots of the change in baseline values (Figure 1a,b) reduced from the variometer records, during heating and cooling clearly demonstrates the thermal effects on magnetic variations. Heating was done using four charcoal braziers, one in each corner of the variometer room, in order to provide uniform heating. Temperature gradients for both heating and cooling cycles were kept approximately the same. The absolute experiments were carried out at 10-minute intervals during the cycles and temperature was recorded every 5 minutes. The thermal coefficients of the La Cour variometers were derived from the plots and found to be -0.34 nT/ºC, for H-variometer and -0.87nT/ºC for Z-variometer. In the plots reproduced here, magnetic field units are γ and not nT, as this experiment was conducted in January 1980!

ESTIMATING EFFECT OF H-VARIATION ON D VARIOMETER IN ASTABLE POSITION

As described above, D-variometer magnet was in astable equilibrium At ETT, the field values are: H ~ 40000n T,D ~ 3° and ∂D ~ 3′. It was desired that the La Cour D Variometer set up, should have sensitivity, such that a deflection of about 2.6 to 3.3 mm on the photographic chart would correspond to a change of 1' arc, in order that the diurnal variation is measurable from the magnetogram. Various quartz fibres were used in the Dvariometer suspension to try and obtain the desired deflection that was tested by giving measured currents in the Helmholtz coils. However, even with the thinnest quartz fibre, in the normal position, the deflection observed on the chart was only 1 mm for every 1′arc. This is constrained by the geometry

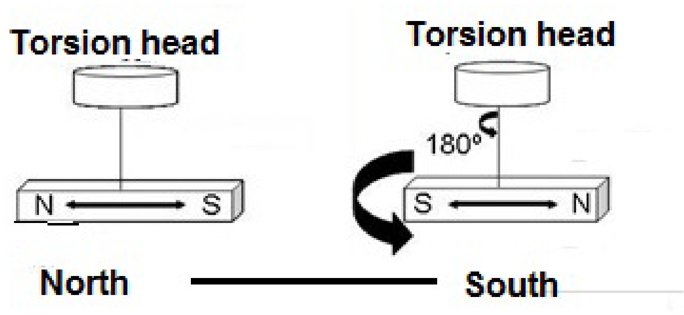

Figure 2a. Schematic illustration of Normal andAstable positions of La Cour D-variometer magnet.

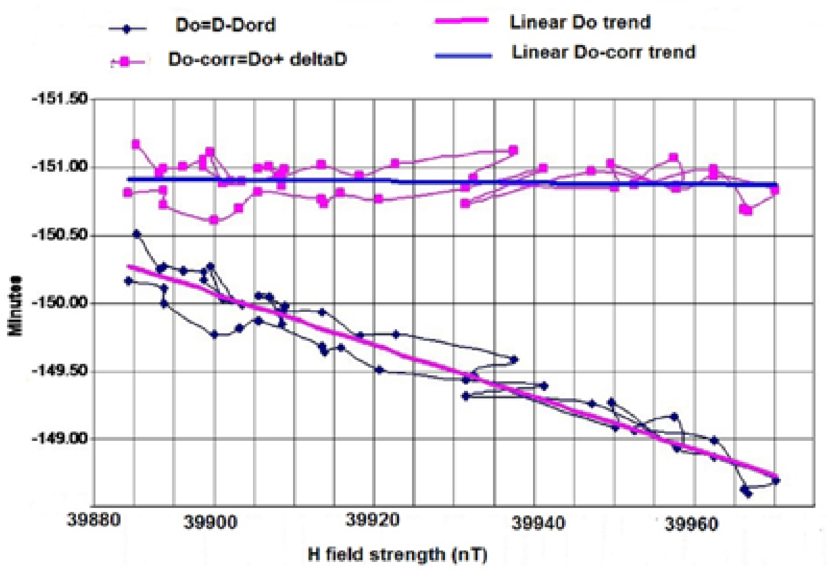

Figure 2b. Comparison of D-baselines reduced without and with corrections for astable position, showing the depeendence of uncorrected Do on values H field, from measurements of 22nd December 1992.

of the photo-registration arrangement and the thickness of the trace on the paper. The diurnal variation would then have a deflection in the record of about 3 mm, which is not at all useful for monitoring diurnal variation of D, from a trace of 1mm thickness. Both normal and astable positions and subsequent sensitivity have been outlined in manuals of observatory practice (*McComb, 1952, Weinert, 1970*).

Normal Orientation: In this orientation, the suspended magnet is oriented in the magnetic meridian with its north pole towards magnetic north with zero torsion in the suspension thin quartz fibre (torsion coefficient is very low) i.e., the magnet orients itself parallel to the direction of H because of zero torsion as shown in Figure 2a. Since the suspended magnet is in the magnetic meridian, it responds ∂Y and is not free to respond to the variations in H.

Astable Orientation: In the astable position of D Variometer, the suspended magnet is oriented with its north pole pointing south with required torsion in the suspension fibre, for which a very high torsion coefficient thick quartz fibre is used (Figure 2a). Therefore it was decided to suspend the magnet of the D variometer, in the astable position. The desired sensitivity was obtained for D variations. However, the effects of diurnal variation in H on D-variation were noticed, during periods of activity and also in the drift of D-baseline values, despite repeated observations with 3 QHM tubes. The magnet orients itself anti-parallel to the direction of H due to high torsion. Since the magnet is suspended in dynamic equilibrium with the ambient strength of H, in the magnetic meridian, it responds to ∂Y and also to ∂H due change in the equilibrium, with H variation ~100nT. Then from the equations:

$$Y = H\sin D \qquad (1), \text{ differentiating,}$$

$$\partial Y = H\,\mathrm{Cos}D.\partial D + H.\ \partial H\,\mathrm{Sin}D (2)\ ,$$

$$\partial Y = X.\partial D + Y.\ \partial H,$$

where Y=0 in the meridian position (normal), then

$$\partial Y = X.\partial D$$

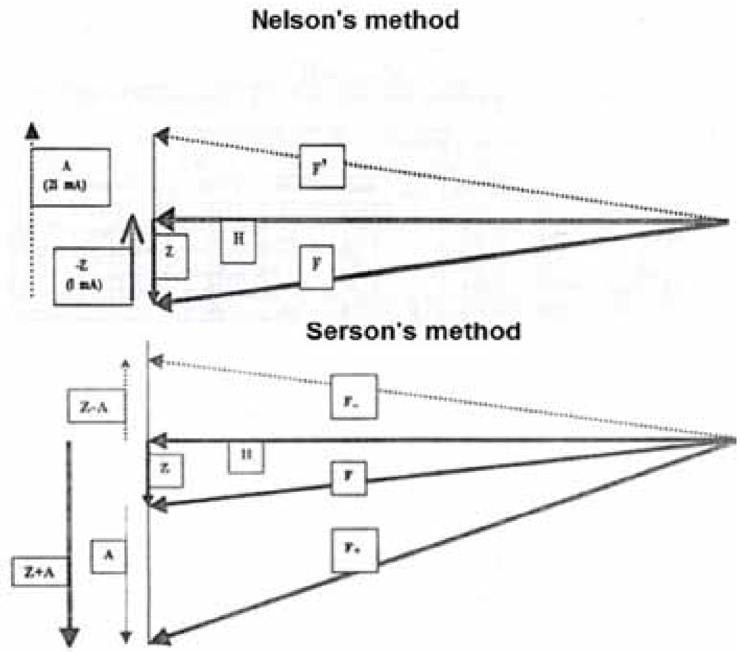

Figure 3a. Schematic to show measurements of F, F′ in Nelsons method, and F, F+ and F- in Serson's method, where the vertical component Z is augmented by a field A, estimated from the constant current source.

And in the astable position, ∂Ycorr. = ∂Y + Y. ∂H, is dependent on both ∂D and ∂H.

In order to accurately report D variation, the baselines had to be stabilised and diurnal variation corrected for the effects of ∂H, on ∂D. An experiment was carried out in 1992, to determine a linear relationship between ∂H and ∂D. Using the Helmholtz coils of the D variometer, an additional H field was added in measured increments. At each step, DIflux measurements of H and D were also carried out. Figure 2(b) show the effect of H variation on the baseline values obtained for D, from the magnetogram, using absolute values conducted throughout the experiment. It is established that the effect of increasing H, is a linear increase in D variation. An effect of 1′ of D variation was observed for a change of 50-60 nT of H. The value of 54 nT/′ as the effect of H variation on D from the continuous observations of DIM-100 for D and the respective baseline plots was accepted and a correction of 0.019′/nT of ∂H variation was applied to hourly means of D Variation.

This procedure was followed in the finalization stage of Do Baseline values and at D data processing stage considering the available H Magnetic data, to output D Magnetic Data independent of H Variations. However, this relationship was not estimated for very large changes in H, viz., likely values of storm ranges. It is also known that torsion suspended variometers can have varying scale values (sensitivity) for large fluctuations. Therefore though this formula to correct D variations was used for the entire series of hourly variations the storm ranges, or short period D ranges were not reported for ETT.

Estimation of Z value by Vector proton magnetometer

The low magnitude of absolute values of Z at low latitudes posed a challenge to accurate measurement. The relatively higher rate of annual variation in Z, in the Indian region, required close monitoring and accurate determination of absolute values at these observatories. Estimation of Z at low and equatorial latitudes has inherent imprecision. The performance of BMZ over time could not be evaluated by inter-comparison, at ETT for reasons given above. Limitations regarding calibration of BMZ also made it desirable to have an independent means of making absolute measurements (*Weinert, 1970*).

A proton precession magnetometer, vectorised with bias coils, to determine absolute 'H' and 'Z' was developed. PPM only measures the magnitude of the total scalar magnetic field (F). However, PPM can be vectorised using suitable bias coils to measure the larger of signal strength (either H or Z) using bias coils. Design and construction of bias coils and a reliable constant current source are critical inputs to obtain vector magnetic measurements using a PPM (*Auster et al, 2007, De Vuyst 1972*). There are intrinsic errors in this instrument set up i) errors in machining the coils, ii) proper orientation and centring, iii) maintaining constant current during vectorisation.

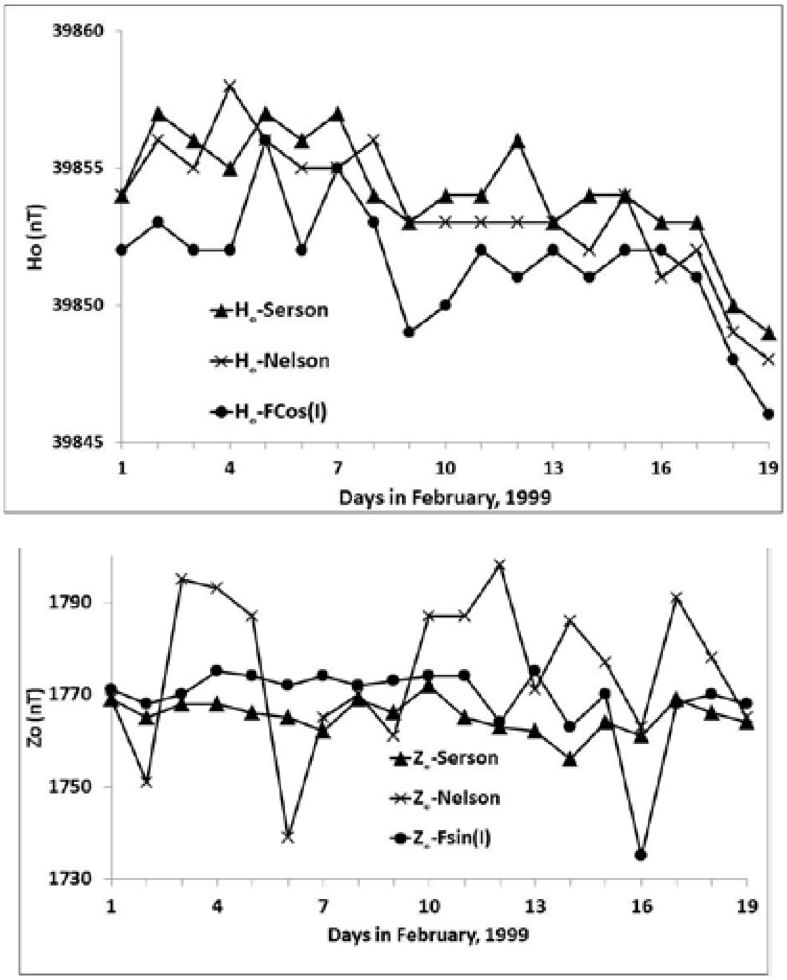

Figure 3b,c. Baselines of H and Z obtained from all VPM measurements: Nelson's method, and Serson's method, compared against F.sin(I) obtained from DI flux measurements, on 19 days in February, 1999.

The bias coil unit and turntable were fabricated at NGRI, replicating one used at HYB observatory (*Sarma et al, 1975*). The coil configuration that was found to produce a volume of uniform magnetic field with most compact coil configuration was the Faneslau-Braunbeck coils. The constant current source was designed specifically for this experiment, the emphasis was on keeping the bias current constant within +/- 10.0 μA, being about 0.65nT. The bias coil constant determined in the laboratory was 65nT/mA (*Sarma et al, 1975, Saratchandra et al, 1999*). The vector PPM (VPM) was used at HYB initially. With improved constant current source, it was felt that the system was sufficiently accurate to obtain reliable vector absolute values even at equatorial station like ETT. The low absolute values of Z at ETT, and inherent errors in determination of absolute values, using BMZ, or VPM, provided suitable conditions to test the vector assembly. Further the relative accuracy of two methods of vector measurements i) Nelson's method and ii) Serson's method were also evaluated. The measurements were compared against absolute values obtained using a DIFlux. A schematic illustrating the two methods is given in Figure 3a.

Nelson's method

Schematic of the magnetic vectors of Nelson's method is given in Figure 3a. F is the total field readout, with zero current in the bias coil. A bias vertical field A, is created in the coil unit by sending a current 2i, which can produce a total field F′ as read on the PPM output, F′=F. Then half that current i produces a total field readout F=H. With readouts of F and H, Z is determined. Five sets of these readings are taken under quiet field conditions and averaged to obtain absolute values of H an Z. In this method F and H are measured and Z is calculated.

However, at low latitudes, this measurement has a high intrinsic estimated error. When F and H are measured using Nelsons method, $Z = \sqrt{(F^2-H^2)}$. Differentiating, the error in Z, $\partial Z=(F+H)/Z$. This error can be large at equatorial stations where F~H and Z <20% of Fafter differentiation error dZ = (F+H)/Z * dF(dH). In∂Z~(40,000+40,000)/1900=42nT*dF(dH) nT.

Sersons method

A schematic of the field measurements is given in Figure 3a. A bias current'i' is used to create a bias vertical field A~3Z. The bias current is kept constant during the measurement cycle, only the polarity is switched. The estimates of F (no bias current), F+ (increased Z and F- (opposing Z) are noted. Five sets of these readings are taken, without altering the current. From the averaged values, Z and H are calculated (*Serson, 1962*).

During these experiments, DI flux measurements of inclination (I) and declination (D) were also made. This was repeated on18 days of February 1999. All the absolute measurements were reduced to baseline values H_o and Z_o. In Figure 3b and c, values of Z_o and $H_o$the baselines obtained from Serson's method, Nelson's method and DIM are plotted for successive days of the experiment in February 1999. Both the VPM methods give similar values for H, with very little scatter (Figure 3b). The values are comparable with the DI Flux measurements, which themselves show some scatter. The stability and similarity of Z baselines obtained by Sersons' method and DIM experiments is clearly seen in Figure 3c.It is seen that Serson's method showed less scatter in Z values. Nelson's method provides more erratic estimates of baselines, due to the inherent errors in determining Z at low-latitudes. It is an acknowledged observation that errors of ~42nT, in Z values, are unacceptable in the measurements at low and equatorial latitudes. The changes in measurement made in Serson's method adequately address this issue and it was demonstrated that stable baselines are obtained at an equatorial station. Further, this experiment, evaluated the performance of the in-house developed PPM, bias coils and constant current source.

CONCLUSION

Due to the isolation of magnetic observatories it was necessary, to periodically test the magnetometers for self consistency, using experiments applying basic concepts of magnetism. Over the past 50 years, when magnetometers were calibrated against secondary standards, extreme care was taken to check and re-check their consistency, as it was not possible to compare and evaluate the performance of variometers and absolute instruments regularly. Further, with the development of modern magnetometers, and the absolute measurements made with proton precession magnetometers, it was once again necessary to compare and calibrate these magnetometers against the older classical instruments. Such experiments help to maintain the validity of a long series of measurements, as in the case of reducingthe effect of ∂H variations on D variometer. Geometry of fields at the magnetic equator, small absolute values and large diurnal variations all provided challenges. These were opportunities to calibrate magnetometers and test methods of measurement using fundamental principles, all the while without disruption of the continuous record of variations.

ACKNOWLEDGMENTS

We thank the LOC of the 16th IAGA Observatory Workshop, 2014, for support to attend the Workshop and the invitation to contribute to this volume. We are grateful for all the assistance and expertise provided by all the staff of ETT observatory, over the years during these experiments and for the fundamental understanding and conceptualisation provided by late Mr Y.S. Sarma.We thank two reviewers for their helpful comments. Support of the Ministry of Earth Sciences (MoES/P.O. (Seismo)/1(124)/2010) is acknowledged (NN).

REFERENCES

Auster V, O., Hillenmaier, R., Kroth, and M. Wiedemann, 2007. Advanced Proton Magnetometer Design and its Application for Absolute Measurement publ. Inst. Geophys. Pol. Acad. Sc., C-99 (398)

De Vuyst, A.P., 1973. Proton and Proton Vector Magnetometers, IAGA Scientific Session, Commission I, Kyoto, Institut Royal Meteorologique de Belgique, Miscellanea Serie C, no 7.

McComb, H.E., 1952. Magnetic Observatory Manual publ. U.S. Department of Commerce, Coast & Geodetic Survey.

Sanker Narayan, 1964. Establishment of a magnetic observatory at NGRI; Bull NGRI, 2, 115-122, 1964.

Sanker Narayan, P.V., Srivastava, B.J., and Sarma.Y.S,1966. Modifications of the temperature compensation systems of the La Cour variometers at the NGRI magnetic observatory, Hyderabad, J. Indian Geophys. Union, 3, 51-58.

Sanker Narayan P.V., Sastry, T.S., Ramanujachary, K.R., Sarma, S.V.S., Morgunov, V.I., Nikonorov, A.M., 1978. Equatorial Geomagnetic and Geo-electric observatory of NGRI at Ettaiyapuram, Geophys Res Bull, pp Vol.16,No.4, 1978.

Saratchandra, K., Nandini Nagarajan, Kumaraswamy, V.T.C. & Nagamani, P.V., 2002. La Cour D- variometer set up- normal and astable orientations, NGRI Equatorial Observatory Ettaiyapuram (ETT). Presented at IGU annual convention, Nagpur, 2002.

Saratchandra, K, Rajendra Prasad, N.P., Sastry, T.S. 1999. Determination of Absolute Z at equatorial latitudes by Serson's method – An Appraisal.-presented at IGU Annual convention, Pondicherry, 1999.

Sarma, Y.S., Sarma, P.L.N., and Ghosh, P.R., 1975. Proton Vector Magnetometer, Geophys Res Bull, 13: 367-374.

Serson, P.H., 1962. Method of Making an Electromagnetic Measurement, , Canadian Patent No.654.552, issued Dec. 25, Class 324-1.

Wienert K.A., 1970. Notes on Geomagnetic Observatory and Survey Practice, publ. UNESCO Publications.

J. Ind. Geophys. Union (January 2016)
Special Volume-2/ 2016 pp: 87-98

On the role of atmospheric tides in the quiet-time variabilities of equatorial electrojet

S. Gurubaran[1,2], S. Sathishkumar[2] and B. Veenadhari[1]
[1]Indian Institute of Geomagnetism, New Panvel (W), Navi Mumbai, India
[2]Equatorial Geophysical Research Laboratory, Indian Institute of Geomagnetism, Tirunelveli, India,
su.gurubaran@gmail.com

ABSTRACT
Simultaneous observations of geomagnetic field variations and upper mesospheric winds by MF radar from low latitudes spanning over a period of 19 years (1993-2011) are utilized in the present work to assess the role of upper atmospheric tides in causing the long-period variabilities of equatorial electrojet (EEJ). Decomposition of ground magnetic data by adopting the method of natural orthogonal components (MNOC) (also referred to as the Principal Component Analysis (PCA))enables the separation of the normal quiet-time behaviour (the expected diurnal variation) and the abnormal (features like counter electrojet (CEJ)) field variation. Using the second principal component as a proxy for CEJ, we show in this work that the CEJs occur more frequently during the solar minimum years and a high degree of correlation is noticed between the enhanced tides during the solar minimum years and the occurrence of CEJs then.

Keywords: Geomagnetism, Equatorial Ionosphere, Equatorial Electrojet, Atmospheric Tides

INTRODUCTION

Tidal winds generate electric fields and currents in the E region of the ionosphere where the transverse conductivities maximize. The ionospheric current system arising during magnetically quiet times is referred to as the solar-quiet (Sq) current system and has been a subject of interest for several decades. During daytime, the Sq current vortices are characterized by an anticlockwise flow in the Northern Hemisphere and a clockwise flow in the Southern Hemisphere, both moving with the apparent motion of the Sun. The principal driver for the Sq current pattern is the solar first symmetrical evanescent (1,-2) diurnal tide (*Tarpley, 1970b*). Surface geomagnetic field observations can be used to deduce equivalent current distributions concentrated in a thin concentric shell. With such an approach, several studies have been carried out in the past since the early work of Chapman and Bartels (*1940*), delineating the structure of the Sq current system and its time and space variations (e.g., *Matsushita and Maeda, 1965; Matsushita, 1967; Malin and Gupta, 1977; Suzuki, 1979; Campbell et al., 1992; Takeda, 1999*). The ionospheric wind dynamo theory that explains the formation of the Sq current system is well documented in the literature (*Richmond, 1995, and references therein*).
An important element in the study of quiet-time ionospheric current system is its significant day-to-day variability. Modelling of Sq faces the challenge of identifying tidal mode or a combination of tidal modes, driving the worldwide ionospheric current pattern, at any instant, that is in agreement with signatures of an equivalent current distribution obtained from the ground magnetic variations. Earlier studies presumed the diurnal tide to be the dominant driver of the current system. Later modelling efforts incorporated the dynamo effects induced by semidiurnal tides (*Stening, 1977; Richmond et al., 1976; Takeda and Maeda, 1981; Hanuise et al., 1983; Takeda, 1990*, to state a few). However, the disagreement between the simulated effects due to semidiurnal tides and observations persisted, despite significant progress in modelling, (*Richmond, 1995*). Other factors like asymmetric tidal components that might be present during solstices and lunar tidal effects have been invoked to explain the discrepancies between models and observations (*Stening, 1989; Tarpley, 1970a; Stening and Winch, 1979*).

Close to the magnetic dip equator, an intense band of eastward electrical current, the equatorial electrojet (EEJ), flows at a height of ~105 km in daytime within a narrow latitudinal belt (*Onwumechili, 1997, on all aspects of EEJ*). The quiet-time eastward current, on some occasions, reverses its direction and manifests as a negative deviation in the horizontal component of the geomagnetic field (*Mayaud, 1977*). This feature is referred to as reverse or counter electrojet (CEJ). The presence of CEJ at the magnetic equator has been linked to a superposition of an additional current system over the normal Sq (*Bhargava and Sastri, 1977; Stening, 1977b, Marriott et al., 1979; Hanuise et al., 1983; Rastogi, 1994; Alex et al., 1998; Gurubaran, 2002*). After examining several CEJ events and possible wind systems that might be driving them, Stening (*1977b*) concluded that various tidal modes might be able to simulate the observational results. However, to better understand the simulation process knowledge of different wind systems are required on different occasions.

Major unresolved issues in the study of EEJ are: (1) the relationship between the Sq current system and EEJ, and (2) the causative mechanisms responsible for the quiet-time CEJ phenomenon. In the first, the daily range in the *H*-component of the geomagnetic field at EEJ stations is poorly correlated with the range at low latitudes (*Kane, 1976; Rastogi, 1993; Yamazaki et al., 2010*). It was also hypothesized that the position of the Sq focus would alter the strength of the EEJ (*Tarpley, 1973*) and the correlation improves when this effect is taken into account. The EEJ itself is treated by some authors as a separate current system flowing at lower altitudes and having its own return current at low latitudes (*Onwumechili, 1997*). A strong indication for this is provided by the narrow latitudinal and longitudinal signatures of CEJ. If the global tidal modes are responsible for this reverse current at the equator, the associated changes in the magnetic field elements should occur globally (*Stening, 1977b*). There is a need to explain why tidal modes of global origin do not always produce such changes in Sq pattern globally. An alternate view envisages vertical winds and gravity wave associated shearing winds to be capable of producing such current reversals in narrow latitude and altitude regions (*Raghavarao and Anandarao, 1987*). In a recent work, Yamazaki et al. (*2014b*) revisited the above problem using a whole atmosphere community climate model. The simulation results from this model reveal the irregularity of zonal winds that seems to be responsible for the spatio-temporal variations of EEJ in shorter time scales. Using the Thermosphere-Ionosphere-Electrodynamics-General Circulation Model (TIE-GCM), Yamazaki et al. (2014a) showed that upward propagating tides compete with the in-situ generated tides to take control of the seasonal variabilities of EEJ. When the upward propagating tides are incorporated into the model, they noticed a doubling of the current intensity and the corresponding ground magnetic signature. The model simulations further indicate that the semi-annual variation in EEJ is caused primarily by the semi-annual variation of the upward propagating tides.

The operation of the medium frequency (MF) radar at Tirunelveli (8.7ºN, 77.8ºE, geographic; 2.2ºN magnetic dip) has produced continuous data,since 1992, on winds in the mesosphere-lower thermosphere (MLT) region in the height range 80-98 km (*Rajaram and Gurubaran, 1998*). This offers an excellent opportunity to explore the long- and short-term variabilities in EEJ, which can be explained by similar variabilities in tidal winds in the MLT region. In the present studywe make use of the information on tidal winds retrieved from the MF radar data and the ground magnetometer observations from Tirunelveli (1999 onwards) / Trivandrum (1993-1998), the dip equatorial stations. These stations are under the influence of both Sq and EEJ. In addition we have also made use of the data from Alibag, a station which is located away from the magnetic equator and is under the influence of only Sq. The EEJ strength for every hour is derived from the difference in the horizontal component of the magnetic field between the two stations for that hour. By taking this difference, contributions arising from magnetospheric currents are expected to be minimized.

We utilize the Method of Natural Orthogonal Components (MNOC) (referred to as Principal Component Analysis (PCA) in this work) to decompose the ground magnetic data for the period 1993-2011 and to express the daily variation as a summation of a few eigen modes. It will be demonstrated here in that the first eigen mode of the EEJ represents the fundamental solar driven diurnal component, whereas the second and third eigen modes reveal the presence of higher order solar driven tidal components. When a comparison of the first two eigen modes is made with the MLT tides, we notice several interesting features: the principal or the first eigen mode that also represents the daily range in EEJ reveals solar cycle variability as expected. However, the tides are stronger during the solar minimum years of 2006-2010 and weaker during the solar maximum years of 1999-2002. They are not correlated well with the daily range in EEJ even in the seasonal time scales. Rather, afternoon CEJs are more prominent during solar minimum. Also they appear to be driven by MLT tides.

SELECTION OF DATA AND ANALYSIS

This study utilizes the hourly values of the strength of the EEJ for all months during 1993-2011,when the data on upper mesospheric winds from the MF radar over Tirunelveli are available. It may be recalled that the solar activity was in the descending phase during the initial years of 1993-1995, whereas the activity went through a deep minimum between 2007 and 2010. Days for which there were gaps in the magnetometer data (either for Tirunelveli / Trivandrum or for Alibag) of few hours or more were excluded from the analysis. The number of days for which EEJ data for the full 24 hours are available is then 6705 instead of a possible 6939.

Like in previous work (*Gurubaran, 2002*), we adopt MNOC to separate the normal and abnormal geomagnetic field variations. Several authors have used this technique to unravel a variety of processes that contribute to the observed field components (*Golovkov et al., 1978; Rajaram, 1980, 1983; Xu and Kamide, 2004; Chen et al., 2007; De Michelis et al. 2010,* to state a few). As described in these reports, the procedure involves expanding the observed field in an orthogonal basis and solving the resultant eigen value problem and looking for some simpler patterns. The method is briefly described below.

The hourly geomagnetic field variation is expressed in terms of a set of basic functions called Empirical Orthogonal Functions (Z_{jk}) as:

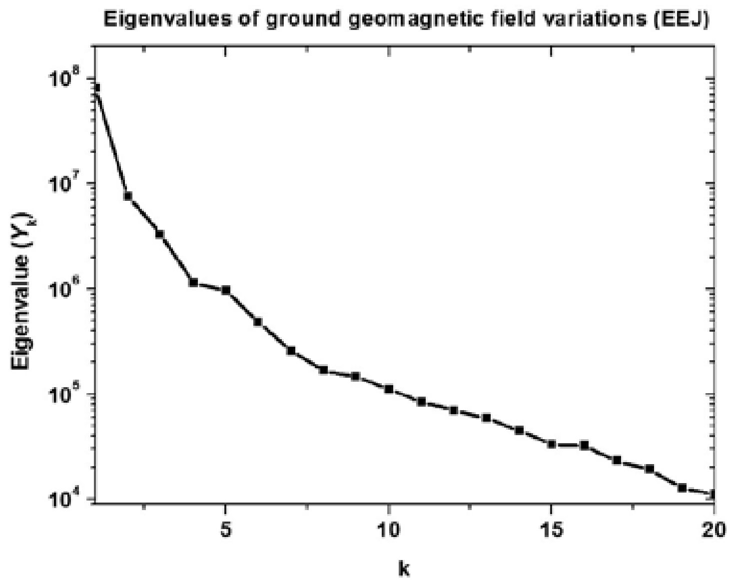

Figure 1. The eigenvalues for the first 20 principal components.

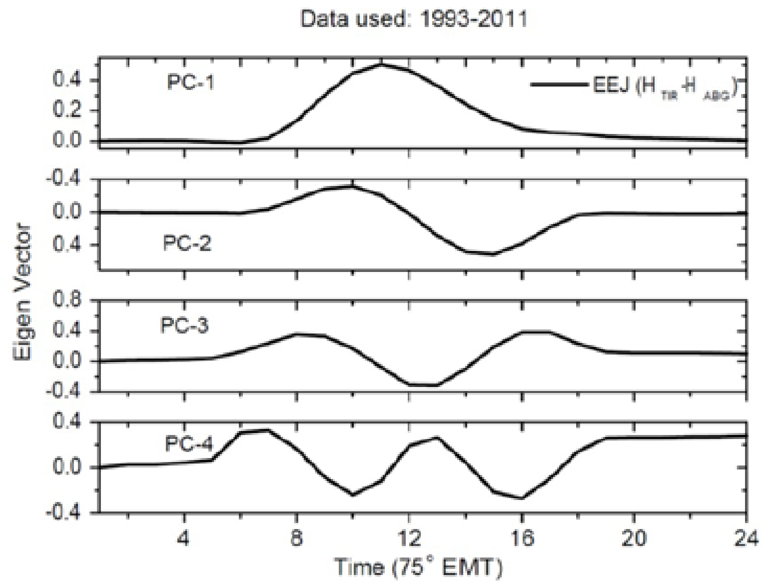

Figure 2. The eigenvectors derived from the MNOC technique.

$$\varphi_{ij} = \sum_{k=1}^{N} h_{ki} Z_{jk} \tag{1}$$

where i = 1,2,..n represents the number of days and j = 1, 2, …24 represents the hour for a given day i. Here k = 1, 2,...and N is the mode number. In short, Z_{jk} is the mode of the kth component (a 24-hour pattern, in our case) and the corresponding principal component (PC) is h_{ki}, which is the amplitude of the mode for the given day i.

If X_{ij} represents the observed hourly variation, we need to minimize the 'error' that might have occurred in the representation of the observed data by the above series expansion:

$$\delta = \sum_{i=1}^{n} \sum_{j=1}^{24} \left[X_{ij} - \sum_{k=1}^{N} h_{ki} Z_{jk} \right]^2 . \tag{2}$$

This reduces to the following eigen value problem:

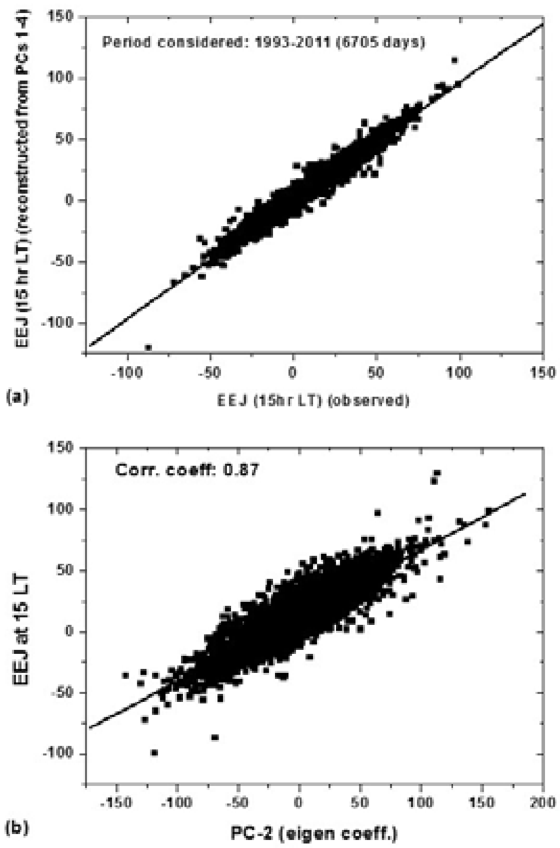

Figure 3. The scatter plots for the observed and reconstructed EEJ strength at 15 LT (top panel) and the PC-2 and EEJ at 15 LT (bottom panel).

$$R_{jk}Z_{jk} = Y_{ki}Z_{jk} \tag{3}$$

where $R_{jk}$is the N x N covariance matrix given by X^TX. Here $X^T$is the transpose matrix.The eigenvalues, Y, and the corresponding eigen vectors, Z, are obtained by solving equation (3).

From equation (1), the amplitudes of the principal components (also referred to as eigen coefficients) for any day, i,can be written as

$$h_{ki} = \sum_{j=1}^{24} \varphi_{ij} Z_{jk}. \tag{4}$$

The eigen values, Y_{ki}, represent a measure of the variance of their corresponding principal components. As we have seen with the large data set chosen for the present work, the observed variation can be explained in terms of the first few eigen modes. Figure 1 reveals the eigen values computed for the first 20 principal components from the EEJ data. The rapid drop of the eigen values is clearly evident. This suggests that the first few eigen modes can almost fully represent the ground geomagnetic field variation.

In Figure 2 we show the results of the PCA for the first four eigen modes. As can be noted, the first eigen mode largely represents the normal quiet day behaviour of EEJ with a maximum around noon hours. Interestingly, the second and third eigen modes reveal features that are characteristic of semidiurnal and terdiurnal components with 12 hour and 8 hour periodicities, respectively. A 6-hour periodicity can be noted in the eigen vector for the fourth PC. As expected, no variation is seen for the night hours (between 18 and 24 and 0 and 6 LT) (time is expressed in local time (LT) or 75°E Meridian Time or in short 75° EMT).

Figure 3a demonstrates how well the first four eigen modes together represent the observed variation field. An excellent comparison has been obtained between the observed and reconstructed EEJ strength for the 15 LT time sector considered for this analysis.

When examined closely, with its characteristic negative minimum around 10 LT and positive maximum around 15 LT, the eigen vector for the second principal component (refer to the second panel from top in Figure 2; also note here that the scale has been reversed) reveals a close relationship with the afternoon CEJ over Tirunelveli (afternoon CEJs are more frequent than morning CEJs). On days of afternoon

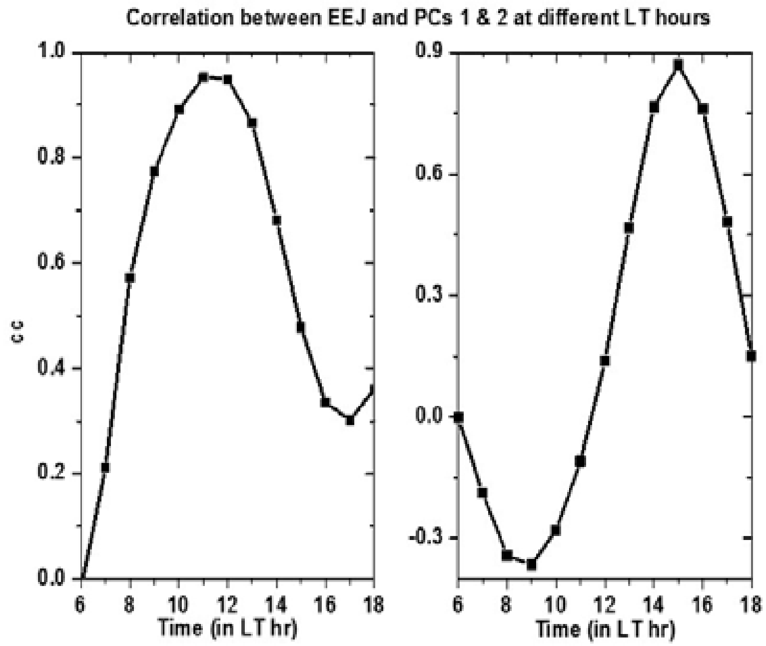

Figure 4. Temporal dependence of the correlation coefficients computed for the EEJ strength at various times and the principal components 1 (left panel) and 2 (right panel).

CEJ, the corresponding eigen coefficient for PC-2 turns out to be negative accounting for the depression of the EEJ in the afternoon hours (refer to equation (1)). This behaviour of PC-2 is evident in Figure 3b, wherein the EEJ at 15 LT is compared with the PC-2 eigen coefficient in the form of a scatter plot. With a correlation coefficient of 0.87 and PC-2 thus contributing to 76% of the variability, we conclude that the PC-2 eigen coefficient can be used as proxy for the afternoon CEJs that are more spectacular and more frequent than the morning CEJs. The small scatter in Figure 3b is likely due to other modes that could have contributed to the rest of the variability at this time. Earlier, Rajaram (*1980*) had successfully adopted the MNOC technique to decompose the normal and abnormal variations of equatorial geomagnetic field. In that work the first principal component was shown to contain information about Sq and EEJ, whereas the second principal component was closely related to CEJ and disturbance field variations.

Before we present the main results, we compare the daily eigen coefficients of PCs 1 and 2 with the observed EEJ at local times between 06:00 and 18:00 hours (Figure 4). Interestingly, PC-1 eigen coefficient shows the largest correlation coefficient of 0.95 at 11 and 12 LT, whereas PC-2 eigen coefficient reveals a small negative correlation in the morning hours and a greater positive correlation in the afternoon hours. We point out here that the high correlation (~0.95) between EEJ and PC-1 for the noon hours indicates that PC-1 represents well the daily range of EEJ. Largest (~0.9) positive correlation for EEJ and PC-2 in the afternoon hours, when EEJ displays a depression, indicates that the afternoon CEJ can indeed be represented by PC-2. As noted earlier, the PC-2 eigen coefficient does become negative on afternoon CEJ days.

Finally, to appreciate how the PCA works on the EEJ data, we present two examples (Figure 5), one representing the occurrence of CEJ on 14 January 2006 (shown on the left panels) and the other, the normal EEJ on 20 January 2006 (shown on the right panels), both days being magnetically quiet. In a series of panels one below the other, we show how addition of PCs (superposition of various modes) one by one tend to capture the observed EEJ variation. On 20 January 2006, PC-1 (black curve) alone almost reproduces the observed EEJ (red curve) with a large positive value of 228 for the corresponding eigen coefficient. On 14 January 2006, EEJ did not develop at all during daytime. Rather, we notice a large afternoon CEJ event with the depression in observed EEJ reaching up to -95 nT on 14 January 2006. Even with a large negative value of 50 nT, one can see that PC-1 is not able to reproduce the CEJ feature on this day. As expected from the PCA, the second and third PCs enable the CEJ feature appearing between 13 and 14 LT. Interestingly, the signs of the first three eigen coefficients were opposite between the two days: PC-1 and PC-2 eigen coefficients were negative on the CEJ day with values of -104 and -114, respectively, whereas they were positive on the normal day (i.e., on 20 January 2006) with values of 228 and 25, respectively. PC-3 amplitude was positive on the CEJ day and negative on the

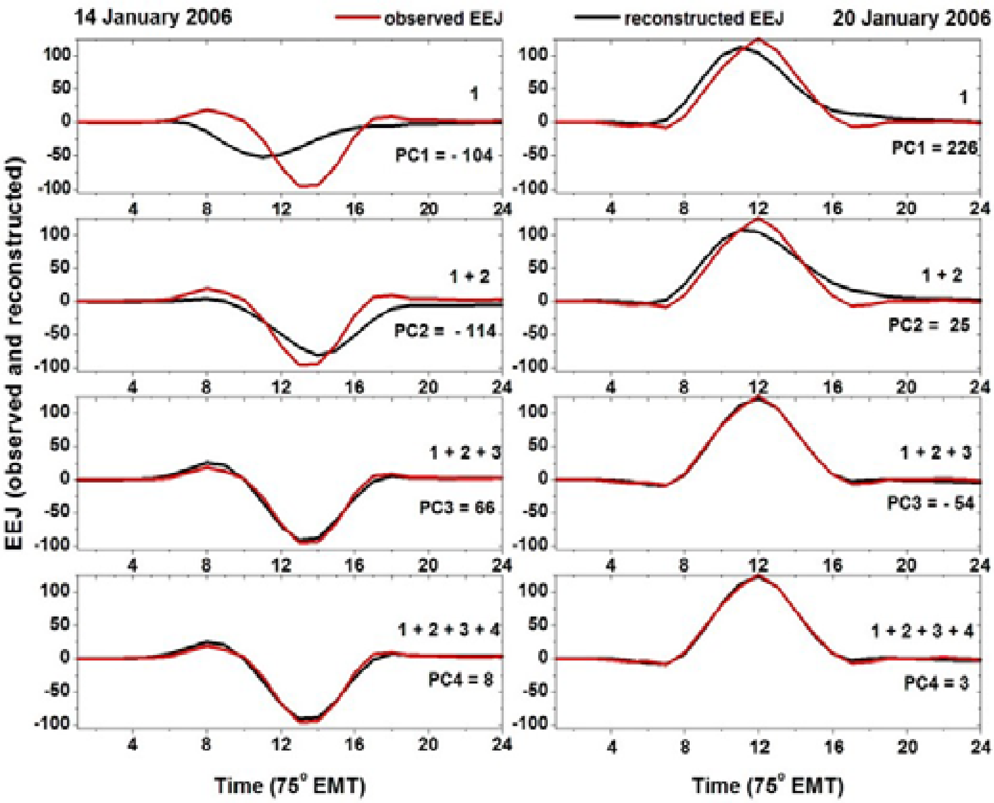

Figure 5. Observed and reconstructed EEJ for 14 January 2006 (left) and 20 January 2006 (right). The observed EEJ is shown as red curves whereas the reconstructed EEJ values are shown as black curves. Increasing number of PCs are used to reconstruct as we slide down from the top (for example, topmost panels were reconstructed from the first PC, second from the top were reconstructed using the first and second PCs together, etc.). The amplitudes of the PCs are also indicated in each panel.

normal day. When several days were carefully examined, it was noticed that on all CEJ days PC-2 amplitudes were largely negative. Further, the greater the CEJ intensity, the smaller (or more negative) was the PC-2 amplitude.

VARIABILITIES OF EEJ IN SEASONAL AND SOLAR CYCLE TIME SCALES

We begin this exercise by examining the first two principal components (essentially, their eigen coefficients) computed for the EEJ strength. The daily values were averaged in monthly time segments and the results are plotted in Figures 6a and 6b. In this exercise we did not remove the disturbed days. A quick look at these plots exhibits the features expected for the normal EEJ and the abnormal CEJ. The equinoctial maxima and the solstitial minima for the first principal component plotted in Figure 6a, which is a measure of the diurnal range of EEJ,are the regular features. This semiannual pattern is clearly modulated by the solar cycle influence. For example, the largest amplitudes(in the range 150-200) for the first principal component are observed during the solar maximum years of 2000 and 2001. During the solar minimum years of 1995-1997 and 2007-2010, the first principal component was relatively weaker (with its eigen coefficient in the range 80-100),implying that the diurnal range in EEJ was smaller during these years.

As discussed earlier, the second dominant principal component, especially when the corresponding eigen coefficient is negative,reveals the abnormal CEJ or reverse electrojet occurring in the afternoon hours. The monthly averaged eigen coefficient for this principal component plotted in Figure 6b exhibits negative values (reaching up to -40) during summer solstices (May-August) and positive values during other months (except for April). Large negative values over an extended period of time are noticed during the solar minimum years (1995, 2009 and 2010). For these years the CEJ occurrences are 221, 242 and 204, respectively, whereas CEJs during the solar maximum years of 2000 and 2001 are 96 and 121, respectively. The frequent occurrence of afternoon CEJs during the summer months and during solar minimum years is a well known feature for the Indian sector (*Rastogi, 1974; Bhargava et al., 1983*). In the present work, we notice 1593 days of CEJ occurrences during summer and 869 and 888 days

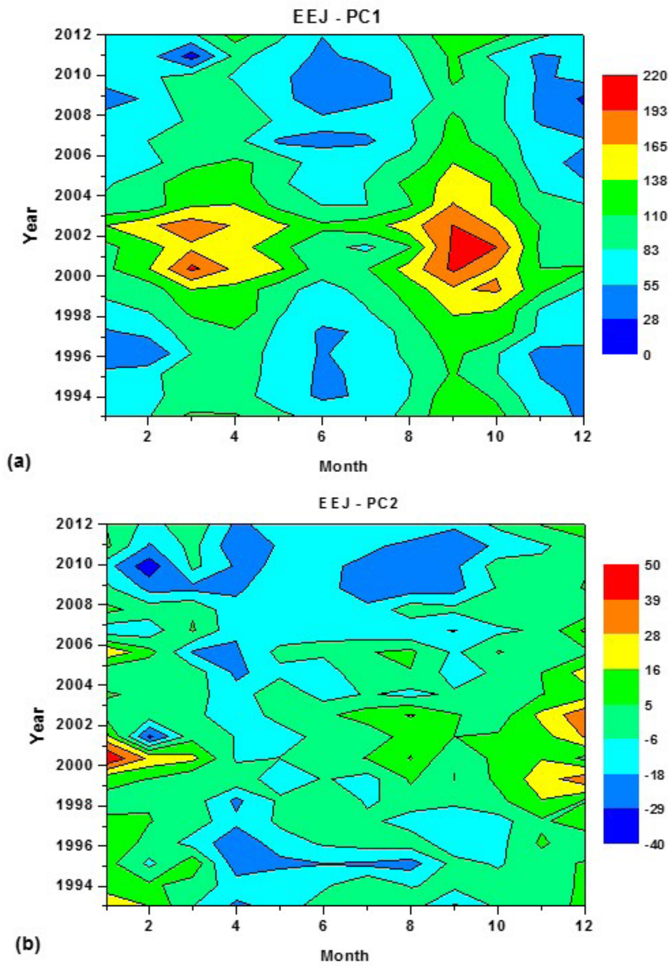

Figure 6. (a) The first principal component of EEJ plotted with season for the years 1993-2011. (b) Same as in (a) but for the second principal component.

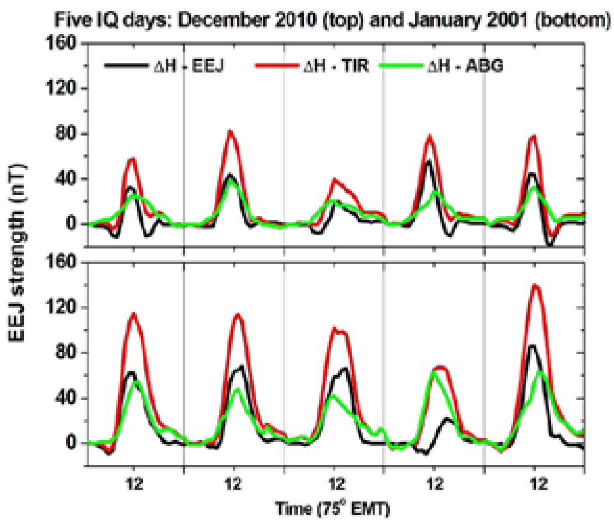

Figure 7. Hourly EEJ strength shown for the internationally classified quiet days during December 2010 (top) and January 2001 (bottom), representing solar minimum and solar maximum years, respectively.

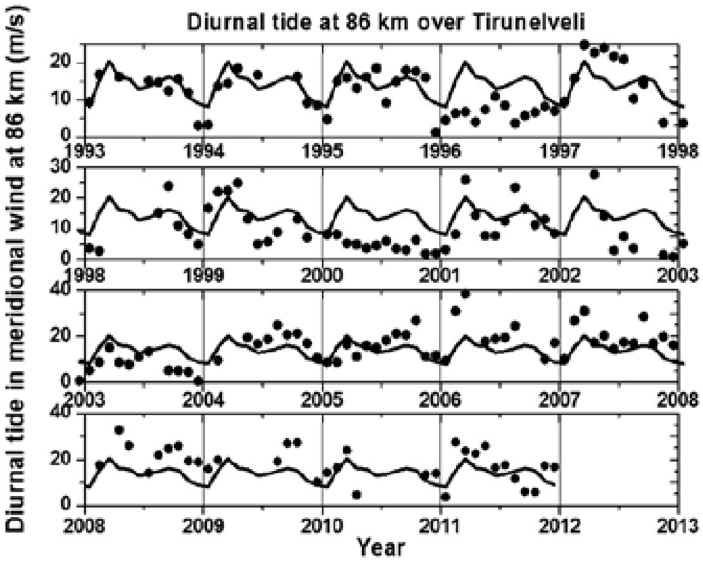

Figure 8. Amplitude of the diurnal tide in meridional wind at 86 km (see text for details).

of CEJ occurrences during winter and equinox months, respectively. With the results from this work agreeing with the previous, on the general behaviour of EEJ and CEJ,one can conclude that the PCA proves to be a valuable tool for assessing the long-term variabilities.

Long-term observations of neutral winds in the mesosphere-lower thermosphere region from Tirunelveli have also helped to examine the role of atmospheric tides in causing the observed variabilities in EEJ in various time scales. Earlier work from this station had shown the links between semidiurnal tides and CEJ during wintertime sudden stratospheric warming (SSW) events (*Sridharan et al., 2009; Sathishkumar and Sridharan, 2013*). During the SSW events that occurred during 1998-1999 and 2005-2006, the semidiurnal tide at 88 km over Tirunelveli was shown to have enhanced amplitudes possibly driving the CEJ events observed during these times (*Sridharan et al., 2009*). The later work by Sathishkumar and Sridharan (*2013*) focused on lunar tides in both mesospheric winds and EEJ during the SSW event of 2008-2009. One of the puzzling aspects of this work has been the enhanced lunar tidal signature in EEJ, whereas the lunar tide in mesospheric winds did not show any enhancement during the SSW.

While carefully examining the diurnal profiles of EEJ, we have noticed the differing nature of the variation during the solar maximum and solar minimum years. In Figure 7 we show the diurnal EEJ curves for the five internationally classified quiet days for December 2010, a solar minimum period (shown in the top panel) and January 2001 (shown in the bottom panel), a solar maximum period. As mentioned earlier, two features can be clearly identified in these curves: (i) Larger diurnal range during January 2001 when compared to December 2010 and (ii) occurrence of afternoon/morning CEJ on four out of five days during 2010.

To better understand the differing nature of EEJ, we have systematically analysed these differences and arrived at more plausibleunderlying causative mechanisms. For this exercise, we have considered tidal amplitudes and phases for the altitude of 86 km by selectively choosing the best radar data acceptance rates. Such a screening and selection has been necessitated as Radar echoes from higher altitudes (92 km and above) are known to be contaminated by EEJ and the radar derived motions are expected to be more closely related to electric fields than to neutral winds at those altitudes (*Gurubaran and Rajaram, 2000*).

In Figure 8 we present the results for the monthly amplitudes of diurnal tide in the meridional wind at 86 km over Tirunelveli for the period 1993-2011. The monthly estimates are shown as symbols, whereas the annual variation in the climatological sense is shown as a thick curve (repeats every year in the figure). One can notice significant deviations of the monthly diurnal tide amplitudes from the climatological mean. During certain years, the tidal activity was greatly enhanced (2007 and 2008, for example),whereas during other years, the monthly tidal amplitudes were smaller than their respective climatological means (1996 and 2000, for example). Especially after 1999, we have noticed a remarkable feature of the upper mesospheric tides over Tirunelveli. The observed strong solar cycle dependence is striking. We have observed presence of larger amplitudes during solar minimum years of 2006-2010 and reduced amplitudes during 1999-2001, when the solar activity was at its peak. Similar solar cycle dependence for the semi-diurnal tide in

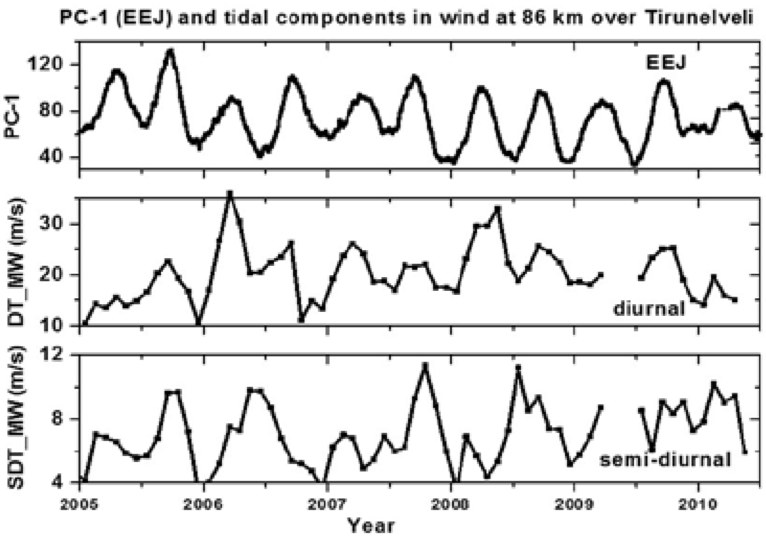

Figure 9. Comparison for the first principal component (top panel) representing the diurnal range in EEJ and the diurnal and semi-diurnal tide components (middle and bottom panels) in wind at 86 km.

the wind components at 86 km over Tirunelveli has also been noticed (not shown here). Earlier, Sridharan et al. (*2010*) noted a negative solar cycle response for the tidal amplitudes over Tirunelveli, while using data obtained over a smaller number of years (1993-2007).

We have also noticed a strong solar cycle dependence of PC-1, which is a measure of the diurnal range in EEJ, with larger values during solar maximum and smaller values during solar minimum (Figure 6a and 6b). This feature is essentially caused by the solar cycle variation of ionospheric electrical conductivity. One can argue that this is not caused by the long-term variability in the mesospheric tides observed over Tirunelveli, as the tidal activity has been weaker during the sunspot maximum years of 2000 and 2001 and stronger during the sunspot minimum years of 2008-2010.

Apart from the solar cycle variability, we also noticed a semi-annual variation in PC-1, which is believed to be partly driven by the in-situ generated thermospheric tides and partly by the upward propagating tides of lower atmospheric origin. In a recent work, using the TIE-GCM simulations that utilize lower atmospheric tidal forcing based on TIMED wind and temperature measurements, Yamazaki et al. (*2014a*) asserted that upward propagating tides play a substantial role in causing the seasonal variability of EEJ.

In Figure 9 we show the comparison for the temporal variation of the first principal component of EEJ and the diurnal and semi-diurnal tidal amplitudes of meridional wind at 86 km over Tirunelveli. The data set chosen for this exercise was for the period 2005-2010. This period was chosen because the solar cycle has already declined and the activity was stable and at its minimum. The 60-day running mean of the eigen coefficient for PC-1represents the EEJ signature. This kind of smoothing enables us to identify the semi-annual variation (two peaks in a year) in EEJ with its characteristic equinoctial maxima and solstitial minima. The tidal amplitudes in the meridional wind at upper mesospheric heights do exhibit a semi-annual variation but during certain years (2006 and 2008, in the case of diurnal tide, for example) larger tidal activity seems to overshadow this behaviour. It is to be noted that these larger tidal amplitudes are not accompanied by similar enhanced variationsin EEJ.

We have also examined the long-term variabilities in the second principal component in EEJ, to explain the tidal wind variabilities. Figure 10(a,b) shows the comparison in monthly time scales for PC-2 and the diurnal and semi-diurnal tide amplitudes in meridional wind at 86 km over Tirunelveli. For this exercise, we have used the principal components only for days for which the geomagnetic activity index, Ap, is less than 6. Further, 6-point running means were considered that would smooth out the short term (~a few months) variabilities in both EEJ and tidal parameters. The entire period range is broken into two parts: 1993-2001 plotted in the left panels and 2001-2011 plotted in the right panels.

An important feature that distinctly appears in both the comparison plots shown in Figure 10 is that beginning with the year 1998 the variations in PC-2 and tidal amplitudes in the longer time scales tend to be similar. When the tidal amplitudes during 1999-2001 (peak sunspot activity) were smaller (5-15 m/s for diurnal tide and 4-6 m/s for semi-diurnal tide), the PC-2 eigen coefficient revealed positive values (also noticed earlier in Figure 6b). During sunspot minimum years of 2008-2010, when the tidal activity was

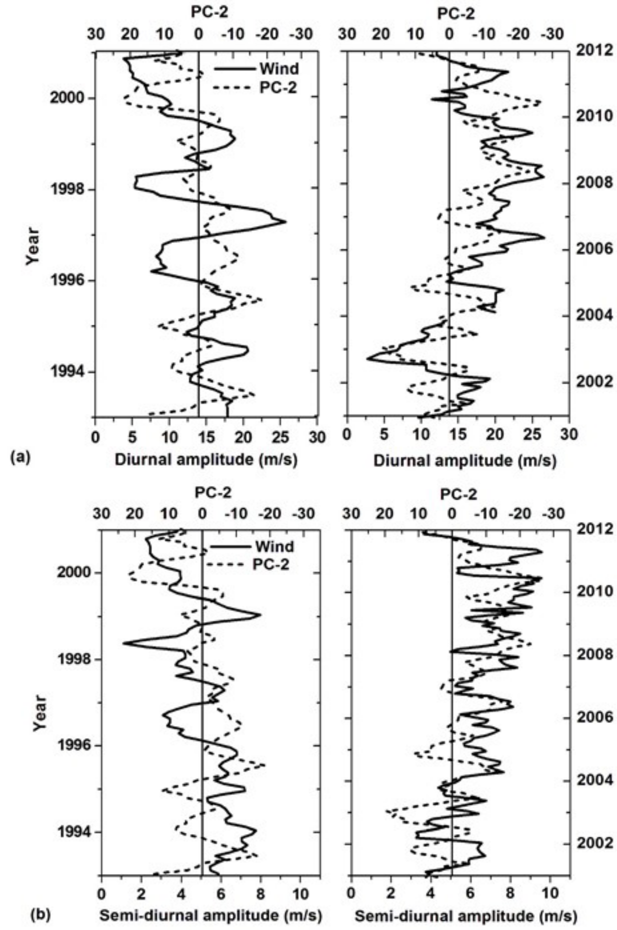

Figure 10. (a) Comparison plot for PC-2 and diurnal tide (top panel). (b) Same as (a) but for the semi-diurnal tide (bottom panel).

enhanced (the amplitudes were greater up to two times their values during high solar activity), the PC-2 eigen coefficient revealed negative values. The eigen coefficients were consistently negative between 2005 and 2011 and both diurnal and semi-diurnal tidal amplitudes were larger than climatological means during these times (also refer to Figure 8 for diurnal tide amplitudes). Further, when the results for the two parameters plotted in Figure 10 were broken into 3-year segments and a correlation analysis performed, a higher correlation (correlation coefficient between 0.5 and 0.9) was obtained for the descending phase of the solar cycle (2002-2008). The correlation during the ascending phase (1996-2001), was, however, negligible or weak.

CONCLUDING REMARKS

With nineteen years of observational data, the present work has demonstrated the utility of the MNOC technique in the analysis of EEJ and its long-term variabilities. The dominant principal components revealed by this technique have very close association with the diurnal range in EEJ and higher order field variation like the CEJ. Availability of MF radar observed winds enabled us to examine the upper mesospheric tidal winds and their variabilities. An important finding of this work has been the enhanced tidal activity during the solar minimum years of 2005-2010, which was likely to be driving the frequent CEJs during this period.

In contrast to the numerical modelling results of Yamazaki et al. (*2014a*), though the semi-annual variation in EEJ is quite regular, the occasional bursts of tidal activity noticed in MF radar observations that modulate the semi-annual variation in tides may not be associated with EEJ. Two issues are needed to be addressed, when one carries out such a comparative analysis: Why do the observed winds confine to lower altitudes of ~85 km, while the EEJ current flows much higher above (~105 km)?Another issue is that it is not known what fraction of the observed tidal wind field is global and what fraction is contributed by local winds. Winds averaged over several days are expected to be of global in origin but this presumption is yet to be tested with satellite data or by other means. It is indeed puzzling that low latitude mesospheric tides show a better correlation with higher order field variation like the CEJ but correlate poorly with the regular diurnal variation in EEJ. This will form a subject matter of further investigation. It is also to be noted that some of the afternoon CEJs were likely to be caused by the disturbance dynamo effects that were not fully removed in the analysis.

ACKNOWLEDGEMENTS

Authors thank the reviewers for critical evaluation and useful suggestions in improving the quality of the manuscript.

REFFERENCES

Alex, S., Kadam, B.D. and Rao, D.R.K., 1998. Ionospheric current systems on days of low equatorial ΔH, J. Atmos. Solar-Terr. Phys., v.60, pp:371-379.

Bhargava, B.N. and Sastri, N.S., 1977. A comparison of days with and without occurrence of counter-electrojet afternoon events in the Indian region, Ann. Geophys., v.33, pp:329-332.

Bhargava, B.N., Arora, B.R. and N.S. Sastri, 1983. Indices of equatorial electrojet and counter-electrojet in the Indian region: Evolution of the indices and their authenticity, Proc. Indian Acad. Sci., v.92, pp:45-55.

Campbell, W.H., Schiffmacher, E.R. and Arora, B.R., 1992. Quiet geomagnetic field representation for all days and latitudes, J. Geomag. Geoelectr., v.44, pp:459-480.

Chapman,S. and Bartels, J., 1940. Geomagnetism, Oxford University Press.

Chen, G.X., Xu, W.Y., Du, A.M., Wu, Y.Y., Chen, B. and Liu, X.C., 2007. Statistical characteristics of the day-to-day variability in the geomagnetic Sq field, J. Geophys. Res., v.112, A06320, doi:10.1029/2006JA012059.

De Michelis, P., Tozzi, R. and Cousolini, 2010. Principal components' features of mid-latitude geomagnetic daily variation, Ann. Geophys., v.28, pp:2213-2226.

Golovkov, V.P., Papitashvili, N.E., Tyupkin, Y.S. and Kharin, E.P., 1978. Division of variations of geomagnetic field on a quiet and disturbed components by a method of natural orthogonal components, Geomag. Aeron., v.18, p:511-515.

Gurubaran, S., 2002. The equatorial counter electrojet: Part of a worldwide current system? Geophys. Res., Lett., v.29, doi:10.1029/2001GL014519.

Hanuise, C., Mazaudier, C., Vila, P., Blanc, M. and Crochet, M., 1983. Global dynamo simulation of ionospheric currents and their connection with the equatorial electrojet and counter electrojet: A case study, J. Geophys. Res., v.88, p:253-270.

Kane, R.P., 1976. Geomagnetic field variations, Space Sci. Rev., v.18, pp:413-540.

Malin, S.R.C. and Gupta, J.C., 1977. The Sq current system during the International Geophysical Year, Geophys. J. R. Astr. Soc., v.49, pp:515-529.

Marriott, R.T., Richmond, A.D. and Venkateswaran, S.V., 1979. The quiet time equatorial electrojet and counter electrojet, J. Geomag. Geoelectr., v.31, pp:311-340.

Matsushita, S., Solar quiet and lunar daily variation fields, 1967. In Physics of Geomagnetic Phenomena, Ed. Matsushita, S. and Campbell, W.H., Academic Press.

Matsushita, S. and Maeda, H., 1965. On the geomagnetic solar quiet daily variation field during the IGY, J. Geophys. Res., v.70, pp:2535-2558.

Mayaud, P.N., 1977. The equatorial counter electrojet – a review of its geomagnetic aspects, J. Atmos. Terr. Phys., 39, 1055-1070.

Onwumechili, C.A., 1977. The equatorial electrojet, Gordon and Breach Science Publishers, 627pp.

Raghavarao, R. and Anandarao, B.G., 1987. Equatorial electrojet and counter-electrojet, Indian J. Radio & Space Phys., v.16, pp:54-75.

Rajaram, M., 1980. Method of natural orthogonal components applied to equatorial geomagnetic variations, Ann. Geophys., v.36, pp:599-603.

Rajaram, M., 1983. Determination of the latitude of Sq focus and its relation to the electrojet variations, J. Atmos. Terr. Phys., v.45, pp:573-578.

Rajaram, R. and Gurubaran, S., 1998. Seasonal variabilities of low latitude mesospheric winds, Ann. Geophys., v.16, pp:197-204.

Rastogi, R.G., 1974. Westward equatorial electrojet during daytime hours, J. Geophys. Res., v.79, pp:1503-1512.

Rastogi, R.G, 1993. Complexities of ionospheric current system at low latitudes, Ann. Geophys., v.11, pp:273-282.

Rastogi, R.G., 1994. Ionospheric current system associated with the equatorial counterelectrojet, J. Geophys. Res., v.99, pp:13,209-13,217.

Richmond, A.D., 1995. The ionospheric wind dynamo: Effects of its coupling with different atmospheric regions, In the Upper Mesosphere and Lower Thermosphere: A review of Experiment and Theory, Geophys. Monogr., v.87, pp:49-65.

Richmond, A.D., S. Matsushita and J.D. Tarpley, 1976. On the production mechanism of electric currents and fields in the ionosphere, J. Geophys. Res., v.81, pp:547-555.

Sathishkumar, S. and Sridharan, S., 2013. Lunar and solar tidal variabilities in the mesospheric winds and EEJ strength over Tirunelveli (8.7ºN, 77.8ºE) during the 2009 major stratospheric warming, J. Geophys. Res. Space Phys., v. 118, pp. 533-541, doi:10.1029/2012JA018236.

Sridharan., S., Sathishkumar, S. and Gurubaran, S., 2009. Variabilities of mesospheric tides and equatorial electrojet strength during major stratospheric warming events, Ann. Geophys., v.27, pp:4125-4130.

Sridharan, S., Tsuda, T. and Gurubaran, S., 2010. Long-term tendencies in the mesosphere/lower thermosphere mean winds and tides as observed by medium-frequency radar at Tirunelveli (8.7ºN, 77.8ºE), J. Geophys. Res., v.115, doi:10.1029/2008JD011609.

Stening, R.J., 1977a. Ionospheric dynamo calculations with semidiurnal winds, Planet. Space Sci., v.25, pp:1075-1080.

Stening, R.J., 1977b. Magnetic variations at other latitudes during reverse equatorial electrojet, J. Atmos. Terr. Phys., v.39, pp:1071-1077.

Stening, R.J., 1989. A diurnal modulation of the lunar tide in the upper atmosphere, Geophys. Res. Lett., v.16, pp:307-310.

Stening, R.J. and Winch, D.E., 1979. Seasonal changes in the global lunar geomagnetic variation, J. Atmos. Terr. Phys., v.41, pp:311-324.

Suzuki, A., 1979. UT and day-to-day variations in equivalent current systems for world geomagnetic variation, J. Atmos. Terr. Phys., v.41, pp:311-324.

Takeda, M., 1990. Geomagnetic field variation and the equivalent current system generated by an ionospheric dynamo at the solstice, J. Atmos. Terr. Phys., v.52, pp:59-67.

Takeda, M., 1999. Time variation of global geomagnetic Sq field in 1964 and 1980, J. Atmos. Solar-Terr. Phys., v.61, pp:765-774.

Takeda, M. and Maeda, H., 1981. Three-dimensional structure of ionospheric currents, 2. Currents caused by diurnal tidal winds, J. Geophys. Res., v.86, pp:5861-5867.

Tarpley, J.D., 1970a. The ionospheric wind dynamo, I, Lunar Tides, Planet. Space Sci., v.18, pp:1075-1090.

Tarpley, J.D., 1970b. The ionospheric wind dynamo, II, Solar Tides, Planet. Space Sci., v.18, pp:1091-1103.

Tarpley, J.D., 1973. Seasonal movement of the Sq current foci and related effects in the equatorial electrojet, J. Atmos. Terr. Phys., v.35, 1063-1071.

Xu, W.-Y and Kamide, Y., 2004. Decomposition of daily geomagnetic variations by using method of natural orthogonal component, J. Geophys. Res., v.109, A05218, doi:10.1029/2003JA010216.

Yamazaki, Y.,, Richmond, A.D., Maute, A., Wu, Q., Ortland, D.A., Yoshikawa, A., Adimula, I.A., Rabiu, B., Kunitake, M. and Tsugawa, T., 2014a. Ground magnetic effects of the equatorial electrojet simulated by the TIE-GCM driven by TIMED satellite data, J. Geophys. Res., v.119, pp:3150-3161, doi:10.1002/2013JA019487.

Yamazaki, Y., Richmond, A.D., Maute, A., Liu, H., Pedatella, N. and Sassi, F., 2014b. On the day-to-day variation of the equatorial electrojet during quiet periods, J. Geophys. Res., v.119, pp:6966-6980, doi:10.1002/2014JA020243.

Yamazaki, Y., Yumoto, K., Uozumi, T., Abe, S., Cardinal, M.G.C., Mcnamara, D.J., Marshall, R., Shevtsov, B.M. and Solovyev, S.I., 2010. Reexamination of the Sq-EEJ relationship based on extended magnetometer networks in the east Asian region, J. Geophys. Res., v.115, doi:10.1029/2010JA015339.

J. Ind. Geophys. Union (January 2016)
Special Volume-2/ 2016 pp: 99-104

Dynamic aspects of the Solar Flare Effects and their impact in the detection procedures

J. J. Curto[(1)], L. F. Alberca[(1)], J. Castell[(1)]
[(1)] Observatori de l'Ebre, (OE) CSIC –Universitat Ramon Llull
C/ Horta Alta, 38, 43520 Roquetes (Spain)
jjcurto@obsebre.es

ABSTRACT
Although crochet shape is conceived as the common manifestation of Sfe, a lot of them present other different shapes and have a sparse variety of rising and ending times. That makes the detection tasks of the observatories difficult. In this work we analyzed the temporal response of the earth's magnetic field to these sudden large energy releases and we assess its consequences in the detection procedures.

We studied the driven mechanisms involved in the decay of the Sfe. The decrease in the ionizing radiation has been found to be one of the main drivers of this decay, which diurnal variation trends very often mask.

Another finding was that the decay time is strongly dependent on the balance in X and UV rays contributions. Finally, we identified the time constant as an important factor for visual detection because it restricts the detected events to those having sharp shape.

Keywords: Sfe, Dynamics, Detection, Time-constant, Decay-time.

INTRODUCTION

Solar flare effects (Sfe) are rapid magnetic variations which are related to the enhancement of the amount of radiation produced during Solar flare events (*Prölss, 2004*). Mostly X-ray and EUV emissions cause variations on the electronic density in the ionospheric layers (*Donnelly, 1976*). From the F to the D regions, there are electron density enhancements during solar flares (*Thome and Wagner, 1971*). On Earth, the magnetic signature of a flare is visible in the illuminated hemisphere (*Dmitriev et al., 2006*), having big amplitudes in the equatorial zone (*Rastogi, 2001*).

Spectral radiation changes from one flare to another. Not every spectral band in the flare contributes equally to the total emission, and radiation with different emission frequencies produce different magnetic effects. What Sfe-s have in common is that, during several minutes, the ionosphere is activated and electron densities, electric conductivities and electric currents are enhanced.

The main characteristics of Sfe can be summarized as: 1) morphology: «crochet» shape; 2) vision: simultaneously in the Earth's sunlit hemisphere; 3) beginning: simultaneous to the flare observation; 4) duration: few minutes (10-20 min); 5) amplitude: few nanoTeslas, about 10 nT.

In order to catalogue these events, the parameters characterizing the Sfe are: Amplitude (A_{sfe}), Rise Time (T_1) and Decay Time (T_2).

The service of Rapid Magnetic Variations (RMVs) was created by the International Association of Geomagnetism and Aeronomy (IAGA) with the aim of obtaining an overall view of the temporal and spatial distribution of RMV as a base for further study of these phenomena. The Ebre Observatory holds this service which has regular daily activities to provide reliable lists of events(Sfe and Sudden Storm Commencements (SSC)) which are published in the IAGA bulletin 32 series. Also, the Ebre Observatory creates normative prospects, aiming to focus the interest of the scientific community on this field and to promote the study of the physics of RMV.

We create lists of Sfe events (preliminary data) from a network of collaborating observatories which report candidate events after visual inspection on the magnetograms. For each event, the observers determine the starting time (T_s) and the ending time (T_e). Both, together with the time of the maximum (T_m) allow us determining T_1 (T_1=T_m-T_s) and T_2 (T_2=T_e-T_m).

DYNAMIC ASPECTS OF THE SFE

A_{sfe} Amplitude

Due to the vortex type of the Sfe current systems, at ground level, amplitudes of the Sfe magnetic variations depend on the latitude and the local time of the observer (*Villante and Regi, 2008*). Thus, just under the center of the vortex one can have nearly no magnetic movements while in observatories located one or two thousand kilometers far away of the focus, one can have variations of several tens of nT. So it is very difficult to establish a unique value of amplitude for an event. The superposed Sq variation being delayed with respect to Sfe variation also generates complex resultants because in some locations they coincide in direction and sense and in other locations they have even opposite senses (*Curto et al., 1994a*). Even for the same event, the configuration of the currents changes as the time goes by (*Gaya-Piqué et al., 2008*).

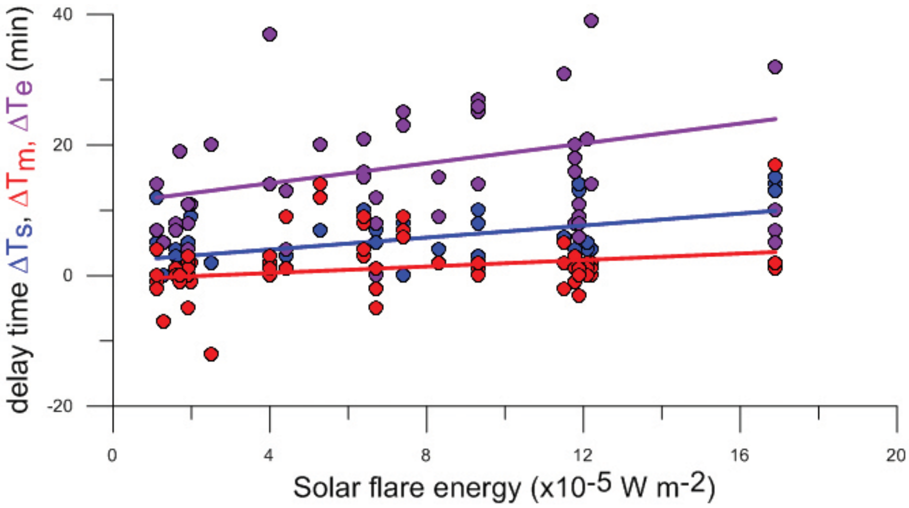

Figure 1. Delay time measured on the magnetogramsby the observers with respect to the corresponding times in the Xray monitors for several solar flares.

Table 1: Main equations ruling both processes: capacitor discharging in an electric circuit (on the left)and electron-ion recombination in the ionosphere (on the right).

$-\frac{Rdq}{dt} = \frac{q}{C}$	$\frac{dn}{dt} = -\alpha_{\mathrm{D}}\, nN_{\mathrm{e}}$
$\int_{q_0}^{q_1} \frac{dq}{q} = -(1/RC)\int_{t_0}^{t_1} dt$	$\int_{n_0}^{n_1} \frac{dn}{n} = -\alpha_{\mathrm{D}} N_{\mathrm{e}} \int_{t_0}^{t_1} dt$
$q = q_0 e^{-\frac{t}{\tau}}$	$n = n_0 e^{-\frac{t}{\tau}}$
$\tau = RC$	$\tau = \frac{1}{2\alpha_{\mathrm{D}} N_{\mathrm{e}}}$

T_s start time &T_e end time

In the reported lists from the collaborating observatories, there is rather unanimity in the T_s and T_m responses of the different observers, which are close to the corresponding times of the flare. However, there is great dispersion in the T_e given by the observers and a long delay (respect X-ray times) (Figure 1). Red points correspond to T_m (delay in the maximum). They are close to zero. Blue points correspond to T_s (delay in the start) they are bigger than Tm, but not much. Violet points correspond to T_e (delay in the end). They present the highest values, and they are much dispersed. Lines are the best linear fits. Delay times grow with the energy of the flares.

T_1 rise time & T_2 decay time

Summarizing, there are concordances in T_m but not in T_e so neither in T_2 (T_2=T_e-T_m). Thus we will concentrate in the study of the decay time to find the reasons of this discrepancy.

Some questions immediately arise: Is the decay time, T_2, conditioned by processes driven by the recombination process in the ionosphere? In that case, can the local conditions of upper atmosphere at the top of an observatory condition T_2?

THE IONOSPHERE AS AN AGENT IN THE DECAY PROCESS

Time constant, τ, in a decay process

To answer those questions, we first consider the main processes producing the ions concentration in the ionosphere. There, the continuity equation

$$\frac{dn}{dt} = Q - \alpha_{\mathrm{D}}\, nN_{\mathrm{e}} \text{-} \Delta.(N\mathrm{v})$$

accounts for the balance between creation and losses and transport. In the equation n is the ion density, t time, Q is the production term; Ne is the electron density and α_D the recombination coefficient, and ν is the electron velocity. During the occurrence of a flare, photochemical

Table 2: Ionizing decrease during a recombination process.

$t = \tau$	$n = n_0/e^1 = 0.37\ n_0$
$t = 2\tau$	$n = n_0/e^2 = 0.13\ n_0$
$t = 3\tau$	$n = n_0/e^3 = 0.05\ n_0$
$t = 4\tau$	$n = n_0/e^4 = 0.02\ n_0$

processes are much faster than transport (*Mitra, 1974*) so the transport term is negligible with respect to production and losses terms and we will not consider it.

There is a formal equivalence in the equations ruling the temporal variations of the ions in the ionosphere and the discharge of a capacitor in a RC electric circuit as shown in Table 1. There, q is the electric charge circulating in the circuit; R is the resistance and C the capacitance. t_1-t_0 represents the time elapsed after the source has been removed (t_0).

Electrons circulating in the electric circuit decay following a power law when we disconnect the source (battery). Then, the main characteristic is the time constant which is proportional to the resistance and the capacitor values.

In analogy, in the ionosphere, ion density also follows a power law, whose main characteristic is the time constant which is inversely proportional to the electronic density, *Ne*, and the recombination coefficient, α_D.

It is worth to note that as in a Capacitor discharging, ionization is significantly reduced after one time constant (about 70%) and dramatically after 2 times the time constant (about 90%) (Table 2).

In the ionosphere several layers can be considered. Some of them (D and E) are directly related to the daily ionizing radiation and disappear at night. Around 100 km high, there is a dynamo region where there are electro-dynamic conditions to sustain electric currents which are able to induce magnetic variations on earth.

In the dynamo region of the ionosphere, the Time constant in the decay process can be computed using the equations given in Table 1 and introducing the usual values of α_D and N_e in this layer: $\alpha_D = 3 \times 10^{-7} s\cdot cm^3$ & $N_e = 10^5\ cm^{-3} \Rightarrow \tau_{ion} = 20$ s !. So the ionization extinguishes shortly after the radiation disappears.

Statistics of T_2

As it was said in the introductory section, Sfe use to have a life time of some minutes. After Curto et al. (1994a), T_2 for Sfe in EBR are: Mode = 7 min, Median = 12 min and Mean = 16 min. So $T_2(sfe) >> \tau_{ion}$. Therefore, although electron-ion recombination plays a role, it is a secondary actor and should be discarded as the main driver of the global decay process as regards the magnetic signature decay.

X-RAY AS IONIZATION DRIVER

Going back to the continuity equation, if the ionization decay process is not mainly driven by the loss term, then we should look at the production term, Q. In principle, the ionization is mainly generated by soft Xray radiation. But no every Xray flare has enough energy to ionize the ionosphere. M and X classes, the most powerful flares, are the main Sfe producers. Most X flares have also a crochet shape with a rapid increase and a slow decay.

After Veronig et al. (*2002*), T_2 for X-ray are: Mode = 3 min, Median = 6 min and Mean = 9 min. SoT_2 (sfe) ≥ T_2 (Xray). Although, now both decay times have the same order of magnitude, T_2 (sfe) is still bigger than T_2 (Xray). We have to search for another agent.

UV RADIATION AS ANOTHER IONIZATION DRIVER

In the dynamo region, in addition to the Xrays, other spectral bands contribute to produce ions (*Richmond and Venkateswaran, 1971*). Curto et al. (*1994b*) built a physical model integrating the main processes involved in the generation of a Sfe. Thus they could evaluate the impact of the different bands at the different highs. They found that, in the dynamo region, UV radiation has an important role, too.

A CASE STUDY: SFE 16/07/2004 AT EBRE (EBR)

To get a deep inside in the problem let's have a case study. Again we chose a Sfe event which happened in a magnetically quiet day: July 16th, 2004 at 13:53 UT. We focused on the Sfe time and compared the decay of the magnetic variation with those in Xray and XUV ray (Figure 2).

In the Xray band((a) panel of Figure 2), we observe a rapid decay with $\tau_1 = 9$ min. In the XUV band ((b) pannel), the decay is much longer with $\tau_1 = 30$ min. Finally, in the magnetogram ((c) pannel), $\tau_1 = 17$ min. The Sfe has a rapid decay in the 10 first minutes following the Xray decay, but then a slower decay happens following the UV decay.

In terms of deposited power (Table 3), the energy delivered in the X ray band reduces the importance of its contribution to the whole XUV band (X+UV) (1-500 Å) as the time goes by. This contribution goes from the 1 % at

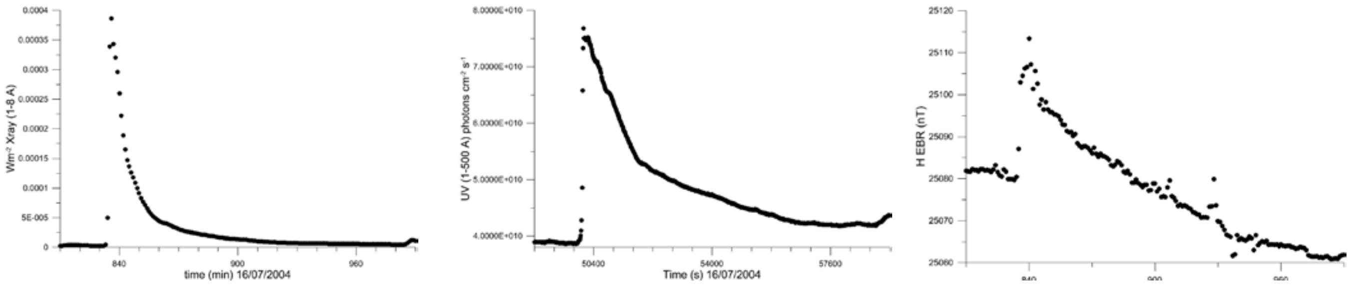

Figure 2. Panoramic view of the 16/07/2004 sfe event. Pannel a) Xray, b) XUV and C) Sfe.

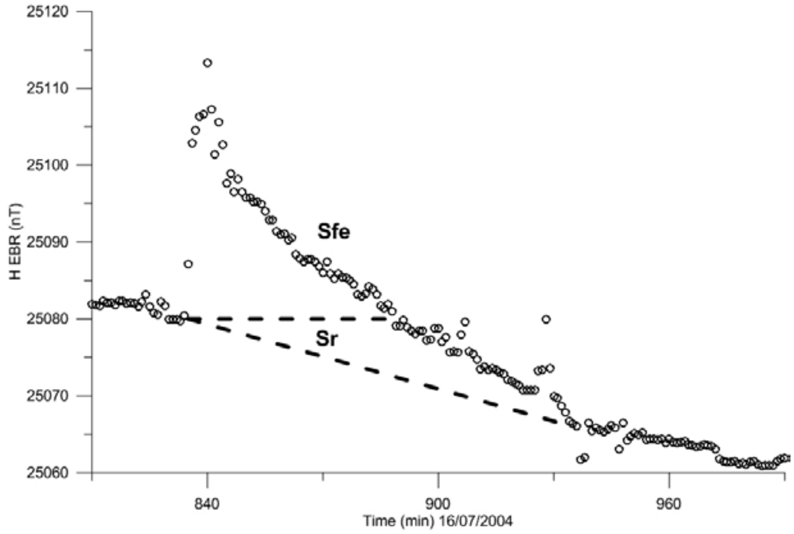

Figure 3. Sfe signature as can be seen in EBR magnetograms (16/07/2014). The starting time is clear enough to be easily determined (13:53). But the ending time depends on the different options of base line according to the Sr extrapolations (dashed lines in the figure).

Table 3. Deposited power rate at the moment of the maximum and ten minutes later for the whole band XUV and for the Xray sub-band.

	XUV ray (1-500 Å) band	X ray (1-8 Å) band
$t = t_0$ (at Sfe maximum)	$P_0 = 5 \cdot 10^{-2}$ W m^{-2}	$P_0 = 4 \cdot 10^{-4}$ W m^{-2} (1%)
$t = t_1 = t_0 + 1_0$ min (after τ_1 Xray)	$P_1 = 4 \cdot 10^{-2}$ W m^{-2}	$P_1 = 1.25 \cdot 10^{-4}$ W m^{-2} (0.3 %)

the moment of the maximum to 0.3 % ten minutes later, when the Xrays have decayed for less than 40% of its value at the moment of maximum.

OTHER CONSIDERATIONS.

Diurnal variation, a quiz

The Diurnal Variation, Sr, is always superposed to the Sfe event. The Diurnal Variation trend very often masks Sfe decay and gives a misleading base level. One should see not only the level at the moment previous to the event but also how the Sr evolves after the event to infer the Sr trend (Figure 3). Having a wrong base line could result in a large error in the T_e determination.

Sfe starts later than the X-ray flare

In general, only the most energetic period of an X-ray flare is Sfe productive. At the moment of the start time, the flare delivers small energy and, only after certain amount of time, it reaches a level of energy sufficient (M or higher) to produce appreciable electric conductivity enhancement which finally manifests itself as a Sfe. This can be seen as a positive delay in Ts (Figure 1). Vice versa, something like this, but in the opposite sense, should happen in the decay time. However, at that moment the UV rays control the ionization and as they have a long recovery, T_e(sfe) takes place much later than T_e(X-ray).

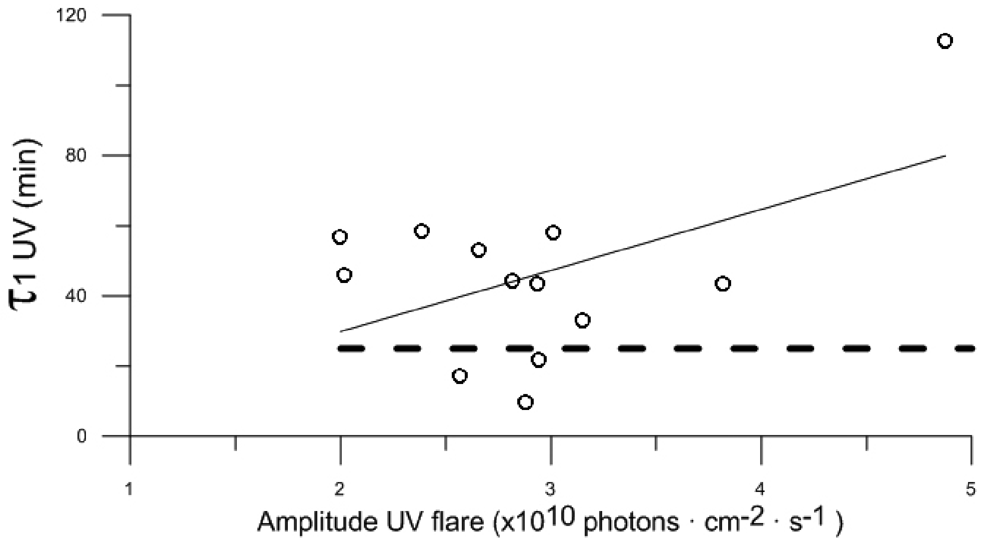

Figure 4. τ_1 versus Amplitude for several UV flares. Only the sfe events under the threshold level (dashed line) were detected and reported in the lists. The best fit (solid line) suggests some kind of dependence between the amplitude of the flare and the value of the time constant.

Big X ray flares not always produce Sfe

Other surprising fact is that having big X ray flares is not equivalent to have big Sfe. Even, in many cases, no Sfe is detected!

According to Curto and Gaya-Piqué (*2009a*), when a flare is only important in X-ray emission, the probability to produce a Sfe is only around 50%. In that study, the authors concluded that other spectral bands contribute and sometimes have more relevance than Xray one. Also Tsurutani et al. (*2005*) have shown that solar flare of 28 October 2003 (X17) produced TEC increase of ~25 TECU whereas a much intense solar flare on 4 November 2003 (X28) produced only an increase of ~5-7 TECU. The cause for such a phenomenon was that EUV flux was nearly double for the 28 October flare as compared to 4 November flare. That study emphasized the importance of the spectra of solar flares for Sfe. Similarly, the solar energetic particles (SEP) associated with some flares can reach the Earth's high latitude ionosphere a little later than the energetic solar photons produced during solar flares (Tsurutani et al., 2009). They can produce extra ionization affecting the Sfe amplitudes, too.

Steepness, a key factor

Going on with this paradoxical fact that most of the biggest XUV flares apparently produce small or no effect in magnetism (Sfe), we compute the time constant of several flares (Figure 4). There, the right most point suggests a kind of dependence between the amplitude of the flare (energy deposited in the ionosphere at the moment of the maximum) and the value of the time constant. The dashed line in the figure separates the events producing Sfe (those under the line) from those events not producing Sfe (those over the line). Only the flares having small τ produced Sfe. The explanation could be that our eyes look for sharp increases of the magnetic field detecting only those with small τ.

CONCLUSIONS

The start and ending times of Sfe are difficult to precisely determine. Very often, ending times of a Sfe event given by the different observatories are very scattered.

The decay in the Sfe is mainly driven by the decrease in the ionizing radiation. In the decay time, after 2 or 3 times the time constant, τ, the signal is reduced drastically to only few % of the total, very close to the "natural" noise level. Moreover, the diurnal variation, Sr, is always superposed to the Sfe event. Diurnal variation trend very often masks Sfe decay.

The decay time is very dependent on the balance in X and UV rays contributions. Only the most energetic period of the Xray enhancement is active producing Sfe.

Finally, visual detection restricts the detected events to those having sharp shape. Very often big XUV events don't appear in the lists because they have large τ.

ACKNOWLEDGEMENTS

This research has been partially supported by Spanish government project CTM2014-52182-C3-1-P of MINECO.

REFERENCES

Curto, J.J., Amory-Mazaudier, C., Cardús, J.O., Torta, J.M. and Menvielle, M., 1994. Solar flare effects at Ebre: Regular and reversed solar flare effects, statistical analysis (1953 to 1985), a global case study and a model of elliptical ionospheric currents, J. Geophys. Res., vol. 99, nº A3, p. 3945-3954.

Curto, J.J., Amory-Mazaudier, C., Cardús, J.O., Torta, J.M. and Menvielle, M., 1994. Solar flare effects at Ebre: Unidimentional physical, integrated model, J. Geophys. Res., vol. 99, nº A12, p. 23289-23296.

Curto, J.J. , Gaya-Piqué, L.R., 2009. Geoeffectiveness of Solar Flares in magnetic crochet (sfe) Production: I - Dependence on their spectral nature and position on the solar disk, J. Sol. Atmos. Terr. Phys., 71, 1695-1704. DOI. 10.1016/j.jastp.2008.06.018.

Curto, J.J. , Gaya-Piqué, L.R., 2009. Geoeffectiveness of Solar Flares in magnetic crochet (sfe) Production: II - Dependence on the detection method, J. Sol. Atmos. Terr. Phys., 71, 1705-1710. DOI: 10.1016/j.jastp.2007.12.003.

Dmitriev, A. V., H.-C. Yeh, J.-K. Chao, I. S. Veselovsky, Su, S.Y. and Fu, C. C., 2006. Top-side ionosphere response to extreme solar events, Ann. Geophys., 24, 1469,

Donnelly, R. F. 1976. Empirical models of solar flare x-ray and EUV emissions for use in studying their E and F region effects, J. Geophys. Res., 81, 4745, doi:10.1029/JA081i025p04745, 1976.

Gaya-Piqué, L.R., Curto, J.J, Torta, J.M., Chulliat, A., 2008. Equivalent ionospheric currents for the 5 December 2006 solar flare effect determined from spherical cap harmonic analysis, J. Geophys. Res., 113, A07304, doi:10.1029/2007JA012934,

Mitra, A. P., 1974. Ionospheric Effects of Solar Flares, Springer, New York

Prölss, G., 2004. Physics of the Earth's Space Environment, Springer, Heidelberg, Germany.

Rastogi, R. G., 2001. Electromagnetic induction due to solar flares at equatorial stations, JASTP, 63, 599-604

Richmond, A.D., Venkateswaran, S. V., 1971. Geomagnetic crochets and associated ionospheric current systems, Radio Sci., 6, 139-164.

Thome, G. D., and Wagner, L. S., 1971. Electron density enhancements in the E and F regions of the ionosphere during solar flares, J. Geophys. Res., 76, 6883, doi:10.1029/JA076i028p06883.

Tsurutani, B. T., Judge, D. L., Guarnieri, F. L., Gangopadhyay, P., Jones, A. R., Nuttall, J., Zambon, G. A., Didkovsky, L., Mannucci, A. J. Iijima, B., Meier, R. R., Immel, T. J., Woods, T. N., Prasad, S., Floyd, L., Huba, J., Solomon, S. C., Straus, P. and Viereck, R., 2005. The October 28, 2003 extreme EUV solar flare and resultant extreme ionospheric effects: Comparison to other Halloween events and the Bastille day event, Geophys. Res. Lett.,32, L03S09, doi:10.1029/2004GL021475

Tsurutani, B. T., Verkhoglyadova, O. P., 2009. Mannucci, A. J., Lakhina, G. S., Li, G. and Zank, G. P., A brief review of "solar flare effects" on the ionosphere, Radio Sci., 44, RS0A17, doi:10.1029/2008RS004029.

Veronig, A., Temmer, M., Hanslmeier, A., Otruba, W., Messerotti, M., 2002. Temporal aspects and frequency distributions of solar soft X-ray flares, Astronomy & Astrophysics, 382, 1070-1080.

Villante, U., Regi, M., 2008. Solar flare effect preceding Halloween storm (28 October 2003): Results of a worldwide analysis, J. Geophys. Res., 113, A00A05, doi:10.1029/2008JA013132.

J. Ind. Geophys. Union (January 2016)
Special Volume-2/ 2016 pp: 105-111

Long-term external field contributions in geomagnetic repeat station results

M. Korte
Helmholtz-Centre Potsdam, GFZ German Research Centre for Geosciences, Telegrafenberg, 14473 Potsdam, Germany, monika@gfz-potsdam.de

ABSTRACT
Geomagnetic repeat station measurements are carried out in several countries to provide additional information on secular variation or to map the field regionally. These measurements are continuously monitored by geomagnetic observatories. However, clear separation of magnetic variations from the different field sources remains a challenge in all geomagnetic observations. This is particularly true for repeat station data, where measurements are only available from one or a few days at a time. Contributions from large-scale magnetospheric fields remain in repeat station data despite careful data processing, and they are modulated by solar activity variations on time scales of several years to decades. Here, the influence of magnetospheric field contribution in repeat station data from Germany and Southern Africa over the past ten years is shown and strategies are discussed to eliminate them by using existing or custom-made geomagnetic activity indices. The disturbed storm time (Dst) index, its derivatives and the CM4 external field extrapolated to recent times clearly do not capture the multi-annual trends accurately. For the satellite era, since about 2000, global spherical harmonic models based on satellite and ground data give the best description of the large-scale magnetoshperic field and can be used to correct ground data time series for long-term external field contributions. It would be desirable to develop a Dst-like index with correct long-term variability and baseline to correct data series further back in time.

Keywords: Repeat station surveys, Decadal variations, Magnetospheric field variation.

INTRODUCTION

Geomagnetic repeat station measurements, observations of the absolute magnetic field vector at well-defined locations over one or a few days at time intervals of one to a few years (*Newitt et al., 1996*) are carried out in several countries to provide information on secular variation on a denser network of stations than provided by permanent geomagnetic observatories. Nowadays modern global geomagnetic core field models based on observatory and satellite magnetic data describe the detailed regional secular variation to high accuracy (*Korte and Lesur, 2012*). Nevertheless repeat station data are still valuable, e.g., to allow regional field mapping independent of the availability of global data or models or to provide information about the lithosphere. Moreover, the modern satellite era only started with the launch of the Ørsted and CHAMP satellites in 1999 and 2000 (e.g. *Olsen and Kotsiaros, 2011*). Long time series of regular repeat station observations that extend back in time well beyond the modern satellite era can be valuable resources to study secular variation on decadal timescales.

The separation of the individual contributions originating inside and outside of the Earth in geomagnetic data remains a challenge for all kinds of magnetic measurements. This is particularly true for repeat station data, where the observations span a few hours to a few days at the most. Short period ionospheric and magnetospheric variations (from seconds up to a few days) can be eliminated by standard data processing (see *Newitt et al., 1996*) ideally using a variometer installed temporarily near the repeat station for that particular purpose, or by comparison with the variations recorded at the nearest observatory. Variations with periods from several days to a year can be eliminated fairly well in most cases by comparison with the nearest observatory recordings, if necessary, taking secular variation gradients into account. However, large-scale magnetospheric fields show additional variations on time scales of several years to decades, e.g. from modulation of the always present magnetospheric ring current by solar activity on time-scales of the 11 year solar cycle. Such variations do not average out in observatory annual means (*Yukutake and Cain, 1987, Verbanac et al., 2007*) and therefore are also present in the repeat station data reduced to annual means. In the following I show that this is also the case for repeat station results reduced to quiet night time values. Elimination of this contribution might not be necessary or not even desirable if repeat station data are used for regionally mapping field components for practical purposes like navigation, but it is important when the data are used for core field secular variation studies as, e.g., for the detection and detailed description of geomagnetic jerks. In the following, German and southern African repeat station and observatory data are used as examples to demonstrate the influence of such long-term magnetospheric field contributions. Some existing geomagnetic activity indices and models aimed at describing the magnetospheric field variation are discussed and methods are suggested to reduce the long-term magnetospheric influence in repeat station data and observatory annual means.

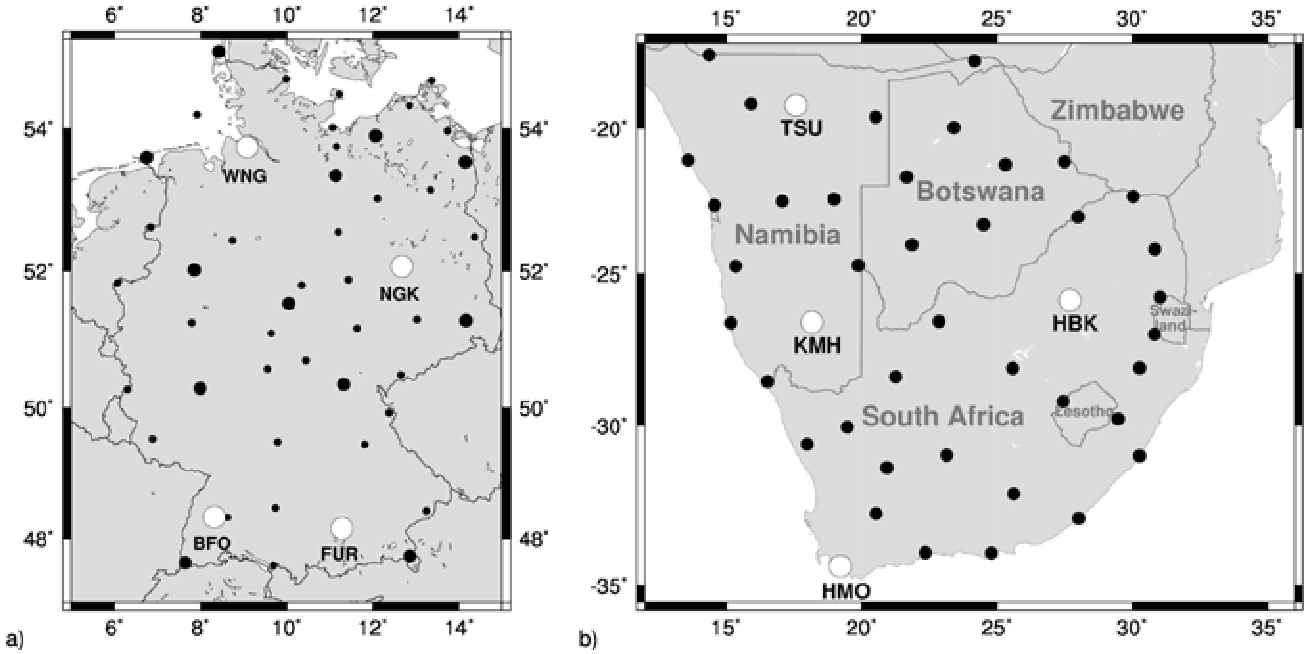

Figure 1. Maps of geomagnetic observatory (white dots) and repeat station (black dots) distribution for a) Germany and b) southern Africa. For Germany, large black dots are first order repeat stations with on-site variometer, small symbols are second order stations not considered in this study.

LONG-TERM MAGNETOSPHERIC SIGNAL IN GEOMAGNETIC GROUND DATA

Data from two regions have been included in this study: from Germany and Southern Africa,encompassing South Africa, Namibia and Botswana. Both regions include four geomagnetic observatories and networks of up to 40 repeat stations. Given the different size of the regions, the data coverage is much denser for Germany. Minimum and maximum distances between the four German geomagnetic observatories Wingst (WNG), Niemegk (NGK), Black Forest (BFO) and Fürstenfeldbruck (FUR) are in the order of 240 to 630 km. The average distance between repeat stations lies in the order of 120 km. For southern Africa, the minimum and maximum distance between the four observatories Hermanus (HER), Hartebeesthoek (HBK), both in South Africa, Tsumeb (TSU) and Keetmanshoop (KMH), both in Namibia, are of the order of 820 to 1680 km, and the average distance between repeat stations of 240 km (Figure 1).

The data are standard data products as made available by the World Data Center for Geomagnetism, Edinburgh. From the observatories, we use the annual mean values from 2001.5 to 2010.5. Observatories BFO and KMH from Germany and Namibia have not been included because they only went into operation in 2004 and 2006, respectively. The repeat station data have been processed in somewhat different ways. From Germany, we only consider a sub-set of 12 repeat stations where a local variometer has been operated for a few days around the absolute measurement. The observations are first reduced to quiet night time values by means of these variometers and then further reduced to annual means by comparison to the NGK observatory recordings (see *Korte and Lesur, 2012*). Repeat station surveys have been conducted bi-annually from 1999 to 2012, and we use the time series from 2001.5 to 2010.5. Repeat station surveys have a long tradition in southern Africa, but here I consider only data from 2005 onwards, when a collaboration between SANSA and GFZ led to intensified survey activity with annual repeat intervals and improved data processing by means of local variometers set up for a full night with absolute observations in the evening and the morning (*Korte et al., 2007*). These data have only been reduced to quiet night time values at the time of observation.

Figure 2 shows the residuals of the data series after a main field and secular variation estimated for the location from a core field model and the constant average value of the remaining signal have been subtracted. The constant average can be seen as an estimate of the lithospheric field contribution which is assumed to be constant over the studied time interval. For the core field and its secular variation the continuous GRIMM3 model spanning the time interval 2001 to 2010 and based on CHAMP satellite and geomagnetic observatory data (*Lesur et al., 2010, Mandea et al., 2012*) was used. The residuals of the annual mean values of the three German observatories and selected six repeat stations very clearly show similar

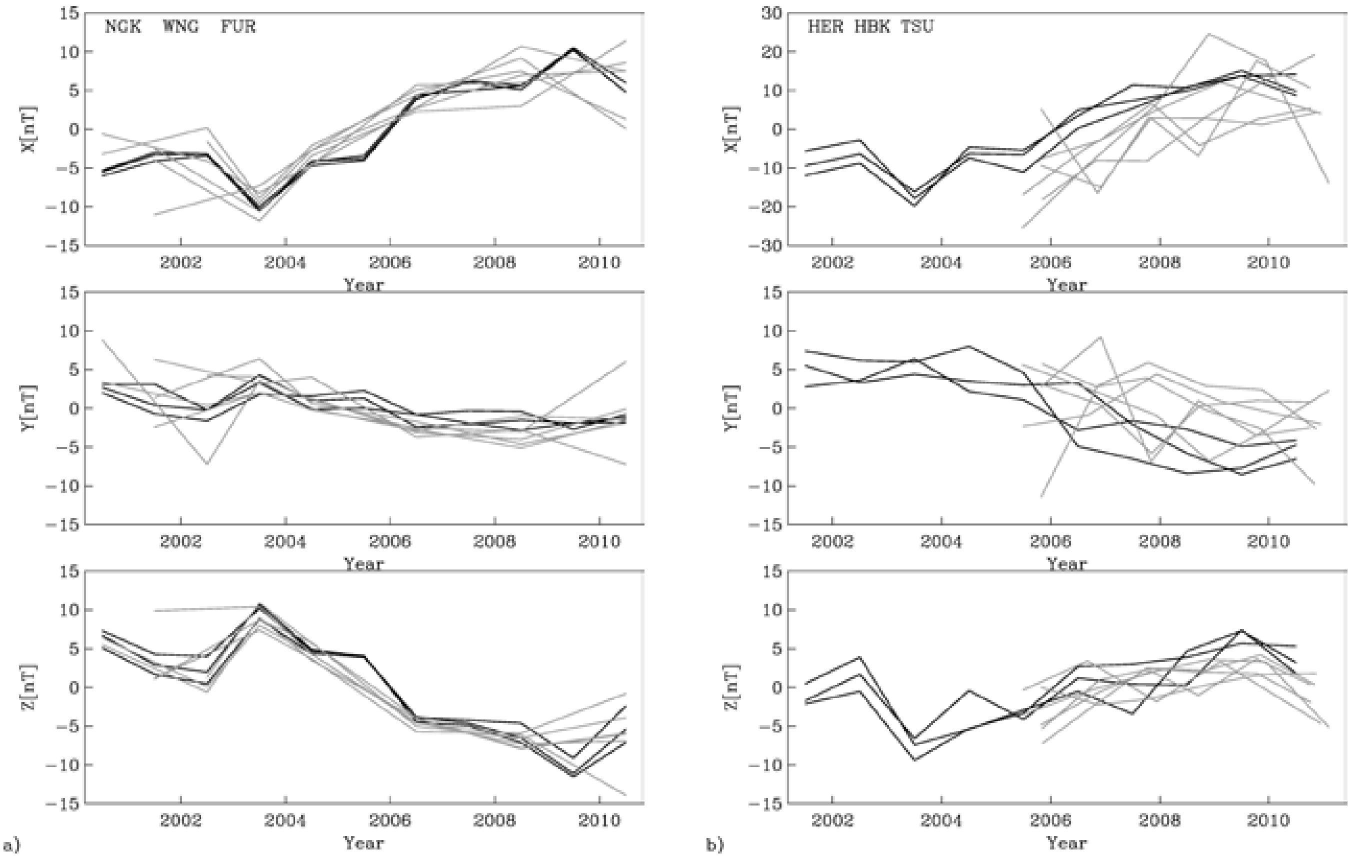

Figure 2. Observatory (black) and repeat station data (gray) residuals after subtraction of core field, secular variation and a constant average to account for lithospheric sources. Geographic co-ordinates are indicated as north (X), east (Y) and vertical (Z) component from top to bottom. a) Annual mean data from the three observatories WNG, NGK and FUR and sixselected repeat stations distributed over Germany. b) Annual means from the three observatories HER, HBK and TSU and night time values from sixselected repeat stations distributed over South Africa, Namibia and Botswana.Scatter in particular in repeat station data is due to data uncertainties or further residual external fields.

long-term trends for the whole area in all components. The residuals from both the annual means of the southern African observatories and the night time values of selected repeat stations, respectively, are noisier but similar trends are obvious. The noise in the repeat station night time values is at least partly due to the fact that these data might contain some further external field influences, which have averaged out better in annual means, indicating that these night time averages may not always be truly quiet time night time averages.

The fact that the residual signal is very similar in northern and southern hemisphere (with slight differences due to different geomagnetic coordinates) of the north (X) and east (Y) component and of opposite sign in the vertical (Z) component indicates a large scale source consistent with a dipole geometry far out in the magnetosphere. Therefore, it is likely due to a modulation of the large-scale magnetospheric currents, mainly the ring current, with solar activity.

ESTIMATING THE MAGNETOSPHERIC CONTRIBUTION

The traditional geomagnetic activity index meant to describe the disturbance field created by a magnetospheric ring current is the Dst (disturbed storm time) index (*Sugiura and Kamei, 1991*), available from the World Data Center Kyoto at *http://wdc.kugi.kyoto-u.ac.jp/dstdir/*. Mursula and Karinen (*2005*) extended the Dst index back in time to 1932 and corrected some errors. Mursula et al. (*2011*) further corrected this index for a semiannual variation arising from seasonal variations at the four contributing geomagnetic observatories that are unrelated to geomagnetic storm activity, which also had an influence on the long-term variability of the index. These two indices, named Dxt and Dcx respectively, are now available derived either from the four traditional observatories or an extended data basis of 17 low- and mid-latitude observatories at *http://dcx.oulu.fi/*.

Two other large-scale magnetospheric indices are obtained by low-degree spherical harmonic analysis of low- and mid-latitude geomagnetic observatories data, the Vector Magnetic Disturbance index (VMD) by Thomson and Lesur (*2007*) and the Ring current (Rc) index by Olsen et al. (*2014*). Both are available upon request from the authors. However, the VMD index is designed to monitor only rapid variations and its long-term average (> 3 months) is close to zero. It thus cannot describe the long-term magnetospheric variation seen in the ground data.

All the indices contain magnetic field contributions originating directly from electric currents in the magnetosphere, but also secondary parts induced in the Earth's crust and mantle by these time-varying fields. A separation of these contributions for the Dst index has been presented by Maus and Weidelt (*2004*), using a one-dimensional conductivity model of the Earth. They have been termed Est (primary external part) and Ist (secondary, induced internal part) and are available at *ftp://ftp.ngdc.noaa.gov/STP/GEOMAGNETIC_DATA/INDICES/EST_IST/Est_Ist_index.lis*. The Rc and VMD indices similarly consist of separate estimates for the direct, external variation and the indirect, internally induced part.

Several recent spherical harmonic global geomagnetic core field models include descriptions of the large-scale magnetospheric variations. The CM4 comprehensive model by Sabaka et al. (*2004*) separately describes the main, large scale lithospheric, primary and induced magnetospheric and ionospheric contributions and toroidal fields generated by field-aligned currents. It spans the time interval 1960 to 2002 and is available at *http://core2.gsfc.nasa.gov/CM/*. The magnetospheric contributions in this model are modulated by the Dst index and thus can be extrapolated to more recent times. (A new model version, CM5, has been published by Sabaka et al. (*2015*) too recently to be included in this study.)

Version 7 of the POMME model series developed by Maus et al. (*2010*) is mainly designed as an internal field model but contains a description of the large-scale magnetospheric currents modulated by the Est/Ist indices and is available at *http://geomag.org/models/pomme7.html*. The latest version of the internal field GRIMM model series, GRIMM3 (*Lesur et al., 2010, Mandea et al., 2012*) co-estimates large-scale magnetospheric fields in the spherical harmonic expansion. It is available at http://www.gfz-potsdam.de/magmodels/.

Predictions for the magnetospheric description included in the spherical harmonic models are obtained for any location on Earth from the respective forward modelling code. Annual means were obtained by averaging hourly values. The POMME7 and GRIMM3 models span approximately the same time interval from 2000 to 2010. They require substantial modification of the provided forward modelling code to obtain the desired time-averaged and purely external annual mean prediction. In particular the POMME7 software requires the implementation of regular input not only of the Est and Ist index, but additionally information on the interplanetary magnetic field By component, the merging electric field and the solar irradiation F10.7 index. While it certainly would be of interest to see the prediction of that model in comparison, it was not possible to include it within the time-frame of this study.

The individual indices (Dst, Dcx, Dxt, Rc, Est, Rc external part) can be considered as describing the strength of a dipolar magnetic field originating from a ring current in the magnetosphere, some with an internally induced dipolar secondary part (Ist, Rc induced part). They can be interpreted as the external and internal (induced) spherical harmonic axial dipole coefficients. Thus their contribution to the magnetic components north (X), east (Y) and vertical (Z) is given by

$$\begin{aligned} X &= ext^*\cos(\lambda) + int^*\cos(\lambda) \\ Y &= 0 \\ Z &= ext^*\sin(\lambda) - 2int^*\sin(\lambda), \end{aligned} \tag{1}$$

with latitude λ and (ext,int) one of the index pairs (Dst,0), (Dcx,0), (Dxt,0), (Rc,0), (Est,Ist), (Rc external, Rc internal). To take into account that the ring current is aligned with the main field dipole axis λ is the geomagnetic latitude and the contributions to the components have to be transformed back from the geomagnetic to the geographic reference frame. A comparison of the large-scale residual signal and several of the magnetospheric descriptions is shown in Figure 3 for the two locations of Niemegk, Germany, and Hermanus, South Africa.

DISCUSSION

The similarity between individual observatory data residuals and averages from three observatories in each of the two regions, both for the long-term trend and year to year variation once more confirms a homogeneous large-scale source of this signal.

Differences between the Dxt and Dcx indices determined from four or 17 observatories respectively are very small in the annual means (order of 1 nT) and only the latter versions based on the extended data distribution are included in Figure 3 (labelled Dxt (17) and Dcx (17), respectively). Treating the primary and induced contributions separately in Dst and Rc can cause differences of a few nT in the vertical component, as can be seen in the case of Dst and Est+Int. Dcx and Dxt as expected are also similar to Dst, with Dxt capturing the year to year variations seen in the data better than Dcx. The long-term, decadal trend seen in the data is not explained well by any of these indices. This is not surprising when considering

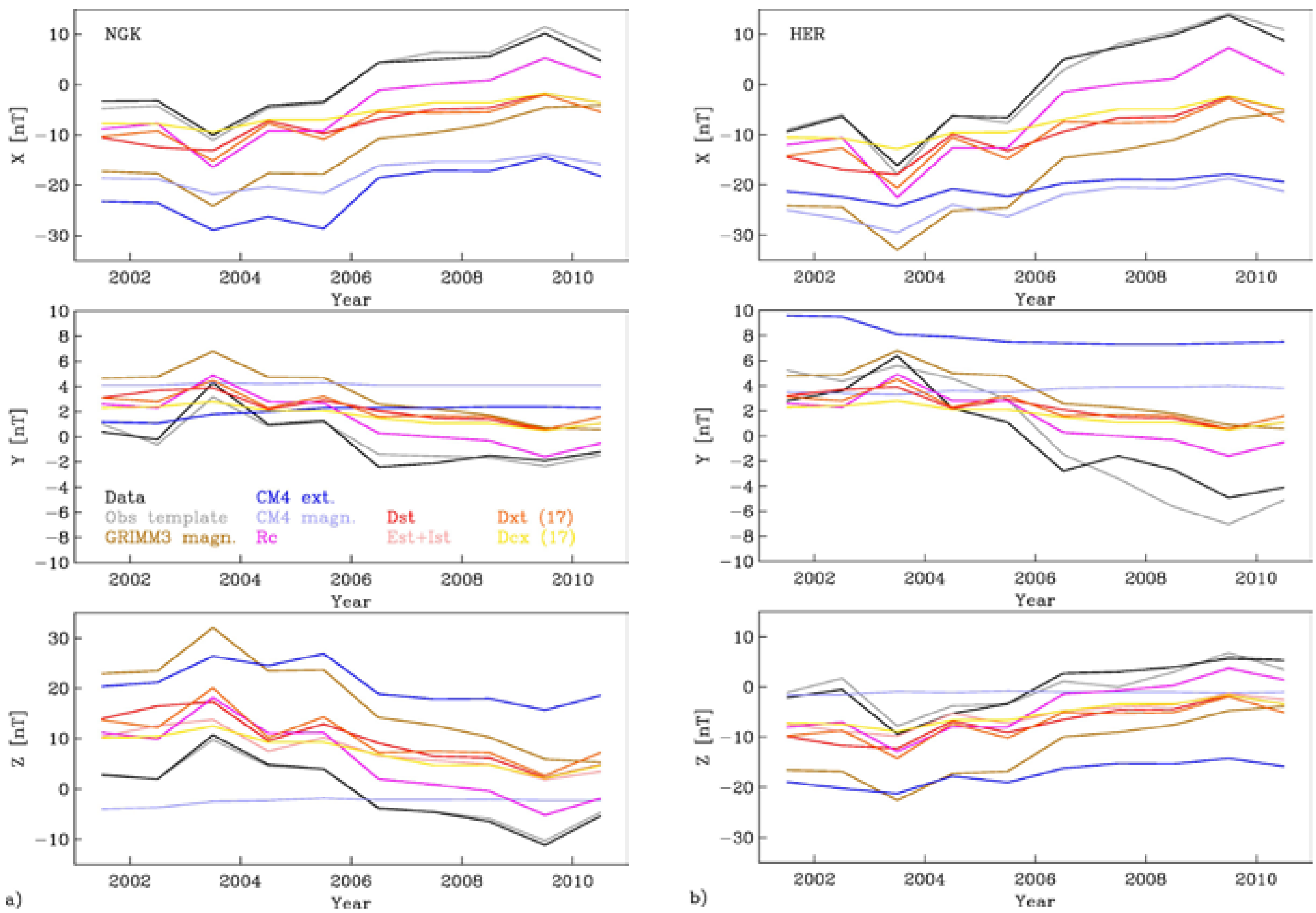

Figure 3. Annual mean observatory residuals (black) as in Fig. 2 for a) NGK (Germany) and b) HER (South Africa) and averaged of the three observatories from each region (gray), respectively, compared to several magnetospheric ring current / large scale external field proxies: based on the GRIMM3 (brown) and CM4 models (light blue: magnetospheric contribution, dark blue: magnetospheric and ionospheric contribution) and using the Dst (red), Est+Ist (light red), Dxt (yellow), Dcx (orange) and Rc(magenta) indices. Geographic north (X), east (Y) and vertical (Z) component from top to bottom.

the derivation of these indices: the core field is subtracted from the data on the basis of a quiet time field estimate on a rather short term basis. The absolute level of the quiet time ring current and long-period variations are not taken into account and the indices have an arbitrary and unstable baseline, as has been noted before by, e.g., Olsen et al. (2005).

The description of primary and induced magnetospheric contribution from the extrapolated CM4 model (CM4 magn.) cannot explain the signal in the Y and Z components, but for X and Z a reasonable description of both long term and year to year variation is given if both magnetospheric and ionospheric contributions are considered (CM4 ext.). However, the recently published CM5 model, which does not rely on a modulation by an independently determined index but co-estimates the magnetospheric contribution (*Sabaka et al., 2015*), would be more appropriate for this time interval and might describe the observed signal better.

Among the investigated large-scale external field descriptions the Rc index and the GRIMM3 model describe the observed long-term trend and year to year variation best, however with different constant offsets in all components. It can be assumed that the GRIMM3 model, which co-estimates the large-scale external field in the inversion gives the most accurate description of the true strength of this contribution even during quiet times. The Rc index in contrast has an arbitrary baseline, although with better long-term stability than Dst, as any quiet time background ring current contribution is eliminated in its derivation together with the constant individual lithospheric field estimates for the observatories.

CONCLUSIONS AND OUTLOOK

Observatory annual mean data series contain clear long-term signals of magnetospheric variations . Repeat station data reduced to annual means are subject to the same influence. Similar magnetospheric field contributions are present in repeat station data reduced to quiet night times. Existing magnetospheric field descriptions could be used to eliminate these external field residuals from ground data to provide cleaner data for internal field secular variation studies. This has been investigated by comparing observatory annual mean data after subtraction of core field, secular variation and a constant time averaged lithospheric field estimate to several existing proxies of large-scale external field / magnetospheric field contributions. Accuracy and availability of these descriptions vary and it is not immediately obvious which one to use. The Dst index, its derivatives and the CM4 external field extrapolated to recent times clearly do not capture the trends accurately. For the satellite era, since about 2000, global spherical harmonic models like GRIMM3 and probably also models POMME7 and CM5 (not included in this study), give the best description of the large-scale magnetoshperic field and can be used to correct ground data time series for long-term external field contributions. In the case of a co-estimation of external field without the need for modulation of the description with a magnetospheric index they should even give the correct absolute level of this contribution, which also is present as a background field during magnetically quiet times. The Rc index is easier to apply and does give the correct trend, if not the absolute value. However, it is only available upon request and does not extend back much beyond the satellite era. In order to be able to easily correct multi-decadal time-series of observatory and repeat station data for the external field residual signal it would be useful to develop a new Rc-like index spanning the whole observatory era with correct absolute level.

ACKNOWLEDGEMENT

I thank the South African National Space Agency, Space Sciences (Hermanus Magnetic Observatory) for providing the Hermanus, Hartebeesthoek and Tsumeb magnetic observatory data and for the ongoing collaboration to collect annual repeat station data in southern Africa. The dedicated work of all the colleagues at GFZ and Hermanus who participated in the fieldwork and carried out the data processing is highly appreciated. The Ludwig Maximilians University in Munich is acknowledged for operating the Fürstenfeldbruck Observatory, the Universities of Stuttgart and Karlsruhe for operating the Black Forest Observatory, and the World Data Center Edinburgh for making the annual mean values available. The results presented in this paper use the Dst index provided by the World Data Center for Geomagnetism Kyoto, Japan and the Dxt and Dcx indices provided by the Dcx server of the University of Oulu, Finland.

REFERENCE

Korte, M. and Lesur, V., 2012.Repeat station data compared to a global geomagnetic field model. Annals of Geophysics, v.55, no.6, pp:1101-1111.

Korte, M., Mandea, M., Kotzé, P. ,Nahayo, E. and Pretorius, B., 2007. Improved observations at the southern African geomagnetic repeat station network. South African Journal of Geology, v.110, pp:175-186.

Lesur, V., Wardinski, I., Hamoudi, M. and Rother, M., 2010. The second generation of the GFZ Reference Internal Magnetic Model: GRIMM-2. Earth Planets Space, v.62, no.10, pp.: 765-773.

Mandea, M., Panet, I., Lesur, V., de Viron, O., Diament, M. and Le Moul, J.-L., 2012. Recent Changes of the Earth's core derived from satellite observations of magnetic and gravity fields. Proceedings of the National Academy of Sciences of the United States of America (PNAS), v.109, no.47, pp.: 19129-19133.

Maus, S., Manoj, C., Rauberg, J., Michaelis, I., and Lühr, H., 2010. NOAA/NGDC candidate models for the 11th generation International Geomagnetic Reference Field and the concurrent release of the 6th generation Pomme magnetic model. Earth Planets and Space, v.62, no.10, pp.: 729-735.

Maus, S. and Weidelt, P., 2004. Separating the magnetospheric disturbance magnetic field intoexternal and transient internal contributions using a 1D conductivitymodel of the Earth. Geophys. Res. Lett., 31, L12614, doi:10.1029/2004GL020232.

Mursula, K. and Karinen, A., 2005.Explaining and correcting the excessive semiannual variation in the Dst index, Geophys. Res. Lett.,v.32, L14107, doi:10.1029/2005GL023132.

Mursula, K., Holappa, L., and Karinen, A., 2011.Uneven weighting of stations in the Dst index, J. Atmosph.and Solar-Terr. Phys., v.73, pp.:316-322.

Newitt, L. R., Barton, C. E. and Bitterly, J., 1996. Guide for Magnetic Repeat Station Surveys. International Association of Geomagnetism and Aeronomy.

Olsen, N., Sabaka, T. J. and Lowes, F., 2005. New parameterization of external and induced fields in geomagnetic field modeling, and a candidate model for IGRF 2005. Earth Planets Space, v.57, pp.: 1141-1149.

Olsen, N. and Kotsiaros, S., 2011. Magnetic Satellite Missions and Data. In Geomagnetic Observations and Models, IAGA Special Sopron Book Series 5, Springer.

Olsen, N., Lühr, H., Finlay, C., Sabaka, T. J., Michaelis, I., Rauberg J. and Tøffner-Clausen, L., 2014. The CHAOS-4 geomagnetic field model.Geophys. J. Int., v.197, pp.:815-827.

Sabaka, T.J., Olsen, N., Tyler, R. H. and Kuvshinov, A., 2015. CM5, a pre-Swarm comprehensive geomagnetic field model derived from over 12 yr of CHAMP, Ørsted, SAC-C and observatory data. Geophys. J. Int., v.200, pp.:1596-1626.

Sabaka, T.J., Olsen, N., and Purucker, M. E., 2004. Extending comprehensive models of the Earth's magnetic field with Ørsted and CHAMP data. Geophys. J. Int., v. 159, pp.:521-547.

Sugiura, M. and Kamei, T., 1991. Equatorial Dst index 1957-1986, IAGA Bull., 40, ISGI Pub. Office, Saint-Maur-des-Fossés, France.

Thomson, A. and Lesur, V., 2007. An improved geomagnetic data selection algorithm for global geomagnetic field modelling. Geophys. J. Int., v.169, pp.:951-963.

Verbanac, G., Lühr, H., Rother, M., Korte, M. and Mandea, M., 2007. Contributions of the external field to the observatory annual means and a proposal for their corrections. Earth, Planets and Space, 59(4),251-257.

Yukutake, T., and Cain, J. C., 1987. Solar cycle variations in the annual mean values of the geomagnetic components of observatory data. Journal of geomagnetism and geoelectricity, 39, 19-46.

J. Ind. Geophys. Union (January 2016)
Special Volume-2/ 2016 pp: 112-119

Geomagnetic Repeat Surveys in India

U. N. Mishra
Geodetic & Research Branch
Survey of India, Dehra Dun – 248 001
un.mishra.soi@gov.in

ABSTRACT
The Survey of India, has a long history of geodetic and magnetic measurements, which have contributed to early editions of topographic and geodetic maps. With successive improvements in international collaborative efforts at geodetic mapping, the Survey of India has improved its observational networks. Early magnetic measurements, since 1820, were scattered around the Indian sub-continent. However, after consolidation of available historical magnetic survey data in 1954, regular repeat surveys were carried out all overIndia. Survey of India maintains 183 repeat stations distributed over the country, as well as a magnetic observatory at Sabhawala (SAB) at Dehradun. Isomagnetic maps are produced for vertical, horizontal intensity and declination every 5 years, since 1965. This valuable repeat data set, spanning over a 100 years, has contributed to obtaining smooth models of secular variation in India and compares well with global secular variation models.

Key words: Secular Variation, Iso magnetic maps, Magnetic observatory, Co-seismic observations, Magnetic declination.

INTRODUCTION

Geodetic & Research Branch (G&RB) of Survey of India (SOI), Dehradun, India has its base station at Sabhawala Digital Geomagnetic Observatory. SAB, which has completed 100 years of its existence and is still going strong. G&RB also carries out repeat magnetic measurements at 183 stations established throughout the country. Archived geomagnetic data with SOI has helped in monitoring secular decrease of the geomagnetic field (*Vestine et al, 1947a*). The observations also provide other interesting results, (*Arora et al, 1983*) which can be used for future research in this field.

Magnetic field intensity measurements on the earth's surface is used to model the main field of the earth. Regional features can be removed from closely spaced measurements to reflect local variations that delineate geological anomalies for resource exploration, a significant contribution towards natural resource augmentation. The knowledge of spatial characteristics of the geomagnetic field is of great significance for geological applications, but as the geomagnetic field also undergoes slow temporal variations, called secular variation, it becomes desirable that a complete description of the magnetic field by analytical functions should incorporate time as well as spatial coefficients. (*Vestine, et al, 1947a, b.; Arora et al, 1983; Campbell W.H.,1997*).

The Survey of India (SOI) has been periodically conducting field magnetic surveys for graphical preparation of regional magnetic charts over the Indian region primarily for navigational needs. A magnetic survey was proposed in India in 1896, and Captain H.A.D. Fraser, Survey of India travelled to Europe to consult Prof. Rucker regarding methods and logistics connected with survey and purchase of necessary instruments. The field work of the first magnetic survey was undertaken during 1901 to 1913. The aim of this detailed survey was to determine three magnetic elements Declination, Horizontal force, and Vertical force with unifilar magnetometer. Dip was observed with Dip Circle at 80 permanent repeat stations and 1401 field stations, uniformly distributed at distance 30 to 40 miles apart over undivided India, Myanmar (Burma) and Srilanka (Ceylon).The field observations were corrected for diurnal variation with the help of data supplied by 5 magnetic observatories located at Dehra Dun, Barrackpore, Toungoo (Myanmar), Kodaikanal and Alibag.

The results of these surveys were reduced to epoch 1909.0 and 1920.0 and published in the forms of charts, contoured manually and tables in the Survey of India (Record volume XIX,1925). These charts were published for Declination, Horizontal force, Dip and Total force. The second magnetic survey was carried out in 1930. Observations were carried out at 37 repeat stations under the aegis of Dehra Dun and Alibag observatories as other observatories had been closed down. The results were reduced to epoch 1931.0 and published (*Survey of India Geodetic Report Volume VII, 1931*).The programme of periodic re-observation at repeat stations of the original survey to keep track of secular variations could not be adhered to. All the repeat stations were occupied between 1943 and 1945, but the results were used without observatory corrections.

After delineation of land borders between newly-independent countries in the Indian sub-continent, in 1947, different regions in India were surveyed in detail with Vertical force variometers, unifilar Magnetometers and

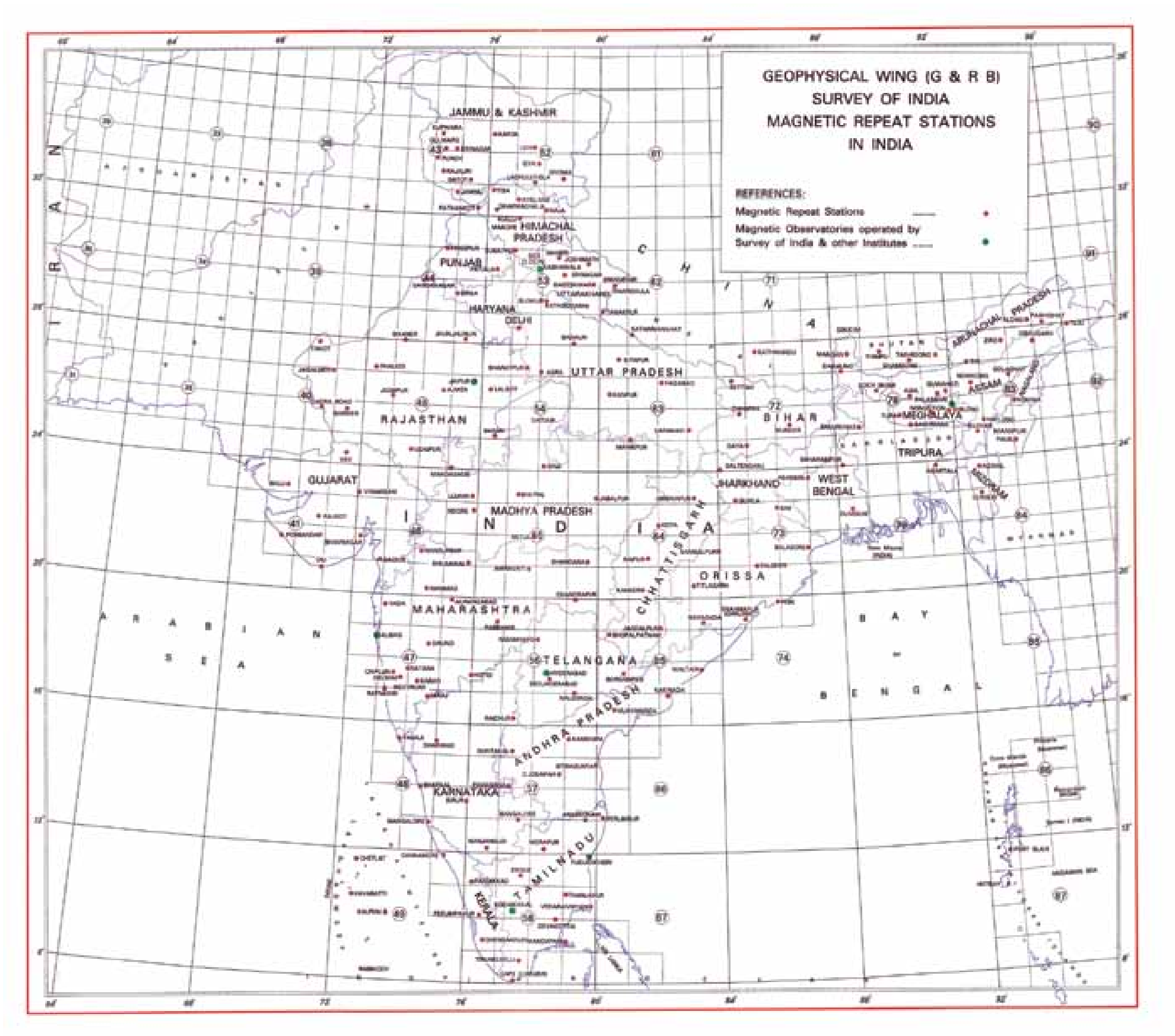

Figure 1. Geo-magnetic Repeat Stations

Dip circles in different years and a considerable amount of data was accumulated, some of which were published in different publications and the various annual Geodetic and Technical Reports of the Survey of India. An attempt was made to utilize all the data for reducing the magnetic elements (Declination, Horizontal force and Vertical force) to epoch 1953.0 and the charts were published in Technical paper No. 7. (*Gulatee, 1954*). Following this, all existing repeat stations were re-occupied and six new stations were established during 1957-59.

During World Magnetic Survey (1961-65) (*Heppner, 1964; Zmuda, 1971*) the magnetic survey of the entire country was carried out in detail. The aim was to occupy the old field and repeat stations with Quartz Horizontal Magnetometer (QHM) and Magnetometric Zero Balance (BMZ), at much closer spacing. Since then, repeat observations are conducted approximately every five years and the data are reduced for preparation of geomagnetic charts of the country. Charts of Horizontal and Vertical Intensity, upto epoch 2000.0 and Declination upto epoch 2010.0 are available. At present SOI maintains 183 Repeat Stations and one Magnetic Observatory where measurements are carried out as per specifications and procedures recommended by International Association of Geomagnetism and Aeronomy (IAGA) (*Newitt L.R., 1996*).

ROLE OF SURVEY OF INDIA

Survey of India is the only organisation in India preparing Isomagnetic charts at different Epochs, at approximately

5 year intervals. Detailed magnetic surveys carried out at the interval of 200 km throughout the country has resulted in establishment of 183 magnetic repeat stations in India (Figure 1). All the geomagnetic observations were made with Q.H.M. and B.M.Z. absolute instruments. This has later been supplemented by PPM and DIFlux magnetometers as well. The three geomagnetic elements i.e. Declination, Horizontal Force and Vertical Force are obtained, on a regular basis.

The geomagnetic data received from the field by SOI is reduced to a particular epoch. The reduced data is used for Publication of Isomagnetic charts by SOI. Details of already published charts are given in Table I.

SABHAWALA (SAB) GEOMAGNETIC OBSERVATORY

The observatory was put into commission in January, 1964. Prior to this there was an underground Magnetic observatory in the Survey of India (Geodetic Branch) compound at Dehra Dun, which had functioned from 1902 to 1943. In 1943, the Dehra Dun underground observatory went out of action (instruments being damaged due to flooding of its underground chambers).

In view of the circumstances prevailing during World War II, the observatory could not be restarted earlier. However, consequent to a resolution passed by the Geophysical Committee in 1947, it was proposed to restart the observatory – by locating it far from anticipated electrical and industrial disturbances. The land for the new observatory was acquired in 1955, and the construction of the building was completed only by 1960. Some of the observatory instruments were received as late as October 1963. After necessary tests and trials with the various instruments, which were received from time to time, and further training and practice of select SOI personnel,the observatory ultimately started functioning, with effect from 21st January 1964, coinciding with the start (on 1^{St} January 1964) of the programme of the International Quiet Sun Year. The compound area of the observatory is about 2 hectares. At present, the building for magnetic observations comprises one absolute room and one magnetograph room. It has a computer room for digital recording besides residential cum office building. It is situated about 34 km west of Dehradun in Sabhawala village. Besides studying the secular changes in the earth's magnetic field, this observatory being the only one in the northern region will help in controlling the field magnetic survey in the northern parts of India.

In 1986, Sabhawala Magnetic Observatory was awarded a gold medal, during the 100 years celebration of the first polar year to the geomagnetic observations around the world. Prof. Naoshi Fukushima, University of Tokyo, Japan presented the medal, for the observatory`s significant contribution to the global geophysical observations.

INSTRUMENTS IN USE IN SABHAWALA OBSERVATORY

La-Cour Variometers as well as the portable Askania Variograph are in use in SAB.The Digital flux-gate magnetometer (DFM) was installed at magnetic observatory on 18^{th} January 2007. Presently 1-minute digital data is reported from SAB.

Field / Observatory Instruments used by SOI:

i) Quartz Horizontal Intensity Magnetometer (QHM): The QHM, a portable instrument is used for measuring the Absolute Horizontal Intensity and Declination of the earth's magnetic field. Accuracy for Horizontal Intensity is ± 5 nT and for Declination ±1′.

ii) Magnetometric Zero Balance (BMZ): The B. M. Z. is a portable instrument used for measuring the Absolute Vertical Intensity of the earth's magnetic field by a zero balance method. Accuracy for Vertical Intensity is ± 5 nT.

iii) ENVI MAG: ENVI system is an easy to use, lightweight, battery powered, portable magnetometer. The magnetometer is a total field instrument using proton-precession techniques to measure the local field / the total intensity.

iv) Theodolite Wild T2:The well-known Wild T2 Theodolite is ideally suited for almost every type of survey task. Being simple tohandle, it has a well-illuminated optical and reading system andcan be used with a large variety of accessories and attachments. The optics are sufficiently good to allow proper observations of normal targets present at distances up to 20 kms. Circle readings are made through one eyepiece, an inverter knob ringing the required circle image into the field of view. Coincidence setting provides a direct measuring of the two diametrically-opposite circle positions. Theodolite is widely used for triangulations up to 3rd and even 2nd order limits, for precise traversing, sub tense measurements, astronomical observations, tacheometry, engineering works of all types, cadastral lay-outs, staking-outstraights and curves and mining surveys. It has least count of 1.0 second.

v) Declination Inclination Magnetometer (DIM): The system permits very precise angular measurements of the terrestrial magnetic field F. The angular components measured are declination D (Variation) and Inclination I (dip). The value of F, together with the components X(horizontal),Y and Z (vertical) may also be measured to an accuracy of 0.25%.

Magnetic Surveys and Charts

The magnetic measurements were made at established repeat stations, using QHM, BMZ and T2 theodolites. At present, the SOI deploys DI flux and proton precession

Table – 1 . List of published magnetic charts of various epochs

Sl. No.		Epoch chart
1	Line of equal magnetic declination	2010.0, 2005.0, 2000.0, 1995.0, 1990.0, 1985.0, 1980.0, 1975.0, 1970.0, 1965.0
2	Horizontal force	2000.0, 1995.0, 1990.0, 1985.0, 1980.0, 1975.0, 1970.0, 1965.0
3	Vertical force	2000.0, 1995.0, 1990.0, 1985.0, 1980.0, 1975.0, 1970.0, 1965.0

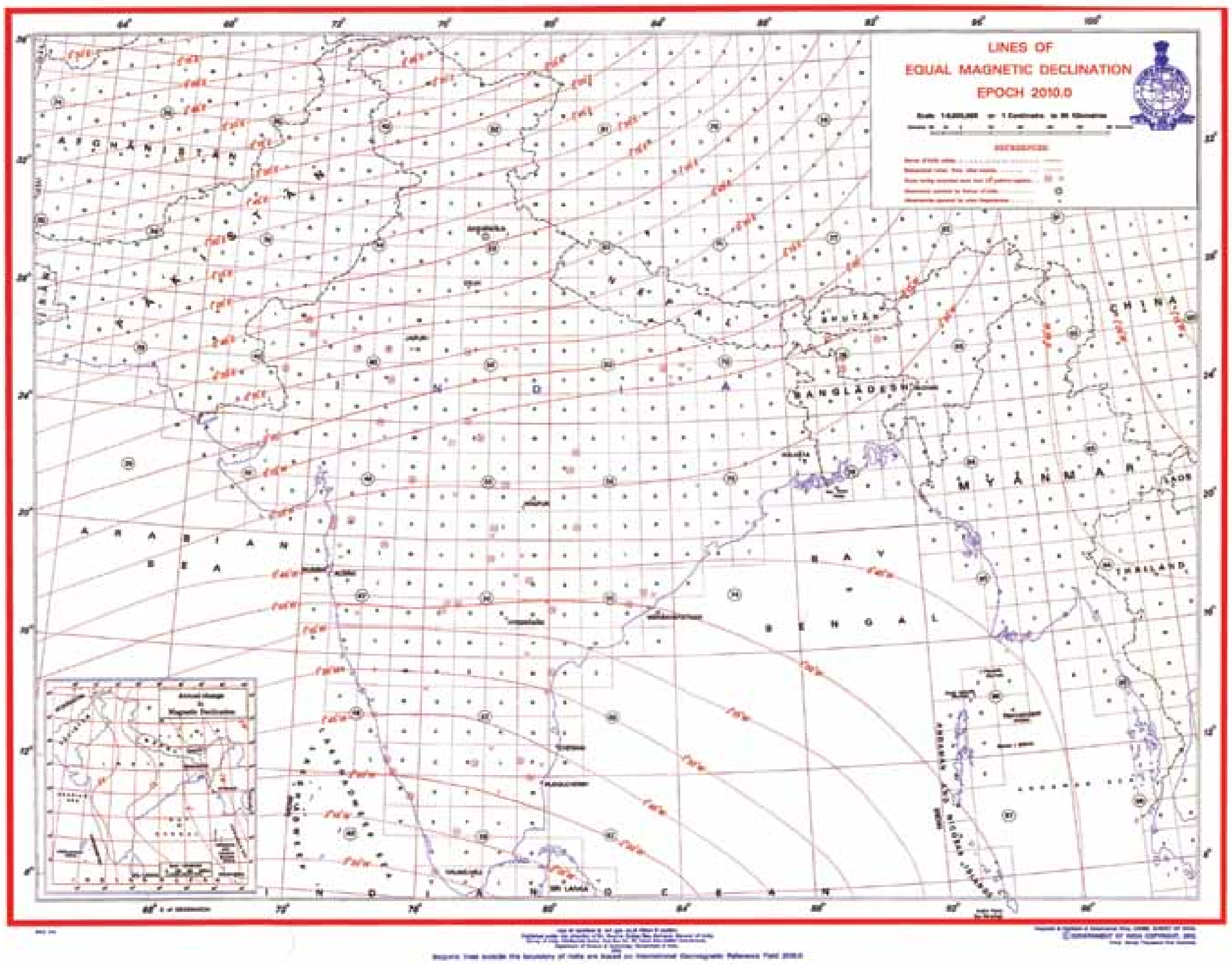

Figure 2. Magnetic Declination Chart

magnetometers, for these measurements. These observations are used to compute horizontal (H), and vertical intensity (Z) & declination (D) at repeat and field stations. The field instruments used in the survey were calibrated against the prime geomagnetic observatory standards, at Alibag (ABG) and other permanent observatories located in different regions of the country. Effects on the data due to instrumental differences are corrected. In addition, the quiet-day daily variation and magnetic disturbance effects are eliminated from the data, by comparing with data from the permanent magnetic observatories. During the magnetic survey of 1962-66, 989 field and repeat stations were covered.

The world magnetic survey Board had recommended a scale of 1:50,000,000 for world magnetic charts and 1:5,000,000 to 1:10,000,000 for regional magnetic charts. In Survey of India a scale of 1:6,000,000 is followed. Following geomagnetic charts are published by Survey of India at an interval of 5 years, since epoch 1965.0.

i) Isomagnetic charts for Horizontal intensity.
ii) Isomagnetic Charts for Vertical Intensity
iii) Isomagnetic Charts for Declination (Figure 2)

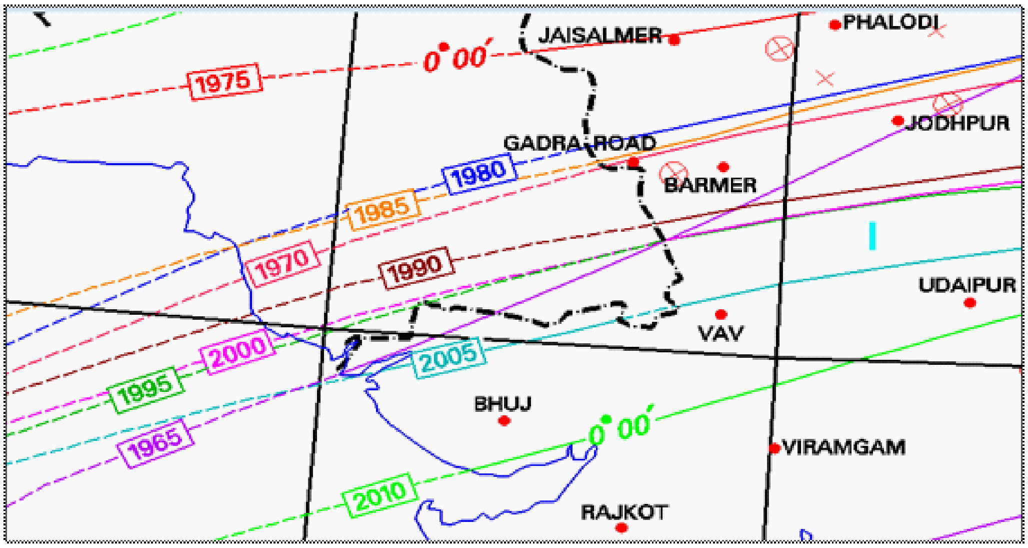

Figure 3. Temporal change of magnetic declination lines over Kutch, Gujarat, 1976-2000

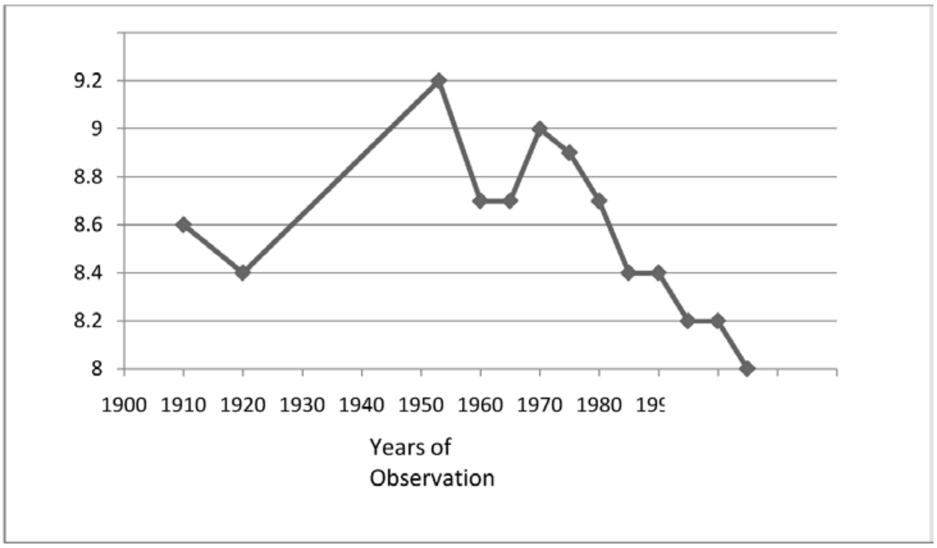

Figure 4. Geographic location / migration of the Dip Equator during last hundred years of Indian Peninsula based on Iso-magnetic Chart published by Survey of India epoch 1909 to 2005 for Z (1953 onwards) and for I (1909 - 1920)

The Survey of India specialises in determining true North at required locations, in addition to determination of declination change, with respect to fixed azimuth markers, to user agencies in India with accuracy of 1″.

STUDIES WITH MAGNETIC DATA

a) Secular variation in India: Repeat stations were established, in addition to those already existing. This survey was carried out over 5 years (1962-1966). The separation between the new field stations ranged from 30-80 km, in contrast to repeat stations,which are about 200-300 km apart. Isomagnetic charts were prepared for epoch 1965.0. Thereafter, repeat surveys were carried out at about 5-year intervals leading to preparation of isomagnetic charts every 5 years.

The reduced data from this survey was used to compute the first analytical isomagnetic chart for Indian region, using 6^{th} degree polynomial. The fit of this model is comparable with that of the IGRF 1965.0. Due to the closely spaced data set, the model could reflect more features of wavelength ~ 1000km. Comparison with IGRF showed agreement in major features. Further models for 1970.0 and 1975.0 were computed with fewer repeat stations. The coefficients of the model obtained for secular change were also found to be similar to the IGRF and also in agreement with secular variation trends observed at the permanent magnetic observatories (*Srivastava and Abbas, 1977*).

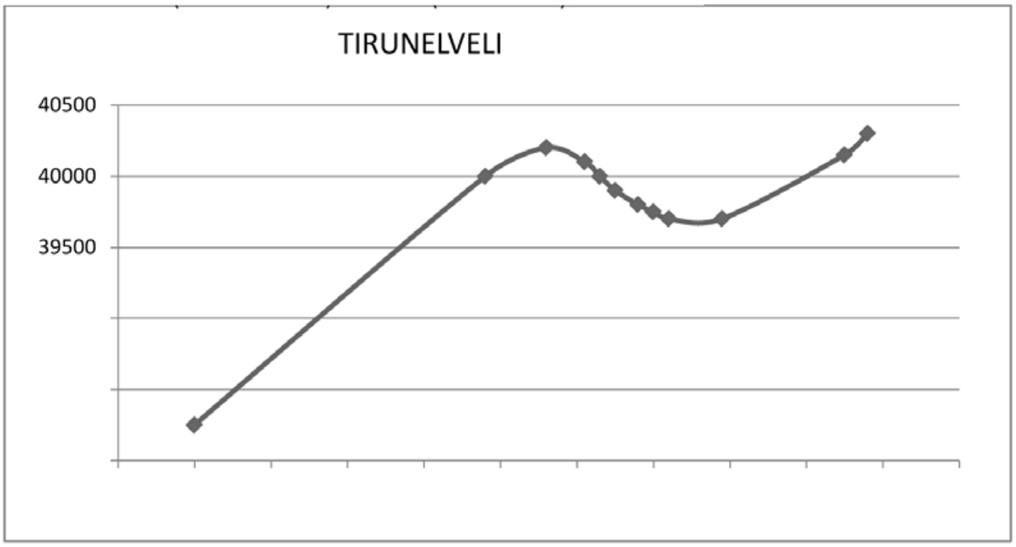

Figure 5. Temporal variation of total magnetic force at Tirunelveli during 1920-2005

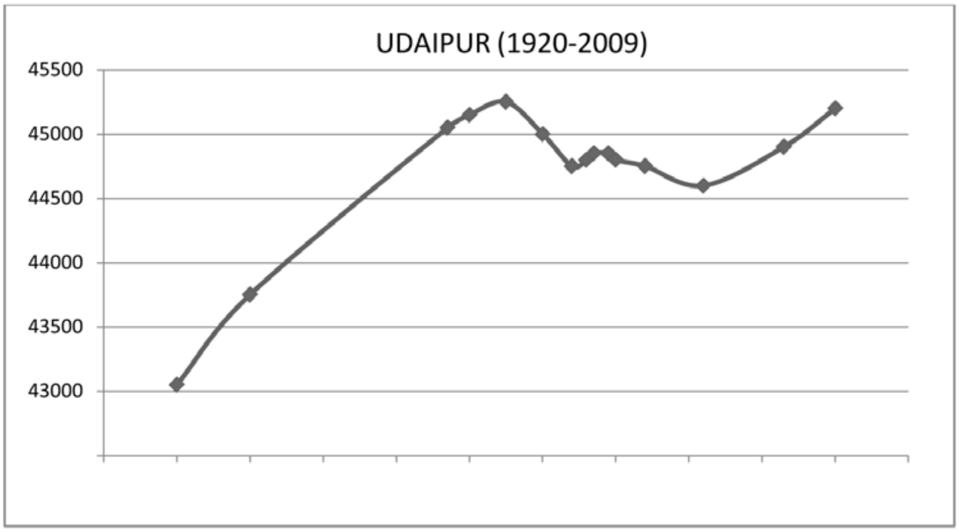

Figure 6. Temporal variation of total magnetic force at Udaipur during (1920 – 2009)

Using the repeat station network data of 1965.0 epoch, Arora et al, (*1983*) made as moothed polynomial fit to the data, including the annual mean of observatory data for 1965.0. The isolines thus obtained, were compared with the IGRF model and found in agreement. Secular variation rates were also estimated, and compared with IGRF. However, detailed observations for secular change in Declination (1965-2000) over Western India (shown in Figure 6), indicate more rapid and complex behaviour. It was also shown that coefficients for secular variation derived, by using 1970.0 and 1975.0 epoch surveys, compare well with IGRF models, as well as secular variation features noted at 6 Indian magnetic observatories (*Srivastava and Abbas, 1977*).

b) **Declination trends in Peninsular India** : The agonic line passes through the Indian region. Long series of measurements, over the region have shown finer details of secular variation in D (*Chatterjee, 1971; Gulatee, 1954*). An example of such variations of the agonic line, in the Western Indian province of Kutch, is shown in the Figure 3. Agonic line variations could be obtained using measurements upto 2005. Migration of Dip equator is shown in Figure 4 and variation of total magnetic forces at Tiruneveli and Udaipur in Figure 5 and Figure 6, respectively.

(c) Co-seismic observations: Geomagnetic studies based on experimental techniques basically determine the electrical conductivity and magnetic susceptibility of the

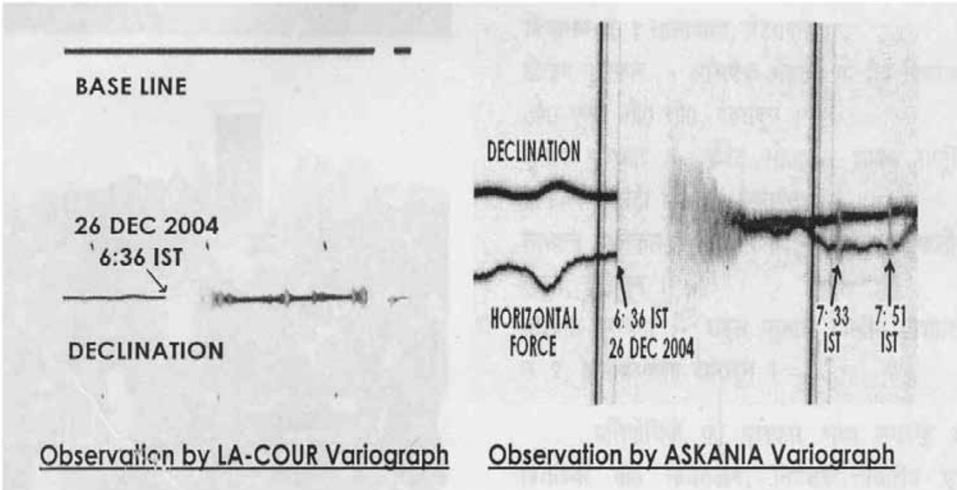

Figure 7. An example of co-seismic effects on magnetic variation is shown for the instant of tsunami 26 Dec., 2004

Earth crust, which in turn are dependent on the chemical composition of the sub-surface material. The magnetic susceptibility is effected by rock – stress; this aspect is known as tectono-magnetism, and efforts have been made to study its efficacy in the prediction of earthquakes (*Arora 1991; Johnston 1997; Johnston 2002*). Signatures of recent earthquakes have been recorded at Sabhawala Geomagnetic observatory in Figure 7 for the 26th December, 2004 tsunami genic earthquake. Signatures of Japan tsunami of 11th March, 2011 and Sikkim earthquake of 18th September, 2011 have also been recorded. Numerous other magnetic field variations have been recorded just prior to local earthquakes such as Uttarkashi and Chamoli earthquakes in Uttarakhand state.

CONCLUSION

A systematic approach to obtain magnetic repeat station data has been initiated by the Survey of India, Geodetic & Research Branch, in last six decades. The data is mainly used for navigation purposes, correction of maps and compasses used in aviation. But,as stated in the foregoing paragraphs, this valuable data can be used for many scientific studies. A collaborative and more systematic study among Indian agencies working in this field and global agencies can derive fruitful results for the benefit of the society.

ACKNOWLEDGEMENTS:

The author thanks the LOC of the XVI IAGA Observatory Workshop, for the opportunity to contribute to this volume as well as to the reviewers for constructive revisions of the manuscript.

REFERENCES

Arora, B.R. 1991. 'Precursory geomagnetic-geoelectric changes to Earthquakes physical mechanism, Indian and contemporary field examples'. Journal of Scientific Research, Benares Hindu University Platinum Jubilee Year, Special Volume 41B. 223-43

Arora, B.R., Badshah, V.H., Singh, B.P., Arur, M.G., Bains, P.S., Jeevan Lal, 1983. Analytical representation of spatial and temporal variations of the geomagnetic field in the Indian region, Proceeding of Indian. Academic Science (Earth&planet.Science), Vol 92, no 1, 15-30.

Arur, M.G., Bains, P.S. and Jeevan Lal 1980. Geophysical Research Bulletin, vol 18, 67-71

Campbell W.H., 1997. Introduction to geomagnetic fields, Cambridge University press.

Chatterji, J., 1970. Geomagnetic anomalies in south India, Proceedings of Seminar on Problems of Equatorial Electrojet.Aug.1970, Ahmedabad (PRL), Paper 8.

Gulatee, B. L., 1954. Charts of declination, horizontal force and vertical force for the epoch 1953.0 and magnetic anomalies (India, Pakistan and Burma), Survey of India Technical Paper. No. 7, (iii)and 9.

Geodetic Report Vol. VII (1931) , Survey of India, Dehradun

Heppner James P., 1964. The World Magnetic Survey, Volume 2109, National Aeronautics and Space Administration, 1964 .

JIG, NGRI, SOI, 1972. Ground geomagnetic survey in the equatorial electrojet region in India-a report, Geophysical Research. Bulletin. 10, 167-180.

Johnston, M.J.S.,1997. Review of electric and magnetic fields accompanying seismic and volcanic activity, Surv. Geophys.,18: 441-475.

Johnston, M.J.S., 2002. Electromagnetic fields generated by earthquakes, International Handbook of Earthquakes and Engineering Seismology, Academic Press, Part A, 621-634.

Newitt, L.R., Barton C.E. and Bitterly, J., 1996. Guide for Magnetic Repeat Station Surveys, NOAA Space Environment Centre, 325, Broadway, USA.

Pramanik, S. K., 1952.Secular variation of the magnetic field at Colaba and Alibag, Journal of Geophysical Research.,57, 339-355

Vestine, E. H., Laporte, L., Lange, I., Cooper, C. and Hendrix, W. E., 1947a. Description of the Earth'smain magnetic field and its secular change 1905-1945. Carnegie Institute of Washington Publ. No. 578.

Vestine, E. H., Lange, I., Laporte, L. and Scott, W. E., 1947b. The geomagnetic field, its descriptionand analysis. Carnegie Institute of Washington Publ. No. 580.

Zmuda A.J., 1971. World Magnetic Survey, 1957-1969, IAGA Bulletin no. 28, 1971, 732 pp.

J. Ind. Geophys. Union (January 2016)
Special Volume-2/ 2016 pp: 120-126

Secular Variation Studies in the Indian Region – Revisited

Nandini Nagarajan, Habiba Abbas and L. Manjula

Hyderabad Magnetic Observatory
CSIR-National Geophysical Research institute
Hyderabad 50007, INDIA
nandini_ngri@yahoo.com

ABSTRACT

This paper provides a retrospective view of some studies on regional secular variation carried out at the Hyderabad Magnetic Observatory, taking into consideration presently available data and models along with an evaluation of the previous results in view of more recent ones. The long term features like quasi-periodic secular variation of horizontal and vertical components, as seen in the annual means of ABG(1850-1975) has been borne out by other studies reporting oscillatory movement based on IGRF models and smoothed spline fitting. Studies of repeat station data over India, as well, have confirmed features of secular variation of D and Z. Ground surveys conducted in the region of the dip equator, also provide confirmation of the rates of migration of the dip equator.

The updated plots of annual means from 1955 to 2010, confirm some important observations of the earlier studies: rapid migration of the dip equator in Indian region that is not reflected in nearby longitudes (East Africa and South-east Asia), and the estimated rates of migration. Other studies have corroborated inferences of quasi-periodic movement of the dip equator, and differences observed in secular change of Declination over Indian region. The predicted northward quasi-periodic oscillation of the dip equator, from 2005, however, has not occurred yet, as seen from the annual means, and from ground surveys.

Keywords: Calibration of observatory magnetometers, Equatorial vertical field measurements, Experiments on magnetometers

INTRODUCTION

This paper provides a retrospective evaluation of early results on secular variation in the Indian region. Three papers that were published during 1977-1992, (*Srivastava and Abbas, 1977, 1984: Srivastava, 1992*), using available information at that time, are discussed here. The results and inferences made are revisited, and examined in the light of the results of subsequent published work.

Recapitulating the results, Srivastava and Abbas (*1977*) used a long series of ABG annual means (Colaba and Alibag data series 1850-1975) to obtain smoothed secular variation trends for the components H, D, and Z by means of a smooth 5th degree polynomial fit to the data. Some of these results are reproduced in Figure 1. A smooth increase (1850-1890) and slight decrease up to 1920, is seen in H (Figure 1a), followed by more rapid increase from 1920 to 1960 and a decrease thereafter. Annual means of Z, show a smooth increase from 1850 to 1930, showing a slow decrease upto 1970 and a slight increase upto 1975 (Figure 1b). Secular change of Declination (D) annual means indicate a smooth increase (easterly) at ABG up to 1880, then a change to decreasing (westerly) declination up to 1960 (Figure 1c). Declination was zero at ABG in 1930. The agonic line passes through Central India, as evident in IGRF charts.The residuals from the smoothed fit to H and Z plots(Figure 1d), were seen to have an oscillatory quasi-periodic variation, 1850-1960 in both H and Z and that they are out of phase with each other. The authors, also inferred a corresponding movement of the dip equator, that is borne out by later studies, in the period 1960-2005. Secular variation rates of D, between 1900-1950, were high at ABG~3.6′/yr (Gulatee, 1954).However, on comparison of annual means at six observatories the authors found that after 1960, secular variation rates for D were found to be slightly less at ABG and HYB, which are near the Agonic line, compared to other observatories in peninsular India.

Using annual means for 1960-1975, of six magnetic observatories, some secular variation trends were obtained by Srivastava and Abbas (*1977*). These are replicated in the updated plots up to 2010, made in the next section(Figure 2). The notable observations were: that H component decreases at all observatories after 1965 (Figure 2a). There is a change in sign of variation of Z-component, but at different years, at each observatory between 1962-1968 (Figure 2c). Secular variation rates for D were found to be slightly less at ABG and HYB, which are near the Agonic line, compared to other observatories in peninsular India (Figure 2b). Table I lists the observatories examined in this study, along with their co-ordinates.

Srivastava (1992), obtained Sq (H),(Z) amplitudes over closely spaced stations, from a magnetometer array study in South India and observed that the line of maximum Sq(H), and of zero dip, are parallel to each other both from the array study and earlier ground survey (*IIG et al, 1972*). He also estimated an increasing gradient of secular change of Z, from 1 km/yr up to 7 km/yr, in 1980, in the Indian region, and predicted the trend of migration of the dip

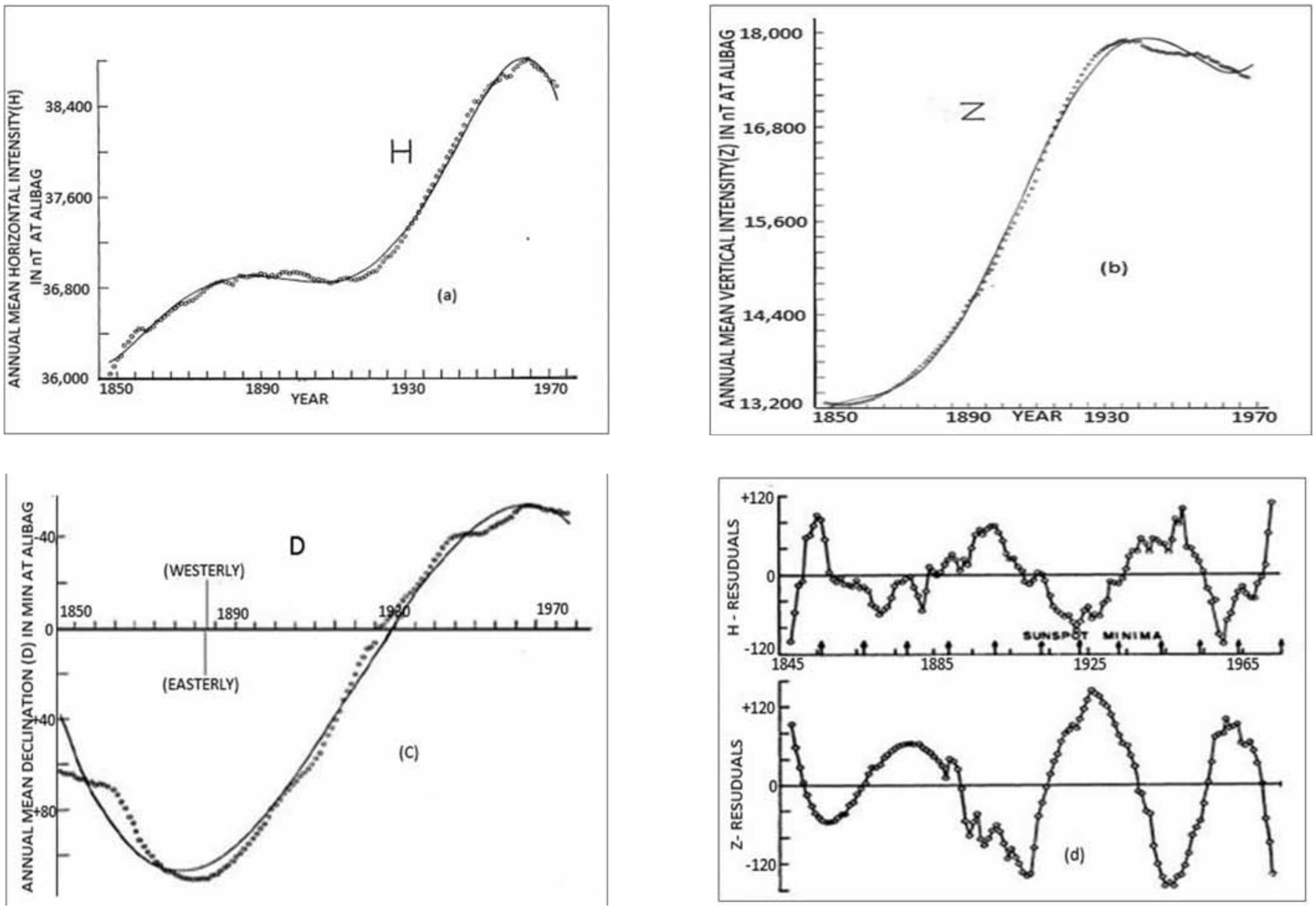

Figure 1. Composite figure showing secular variation in (a) H, (b) Z, (c) D components from annual means of Colaba-Alibag (1850-1975)together with the fit of a smooth polynomial and (d) residuals in H and Z, obtained by subtracting the smoothed trend, showing quasi-periodic variation (reproduced from Srivastava and Abbas, 1977).

equator, further south of the Indian peninsula up to 2005 and noted a corresponding northward movement of the dip equator at Huancayo observatory (285º longitude) in comparison (*Golovkov et al., 1983*), in the American sector.

Srivastava and Abbas (*1984*) examined annual means from Indian observatories for signs of the geomagnetic jerk of 1969, (*LeMouel, et al, 1982*). This jerk was not seen in the annual means of declination at Indian observatories.

Subsequent work on secular variation in the Indian region have been presented by several authors, their inferences taking into account the availability/access to latest IGRF models and techniques. Their results refine global and regional features of secular variation, and estimation of migration of the dip equator and have largely corroborated the earlier findings. One of the earliest studies (*Arora et al, 1983*) focuses on the estimation of polynomial fit to a network of repeat station measurements and observatory data in India at 3 epochs,(1960-1975)and comparison of region secular variation patterns with IGRF (1965.0 – 1975.0).The rates of change have also been estimated. The most significant feature is the rapid change in rate of secular change in D, over the Indian peninsula. Studies on migration of the dip equator, estimated directly from ground surveys conducted approximately every 10 years (*IIG, et al,1971;Sanker Narayan and Ramanujachary 1971;Murty et al 1983; Rangarajan and Deka, 1991;Paramasivan et al, 1999; Deka et al 2005*), have delineated the position of the dip equator, along traverses in southern peninsular India and confirmed its southward migration until 2000. In the last survey in 2003, it was inferred that the equator was situated south of the landmass of the Indian peninsula. Deka et al, (*2005*), report that the movement of the dip equator at 77.5 °E longitude, along the centre of the Indian peninsula, over past hundred years, as derived from IGRF values, and the migration determined from ground surveys over 30 years (1971-2003), follow a similar trend. Oscillations of the position of the dip equator, have also been extracted from IGRF values (1910-1980) (*Rangarajan and Baretto, 2000*). The oscillatory southward movement (1900-1930)

Table 1. Co-ordinates of the magnetic observatories used in this analysis and availability of annual means.

STATION	Abbreviations	Geographic		Data Length (in Years)	Data Gaps
		Lat.	Long.		
TRIVANDRUM	TRD	8° 29' N	76° 57' E	1957-1999	
TIRUNELVELI	TIR	8° 42' N	77°48' E	2000-2010	
ETTAIYAPURAM	ETT	9° 10' N	78° 01' E	1980-2000	
KODAIKANAL	KOD	10° 14' N	77° 28' E	1955-2004	
ANNAMALAINAGAR	ANN	11° 22' N	79° 41' E	1957-1993	
PONDICHERRY	PON	11° 55' N	79° 55' E	1994-2010	
HYDERABAD	HYB	17° 25' N	78° 33' E	1965-2010	
ALIBAG	ABG	18° 37' N	72° 52' E	1955-2010	
SABHAWALA	SAB	30° 22' N	77° 48' E	1965-2010	
MUNTINLUPA	MUT	14° 22' N	121° 1' E	1955-2002	1989-1994,1997 &1999
ADDIS ABABA	AAE	9° 2' N	38° 46' E	1958-2010	

followed by northward movement (1930-1975) and again southward movement (1975-2005) clearly demonstrates a quasi-periodic feature.

PRESENT DATA SETS

In the present work, we have extended the datasets of annual means of six magnetic observatories, in India up to 2010. As in the work of Srivastava and Abbas (*1977*), we compare this regional trend against trends in Africa (AAE) and south-east Asia (MUT). Location, and details of all the observatories is given in Table I.

The annual means series for TRD, has been extended using the proximate observatory TIR, from 2000 and series for ANN is extended using annual means of PON. We compare this data series 1955-2010, against improved IGRF models and subsequent published work and evaluate the inferences made in the earlier papers, with knowledge presently available.

Plots of annual means (1955-2010) at all six Indian observatories and AAE(blue) and MUT(yellow) are presented in Figure 2a,b,c. Coloured lines show trends of annual means and dots of same colour show IGRF value at 5-year intervals at each observatory. Appropriate constant offsets have been added to mean value series of each observatory in order to bring all the plots into the same range. Also, the corresponding IGRF values at 5-year intervals have been shifted by known amounts to coincide/ align with the annual means shown as continuous lines for each observatory. In Figure 2a, the annual means of H-field at all six observatories show similar trends: slow decrease from 1965 to 1988 and increase thereafter. This decrease is in agreement with the plots of ABG in Figure 1a (*Srivastava and Abbas, 1977*).The rate of increase (1988-2010) is faster at the southern observatories ANN-PON, KOD, TRD-TIR compared to SAB, ABG and HYB. The plots of AAE(East Africa) and MUT(Philippines) in the same figure indicate similarity between AAE and the Indian region. In contrast secular variation at MUT is in opposite phase, showing increase up to 1989, and decrease thereafter.

Figure 2(b) shows plot of annual means of Declination along with IGRF values for the period (1955-2010). It is noted that there is a steady decrease in D (westward declination at Indian observatories) from 1965. SAB shows slightly different trend compared to others, with marked change between 1990-2000. This rapid change in D variation, on either side of the agonic line passing through central India, is also reflected in the IGRF models, for the Indian region (*http://www.ngdc.noaa.gov/IAGA/vmod/igrf_old_models.html*) and also pointed out from theisolines derived from repeat station data (*Arora et al, 1983*). Secular variation trends for D are similar at all peninsular observatories in Indian region. After 1960, there is slight divergence between trend at ABG and HYB as seen from IGRF values. At the three (TRD, ANN & KOD) southern observatories, similar trends are seen. The anomalous trends in rate of change of D, noted by Gulatee (*1954*) and Srivastava and Abbas (*1977*), are not seen in this data set. Secular variation at SAB is in the opposite trend showing gradual increase. In contrast, trends seen at AAE (East Africa) and MUT (East Asia) vary widely.

Figure 2(c) shows plots of annual means of Z variation at all six Indian observatories as well as those from AAE (Africa) and MUT (Asia). Z variations show a slight decrease from 1955 to 1975 and also at AAE & MUT. AAE shows a similar trend as ABG and HYB, the rate of increase is slightly less. MUT, on the other hand shows little variation up to 1981, and gradual increase thereafter. Rate of increase is more rapid from 1995 at all Indian observatories.

The Z annual mean values at 10 year intervals, for the four observatories in South India (TRD-TIR, ETT, KOD,

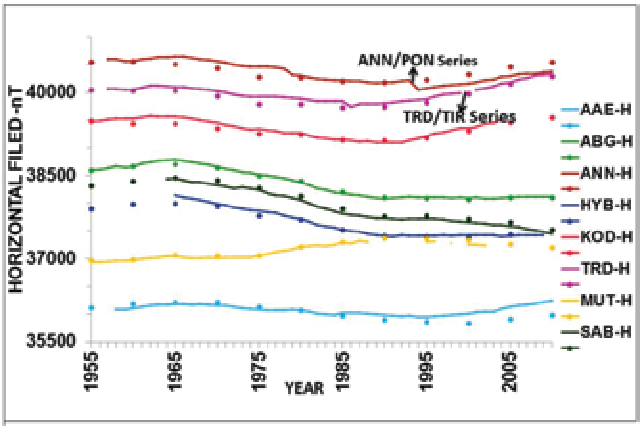

Figure 2a. Plots of annual means (1960-2010) at all 6 Indian observatories and AAE(blue) and MUT(yellow) of Horizontal intensity, along with IGRF values shown as dots..

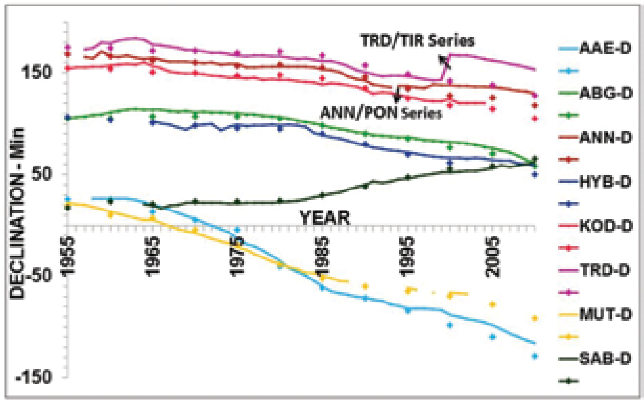

Figure 2b. Plots of annual means (1960-2010) at all 6 Indian observatories and AAE(blue) and MUT(yellow) of Declination, along with IGRF values shown as dots..

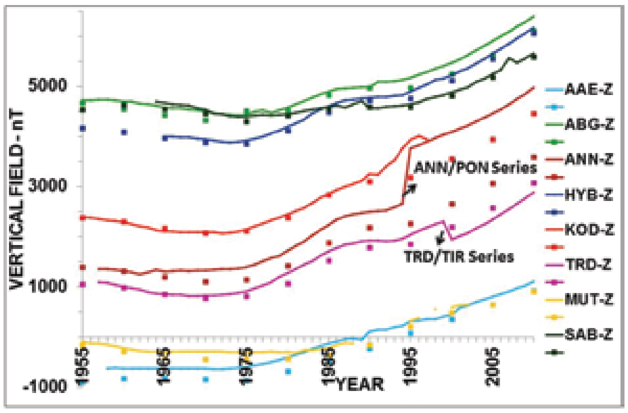

Figure 2c: Plots of annual means (1960-2010) at all 6 Indian observatories and AAE(blue) and MUT(yellow) of Vertical intensity, along with IGRF values shown as dots

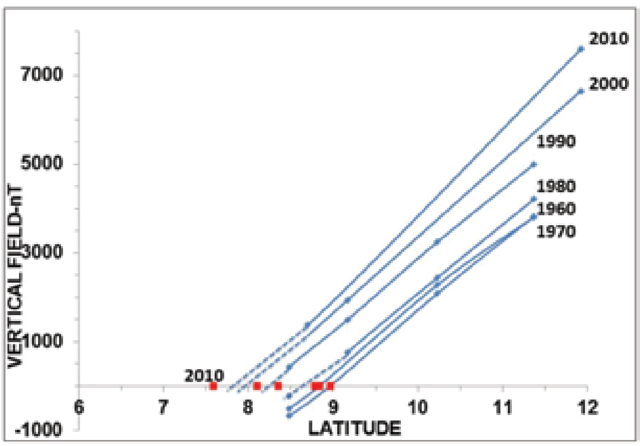

Figure 2 (d). Position of the dip equator (1960 -2010) as deduced from plots of annual means of Z,at observatories in the Indian region, at 10 year intervals. The location of the dip equator derived from IGRF of the same epoch is shown (red squares) at the latitude 77°E.

ANN-PON) are plotted against their respective latitudes, in Figure 2(d). The position of the dip equator, as obtained from observatory annual means is evident from these plots for epochs 1970.0 and 1980.0. Upto 1990, the dip equator, as delineated from observatory data and ground surveys, differed slightly from IGRF positions (*Deka et al, 2005*). After 1990, we can only extrapolate the location of the dip equator from observatory data, in the ocean south of the Indian peninsula. For the next 3 epochs, the position of the dip equator is found by extending the trend in decreasing Z, to find the latitude of the inferred location of the dip equator. With present data, we have projected the latitude at which Z would become zero, along the 77° longitude, based on the rate of increase of Z values at the four observatories in the Indian peninsula. The positions of the dip equator at 77° E longitude was obtained from IGRF and shown along the latitude axis, in red. The positions show a good fit with observatory data, except for the extrapolated values for 2010 and 2015. This plot shows the decadal change to be large between 1990-2010 compared to earlier period. From the annual mean values of Z from several low latitude observatories of the world for 1945 to1995, Rangarajan (*1994*) showed that at most of the observatories the secular trend in Z is consistent with the direction of the meandering dip equator.

DISCUSSION

Preliminary trends inferred up to 1975 (*Srivastava and Abbas, 1977*), and separately in repeat station data (1965-1975) by Arora et al, (*1983*), continue in the present data set, shown here (1955-2010). The regional differences noted between Indian region when compared with East Africa and Asia, also continue up to 2010. These results are also corroborated by values obtained from IGRF models over the period.

Rates of migration of dip equator

The differences in dip equator migration at different longitudes, was inferred by comparing annual means in the Indian region with observatories in Africa and East Asia by Srivastava (*1992*). The extended series (1955-2010) is presented here. Similar observations were extracted from IGRF values (1900.0-2000.0) and discussed in detail by Rangarajan & Baretto (*2000*). The extended series of annual means (1960-2010) plotted here, also reiterate the differences between Indian, African and East Asian sectors.

The long series of annual means of ABG (1850-1975) is a unique dataset and provides independent corroboration of secular variation models. The features noted by Srivastava and Abbas (*1977*), have thus been subsequently corroborated (*Baretto, 1987;Rangarajan and Baretto, 2000 and Deka et al, 2005*). Locally, from direct ground surveys, trace of the dip equator in India (76-78° E longitude) was plotted in 1971, 1983,1991 and 2003 (*IIG et al, 1972; Murty et al, 1984; Paramasivan et al 1999; Deka,et al 2005*) describing the migration up to 1991, after which the dip equator could not be located on the Indian peninsula.

Most significant is the quasi-periodic variation of Z, and migration of the dip equator, over a 80-year cycle. It was also inferred from these results that southward migration would reverse around 2005 (*Srivastava, 1992; Deka et al, 2005*). The dip equator migrated southwards up to 1925 and then reversed to a northward direction smoothly. After 1970, a southward migration is again noticed. Between 1945 and 1980, it is seen that the dip equator was confined to a narrow latitude belt between 8.5° and 9°N (*Deka et al, 2005*) and migrated southward rapidly (1990-2010) subsequently.

The quasi-periodic movement of the dip equator, postulated by Srivastava, (*1992*), predicts a northward movement after 2005. Present results from annual means plotted up to 2010 and values available up to 2014(quasi-definitive)and IGRF values up to 2015, show that southward migration of the dip equator continues and has not changed direction in 2005, as suggested earlier (*Srivastava, 1992; Deka et al, 2005*). The rate of southward migration has also increased after 1990. Differences are seen between the inferred location the dip equator for epochs between 1970-2010, and location derived from IGRF models of the same epochs. There is no evidence that northward migration of the dip equator has commenced.

Quasi-periodicity in secular variation

In Srivastava and Abbas (*1977*), annual means were compared against available values from the Survey of India charts of isolines (*Chatterjee, 1970; Gulatee, 1954*) and migration of the dip equator was further confirmed by a ground magnetic survey in 1971(*IIG et al, 1972*). The residuals derived from ABG data from 1910-1970 in that study, showed an oscillatory behavior of Z and also in H, but directly opposite in phase. From survey results collated over 60 years, it was inferred that the northward migration of the dip equator continued to occur during 1927-1967, and ground surveys confirmed its position near 9°N latitude in 1971. These observations together with the residuals obtained from the secular change at ABG, led to the inference that the migration is probably cyclic in nature and would complete its southward movement in further 40 years. Trends obtained from the long series of annual means at ABG, could only be compared against early IGRF models, available from 1900 (Rangarajan and Barreto, 2000), wherein an oscillatory movement of the dip equator (and inferred change in Z), was obtained for the Indian sector (longitude 70-80°E). This appears to have a period of nearly 80 years. When compared with the results of Srviastava and Abbas (*1977*), in Figure 1 above, some questions arise. The plot Figure 1(d), shows a maxima before 1845, and at 1880, 1925, and 1965. As presented in that paper, they indicate a periodicity (~40 years), but this has been subsequently attributed to 80yr Geissburg Cycle (*Bhardwaj & Subba Rao, 2013*). It must be acknowledged that the method of obtaining these residual curves using a polynomial fit to the 1850-1970 annual means series, is probably subjective. However, quasi-periodic structure of secular variation (~50 yr) has also been identified in the region (*Rotanova et al, 2003*).

Secular variation of D

The large changes in rate of secular variation in D, over the Indian region have been corroborated by later studies (*Arora et al, 1983; Bhardwaj & Subba Rao, 2013*). The rapid changes in D, taking place in the vicinity of the agonic line that passes through central India, has also been documented in IGRF maps. The more westerly change in declination has been documented earlier and compared with IGRF models (*Arora et al, 1981; Bhardwaj and Subba Rao, 2013*), wherein, ABG and HYB, along with SAB, in the Himalayan foothills show decreasing declination. A single trend of westward secular change is seen over the entire peninsula. The rate of change is about 0.25'/yr. The same decreasing trend is seen more sharply at AAE and MUT in our plot (Figure 2b), where the rates at AAE and MUT is about 0.35'/yr. Between 1980 and 2000, a slightly larger change in seen at ABG, compared to HYB. Similar trends are seen at the southern observatories ANN-PON, KOD, TRD-TIR. Rapid changes in D variation were reported (*Gulatee, 1954; Arora et al, 1983*) and is also evident in rates of secular change in IGRF models.

COMPARISON WITH GLOBAL SECULAR VARIATION

An attempt to identify the global geomagnetic jerk of 1969 (*Le Mouel, et al, 1982*) was made by Srivastava and Abbas, (*1984*). The signature of the geomagnetic jerk of 1969, could not be detected in regional secular variation trends in the Indian region. The residuals in first and second derivatives of secular variation, were large in this region (*McLeod, 1989*). However, wavelet analysis of the jerk, showed some regional differences in phase of the Jerk (*Alexandrescu et al, 1996*) that supported the original observations. Further global analysis of first and second derivatives of secular variation in the Indian and African regions delineated separate trends, one for Indian region, correlating well with the East African region, and that of West Africa with Europe (*Nandini Nagarajan, 1992*). Wavelet analysis of secular variation also indicated 60-yr periodicity, prominent over East Africa and Indian peninsular (*Rotanova et al, 2003*).

CONCLUSION

Cumulative results from successive IGRF estimates of migration of the dip equator, conclusively report that an oscillatory movement with periodicity of 80 years, is seen in the Indian region. This is partially corroborated by repeated ground surveys to determine the position of the dip equator, in India over the past 50 years. Early indications of this migratory, as well as oscillatory behaviour could be shown from the residual variation of annual means from the annual means of a single observatory (Colaba-Alibag). Further, observations made from analogue information, solely from reports of observatory data from other stations, also provided evidence that this migration is clearly seen in some longitude zones while absent at others. Observations of the secular change of declination made from repeat surveys and observatory means (1950-1975) indicating rapid changes over the Indian peninsula have been corroborated by subsequent IGRF models.

Regional estimates of secular variation from six magnetic observatories, in the Indian region, correspond well with global models. However, in respect of geomagnetic jerks, early indications of regional differences were also provided from this data series. These variations have been corroborated by subsequent analyses.

The trends found in a long, extremely valuable, series of annual means from a single station, as well as first results from 15 years of means from five other Indian observatories, have been corroborated by global models and subsequent analyses. The significant result of extending these series, in the present study, has been that the oscillatory migration of the dip equator, has not reversed in 2005, as hypothesised.

ACKNOWLEDGEMENTS

Authors thank LOC of IAGA XVI Workshop on Magnetic Observatory practice for support to attend the Workshop, and the invitation to contribute to the this special volume. We thank the reviewers for helpful comments that have expanded the discussion. Support of the Ministry of Earth Sciences(MoES/P.O.(Seismo)/1(124)/2010) is acknowledged (NN).

REFERENCES

Alexandrescu, M., Gibert, D., Hulot, G., Le Mouël, J.-L. and Saracco, G., 1996. Worldwide wavelet analysis of geomagnetic jerks, J. Geophys. Res., 101 (B10), 21975–21994, *doi:*10.1029/96JB01648.

Arora, B.R., Badshah, V.H., Singh, B.P., Arur, M.G., Bains, P.S. and Jeevan Lal, 1983. Analytical representation of spatial and temporal variations of the geomagnetic field in the Indian region, Proc. Ind. AcadSci. (E & planet.Sci), 92, 1, 15-30.

Barreto, L.M., 1987. Consideracoessobre a variacao secular e o modelamento de campo geomagnetico no Brasil, Publ. Observatorio Nacional do Brasil, 5/87.

Bhardwaj, S. K. and Subba Rao, P. B. V., 2013. Secular trend of geomagnetic elements in the Indian region, Earth Planets Space, 65, 1515–1523.

Chatterjee, J., 1970. Geomagnetic anomalies in south India, Proc. Seminar on problems of Equatorial Electrojet Ahmedabad, 8.

Courtillot, Ducruix, V., J. and Le Mouel, J.-L. 1978. 51, Sur uneaccdldrationrdcented e la variation s•culaire du champ magn•tiqueterrestre, C. It. Acad. Sci. Set. D, 287, 1095-1098,

Deka, R. C., D'Cruz, L. A., Jacob, V. J., Iype, A. and Elango, P., 2005. Location of the dip equator over Peninsular India,J. Ind. Geophys. Union,9, 41–46.

Golovkov V. P., Kolomijtzeva G. I., Konyashchenko I. P. and Semyonova G. M, 1983. The Summao, ~(the Annual Mean Values o['Magnetic Elements at Worm Magnetic Observatories,21,279 (for Trivandrum) and 21,295 (for Huancayo). Izmiran, Moscow,

Gulatee, B. L., 1954. Charts of declination, horizontal force and vertical force for the epoch 1953.0, and magnetic anomalies (India, Pakistan and Burma), Surv. India Tech., 7(iii) & 9.

1972. IIG, NGRI and SOI, Ground geomagnetic Survey in the Equatorial Electrojet region in India – A Report.Geophy. Res.Bull., 10,167-180,

McLeod, M .G., 1989. Geomagnetic secular variation in Geomagnetism and Paleomagnetism, edited by F.J. Lowes D, .W.Collison, J.H. Parry, S.K. Runcorn, D.C. Tozer and A. Soward Kluwer Acad., Boston,M ass.,19-30.

Murty, A.V.S., Ahmed,K. and Rao,D.R.K., 1984. Migration of the dip equator in the Indian region, Proc.IndianAcad.Sci.(Earth & Planet Sci), 93, 129~133.

Nandini Nagarajan, 1992. A comparison of geomagnetic secular variation in the Indian region with world-wide trends, Mem.Geol. Soc. Ind.24, 253-261,

Paramasivam,B., Vijaykumar,K. and Elango,P., 1999. Migration of dip equator-Ground geomagnetic Survey, The J. Ind. Geophys.Uni., 6 (1), 19-23.

Rangarajan, G. K., 1994. Secular variation in the geographic location of the dip equator PAGEOPH, 143, 697~71.

Rangarajan, G. K. and Barreto, L.M., 2000. Secular change in the location of the magnetic dip equator in the twentieth century. Geofisica Inter.,39, 323-336.

Rangarajan, G. K. and Deka, R. C., 1991. The dip equator over peninsular India and its secular movement. Proc. Indian Aca.Sci. (Earth & Planet Sci), 100, 361~368,

Rotanova, N. M., Bondar, T. N., and Kovalevskaya, E., V.2003. Wavelet analysis of secular geomagnetic variations, Russian J. of Earth Sciences, 5, 5,

Sanker Narayan, P. V. and Ramanujachary, K.R., 1971. Nature (London), 231-37.

Srivastava, B. J., 1977. New results on the dip equator and the equatorial electrojet in India, J.Atmos. Terr. Phys., 54,871-880, 1992.

Srivastava, B. J.and Abbas, H.,Geomagnetic secular variation in India-Regional and local features, J.GEOMAG.Geoelectr.29, 51-64.

Srivastava, B. J. and Abbas, H., 1984. Global geomagnetic impulses in annual intensity changes, J. of Geophysics - Zeitschrift fur Geophysik, 54, 2, 157-161.

J. Ind. Geophys. Union (January 2016)
Special Volume-2/ 2016 pp: 127-132

Preliminary studies of ionospheric behavior during a seismic event of Mw~6.9 at Qinghai station (geog. 33.19° N, 96.75°E)

Malini Aggarwal[1*], D. K. Sharma[2] and Ananna Bardhan[2]
Indian Institute of Geomagnetism, New Panvel, Mumbai, India
Department of Physics, Manav Rachna University, Faridabad, India
asmalini@rediffmail.com

ABSTRACT
The prediction of one of the natural hazards, namely, earthquakes continues to be most challenging for earth scientists. Several recent studies have shown examples from different regions of the world, by which an association noticed between possible electromagnetic precursors and earthquakes has become more authentic. We have investigated the response of ionospheric parameters to the seismic conditions for one of the seismic events of 13 Apr 2010 (Mw~6.9, depth~13.8 km) over Qinghai station (**geog. 33.19° N, 96.75°E**), using the available online information from the US Geological survey (USGS) website for seismic and space-based GPS-TEC (GPS based total electron content) measurements, for the ionospheric behaviour. The preliminary result shows anomalous depletions in GPS-TEC observed 3-4 days before the seismic event in the ionosphere over nearby stations: Lhasa, Kunming and Urumqi consecutively for ~7-10 hrs.

Keywords: Ionosphere, Seismo-ionosphere coupling, GPS-TEC.

INTRODUCTION

Since last few decades, a connection between the earthquake (EQ) phenomena and the earth's ionosphere is proposed and many scientific investigations have been carried out to understand if it exists, using various satellite and ground-based measurements (eg. *Pulinets et al.,1998; Pulinets and Boyarchuk, 2004; Liu et al., 2009*). But still the ambiguity of seismo-ionospheric effects exists and the conclusions are not very clear. This is because the EQ phenomenon is a complex chain of various physical processes, which reflects the physical nature of different geochemical, atmospheric, ionospheric and magnetospheric anomalous variations (*Pulinets and Ouzounov, 2011*). Along with this, the earth's ionosphere also exhibits the day-to-day, seasonal, longitudinal, latitudinal and annual variabilities, which mainly are driven by solar activity. Apart from the solar-driven variations, 27 day variations (*Kakinami et al., 2009*), the ionospheric variabilities existed due to the dynamics of thermosphere and occurrence of a variety of geophysical phenomena like planetary waves, atmospheric and lunar tides etc. The occurrence of a geomagnetic storm also changes the ionospheric behavior, which changes the background conditions during disturbed period (*Afraimovich and Astafyeva, 2008; Astafyeva and Heki, 2011; Aggarwal et al., 2013*). Recently, *Le et al., 2013* investigated the ionospheric behaviour using GPS-TEC measurements prior to the 11 Mar 2011 Tohoku-Oki EQ and found a significant increase in TEC adjacent to the epicenter and its magnetic conjugate for 16 hr on 8 Mar 2011. This was considered to be related to the EQ and the geomagnetic disturbances on 7 Mar (Kp=4). Besides the storms, it was recently shown that even under geomagnetically quiet conditions and during low solar activity, a decrease of the Bz component of the IMF to -5 nT is enough to produce ~15-25% increase in the equatorial afternoon TEC (*Astafyeva and Heki, 2011)*. *Pulinets and Boyarchuk (2004)* explained the variations of near-earth plasma densities observed over seismically active areas several days/hours before strong seismic shocks. They demonstrated the seismo-ionospheric coupling to be a part of the global electric circuit and the anomalous electric field observed in the active seismic areas to be the main carrier of information from the earth's ground surface to the ionospheric altitudes. Besides this, another factor considered responsible for the co-seismic disturbances is the atmospheric gravity waves (AGWs). These waves are produced by the vertical sudden displacement of the ground and sea surface caused by the EQ and tsunami (*Watada et al., 2009*). Considering the various complexities, we probed the ionospheric behaviour during a seismic event (Mw~6.9, depth~13.8 km) of 13-14 Apr, which occurred at Qinghai (geog. 33.19° N, 96.75°E) station in China to study and understand the changes in the physical ionospheric behavior before the EQ event.

THE EQ DESCRIPTION

The strong EQ of magnitude 6.9 occurred on 13 Apr, 2010 around 23:49:38 UT (14 Apr 2010 around 07:49:38 LT) and its aftershock (14 Apr 2010, 6.1 magnitude, ~ 01:26:16 UT) at the epicenter (geog. 33.19°N, 96.75°E, geom. 23.90°N, 169.98°E), with shallow depth ~13.8 km in the Southern Qinghai, China (as reported on the United State Geological Survey (USGS) website *www.earthquake.usgs.gov.in*). This EQ occurred as a result of strike-slip faulting in the tectonically complex region of the eastern

Tibetan Plateau and is one of the largest known historic earthquakes within several hundred kilometers of its location. The radius of the earthquake preparatory zone in the lithosphere is found to be ~930 km. This was obtained by using the expression, R = 10^(0.43M), where M is the magnitude of the earthquake (*Dobrovolsky et al., 1979*).

DATA SET AND ANALYSIS

To investigate the spatial and temporal irregular behavior of the ionosphere before and during the earthquake event, the hourly total electron content (TEC) is obtained by the GPS using 10 IGS stations in the Chinese sector, by using a method of thin layer approximation (~350 km) (*Klobuchar, 1986*) with >20° elevation angle to minimize the time shift and avoid unwanted errors due to multipath (*Aggarwal et al., 2012*). The GPS-TEC is defined as the total number of electrons from the ground to the height of GPS satellite (20,500 km) in 1 m^2 area. **Figure 1(A)** shows the location of the epicenter (starred) and the relative distance of the considered GPS receivers (symbol). The stations considered are: Lhasa (LHAZ, geog. 29.65°N,91.1°E), Kunming (KUNM, 25.02°N, 102.79°E), Urumqi (URUM, 43.8°N, 87.6°E), Wuhan (WUHN, 30.53°N, 114.35°E), Fangshan (BJFS, 39.6°N, 115.89°E), Sheshan (SHAO, 31.9°N,121.2°E), 2 stations at Hsinchu (24.79°N, 120.98°E, TCMS and TNML), Taoyuan (TWTF, 24.95°N, 120.98°E) and Changchun (CHAN, 43.79°N, 125.44°E). The circle represents the preparatory or influence zone of the earthquake of radius ~930 km. Out of these stations, we found that LHAZ lies in the preparatory zone of earthquake, whereas KUNM is just at the boundary. The three stations (BJFS, CHAN and URUM) are further north of Qinghai, whereas others are toward the equator side. The LHAZ and URUM lie in the west, whereas other stations are in east-side of the epicenter. To compare the behavior of ionosphere away from the occurrence of EQ event, 6 more IGS stations are considered: Chumysh (CHUM, 42.99°N, 74.75°E, Kazhakstan), Kitab (KIT-3, 39.14°N, 66.88°E, Uzbekistan), Ulaanbataar (ULAN, 47.67°N, 107.05°E, Mongolia), Tehran (TEHN, 35.69°N, 51.33°E, Iran), Suwon-Shi (suwn, 37.27°N, 127.05°E) and Daejeon (DAEJ, 36.39°N, 127.37°E) in South Korea, respectively. All these stations are also shown in **Figure 1 (A)**.

To detect abnormal signals in the GPS TEC, we used the method of *Liu et al. (2009)*,which is gaining significance in determining the possible EQ precursors (e.g *Astafyeva and Heki, 2011; Pundhir et al., 2014*). We computed the hourly median M, lower (first) quartile (LQ) and upper (third) quartile (UQ) for the successive previous 15 days of GPS-TEC for same UT over each station. Under the assumption of a normal distribution with mean (m) and standard deviation (s) for the GPS TEC, the expected values of M and LQ or UQ are noted as m and 1.34s, respectively (*Klotz and Johnson,1983*). Then the isolated TEC anomalies are obtained as the lower bound (LB)=M-1.5(M-LQ) and upper bound (UB)=M+ 1.5(UQ-M), respectively. Here, the probability of observed TEC in the interval (LB, UB) is approximately 65%. Thus when an observed TEC (Obs) on the 16th day is found to be higher or lower than its previous 15-day-based median by UB or LB, we confirmed presence of an upper or lower abnormal GPS TEC signal.

RESULTS AND DISCUSSION

The earth's ionosphere is subjected to numerous influences, from both above as well as below due to the variability of solar activity, geomagnetic activity, meteorological events, and anthropogenic effects. The ionosphere also exhibits normal day-to-day, seasonal and diurnal variations making it difficult to identify possible pre-seismic ionospheric anomalies (*Afraimovich and Astafyeva, 2008*). Hence, we also firstly looked into the prevailing background conditions during our study period. The **Figure 1(B)** represents the variability of Dst (storm-time disturbance) and F10.7 (solar flux) in the upper panel along with the observed TEC, M, LB and UB on each day over LHAZ, KUNM, URUM and CHAN stations during 5-14 Apr 2010. Though we obtained the TEC variabilities over each station, only 4 stations are shown here (**Figure 1 (B)**).Out of which CHAN is farther station in China, whereas other 3 stations are near the epicenter.

A coronal mass ejection (CME) occurred on 3 April 2010 and arrived at the earth 2 days later (*Mostl et al., 2010*). On 5 April 2010, an interplanetary (IP) shock was detected by the Wind spacecraft ahead of Earth, followed by a fast (~ 650 km/s, average speed) IP CME. This CME was associated with a magnetic cloud. A moderate geomagnetic storm occurred that lasted 3 days (5-7 April 2010). The Kp index became higher ~7.7 (0900-1200 UT) on 5 Apr with Dst min (~-81 nT) on 6 Apr around 1500 UT. Despite being a relatively moderate storm, it nevertheless had some devastating space weather impacts, including the malfunction of the Galaxy 15 communication satellite (at ~35,785 km) (*Allen, 2010*) and widespread GPS scintillations ranging from the Arctic to Antarctic (*Prikryl et al., 2011; Kinrade et al., 2012*). *Smirnov et al., (2014)* studied the effects on the electric parameters of the amospheric near-ground layer during this storm. They found that air electro-conductivity decreased by a factor of 2, 4 hrs before the sudden commencement (SC) of storm and lasted for 20 hrs. The storm's SC caused potential gradient oscillations with amplitudes up to 300 V/m. This storm was associated with higher solar flux (F10.7~76-79 sfu) as compared to other days during our study period. Another weaker storm occurred on 11-12 Apr with Dst min ~-67 nT around 0200 UT on 12 Apr.

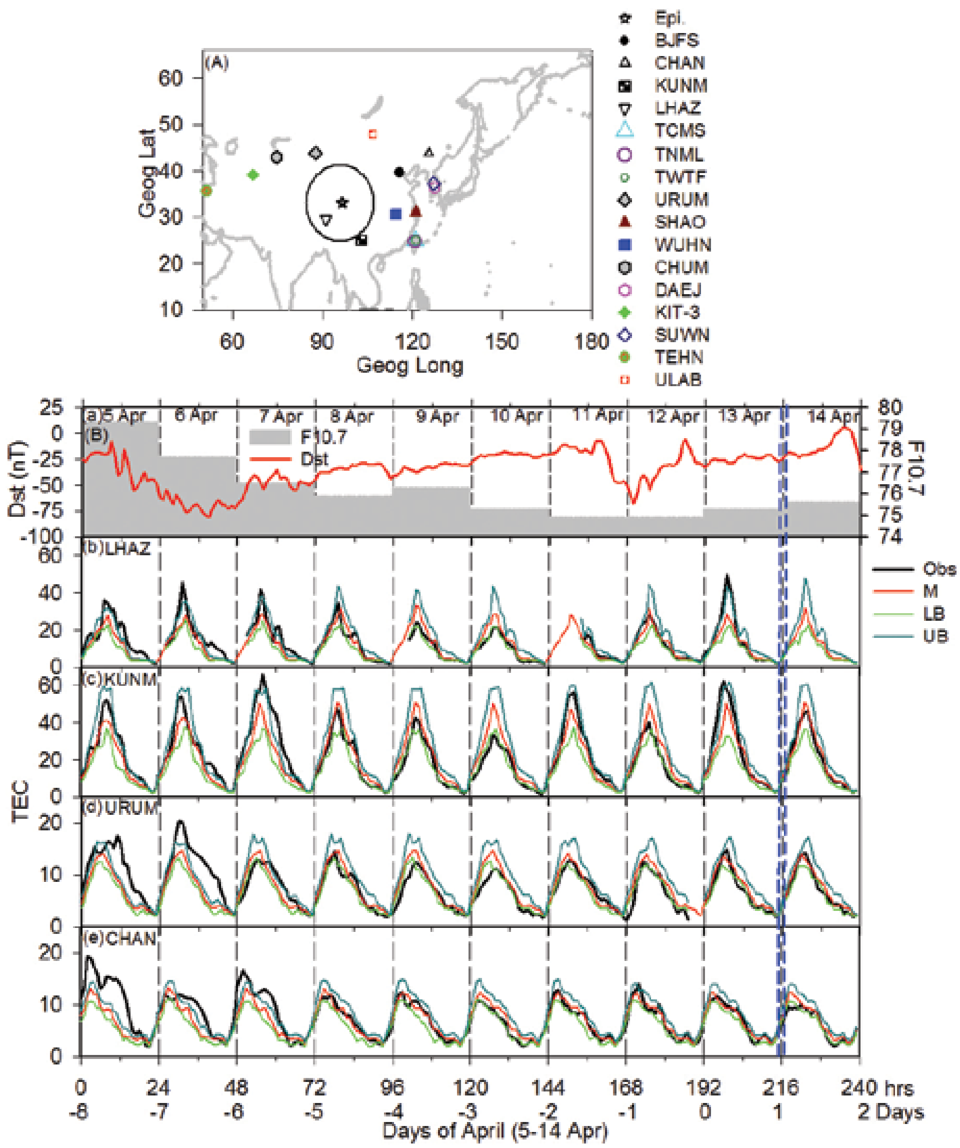

Figure 1. Upper panel (A): Represents the locations of the epicenter (star) with 16-IGS stations (symbols) considered in the study. Circle shows the preparatory zone of EQ (~ 930 km radius). Lower Panel (B): Variability of various parameters during 5-14 Apr 2010 with time: (a) Dst and F10.7 and obs TEC (Obs), Median (M), lower bound (LB) and upper bound (UB) over (b) LHAZ, (c) KUNM, (d) URUM and (e) CHAN respectively. The vertical line shows the occurrence time and day of EQ and its after shock.

To investigate the anomalies in the ionospheric behavior, which may have occurred during the earthquake, we examined the diurnal variability of observed TEC (Obs TEC), median (M), LB and UB (Figure 1(B)) as described in the 'data set and analysis' section. The TEC comprises electron densities in the D, E and F layer of the ionosphere with main contribution from F-layer. The well known diurnal pattern of TEC exhibits a steady increase during early morning when the photoelectron production begins and is maximum during noon time and then decreases due to the competitive effects of absence of photo-ionization and recombination of electrons with neutrals and ions during nighttime. It is well known that in the F region, the production rate of electrons depends on the atomic oxygen concentration [O], whereas the loss rate depends mainly on the molecular nitrogen concentration [N_2] with some contribution from the molecular oxygen [O_2]. We found from different stations that the observed TEC is minimum (≤ 5 TECU) through-out the nighttime at all stations and start increasing early in the morning. The rate of increase of TEC and the magnitude of noon-time TEC is higher over the low-latitude (≤ 30 deg) stations

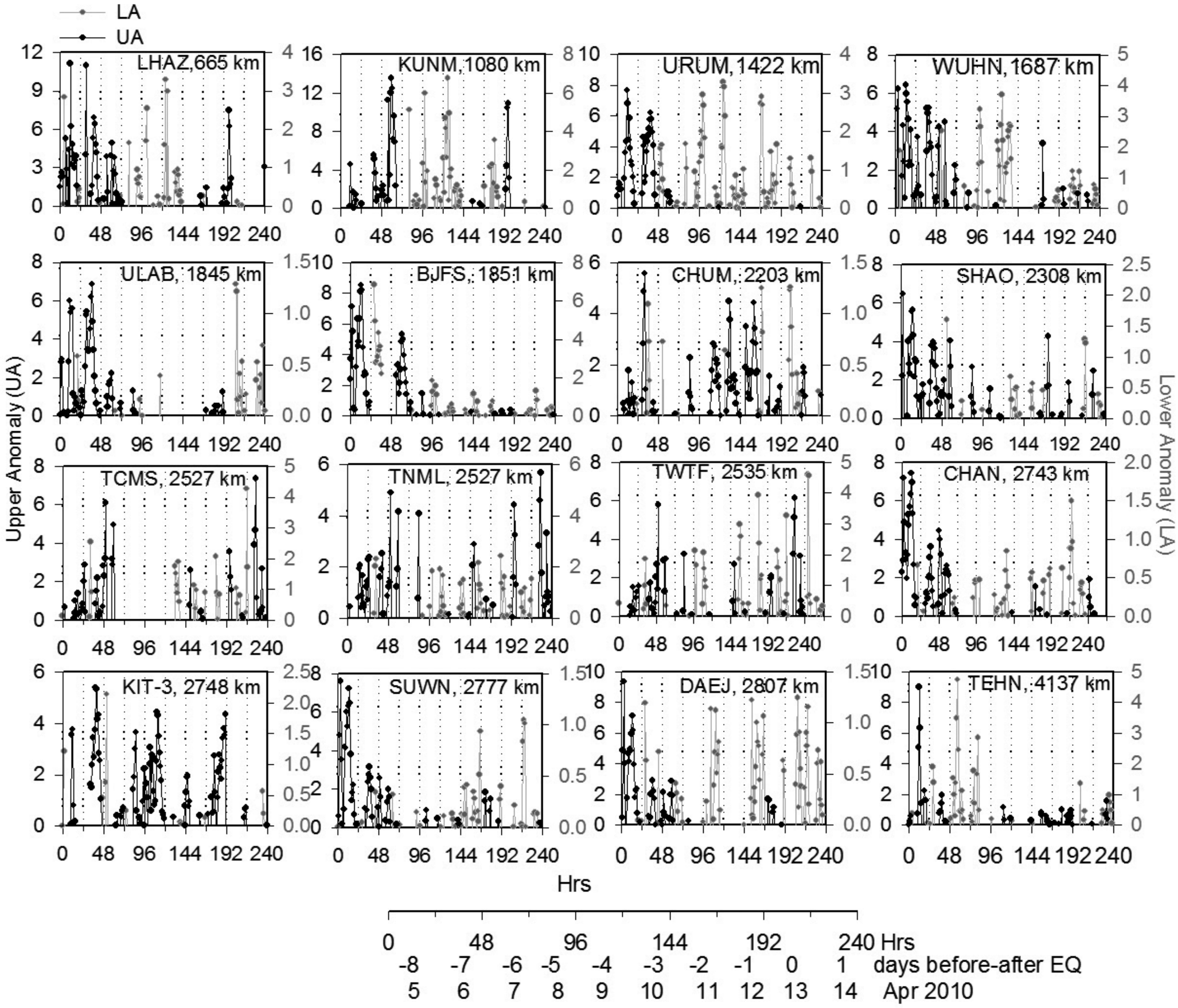

Figure 2. Represents the quantitative hourly anomalies in the upper bound (ObsTEC-UB, upper anomaly, UA, left-axis) and lower bound (LB-ObsTEC, lower anomaly, LA, right-axis) respectively over all 16-IGS stations during 5-14 April. The stations are arranged with the increase in the distance from the epicenter mentioned in each panel.

(LHAZ, KUNM, TCMS, TNML, TWTF), whereas at other higher mid-latitude stations (URUM, WUHN, BJFS, SHAO, CHAN, CHUM, KIT-3, ULAB, TEHN, SUWN and DAEJ) the response is weaker, showing a latitudinal response of production processes of electrons in the ionosphere.

The hourly anomalies in both the upper bound (ObsTEC-UB, UA) and lower bound (LB-ObsTEC, LA) over each station is examined and is presented in **Figure. 2**. The stations in **Figure 2** are arranged with the increase in the distance from the epicenter ,which is obtained by using the Haversine formula. The positive values of UA/LA indicate an enhancement/depletion of obs TEC from the UB/LB, respectively. When consecutively more than one third of hourly values (>7) of obs TEC in a day are higher or lesser than the upper and lower bounds of that particular day, we called that as an anomalous day. The higher anomalous TEC is observed during 5-7 Apr over all stations. Another increase in TEC is observed on 13 Apr (also an EQ day) over all the stations but the magnitudes are different, being higher at lower-latitude stations than over mid-latitude stations, which may again be attributed to the moderate storm period (Dst ~ -67 nT) of 12 Apr in the background. The ionospheric effect of a geomagnetic storm is considered a global phenomenon ,whereas EQ is a local phenomenon

(*Pulinets, 1998*). Considering this, we have looked into the ionospheric variabilities above the available stations, which are near-by and away from the epicentre. We found the method developed by *Liu et al., 2009* ,a robust method to remove the anomalous changes in hourly values. The storm time behavior is also distinct. During geomagnetic storms, strong electric fields and currents are transmitted between the magnetosphere and the high-latitude ionosphere, producing enhanced Joule heating and auroral particle precipitation in the auroral region. The conductivity of the ionosphere increases, neutral winds are accelerated, the thermosphere is heated up and the composition gets altered, and ionospheric plasma convection gets intensified and highly distorted. The perturbed neutral winds and composition propagates equator ward ,creating ionospheric and thermospheric disturbances over the entire globe (e.g., *Prolss, 1995; Aggarwal et al., 2013*).

From the lower panels of **Figure 1(B) and 2**, it is clear that on some days the Obs TEC lies between LQ and UQ, whereas on other days it is either higher or lower than UQ or LQ, respectively. Here mainly the days 5, 6, 7, 10 and 13 Apr exhibit the anomalous features. As said before also 5-7 and 12-13 Apr are disturbed periods when the TEC gets enhanced. But, it was not for a longer period (<7 hours). Whereas, on 10 Apr, the Obs TEC is close to LQ, which is even slighty lower than LQ for 7-10 hours. This anomalous decrease in Obs TEC is observed over LHAZ, KUNM, URUM and WUHN, whereas not over the stations far-away from the epicenter.

We can conclude from **Figure 2** that 6-8 days before the EQ, the TEC has enhanced on few days (UA) ,which has contributed to the high solar activity and disturbed period, as discussed earlier. And the anomalous depletions in TEC (LA) are observed 3-4 days (on 10 Apr) before the EQ in the ionosphere over nearby stations: LHAZ, KUNM, URUM and WUHN consecutively for ~7-10 hrs. Now, the question comes that how the variability in the plasma (electrons, TEC) may occur in the ionosphere few days before the earthquake. Although, the exact mechanism of the lithosphere-ionosphere coupling is still not known, possible explanations have been advanced by many workers in terms of E x B drift mechanism where the electric field (E) triggered by an earthquake preparatory process penetrates the ionosphere and, in the presence of local magnetic field (B), causes upward or downward movement of the ionization depending upon the direction of the electric field (Devi et al., 2008). The radon element, which is also a radioactive material is considered a source of ionization for the electric field generation mechanism. During the EQ, each α-particle emitted by ^{222}Rn (5.46 MeV) and its progeny, ^{218} Po (6 MeV) can produce $\sim 10^5$ ion-electron pairs. The heat released during the EQ depends on the number of H_2O molecules attached to the ion (*Pulinets and Ouzounov, 2011*). According to *Pulinets et al., (2006)*, the ion concentration increases in the area of the EQ preparation to $\sim 10^5$-10^6 cm^{-3}, which essentially changes the electric properties of the near ground layer of the atmosphere. The consequence of this process is the change in the air conductivity, which creates the possibility of the anomalous electric field generation. As a result of the local changes in the atmosphere electricity, the local changes of the electron concentration variability are induced in the ionosphere, which can be registered by different ionospheric techniques. From our observations, we found that spatial distribution of the anomalies was very local, which probably indicates association with seismo-ionospheric coupling processes. Some more detail investigations are needed to obtain quantitatively the changes in the other plasma and neutral parameters in the ionosphere to understand the seismo-ionosphere coupling.

ACKNOWLEDGEMENT

MA is grateful to the Department of Science and Technology (DST), India for awarding the Ramanujan Fellowship to carry out the work. She is also grateful to Prof. D.S Ramesh, Director of IIG, Mumbai for providing the hosting facilities at the Institute. The GPS data collected from various IGS stations, OMNI website and the USGS community are also highly acknowledged for making the data available. We are also grateful to the reviewers for their fruitful comments and suggestions.

REFERENCES:

Afraimovich, E. L., Astafyeva, E. I., 2008. TEC anomalies Local TEC changes prior to earthquakes or TEC response to solar and geomagnetic activity changes? Earth, Planets and Space, 60, 961-966.

Aggarwal, M., Joshi, H. P., Iyer, K. N., Kwak, Y.-S., Lee, J. J., Chandra, H., Cho, K. S, 2012. Day-to-day variability of equatorial anomaly in GPS-TEC during low solar activity period, Adv. Space Res., 49, 12, 1709-1720.

Aggarwal, M., Joshi, H. P., Iyer, K. N., Kwak, Y. S., 2013. Response of the EIA ionosphere to the 7-8 May 2005 geomagnetic storm. Adv. Space Res. 52, 4, 591-603.

Allen, J., 2010. The Galaxy 15 Anomaly: Another satellite in the wrong place at a critical time. Space Weather, 8, S06008, doi:10.1029/2010SW000588.

Astafyeva, E., Heki, K., 2011. Vertical TEC over seismically active region during low solar activity. J. Atmos. & Sol. Terr. Phys. 73, 13, 1643-1652.

Devi, M., Barbara, A. K., Depueva, A., Depuev, V., 2008. Preliminary results of TEC measurements in Guwahati, India. Adv. Space Res. 42, 753–756.

Dobrovolsky, I.P., Zubkov, S.I., Miachkin, V.I., 1979. Estimation of the size of earthquake preparation zones. Pure Appl. Geophys. 117, 1025–1044.

Kakinami, Y., Chen,C.H., Liu,J.Y., Oyama,K.-I., Yang,W.H., Abe,S., 2009. Empirical models of total electron content based on functional fitting over Taiwan during geomagnetic quiet condition. Ann.Geophys.27, 3321–3333.

Kinrade, J., Mitchell, C. N., Yin, P., Smith, N., Jarvis, M. J., Maxfield, D. J., Rose, M. C., Bust, G. S., Weatherwax, A. T., 2012. Ionospheric scintillation over Antarctica during the storm of 5-6 April 2010, J Geophys. Res., 117, A5, CiteID A05304.

Klobuchar, J., 1986. Design and characteristics of the GPS ionospheric time-delay algorithm for single frequency users, in: Proceedings of PLANS'86 – Position Location and Navigation Symposium, Las Vegas, Nevada, 4–7 November, pp. 280–286,

Klotz, S., Johnson, N.L. (Eds.), 1983. Encyclopedia of Statistical Sciences. John Wiley and Sons.

Le, H., Liu, L., Liu, J.Y., Zhao, B., Chen, Y., Wan, W., 2013. The ionospheric anomalies prior to the M9.0 Tohoku-Oki earthquake // Journal of Asian Earth Sciences, 62, 476-484.

Liu, J.Y., Chen, Y.I., Chen, C.H., Liu, C.Y., Chen, C.Y., Nishihashi, M., Li, J.Z., Xia, Y.Q., Oyama, K.I., Hattori, K., Lin, C.H., 2009. Seismoionospheric GPS total electron content anomalies observed before the 12 May 2008 Mw7.9 Wenchuan earthquake. J. Geophys. Res. 114, A04320, doi:10.1029/2008JA013698

Möstl, C., Temmer, M., Rollett, T., Farrugia,C. J., Liu, Y., Veronig, A. M., Leitner,M., Galvin, A. B., Biernat, H. K., 2010. STEREO and Wind observations of a fast ICME flank triggering a prolonged geomagnetic storm on 5–7 April 2010. Gophys. Res. Lett, 37, L24103, doi:10.1029/2010GL045175, 2010

Prikryl, P., Spogli, L., Jayachandran, P. T., Kinrade, J., Mitchell, C. N., Ning, B., Li, G., Cilliers, P. J., Terkildsen, M. , Danskin, D. W., Spanswick, E., Donovan, E., Weatherwax, A. T., Bristow, W. A., Alfonsi, L., De Franceschi, G., Romano, V., Ngwira, C. M., Opperman, B. D. L., 2011. Interhemispheric comparison of GPS phase scintillation at high latitudes during the magnetic-cloud-induced geomagnetic storm of 5–7 April 2010, Ann. Geophys., 29, 2287–2304, doi:10.5194/angeo-29-2287-2304.

Prolss, G.W. 1995. Ionospheric F region storms. H. Volland (Ed.), Handbook of Atmospheric Electrodynamics, CRC Press, Boca Raton, pp. 195–248.

Pulinets S.A., 1998. Seismic activity as a source of ionospheric variability. Adv Space Res. 22, 903-906.

Pulinets S. A. and Boyarchuk, K.A. 2004. Ionospheric precursors of earthquakes (Springer, Berlin, Germany).

Pulinets, S. A., Ouzounov, D., Ciraolo, L., Singh, R., Cervone, G., Leyva, A., Dunajecka, M., Karelin, A. V., Boyarchuk, K. A., Kotsarenko, A. 2006. Thermal, atmospheric and ionospheric anomalies around the time of the Colima M7.8 earthquake of 21 January 2003. Ann. Geophys., 24, 835–849.

Pulinets, S., Ouzounov, D. 2011. Lithosphere–Atmosphere–Ionosphere Coupling (LAIC) model – An unified concept for earthquake precursors validation. J. of Asian Earth Sciences, 41, 371–382.

Pundhir, D., Singh, B., Singh, O. P., 2014. Anomalous TEC variations associated with the strong Pakistan-Iran border region earthquake of 16 Apr 2013 at a low latitude station Agra, India. Adv. in Space Res. 53, 2, 226-232.

Smirnov, S. 2014. Reaction of electric and meteorological states of the near-ground atmosphere during a geomagnetic storm on 5 April 2010 // Earth, Planets and Space, 66: 154.

Watada, S. 2009. Radiation of acoustic and gravity waves and propagation of boundary waves in the stratified fluid from a time-varying bottom boundary, J. Fluid Mech., 627, 361–377, doi:10.1017/S0022112009005953.


IAGA OBSERVATORY WORKSHOP
2014 HYDERABAD INDIA
IAGA
XVI IAGA WORKSHOP
ON
GEOMAGNETIC OBSERVATORY
INSTRUMENTS, DATA ACQUISITION
AND PROCESSING
October 7-16, 2014 Hyderabad, India
Sponsored by
CSIR
IUGG
INCOIS
INSA
DST
MoES
ICSU
Jointly Hosted by
CSIR - National Geophysical Research Institute
Uppal Road, Hyderabad -500606 Telangana, India
Indian Institute of Geomagnetism
Kalamboli Highway, New Panvel, Navi Mumbai - 410218